A METHODOLOGY FOR RISK-INFORMED LAUNCH VEHICLE ARCHITECTURE SELECTION

A Dissertation
Presented to
The Academic Faculty

By

Stephen J. Edwards

In Partial Fulfillment
of the Requirements for the Degree
Doctor of Philosophy in the
School of Aerospace Engineering

Georgia Institute of Technology

December 2017

Copyright © Stephen J. Edwards 2017

A METHODOLOGY FOR RISK-INFORMED LAUNCH VEHICLE ARCHITECTURE SELECTION

Approved by:

Dr. Dimitri Mavris, Advisor
School of Aerospace Engineering
Georgia Institute of Technology

Dr. Daniel Schrage
School of Aerospace Engineering
Georgia Institute of Technology

Dr. Mitchell Walker
School of Aerospace Engineering
Georgia Institute of Technology

Dr. Charles Domercant
Electronic Systems Lab
Georgia Tech Research Institute

Mr. Mark Rogers
Advanced Concepts Office
NASA Marshall Space Flight Center

Date Approved: May 4, 2017

Soli Deo Gloria

For Amy

I left you in the morning,
And in the morning glow
You walked a way beside me
To make me sad to go.
Do you know me in the gloaming,
Gaunt and dusty gray with roaming?
Are you dumb because you know me not,
Or dumb because you know?

All for me? And not a question
For the faded flowers gay
That could take me from beside you
For the ages of a day?
They are yours, and be the measure
Of their worth for you to treasure,
The measure of the little while
That I've been long away.

Robert Frost

TABLE OF CONTENTS

LIST OF TABLES

LIST OF FIGURES

SUMMARY

Modern society in the 21st century has become inseparably dependent on human mastery of the near-Earth regions of space. Billions of dollars in on-orbit assets provide a set of fundamental, requisite services to such diverse domains as telecom, military, banking, and transportation. While these services are provided by orbiting satellites, launch vehicles (LVs) are unquestionably the most critical piece of infrastructure in the satellite industry value chain.

The past decade has seen a significant level of activity in LV development, including some fundamental changes to the industry landscape. Every space-faring nation is engaged in new program developments: Russia with its Angara family of launchers; China with its Long March V vehicle; India with its Geosynchronous Satellite Launch Vehicle (GSLV); Japan with its Epsilon launch vehicle; Europe, with the Ariane 6; and the United States with the Space Launch System (SLS). Most notable, however, is the surge in activity by commercial players, whose investments and development efforts have been spurred by a combination of private investments by wealthy individuals, new government policies and acquisition strategies, and the increased competition that has resulted from both.

In all the LV programs of today, affordability is acknowledged as the single biggest objective. Governments seek assured access to space that can be realized within constrained budgets, and commercial entities vie for survival, profitability, and market-share. This marks the culmination of a shift in the space launch industry away from its roots in the ballistic missile programs of the Cold War. In this coming of age, how sustainable affordability will be achieved stands as the most imminent question to be answered.

From literature, it is clear that the biggest opportunity for affecting cost savings resides in improving decision-making early on in the design process. The NASA Systems Engineering Handbook estimates that 50 to 70 percent of the total life-cycle cost is locked in by the time an architecture has been selected. It goes on to say that “by the time a preliminary

system design is selected, this figure may be as high as 90 percent." Launch vehicles are no exception to this rule, as another NASA author states that "at least 80 percent of the life-cycle costs are determined by decisions made during the conceptual design stage."

Despite these observations, a review of historical LV architecture studies shows that very little has changed over the past 50 years in how early architecting analysis of alternatives are performed. In particular, architecture analyses of alternatives are still conducted deterministically, despite uncertainty being at its highest in the very early stages of design. All of the "design freedom" that is held by designers early on manifests itself as volitional uncertainty during the LV architect's decision-making. This perspective motivates the objective for this thesis, which is "to develop a methodology for enabling risk-informed decision making during the architecture selection phase of LV programs."

This thesis adopts NASA's Risk-Informed Decision Making process, and tailors the methods and techniques applied in its execution to the LV architecture selection problem. The most significant challenge is found to be LV trajectory performance modeling, which does not lend itself to probabilistic analsyses in a full numerical optimization form. To overcome this challenge, an empirical modeling approach is proposed. However, this in turn introduces the challenge of generalizing the empirical model, as creating distinct performance models for every architecture concept under consideration is deemed infeasible.

A review of the main drivers in LV trajectory performance observes the thrust-to-weight ratio (T/W) not only to be one of the parameters with most sensitivity, but also reveals it to be a functional in its true form. Based on the performance driving nature of the T/W profile, and the fact that in its infinite-dimensional form it offers a common basis for statistical modeling across architectures, functional regression techniques are proposed as a potential means of constructing an architecture-spanning empirical performance model. A number of techniques are formulated and tested, and prove capable of supporting the LV performance modeling in support of risk-informed architecture selection.

CHAPTER 1
INTRODUCTION & MOTIVATION

1.1 The Challenge in Launch Vehicle Design

1.1.1 Importance of Launch Vehicles

Modern society in the 21st century has become inseparably dependent on human mastery of the near-Earth regions of space. Billions of dollars in on-orbit assets provide a set of fundamental, requisite services to such diverse domains as entertainment, military, banking, and transportation.[1] These, among others, are depicted by a cross-section of satellite applications in Figure 1.1. While these services are provided by orbiting satellites, launch vehicles (LVs) are unquestionably the most critical piece of infrastructure in the satellite industry value chain. Launch and orbit insertion, both activities that are completed in a matter of minutes to hours, comprise the biggest risk of loss in spacecraft life cycles that are usually measured on a scale of months to years.[2] Similarly, launch insurance and launch costs can together represent up to 50 percent of a satellite's cost, but the revenue generating capabilities (or value generating, in the case of entities that may not seek revenue, such as militaries) reside exclusively in the spacecraft. [3]

The past decade has seen a significant level of activity in LV development, including some fundamental changes to the industry landscape. Every space-faring nation is engaged in new program developments: Russia with its Angara family of launchers;[4] China with its Long March V vehicle;[5] India with its Geosynchronous Satellite Launch Vehicle (GSLV);[6] Japan with its Epsilon launch vehicle [7]; Europe, with the Ariane 6 [8]; and the United States with the Space Launch System (SLS).[9] Most notable, however, is the surge in activity by commercial players, whose investments and development efforts have been spurred through a combination of private investments by wealthy individuals,

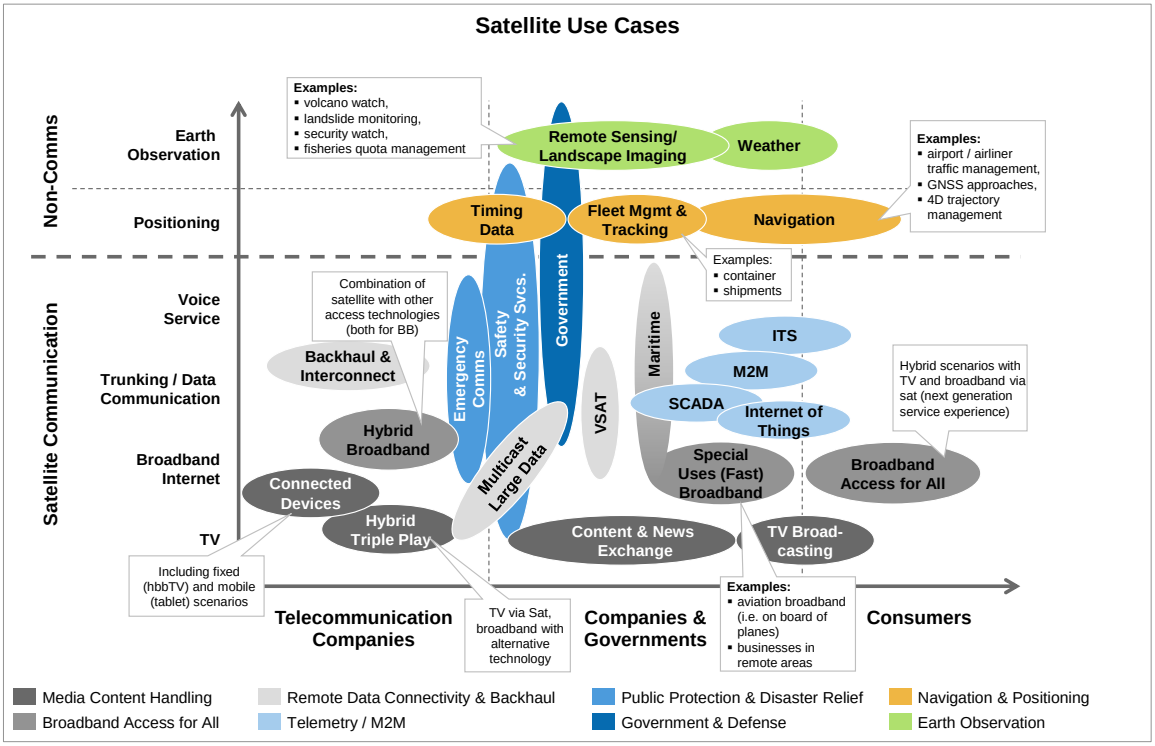

Figure 1.1: Domains and services dependent on space-based assets [1]

new government policies and acquisition strategies, and the increased competition that has resulted from both.[10]

Competitive pressure from new entrants has forced the "old guard" of the industry to adapt and innovate in order to remain relevant. United Launch Alliance's new Vulcan LV and Arianespace's Ariene 6 are viewed largely as responses to the rise of SpaceX and its industry beating prices. Blue Origin, the other major new player in the launch services and technologies front, has not yet taken a stance in direct competition to existing launch service providers. Its impact has been felt nonetheless, as Blue Origin-developed engines have gone into competition with a consolidated Aerojet-Rocketdyne, being the front-runners for powering ULA's planned Vulcan LV.

1.1.2 Elusive Affordability

Historically, LV developers and operators have been either government agencies or heavily subsidized defense industry ventures. This arrangement makes sense due to the nature

of access-to-space as a critical national infrastructure. The industry operated as a sort of oligopoly, with the government as the only customer. [11] This subjected high-visibility LV development programs to the unpredictability of politics, with potential strategy and requirements changes coming at every new election. Launch vehicle design itself already presents an engineering challenge of the highest degree, requiring systems that operate at the furthest extremes of the performance envelope to carry expensive, one-of-a-kind payloads on missions that allow practically no margin for error. When combined, all of these factors together produce a design process that proceeds on a knife's edge, simultaneously pulled towards conservatism and the use of advanced technologies.

Affordability has proved elusive in this system, as evidenced by the fact that more LV programs have been canceled due to cost overruns than have made it into operation.[12, 13] Figure 1.2 provides a glimpse of this, presenting a two decade timeline of human space flight development programs in the United States. Even with a scope limited to manned development programs, this survey concludes that over twenty billion dollars were spent in programs ultimately destined for cancellation. Bekey, writing in "Exploring the Unknown," a NASA History Series publication, succinctly captures this same trend for the larger scope of both NASA and Air Force LV programs in one of his section titles: "Lots of Studies, But Little Progress." [12] Many would-be programs never make it past the paper study phase.

Even programs that have managed to complete development and enter into operation have not necessarily met their affordability targets. The Space Shuttle program, initially cast as a more cost effective alternative to Apollo-style expendable vehicles, was retired in 2011 with an estimated total program cost of close to $1.5 billion per flight. [14] A replacement LV was not immediately available because the Shuttle operating costs prevented the execution of a new LV development program in parallel. More recent LV programs, aimed specifically at reducing costs, have also fallen short. The Air Force's Evolved Expendable Launch Vehicle (EELV) program was initiated in 1996 with the stated goal of a 25% cost reduction over its predecessors, namely the Medium Launch Vehicle (MLV) and Titan pro-

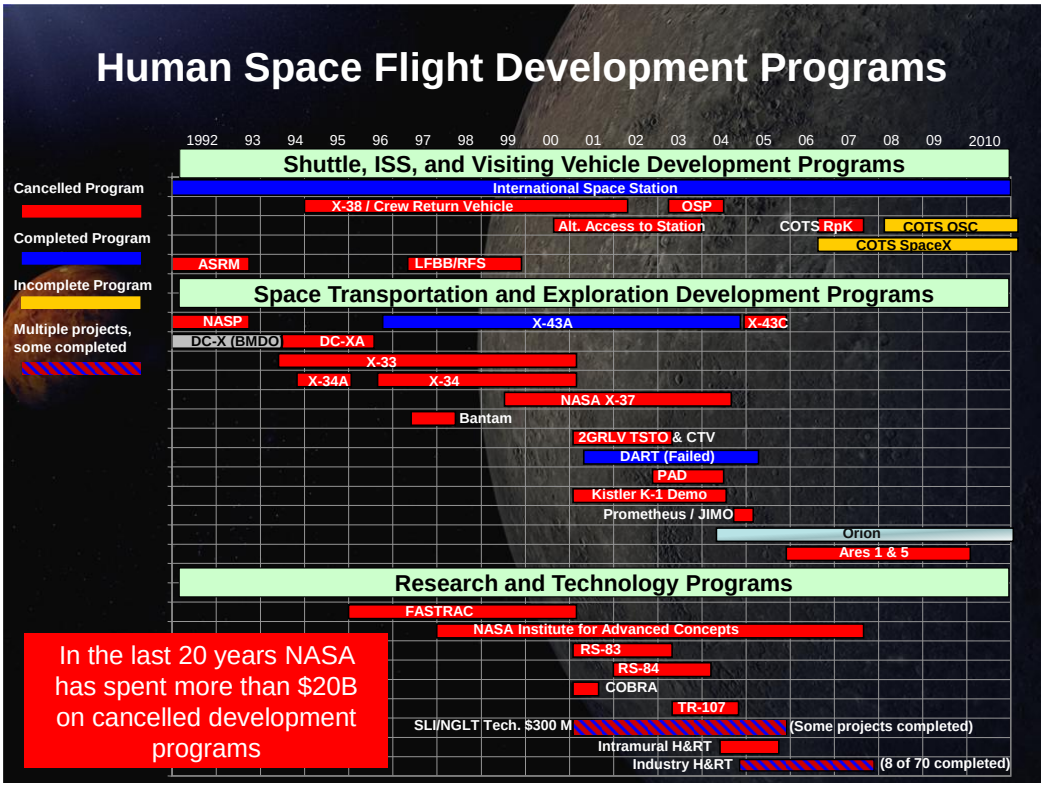

Figure 1.2: A sampling of canceled space launch programs [13]

grams. [15] These closed out with average costs of approximately $51 and $187 million per flight, respectively. [16, 17] However, recent Air Force budget documents place the estimated cost per launch of the EELV program as a whole at over $400 million per flight. [18] Even when accounting for inflation and cost per unit payload mass, EELV costs are significantly higher than its predecessors.

In all the LV programs of today, affordability is acknowledged as the single biggest objective. Governments seek assured access to space that can be realized within constrained budgets, and commercial entities vie for survival, profitability, and market-share. This marks the culmination of a shift in the space launch industry away from its roots in the ballistic missile programs of the Cold War. In this coming of age, how sustainable affordaiblity will be achieved stands as the most immminent question to be answered. It is important to emphasize that, while linked, affordability and cost are not the same thing. A high-cost program can be deemed affordable if the cost is considered to be reasonable given

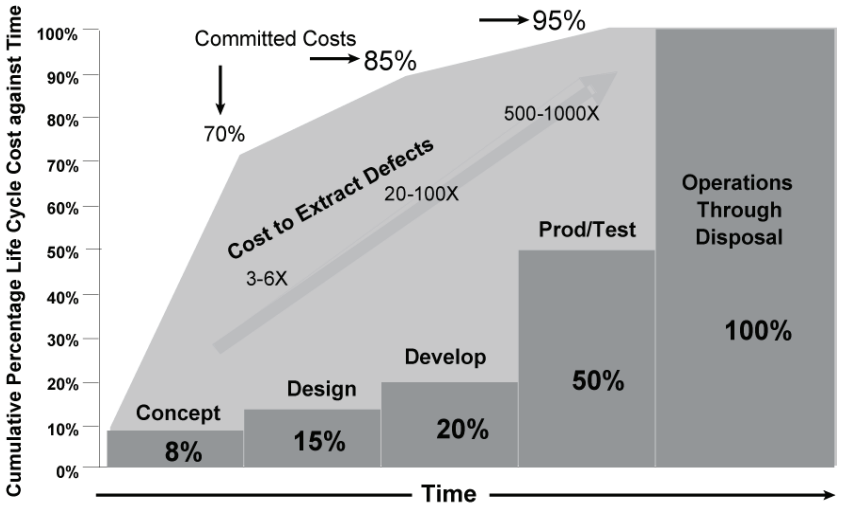

Figure 1.3: Lifecycle cost trends for engineered systems [19]

the capabilities provided and the requirements being satisfied. For example, affordability for NASA's Space Launch System, an LV intended to enable deep space exploration, is defined as "the ability to develop and operate...within the national means to sustain funding for the program." [20] It is expected that such an exploration class vehicle will have a high cost; in return, it should provide a one-of-a-kind mission capability.

In a way, affordability can be understood to represent some form of cost-benefit trade. It is not surprising, then, that in the design and development of such constrained systems as LVs, where competing requirements between the various "-ilities" must be traded, affordability presents itself as a leading challenge.

1.1.3 The "-ilities"

If LV affordability is truly tied up in the cost-benefit ratio, then improving affordability must require some improvement in a set of metrics known as the "-ilities." These measures of "benefit" include such things as reliability, manufacturability, operability, sustainability, and performance capability. [21] Any improvement in affordability will manifest as either a decrease in cost, an improvement in the "-ilities," or both.

While the EELV program as cited in the previous section clearly misses the origi-

nal cost-savings intent for that program, it may not be straight forward to conclude that the program is wasteful, or even that it is unaffordable. United Launch Alliance has also achieved outstanding reliability and operability for their families of LVs, "-ilities" of particular importance to their primary customer, the Department of Defense. The company seeks to assign a monetary value to these "-ilities" on its Rocket Builder website (www.rocketbuilder.com), where reliability, schedule certainty, and orbit optimization are estimated together to provide an additional $\$65$M in value over their competition.

The affordability tradeoff resulting from the interplay of the "-ilities" with cost was explored quantitatively by Krevor. [22] In his thesis, Krevor showed the ability to trade cost for reliability, while holding vehicle performance fixed. This was accomplished by modifying LV propulsion system designs, optimizing the number of engines, stage thrust-to-weight ratios, and enabling engine-out capabilities. The results showed a 670% increase in Mean Flights Between Failure (MFBF) and a $\$32$B cost increase from the minimum cost configuration to the maximum reliability configuration. Clearly, the "-ilities" have a significant tradeoff with cost.

1.2 Decision Making in Design

The life-cycle for any engineered system stretches from paper concept studies through design maturation, production, operation, and retirement. It is common practice to discretize this timeline into different "phases" associated with the activities, objectives, and requirements of the particular life-cycle models being followed. The exact definitions of these phases and the milestones that mark the transition between them differ between various entities and domains; Forsberg et al. review life-cycle models from NASA, the Department of Defense (DoD), the International Organization for Standardization (ISO), and a typical high-tech commercial business on the way to developing their own generalized life-cycle template. [23]

Figure 1.4 provides representative examples from both NASA and the European Space

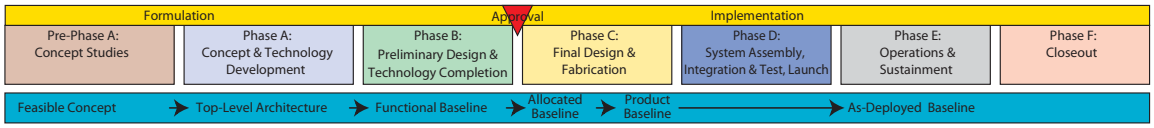

(a)

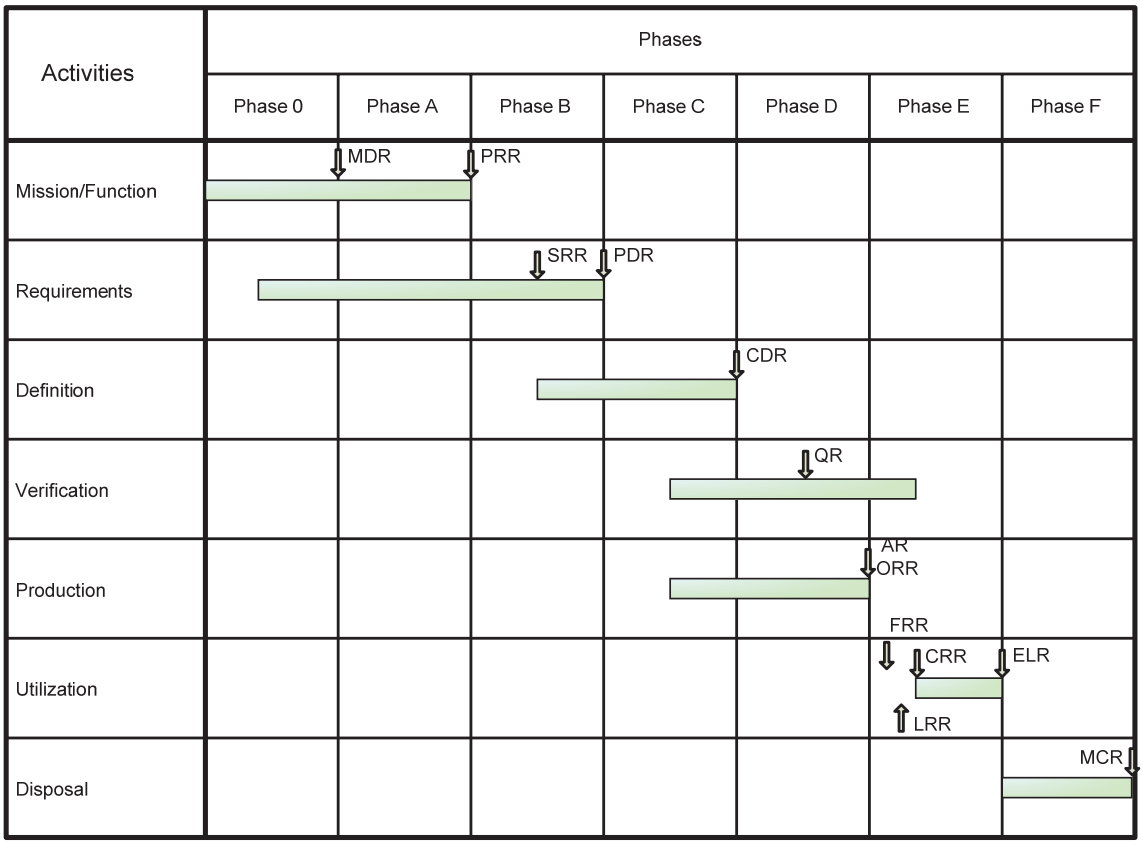

(b)

Figure 1.4: Life-cycle phases from (a) NASA [24] and (b) ESA [25]

Agency (ESA). At the beginning, the goal is "to produce a broad spectrum of ideas and alternatives." This goal shifts subsequently to establishing an initial baseline, developing the baseline's system structure, and finalizing the design details at each level of the structure. [24] This apparent down-selection process is performed by designers as a decision making exercise. It is structured into a sequence of key decision points and design reviews that serve as "tollgates" for the design, as it moves from broad to focused in scope.

It is clear that the design life-cycle of complex aerospace systems entails a sequence of "key decision points," but it can be stated more generally that the very essence of design consists of decision making, often in the presence of multiple attributes and objectives. [26] An excellent working definition for decision making is provided by Ignacy Kaliszewski:

> *"given a set of alternatives, choose a feasible alternative, which according to decision making circumstances is the most preferred"* [27]

Dieter's *Four C's of Design* describe the key elements at play in design as: [28]

Creativity: Requires creation of something that has not existed before or not existed in the designer's mind before

Complexity: Requires decisions on many variables and parameters

Choice: Requires making choices between possible solutions at all levels, from basic concepts to smallest detail of shape

Compromise: Requires balancing multiple and sometimes conflicting requirements

Real-world design decisions always exhibit these qualities, involving multiple alternatives that must be evaluated and down-selected on the basis of multiple criteria. If there are not multiples of either alternatives or criteria, there is no decision to be made; in the first case, with only one option, there is no choice; in the latter, with only one criteria, there is no trade. [29] Many different decision making algorithms or routines have been formulated to aid in addressing the non-trivial case. Because of the multiple criteria at play,

the decision-making methods and techniques used fall within the scope of Multi-Criteria Decision Analysis (MCDA).

1.2.1 Impact of Early Decisions

From literature, it is clear that the biggest opportunity for affecting cost savings resides in improving decision-making early on in the design process. In its *Systems Engineering Handbook*, the International Council on Systems Engineering (INCOSE) provides a critical insight into the life-cycle costs for engineered systems, observed in Figure 1.3, that the majority of life-cycle costs are committed early in the design process. [19] The NASA Systems Engineering Handbook seconds this, acknowledging early conceptual design decisions as significant drivers of the life-cycle costs for aerospace systems, estimating that 50 to 70 percent of the total life-cycle cost is locked in by the time an architecture has been selected.[24] It goes on to say that "by the time a preliminary system design is selected, this figure may be as high as 90 percent." Launch vehicles are no exception to this rule, as "at least 80 percent of the life-cycle costs are determined by decisions made during the conceptual design stage." [30]

Figure 1.3 provides the motivation behind focusing on decisions made in the earliest phase of design, depicting the majority of life-cycle cost being committed by these early decisions. A second observation that can be drawn from Figure 1.3 is that a very small amount of any program's budget is spent during these initial design stages, a fact that stands in contrast with the clear significance of the decisions made in early design. INCOSE's graphic shows approximately eight percent of costs being incurred in conceptual design. In another source, Havskjold presents a review of historical development programs at Rocketdyne, noting in Figure 1.5 that approximately two percent of the development program budgets were allocated to initial design. [31] Similarly, Blair states that for LVs "about 6 percent of the technical effort is allotted to the conceptual design stage." [30]

These observations concerning the leverage early design decisions have on cost and

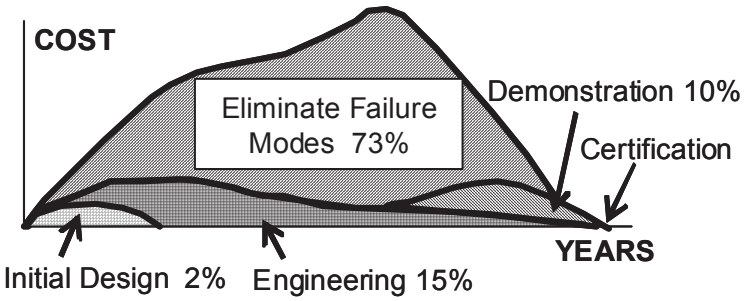

Figure 1.5: Cost profile for historical Rocketdyne development programs [31]

the fraction of program budgets allocated to early design phases are not difficult to understand if considered separately. The earlier a design decision is made, the more sweeping consequences to the scope, ground rules, and assumptions that will shape the rest of the program; for example, NASA's Exploration Systems Architecture Study of 2005 started their LV design trades by choosing non-assisted launch, vertical take-off, no propellant tanking during ascent, pure rocket-based propulsion, and ruling out fully reusable options. [32] Choosing differently on any of these items would have resulted in radically different design considerations. At the same time, though, making such decisions does not require a massive workforce, and is often performed by a very small group of experts. In contrast, later phase activities such as detailed design, manufacturing, and assembly all require much larger workforces to perform the detailed tasks and handle the vast amounts of information that must be managed. Thus, by payroll alone, it would be expected for later phases of design to cost more than early phases. This gap only widens when the required infrastructure and material costs are taken into account.

When considered together, though, there is clearly a mismatch between the leverage early design decisions have on cost and the actual program budget allocations. Ensuring adequate funding in early phases when key decisions are being made would seem to be a logical approach to controlling program affordability, if indeed these early decisions are so critical. Figure 1.6 presents evidence in support of this idea. Werner Gruhl, a cornerstone of NASA cost engineering during the '70s and '80s, observed a significant negative

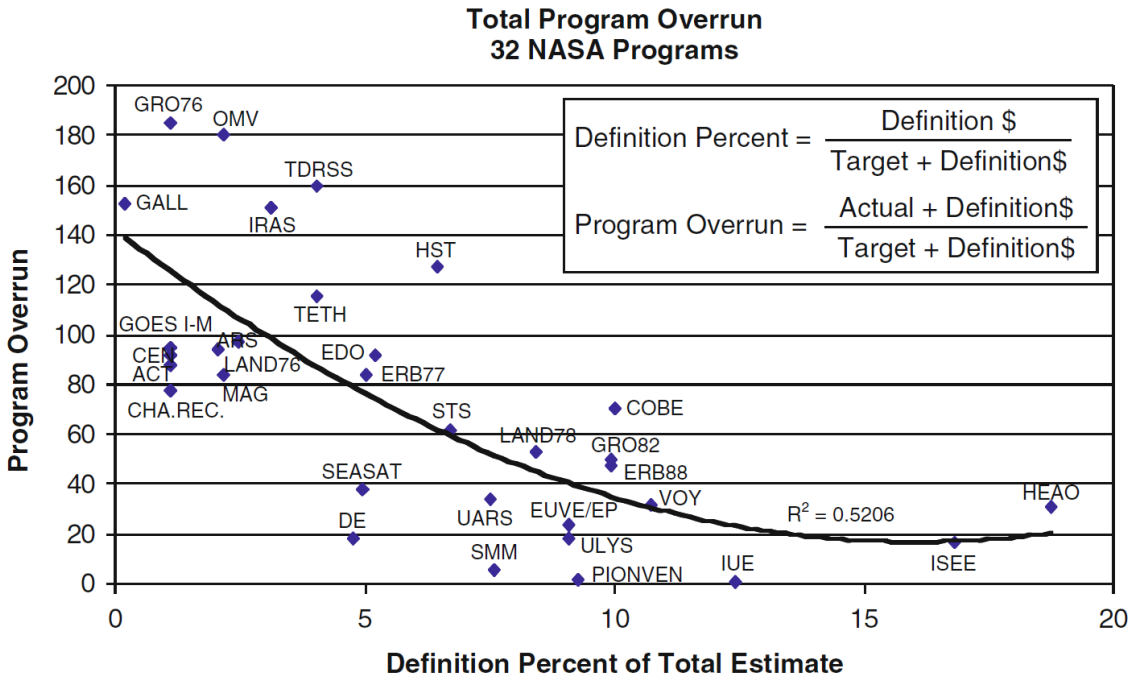

Figure 1.6: System definition versus budget overrun. [33]

correlation between the level of investment in "system definition" and the percent budget overrun that a program experienced. [33, 34] In this data, "Definition $" represents the program expenditures during Phases A and B, "Target" represents the anticipated/planned costs for Phases C and D, and "Actual" the costs ultimately incurred in these later phases.

Havskjold's review of Rocketdyne development programs also provides insight into one of the primary drivers of the trend Gruhl observed. Figure 1.5 reveals that while two percent of development costs were spent on initial design, fully 73 percent of the costs were incurred in redesign cycles to eliminate failure modes. It is not difficult to imagine that with some additional investment in the initial design effort, some of the defects could have been prevented; doubling the up-front investment, at a cost of two percentage points in program budget, could very well yield far more than two percentage points of cost savings. This effect has come to be known as the "quality lever," and is also supported by the "Cost to Extract Defects" depicted in Figure 1.3.[35]

The mechanism through which increased investment in early design efforts would de-

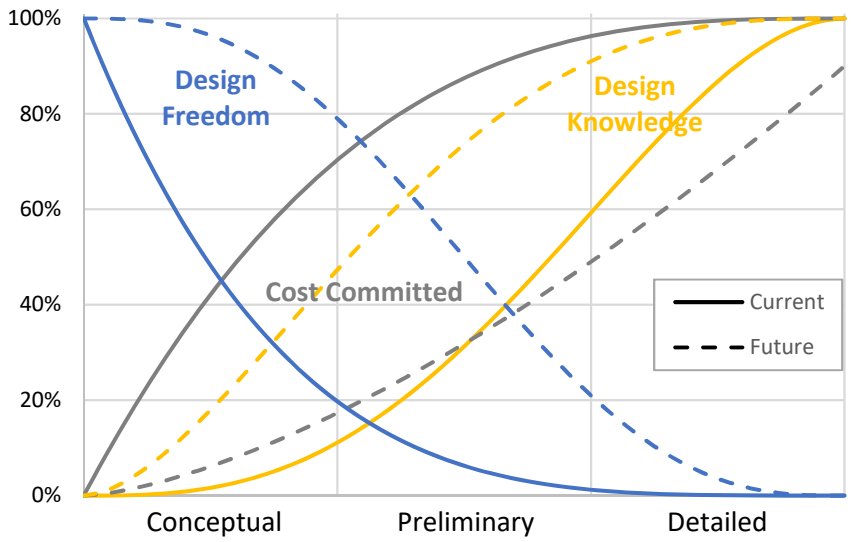

Figure 1.7: Current and future trends in design, adapted from [36, 37]

liver a payoff is through increasing decision makers' understanding concerning the pertinent design trades, sensitivities, and risks. Generating this knowledge early allows for adjustment of decisions and strategies when there is still significant flexibility in the design. The resulting cost savings would come by both the avoidance of potential design flaws, as well as by the fixing of design flaws when it is still relatively inexpensive to do so. These ideas are not new, having been first encapsulated and put forward in the white paper published by the American Institute of Aeronautics and Astronautics' (AIAA) Multidisciplinary Optimization (MDO) Technical Committee (TC) in 1991. [36] Figure 1.7 summarizes them graphically, capturing many of the same elements as Figure 1.3.

The goals implied by Figure 1.7 are that: Cost committment should be delayed until later in design, if possible; design freedom should be retained for as long as possible; and more knowledge should be generated earlier. Cost committed is a concept already introduced through Figure 1.3. Design freedom represents the degrees of freedom still available for decision-makers to exercise at any given point in time. As decisions are made, by definition this quantity is decreased. Design knowledge is a bit more abstract to define, but is critical to understand, as it forms the basis on which decision-makers act. This

concept will be explored in the following section.

1.2.2 Design Knowledge

While pedestrian use of the word "knowledge" is uncomplicated, in the realm of philosophy there are few ideas more debated and studied. The study of knowledge is called epistemology, which is more properly defined as "the philosophical study of the nature and scope of knowledge." [38] In traditional epistemology, there are three primary elements that play into the nature and existence of knowledge: Justification, Belief, and Truth. [39] To aid in discussing the interplay between these, some working definitions are as follows:

Truth The property of being in accord with fact or reality [40]

Belief A state or habit of mind in which trust or confidence is placed in some person or thing [41]

Justification "Sufficient reason" [42] Philosophically, two revealing perspectives on the necessary conditions for justification are: [39]

- Deontological: S is justified in believing that p if and only if S believes that p while it is not the case that S is obliged to refrain from believing that p
- Non-Deontological: S is justified in believing that p if and only if S believes that p on a basis that properly probabilifies S's belief that p

Each of these elements of epistemology are a field in and of themselves; the various forms of Truth, Belief, and Justification, and the intricacies of their interactions, have been debated and discoursed since the days of Plato and Aristotle. While it is not the intent here to delve into the interstitials of epistemology, it is helpful to establish a high level interpretation of these concepts in order to facilitate the understanding of knowledge, and eventually uncertainty, in design.

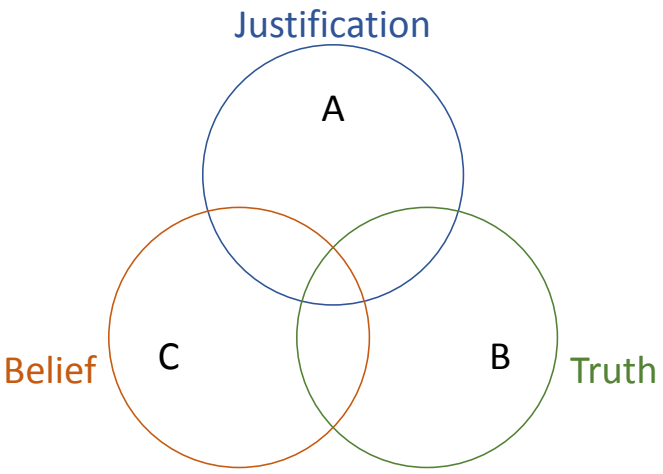

Figure 1.8: The Venn Diagram of Epistemology

Table 1.1: Description of areas enclosed in Venn diagram from Figure 1.8

Diagram Area	**Description**
A	The set of all things that have been justified.
B	The set of all things which correctly constitute reality.
C	The set of all things in which trust and confidence are placed.
$A \cap (B - C)$	Just because something has been justified does not mean it has yet been believed.
$A \cap (C - B)$	Trust placed in a source of justification that is lying.
$B \cap (C - A)$	A lucky guess. For example, a wrong decision may still turn out to be a good one. [43]
$A \cap B \cap C$	Often referred to as the only true "knowledge."

Figure 1.8 presents Truth, Belief, and Justification in a Venn diagram that allows for the various potential states of "knowing" to be identified. A brief description of each enclosed area is included in Table 1.1. While the philosophical framework of epistemology is general, and thus broadly applicable, an engineering design oriented interpretation is necessary to get at the question regarding the nature of design knowledge and its measurement. Section 1.2.2 establishes this interpretation, and Section 1.2.3 carries the interpretation into the specific context of LV architecture selection.

Establishing a philosophical interpretation of the knowledge economy at play during

design is helpful for providing a solid foundation on which to build design methodologies.

Belief In Design

Acknowledging design as a decision making process, as was done in Section 1.2, places the designer's beliefs at the center of design. While epistemology shows that knowledge is difficult to secure, beliefs are always numerous and easy to come by. Therefore, it is important in design to execute a process that documents and builds beliefs in a structured and traceable manner.

Truth In Design

According to the definition for truth provided previously, truth consists of fact and reality. Philosophers employ a large array of mental calisthenics to demonstrate that on very few, if any, occasions can truth ever be known. However, the truth sought by designers relates to the properties, behaviors, and performance the system under development will actually realize when it enters operation. This "truth" is guaranteed to become known, so long as the system makes it through the various design phases and reaches operation.

Justification In Design

Justification provides the "sufficient reason" for design decisions to be based off of. Sources of justification can be as abstract as a designer's intuition, or as concrete as the results from a physical test or demonstration. In either case, "models" lie at the root of a decision maker's beliefs (intuition is considered a form of mental model [44]). So, Modeling and Simulation (M&S) is the primary source of justification for designers in engineering. Modeling and simulation are both terms used frequently in many diverse contexts, and accordingly have many variations to their definitions. Dispensing with an exhaustive review of all possibilities, these two terms will be distinguished in this document by the following definitions:

Model: A simplified image of a partial reality [45]

Simulation: Experimentation performed with, on, or in a model [46]

Models are used in lieu of the referent, or primary, systems because they are more cost-effective, convenient, or safe. [47] Justification via M&S seeks to shed some light on the truth, without paying the full price of observing truth directly. If, as the description in *Truth in Design* proposes, truth for a designer resides in the actual realized system, it is clear that its acquisition for the sake of decision making in early design may be prohibitively costly. There is a tradeoff to be made in M&S, though, as how "simplified" the image and how "partial" the reality impacts the strength of the justification that can be provided by the model. This introduces the need for the concept of fidelity, which can be thought of as the degree of "correspondence with reality," or according to the previous section, correspondence with truth. [48] The idea that some models provide greater justification than others is directly related to uncertainty, which is discussed in Section 1.2.3.

Tying Them Together

Decision makers invariably take action according to their beliefs; to do otherwise is either dishonest or an abdication of responsibility. These beliefs, whether long held or recently acquired, are generally based on some form of justification; without justification, a belief is merely a guess. The hope is that whatever has been justified is in agreement with "truth," so that the decision maker is not misled by the source of justification. However, because models are used in the justification process, there is always the potential for something to be justified that is not true. Similarly, there may be occasions in which belief is not grounded firmly in justification; or rather, when a decision maker may perceive something to have been justified when in fact it hasn't.

A key factor in enabling better decision making in early design was identified over two decades ago in the frequently cited "White Paper on Current State of the Art" published by the American Institute of Aeronautics and Astronautics' (AIAA) Multidisciplinary Design

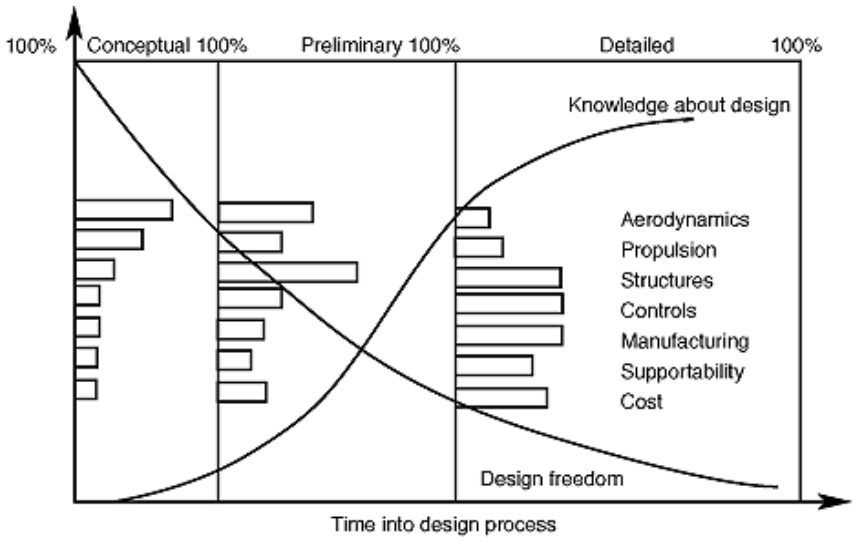

Figure 1.9: Notional depiction of disciplinary emphases in traditional design [36]

Optimization (MDO) Technical Committee. [36] The observation was made that while traditional design focused on performance-based synthesis in the conceptual phase, the need to better leverage design freedom available early on required the consideration of other disciplines typically not addressed directly until later phases. A notional depiction of this shift is provided in Figures 1.9 and 1.10. By generating more design knowledge through more comprehensive analyses early on, decision makers could be more informed as to the ramifications of the choices they make. This entails a more holistic treatment of the disciplines, along with more careful attention being paid to the broader context of the "-ilities."

A significant body of research has been motivated by these observations, aiming to provide conceptual level representations not only of the traditional engineering disciplines involved in design, but also of other domains of analysis responsible for quantifying a concept's "-ilities." Reliability has been introduced into conceptual LV design by methods acknowledging its cost [22] and maturation path [49]; techniques focusing on manufacturing considerations, especially on capturing the impacts of new materials and technologies, have been developed [50, 51]. Some methodologies have even been demonstrated which

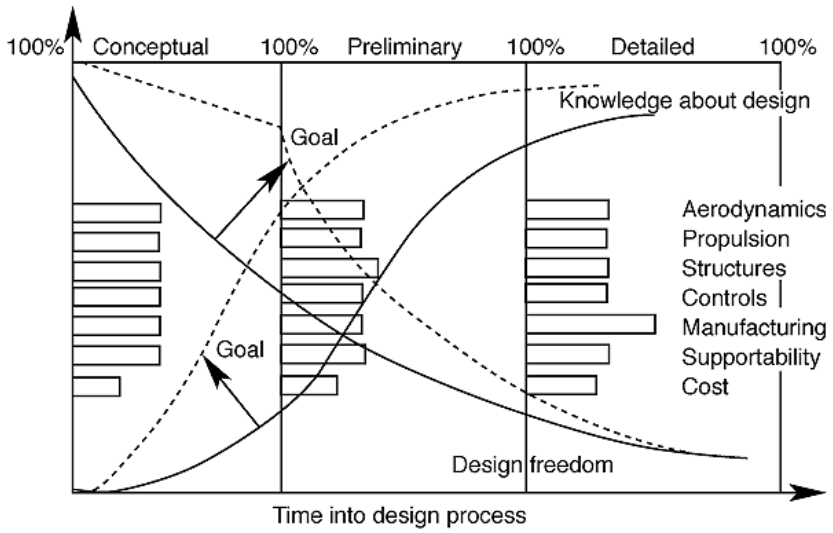

Figure 1.10: Shifted disciplinary emphases, aiming at improved design knowledge for earlier decision making [36]

model the LV development programs themselves, recognizing that cost and schedule actually emerge only at the intersection between program management/planning decisions, and vehicle design decisions. [52]

A common theme through all of these developments is a recognition of the need to implement probabilistic approaches in order to account for the uncertainties present in such early phases of design. In fact, given the preceding discussion on the nature of design knowledge, uncertainty could notionally be plotted on Figures 1.7, 1.9, and 1.10 as the inverse of the Design Knowledge curves. In this way, replacing deterministic analyses with probabilistic ones, regardless of the discipline area in question, can be viewed as a significant step towards providing increased design knowledge to early decision makers.

Probabilistic analysis is commonly practiced for traditional LV development programs in the area of margin allocation: First for design margins, which get consumed over the course of a development program; then for performance and safety margins, which are built in to account for aleatory uncertainties and those epistemic uncertainties that were not completely driven out by the time of first flight. [44] However, these activities typically take place late in the conceptual phase and into preliminary design, once a baseline

vehicle architecture has been selected. The new design methodologies aimed at promoting more informed early decision making advocate for moving these more comprehensive assessments earlier into conceptual design; however, as will be seen in a subsequent section, probabilistic analyses are very far from practiced in LV architecture selection.

1.2.3 Uncertainty and Risk

To say something is uncertain is to say that it is "not definitely known." [53] By this definition, every aspect of life involves some amount of uncertainty, especially in engineering and design. Another definition for uncertainty in the context of decision making is "the discrepancy between the actual state of the world at any time and the information available to the decision maker." [54] Applying the designer's interpretations of truth and justification developed in the previous section, this definition could be restated as "the discrepancy between the truth and what has been justified." This definition fails to provide a complete picture of uncertainty, though, as it would seem to imply that uncertainty could be reduced to the point of eradication by simply providing more information to the decision maker.

There is, however, information that cannot be known, and thus, uncertainties that cannot be reduced. For example, a designer cannot know the ambient temperature or the atmospheric winds that will be encountered on the day of launch ten years into the future; these do, however, have a meaningful impact on performance for LVs employing solid rocket propulsion. [55] This leads to the identification of two top level categories of uncertainty:

Aleatory "The uncertainty or randomness inherent to a process" [56]

Epistemic "The uncertainty resulting from lack of information about that process, that is, the relationship between human knowledge and the process" [56]

The decision maker must clearly take into account both types of uncertainty, but the means of dealing with each differs. Aleatory uncertainties, which cannot be "burned down" by design actions or test programs, remain with the vehicle through all of design and into op-

eration. They are accounted for by establishing a "cushion" between the resources allocated and those calculated deterministically; this "cushion" is variously referred to as "reserve," "margin," or "contingency," depending on the context or perspective taken. [57] An excellent example of this for LVs is the practice of allocating Flight Performance Reserve (FPR) to account for day-of-launch uncertainties such as atmospheric winds. [58]

Epistemic sources of uncertainty, as stemming from some lack of knowledge, are addressed through practices such as trade studies, testing, and demonstration programs. These all are intended to provide uncertainty mitigating knowledge to decision makers; in a way, the entirety of the Design, Development, Testing and Evaluation (DDT&E) phase of a program, corresponding to NASA project life cycle Phases A through D, is aimed at uncertainty reduction in support of the program's key decision points and reviews. Because of this, and because epistemic uncertainties intersect more directly with the human nature of the designer, many researchers have decomposed the epistemic branch to reveal a more granular view of uncertainty sources.

Uncertainty Taxonomy

In his 2013 dissertation, Robertson developed a taxonomy specifically tailored to the uncertainties associated with LVs; this is reproduced in Figure 1.11. [44] At the top level, Robertson differentiates between epistemic and aleatory uncertainty. Within the epistemic, he further delineates between those uncertainties directly under the control of the program, and those coming from outside sources. Table 1.2 provides brief definitions for each of Robertson's epistemic uncertainties.

While most of these may be present at any given point in the design, typically only specific ones are targeted by any given mitigation action. The fact that some sources of uncertainty are scrutinized very carefully while others are ignored altogether is due to the differing severity of the consequences associated with each source of uncertainty. If doubling or halving a particular parameter in a design makes very little difference to anything

Table 1.2: Epistemic uncertainty definitions from Robertson's dissertation [44]

Uncertainty Type	**Description**
Phenomenological	Due to an acute lack of knowledge of phenomena, physical or otherwise; this lack of knowledge is characterized by the inability to recognize potential risks or opportunities.
Human Error	Blunders occurring in the design, manufacture, test, or operation of a system.
Model	Refers to the fidelity level of engineering analyses and models, as well as the fidelity level of the engineers' and designers' mental model of the system under development.
Technological	Stemming from the incorporation of new technologies in a system.
Volitional	Due to future decisions of actors within the design process of the system.
Requirements: Scope	Due to potentially evolving functional requirements.
Requirements: Constraints	Due to potentially evolving non-functional requirements
Requirements: Linguistic	Due to the natural language used to specify requirements.
Political	Due to program funding instability.
Integration	Due to asynchronicity between subsystem/component development efforts.

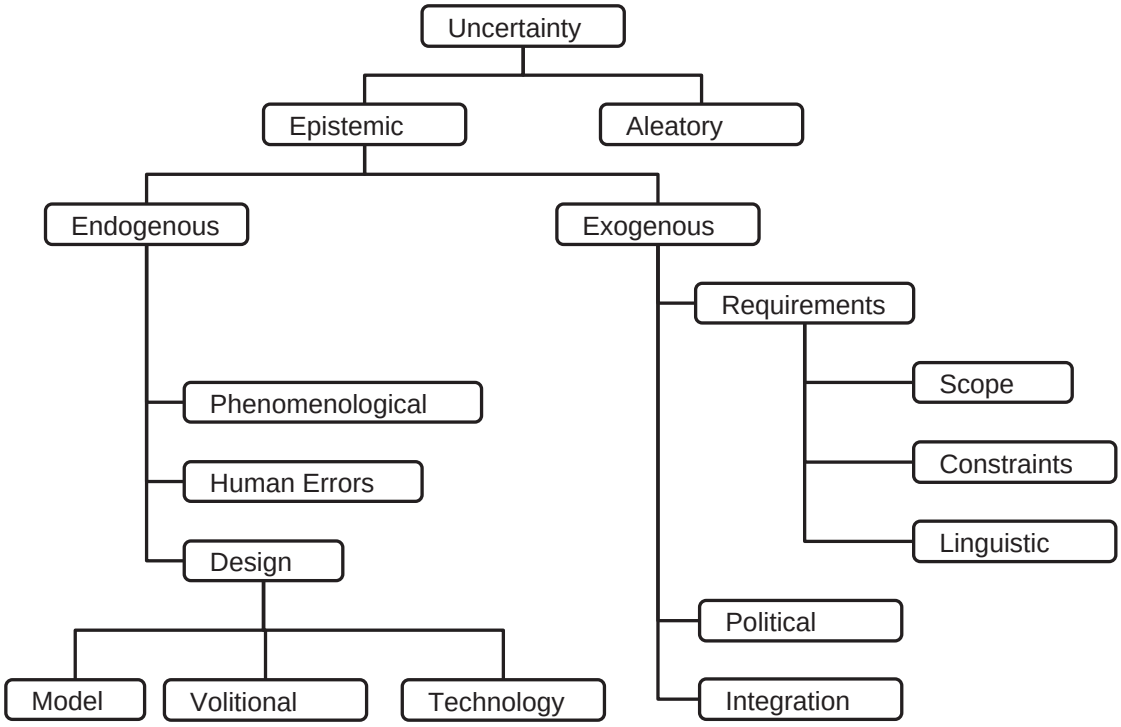

Figure 1.11: Taxonomy of LV development program uncertainties [44]

of importance, a large amount of uncertainty in its value is easily tolerated; on the other hand, if the parameter in question exhibits a strong influence on the program Figures of Merit, a great deal of attention and effort is put towards reducing its uncertainty. The issue at work here amounts to an assessment of risk.

Risk Analysis

The *NASA Risk Management Handbook* characterizes risk as an interplay between three key factors, namely: Scenarios, likelihoods, and consequences. [59] The scenario captures the fundamental uncertainty, describing where the subject uncertainty resides and the extent of potential deviation from the expected behavior. Likelihood measures the probability of a particular scenario occurring, and consequence communicates the impact a scenario would have if it did play out. Although it does not present the scenario aspect explicitly, a Risk Matrix such as is shown in Figure 1.12 is commonly used to understand this interplay.

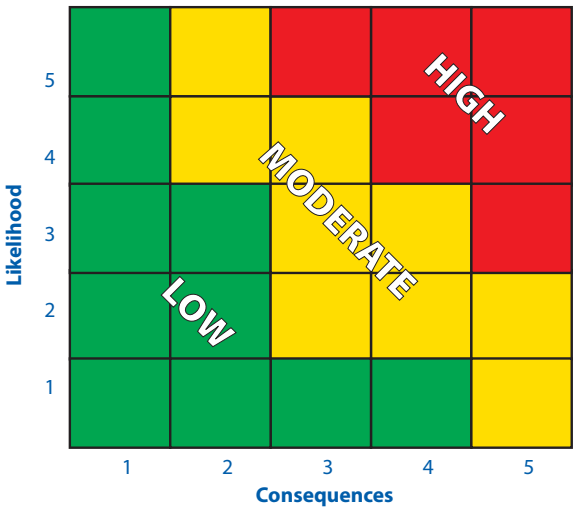

Figure 1.12: Generic risk matrix [24]

Here, things of little consequence are considered to be low risk regardless of how likely they are to occur; conversely, things of very low likelihood are still considered moderate risks if their consequences are perceived as severe.

Rychlik points out that "the term risk is often used informally to mean the probability of a hazard occurring." [60] This informal use is acceptable, so long as the consequence of the subject risk is understood in context. For example, two of the most common risk assessments performed in LV reliability are the probabilities of *Loss of Mission* (LOM) and *Loss of Crew* (LOC). [59] While the quantitative likelihood values are generally referred to as the risk (e.g. "there is a 5% risk of LOM"), the consequences implied by LOM and LOC are well understood. Likelihoods in risk analysis are quantified by propagating all relevant sources of uncertainty to produce probability distributions on the metrics of interest. The likelihood value is then computed as the total probability of the metric being at least as extreme as some target threshold. For example, the probability of a negative value being drawn from the distribution in Figure 1.13 is the total area under the distribution that lies to the left of 0.

Risk mitigation strategies generally take one of two forms, margin allocation and uncertainty reduction. As discussed previously, margin establishes a cushion between the de-

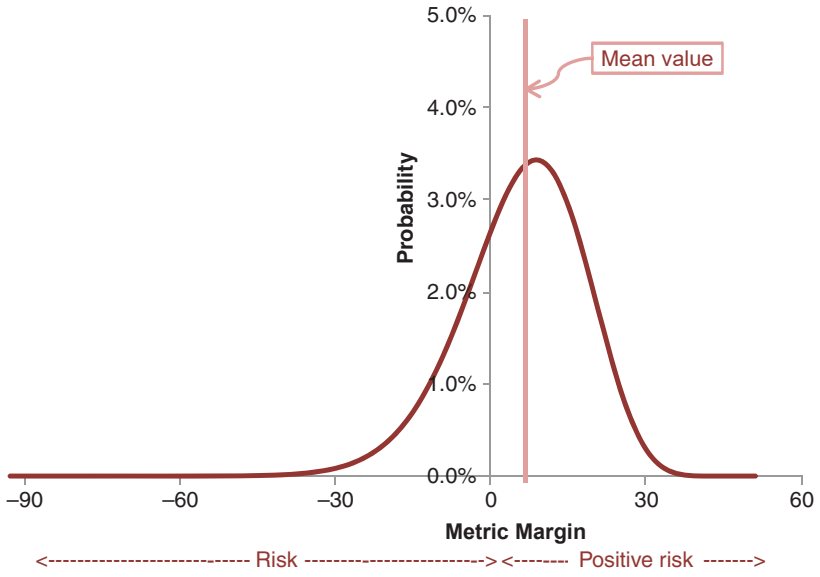

Figure 1.13: Generic probability distribution. Negative metric margin indicates event occurrence. Adapted from [61]

signed system and any critical threshold values, in effect shifting the distribution in Figure 1.13 to the right. Uncertainty reduction efforts reduce risk by shrinking the distribution's spread, pulling the tails inwards, in effect reducing the area under the curve that falls to the left of zero. Remembering that the definition of uncertainty relates to a lack of knowledge, uncertainty reduction studies aim to generate increased knowledge that will result in lower probability of undesirable or unexpected outcomes.

1.3 Launch Vehicle Architecture Selection

The characteristics and principles of design described in the preceding sections are true for engineered systems in general. To understand how these intersect with LV design, and where the challenges lie in LV architecture selection, it is necessary to introduce some of the fundamentals of LV design.

1.3.1 Architecture Decomposition

Up to this point, the term "architecture" has been used without a formal definition. However, architecture is a word that assumes various meanings and scopes depending on the context and community in which it is spoken, and so it is important to establish a precise definition for use here. Comprehensive reviews of the different definitions of the word have been performed in both [62] and [63], and it is not the aim here to reproduce those efforts. Of the definitions reviewed, the one that most naturally encompasses and describes the context for LVs is from *The Art of System Architecting* [62]:

> "The structure (in terms of components, connections, and constraints) of a product, process, or element"

The decisions at stake during architecting activites revolve particularly around the components to be used in the LV design. The following sections provide descriptions and examples of the types of design features that are commonly involved during architecture selection.

Physical Elements

Figure 1.14 shows an exploded view of a LV from the Delta II family of vehicles. The 7920-10 consists of a generic payload element, a ten foot diameter payload shroud, an $N_2O_4/Aerozine-50$ fueled upper se, a $LO_2/RP-1$ fueled core stage, and nine strap-on solid rocket motors. The physical elements of the LV depicted, and indeed of any LV, can be generalized as being made up of three classes: Payload, Jetsam, and Stages.

Within the context of a pre-conceptual LV architecture definition, the Payload element is the simplest to describe, as it consists merely of a mass (and possibly physical dimensions, if volumetric sizing is being taken into account). In reality, a LV can lift multiple "payloads" – that is, the Payload element can be a compound one, made up of multiple

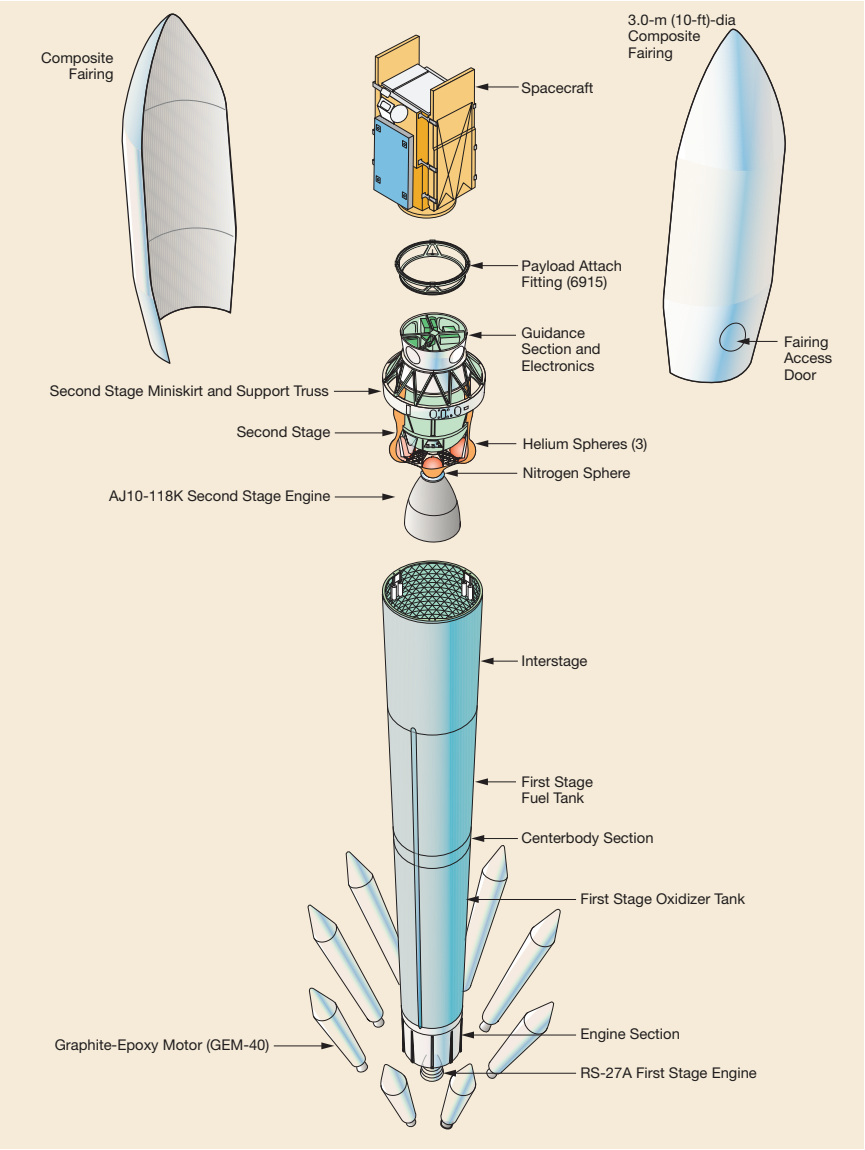

Figure 1.14: Elements of a Delta II 7920-10 launch vehicle [64]

spacecraft. However, from an ETO performance perspective, the Payload can be considered as a simple lump mass.

Jetsam is not a term typically used with LVs; however, its verb form, jettison, is commonly used to refer to events when LV components separate and are cast off of the main vehicle. Jetsam is an old word originating from the naval domain. Its definition, according to Webster, is "the part of a ship, its equipment, or its cargo that is cast overboard to lighten the load in time of distress and that sinks or is washed ashore." [65] While some parts of this definition are not particularly applicable in the LV context, the first part of the definition is helpful in generalizing a class of LV physical elements. Here Jetsam will be defined as "launch vehicle equipment or cargo that is cast overboard to lighten the load." With this new definition, the Jetsam class can be used to describe LV physical elements such as payload shrouds (like the one depicted in Figure 1.14), other aerodynamic fairings (such as the Orion Service Module Fairing [66]), or any other equipment that is jettisoned during ascent (such as Orion's Launch Abort System [66]).

Propulsion Stages make up the remainder of the architecture, and account for the vast majority of LV gross mass. They are the most complex of the three elements identified, being composed of a variety of subelements that come into play even during architecting activities. Stages can be arranged in a number of different configurations; strap-on boosters are considered a type of stage within this taxonomy, so LV stage configurations can be not only 2- or 3-stages, but also 1.5- or 2.5-stages (where the half indicates the presence of strap-ons). LV stages are discarded once their propellant is consumed. This is not to say that they are necessarily expendable, but from the perspective of the vehicle flying to orbit, stage separation looks much the same whether or not there is an intent to recover it.

Operational Elements

The physical elements alone do not provide enough definition to fully analyze a LV's trajectory performance; a functional mapping of the physical elements to a LV mission profile

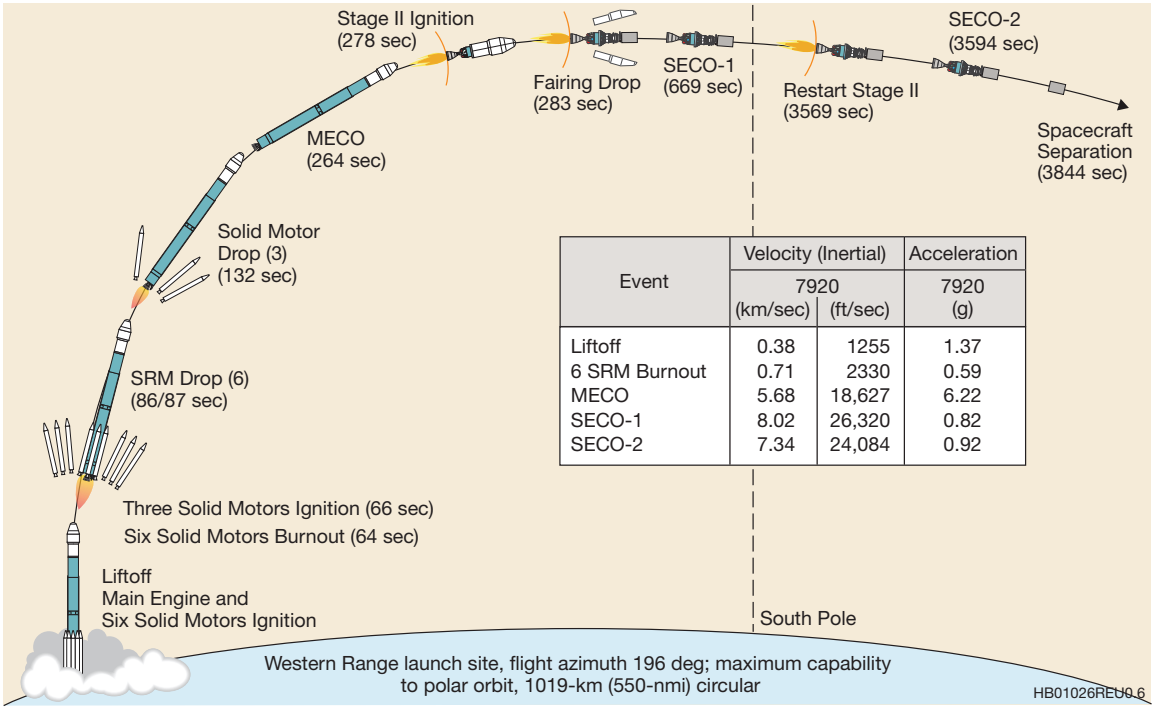

Event	Velocity (Inertial)		Acceleration
	7920		7920
	(km/sec)	(ft/sec)	(g)
Liftoff	0.38	1255	1.37
6 SRM Burnout	0.71	2330	0.59
MECO	5.68	18,627	6.22
SECO-1	8.02	26,320	0.82
SECO-2	7.34	24,084	0.92

Figure 1.15: Example CONOPs of a Delta II 7920 ascent to polar orbit from Vandenberg [64]

or concept of operations (CONOPs), is also needed. Figure 1.15 provides an example CONOPs for a Delta II 7920 ascent to Polar orbit. From this figure it is revealed that three of the nine strap-on solids are not thrusting at the time of liftoff; instead, they ignite after burnout of the first six boosters, producing a staged thrust assist to the core stage that lasts twice as long as would have been guessed if assuming a more typical CONOPs where all boosters fire in unison.

Other operational elements that impact LV ascent performance involve various event sequencing and timings. Some of these are dictated by physical properties of the LV, such as burnout occurring when all propellant has been consumed; others are triggered by trajectory constraints, such as jettison of a payload shroud once a threshold free-molecular heating rate has been passed.

Virtual Stages

The effect of functionally mapping the LV physical elements to the mission CONOPs is to produce what will be referred to here as "virtual stages." The logic for defining virtual stages proceeds from the observation that staging events manifest themselves as discrete changes in the LV's state and/or attributes. The inert mass of the spent stage is jettisoned, producing a step change in LV mass; the next stage's propulsion system ignites, producing a change in thrust and exhaust velocity. However, strictly speaking, staging events are not the only times when these kinds of changes are observed. Jettison of any elements from the Jetsam class will also produce a step change in mass; changing the propulsion system operating point will similarly produce changes to the thrust and/or exhaust velocity. These events can be viewed as virtual staging events, a perspective that addresses much of the complexity associated with modeling real-world LVs such as the Delta II 7920-10.

The motivation for introducing the concept of virtual stages is twofold: First, interpreting the functional mapping of the physical elements to the mission CONOPs as virtual stages provides a basis for generically describing LVs such that significantly different architectures can be compared. For example, comparing one concept that jettisons a payload shroud to another that jettisons a tractor launch abort system can be done very easily once each vehicle's operational concept has been abstracted to a description via virtual stages. Second, any LV performance modeling methodology that seeks to leverage some form of the Rocket Equation must provide a serialization of the LV stages to be evaluated using (1.2), and computing virtual stages provides this, even for vehicles that employ parallel burn or other diverse CONOPs.

1.3.2 Launch Vehicle Synthesis & Sizing

A high-level description of the earth-to-orbit (ETO) mission is deceptively simple: To lift a payload from the surface of the earth to a specified final state, such that the payload is inserted into the desired orbit. However, a look at the energy implications of this statement

provides a first glimpse of the challenge in the ETO mission. The energy delta required to place an object in low earth orbit (LEO) is approximately 35 MJ/kg. For LVs that meet these requirements by extracting the energy stored in chemical fuel – that is, for all LVs in existence today – the vast amount of energy required to achieve orbit translates into the need to burn a similarly vast amount of fuel. Contributing to this large propellant loading is the fact that every unit of propellant burned imparts its energy not only to lifting the LV and payload, but also to lifting the unburned propellant still onboard; therefore, every unit of propellant expelled results in a loss of a fraction of the energy contribution of the previously burned fuel. The result of this is that LVs essentially consist of large, flying propellant tanks, with engines attached to the aft end and a payload strapped to the fore.

An analytic view of these trends presented in Figure 1.16 shows the extreme nature of LV scaling. The performance required for a nominal ETO mission to low earth orbit (LEO), quoted in the customary units of velocity, stands at $9,000\frac{m}{s}$. This requires that fully 89.5% of a single-stage LV's gross liftoff mass ($GLOM$) consist of propellant for an assumed v_e of $4,000\frac{m}{s}$ (representative of the Space Shuttle Main Engine, or RS-25), as depicted in Figure 1.16a. With a favorable propellant mass fraction (PMF) value of 0.9, Figure 1.16b indicates that for every one unit of payload mass inserted into LEO, the LV $GLOM$ will exceed 160 units of mass!

For reference, the PMF as used here is defined as a function of the usable propellant mass m_p and the stage inert mass m_i:

$$PMF = \frac{m_p}{m_p + m_i} \tag{1.1}$$

The relationship governing these sizing relationships is the Ideal Rocket Equation, (1.2). The source and implications of the Rocket Equation will be discussed in Section 2.4.1.

$$\Delta V = v_e ln(\frac{m_0}{m_f}) \tag{1.2}$$

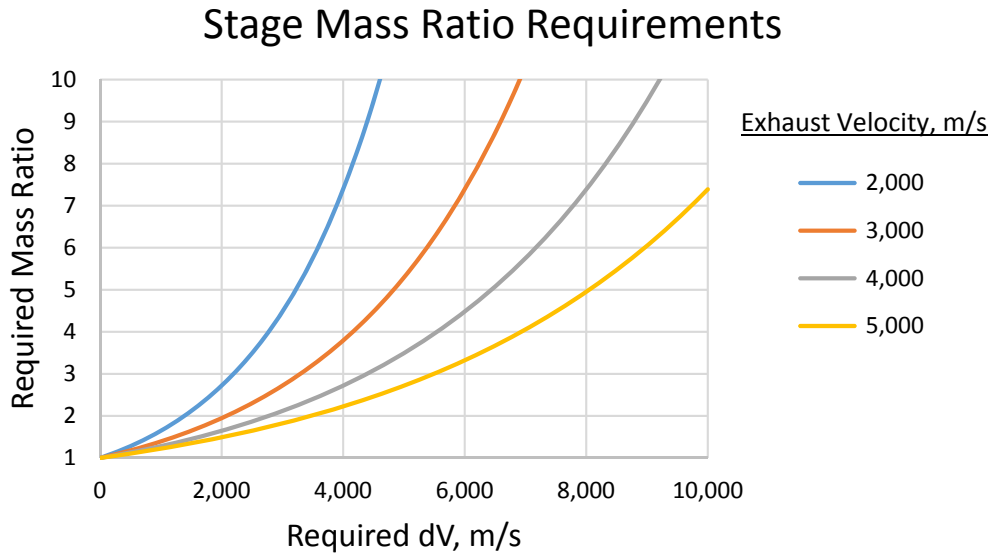

(a)

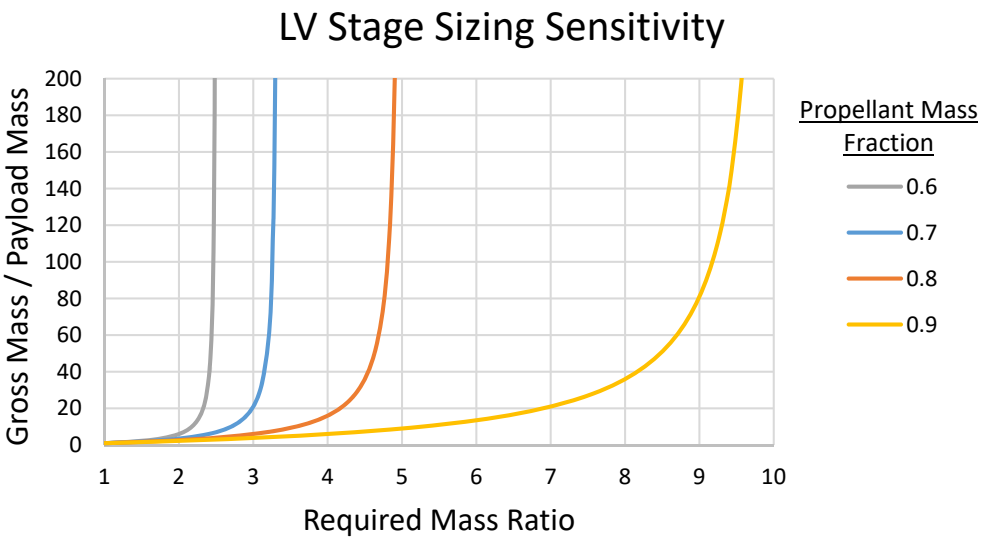

(b)

Figure 1.16: LV sizing trends, with (a) Mass Ratio requirements, and (b) stage sizing trends

Although this notional sizing exercise adequately establishes the extreme scaling behavior of LVs, the greater challenge in LV design lies not in the actual scaling, but in the sensitivity to changes in the design parameters. A feel for this sensitivity can be obtained by visual inspection of the slopes of the curves in Figure 1.16, but an explicit depiction in Figure 1.17 drives the point home. For an extremely small perturbation of any of the three design parameters ΔV, PMF, or v_e, a very significant impact is seen in the overall vehicle sizing. This sensitivity becomes a major challenge when one takes into account the inherent uncertainties present in the various phases of design. Any deviations from the expected propulsion system performance or structural efficiency can have dire implications to the LV's ability to perform its design mission. The same can be said of any changes in the mission required ΔV, due either to inaccurate initial estimates or to actual requirement changes. The main design strategy used to mitigate these sensitivities is to segment LVs into multiple stages, each responsible for providing a fraction of the total ΔV required by the mission. While effective, this approach does not mitigate these sensitivities entirely.

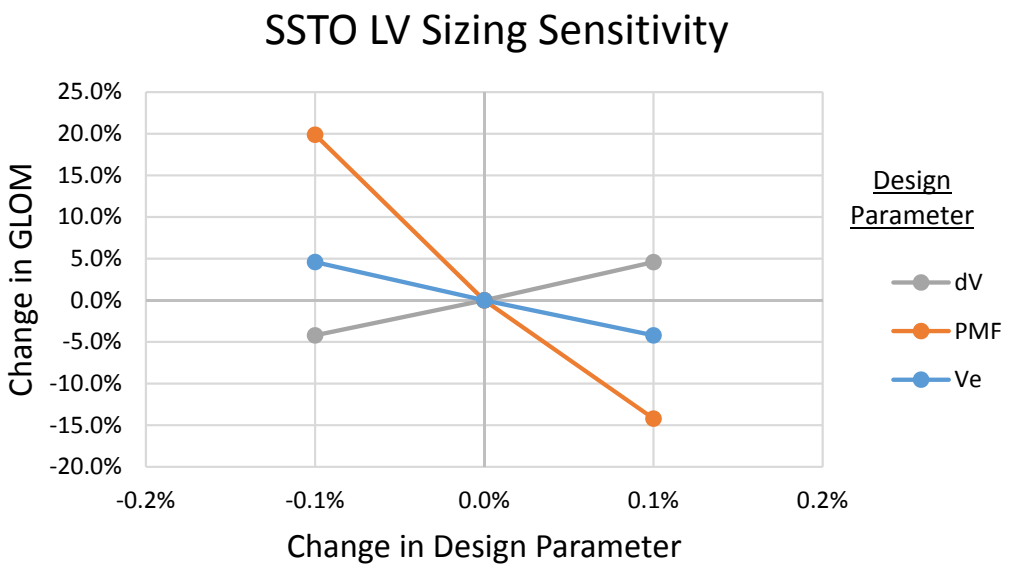

(a)

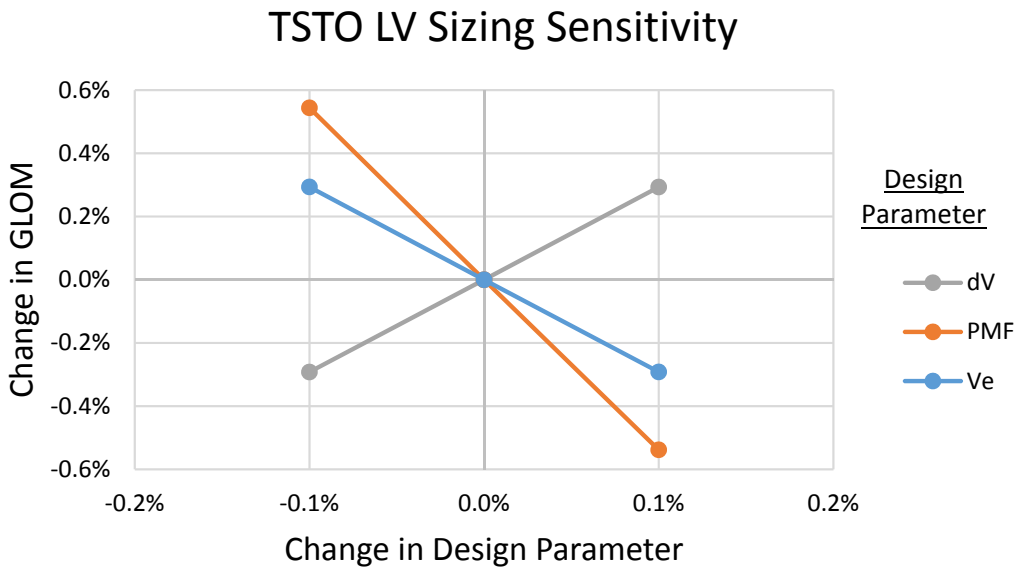

(b)

Figure 1.17: Sizing sensitivities of (a) single-stage and (b) two-stage LVs performing the subject notional mission

Evaluating a LV concept entails quantifying the FOM values the concept achieves subject to all relevant requirements and design constraints. This is the "transfer function" employed in the mapping between Design and Objective spaces discussed in the previous section. The specific analyses required to perform the LV evaluation are dictated by the FOMs of interest; however, analyses ranging from cost to safety and reliability all require

some inputs from either the vehicle's geometry, weight breakdown, or trajectory simulation. Because of this, sizing and synthesis is almost invariably required for the analysis of LV concepts, even in very early design studies.

Sizing and synthesis is an inherently multidisciplinary activity, bringing together analyses from all of the relevant disciplines to develop a fully "closed" quantitative description of a vehicle design. [30] This "closure" implies that a consistency, concurrency, and consensus has been established between each of the subsystems, disciplines, and requirements, subject to any active ground rules and assumptions. Launch vehicle sizing imposes a very tight coupling between disciplines, especially propulsion, mass estimation, and mission performance. Because of this, it is often approached as a multi-disciplinary optimization (MDO) problem, where rigorous convergence algorithms and optimization routines work to achieve "closure" while informed by some overall objective function. [67] Many different MDO techniques have been developed and demonstrated, with some of the most common being Multi-Discipline Feasible (MDF), Individual Discipline Feasible (IDF), and Collaborative Optimization (CO). [68]

The multidisciplinary coupling in LV analysis has its epicenter in the mission performance evaluation, which can be observed in the equations of motion that govern LV mission performance. The system of equations presented in (1.3) demonstrate this coupling. These are adapted from [69], and derived subject to the following assumptions: (1) Non-rotating earth, (2) Planar ascent trajectory, (3) Spherical Earth, (3) Inverse-square gravitational field,

and (4) Stationary atmosphere.

$$\begin{aligned}
\dot{V} &= \frac{T_i \cos\alpha - D_i}{m} - \frac{\mu}{r^2}\sin\gamma \\
\dot{\gamma} &= \frac{1}{V}\Big[\frac{T_i \sin\alpha + L_i}{m} - \big(\frac{\mu}{r^2} - \frac{V^2}{r}\big)\Big] \\
\dot{\phi} &= \frac{V\cos\gamma}{r} \\
\dot{r} &= V\sin\gamma \\
\dot{m} &= -\eta\frac{T_{vac_i}}{v_{e_{vac_i}}}
\end{aligned} \tag{1.3}$$

where

$$\begin{aligned}
T_i &= \eta T_{vac_i} - p_a A_e \\
D_i &= qS_i C_D(V,\alpha) \\
L_i &= qS_i C_L(V,\alpha) \\
\eta &= \eta(t)
\end{aligned} \tag{1.4}$$

While aerodynamics, propulsion, and structures/weights are all represented explicitly, stability and control, material thermal properties, and structural elasticity aspects are all frequently represented via constraints imposed on the trajectories flown. [70]

Because the ascent to orbit places such stringent requirements on LV sizing, accurately estimating the ascent performance of a particular LV concept is a critical task during all phases of design. As was shown earlier, the ideal rocket equation is not suitable for this task due to its inherent assumptions. For this reason, estimation of losses is done today almost exclusively via trajectory simulation. Because there are theoretically an infinite number of paths that a LV could take on its way to a particular target orbit, LV trajectory

simulation requires the solution of an optimal control problem - it would be undesirable to design a vehicle based on a suboptimal performance estimate. This trajectory optimization is acknowledged as one of the biggest challenges in performing LV architecture and early conceptual design trades; a few quotes from literature help communicate the general impression:

> "The specificity (and also the difficulty) of launch vehicle design is to include, within the global design, a trajectory optimization by using an optimal control law calculation subject to equality constraints" [68]

> "In general, the numerical solution of aerospace trajectory optimization problems is not trivial" [71]

> "a rather good initial approximation of the optimal trajectory is needed and a rather large amount of work has to be done by the user" [72]

In short, trajectory optimization is a very man-hour intensive discipline. [73]

Explicit trajectory simulation provides a host of information critical for designing various LV subsystems and components; for example, structural design load cases are taken from critical flight conditions, and thermal protection systems are sized based on trajectory heating environments. The majority of these additional details go to waste on early design feasibility assessments, however, as only basic performance estimates are needed. [70] It has even been suggested that using these higher fidelity analyses may be questionable when used in concert with other models that are of much lower fidelity. [74]

1.3.3 Sources of Uncertainty

Robertson's taxonomy of LV uncertainties was already presented in Section 1.2.3. Unless approached in a very targeted manner, addressing uncertainty during architecture selection would seem to be an untenable proposition. Every epistemic source of uncertainty exists in its most unreduced form at this stage: Few, if any, design decisions have yet been

made (Volitional uncertainty); due to a lack of detail in the design, the models available for analysis are naturally low-fidelity in nature (Model uncertainty); and many uncertainties will only emerge once more specific design features are resolved (Technological and Phenomenological uncertainties). Of course, uncertainties associated with the flaws of a human designer are always present.

As stated in Section 1.2.3, uncertainties perceived as contributing the greatest amount of risk are usually prioritized, especially as they pertain to the decisions at hand. Any uncertainties preventing a decision maker from resolving the differences between options under consideration must be dealt with, while uncertainties that do not impede the current decision making process can be deferred until later.

As presented in Section 1.3.1, a LV architecture defines at a high level the major constituent elements of the vehicle; selection of a unique architecture concept entails a decision regarding each major category of morphological variation laid out in the architecture trade space. However, for any unique architecture concept there is an underlying design space from which the a representative vehicle design must be formulated. What this means practically for the LV arhcitect is that the evaluation of any architecture concept through sizing and synthesis of a specific LV design point is in fact obscuring a vast amount of information regarding a decision space that has not yet been traversed. The interesting fact is that this "design freedom" that exists within the design space of any given architecture manifests itself as a significant source of volitional uncertainty during the architecture selection process. While no quantitative comparison of uncertainty impacts is to be found in the literature, intuition and an understanding of the hierarchy of uncertainty sources leads to the formulation of the following assertion: **Volitional uncertainty is the single most significant source of uncertainty at play during LV architecture selection decisions**

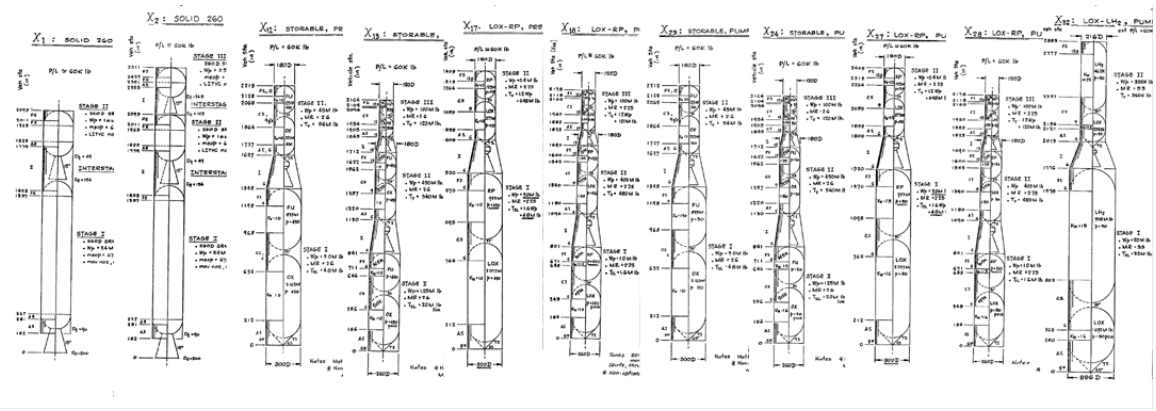

Figure 1.18: Example line-up of LV architectures evaluated in Integral Launch and Reentry Vehicle study [75]

1.3.4 Past Studies

Integral Launch and Reentry Vehicle Study

A review of historical LV architecture studies shows that very little has changed in how early architecting analysis of alternatives are performed. The Integral Launch and Reentry Vehicle study (ILRV), performed in 1969 as a precursor study for what would become the Space Shuttle program, sought to identify expendable LV configurations for launching reusable spacecraft that showed the most promise of low costs. [75] Based on subject matter expert judgment, 32 launch vehicle architectures were selected for their low-cost potential, and were evaluated through a detailed sizing and parametric costing analysis.

Advanced Transportation System Studies

In 1995, Lockheed Martin delivered its Advanced Transportation System Studies final report to NASA, detailing 29 different LV configurations. [76] These were sized and assessed in much the same way as the ILRV study. For the trade space considered, over 250,000 possible discrete architecture combinations were possible; however, the logic for downselecting to those analyzed was not presented.

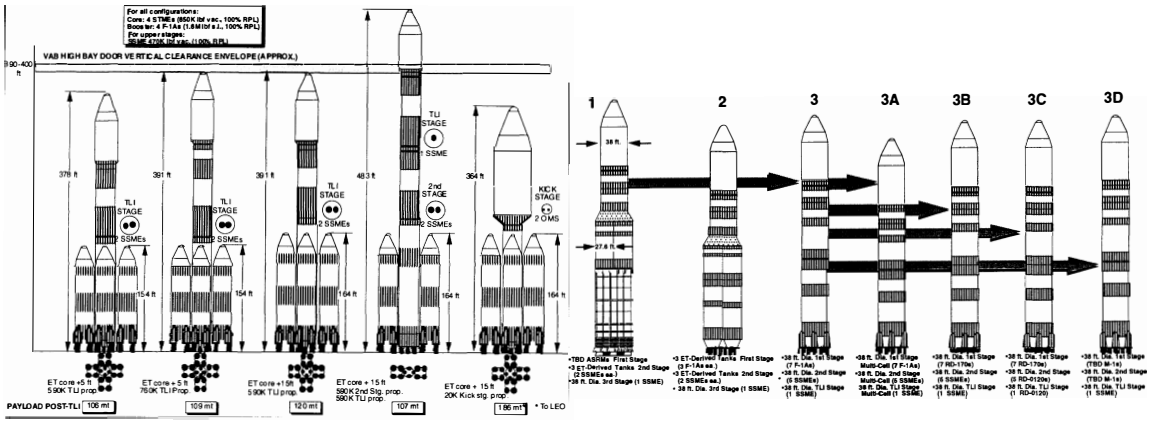

Figure 1.19: Example line-up of LV architectures evaluated in Advanced Transportation System Studies [76]

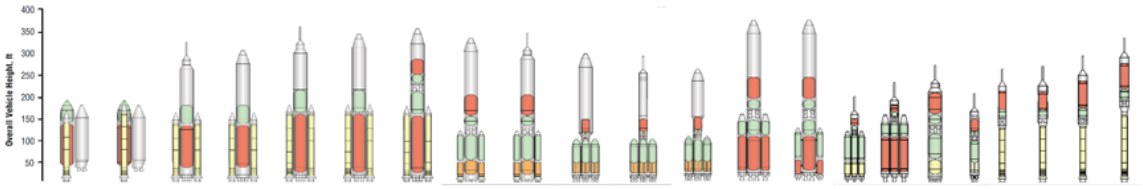

Figure 1.20: Example line-up of LV architectures evaluated in Exploration Systems Architecture Study [32]

Exploration Systems Architecture Study

In 2005, NASA performed the Exploration Systems Architecture Study from which the Constellation program emerged. [32] In this study, crew and cargo launch vehicles were considered separately; 28 LV architectures were evaluated for each type. Down-selection from the tree presented in Figure 2.2 was rationalized qualitatively but clearly; however, only engineering judgment was applied in selecting the specific variants studied, as the combinatorial space comprising all of the architectural elements remaining after the initial pruning still contained many thousands of possible architectures.

Heavy Lift & Propulsion Technologies Study

In a more recent architecture study, as part of NASA's Heavy Lift & Propulsion Technologies Broad Agency Announcement, Orbital Sciences Corporation initially analyzed

"several hundred concepts," and then selected 29 for further study. [77] It is unclear what level of analysis was performed in the initial screening, but the final set of 29 were defined and evaluated to a similar level of fidelity as all of the previous studies.

Aliakbargolkar

Aliakbargolkar et. al. evaluated 192 architecture alternatives, analyzing a comprehensive set of factors affecting feasibility and viability of the concepts considered. [78] Ttheir analyses took into account factors such as manufacturability, ground systems integration, and commonality, addressing many of the "-ilities" in an attempt to better inform architecture downselection. However, vehicle analysis was performed via a combination of very simple assumptions regarding vehicle sizing and an ascent performance model that assumed the same ΔV trajectory for all vehicles, regardless of propulsive performance. This the larger number of alternatives considered was achieved

Villeneuve

Villeneuve analyzed $186,000$ LV concepts, an astounding number when compared to all the other studies reviewed. [79] This was achieved with a vehicle sizing technique in line with the standard approach employed in industry and government conceptual design studies. The key enabler to the number of concepts Villenueve was able to evaluate lies in the use of surrogate (or empiric) models of the trajectory performance.

Summary

The clear standout in this brief review is Villeneuve's study, as it demonstrated three orders of magnitude more design points evaluated. This provides a strong statement regarding the potential for empirical models to enable broad design space exploration. This will also be shown to be critical to any methodology seeking to improve decision making by quantifying uncertainty.

A couple of high level observations can be made of these and other LV architectures studies from the literature. First, the total number of alternatives comprehensively evaluated in any given study is quite limited. In most government and industry studies, the LV architectures considered seem to be hand-picked by a combination of subject matter expertise and subjective, a priori assessments of anticipated costs. Second, the architecture evaluations are definitively "point design" in nature, consisting of a single optimized vehicle representative for each architecture alternative. No form of probabilistic design space exploration takes place, even in the case of Villeneuve, who seems to have had the apparatus for performing such analysis.

1.4 Overarching Hypothesis

Launch vehicle architecture selection was identified as a problem of interest due to two top-level observations, namely: The difficulty LV programs have had historically in achieving a viable cost-benefit trade (affordability), and the critical role the earliest design decisions play in locking-in cost. The brief review of LV architecture analysis of alternatives studies performed in Section 1.3.4 found no treatment of uncertainty anywhere other than reliability assessments (and that only in the case of the ESAS study), despite all forms of uncertainty existing at their highest levels in such early stages of design. For this reason, the overall objective of this thesis is formulated as: **"To develop a methodology for enabling risk-informed decision making during the architecture selection phase of LV programs."**

Because of the abundance of uncertainty sources present in the architecting stage of design, it is important to identify which types of uncertainty are to be targeted in the development of a risk-informed LV architecture selection methodology. It was observed in Section 1.3.3 that the "design freedom" that exists within the underlying design space of any given architecture manifests itself as a significant source of volitional uncertainty during the architecture selection process. Since a significant element in advanced design philoso-

phies involves the retention of design freedom for as long as possible, the accompanying volitional uncertainty must be understood and quantified to the greatest extent possible. For this reason, the overarching hypothesis for this thesis is stated as follows:

> **If volitional uncertainty in the form of design freedom is quantified and propagated, decision makers will be able to perform risk-informed LV architecture selection.**

The rest of this document is organized as follows: A framework for probabilistic architecture selection is presented in Chapter 2, where a more focused research objective is identified; potentially useful approaches and techniques are reviewed in Chapter 3, leading to a set of research questions and the formulation of hypotheses; and Chapter 4 designs and executes a series of experiments in support of answering these research questions and testing the hypotheses. Finally, Chapter 5 summarizes the observations drawn from literature, and synthesizes them with observations from the experiments performed, presenting a response to the overarching research question.

CHAPTER 2
PROBLEM FORMULATION

The greatest challenge for decision makers in the early stages of design is a lack of knowledge. As has been discussed, lack of knowledge is the very definition of uncertainty, and so where it is stated that "design knowledge can improve the quality of design decisions," it could also be said that uncertainty reduction can improve the quality of design decisions. [43] Taguchi, a pioneer of both quality and systems engineering, held this same view, considering the primary means of improving the quality of the engineered product to be the reduction of variability in the outcome. [28] Variability, in its mathematical representation variance, is a measure of uncertainty; indeed, Taguchi's aim was for a "robust" product, insensitive to sources of "noise," or uncertainty.

The potential rammifications that uncertainty has on decision outcomes are a well known challenge in design. Many processes and methodologies have been put forward to address this challenge in some way. [80, 81, 82, 83, 84, 85] None of them is able to fully inoculate the design process, but limitting the scope of potential impact to the outcomes of design is still of great importance.

From a high level, there are two primary thrusts identified in the literature on design and decision-making under uncertainty, taking proactive and reactive stances. The proactive stance seeks to make "stable decisions" which reduce the number of scenarios in which future redesign actions would have to be taken. [86, 87] Within this proactive category exist the two perspectives of robust design and reliability-based design. [88] Reactive strategies strive for flexibility in design, seeking to make responding to unexpected outcomes or scenarios easier. The primary means for achieving flexibility are by putting off final decisions for as long as possible. [86, 87] This strategy mirrors that at play in set-based design methods, which will be briefly introduced in Section 2.1.3.

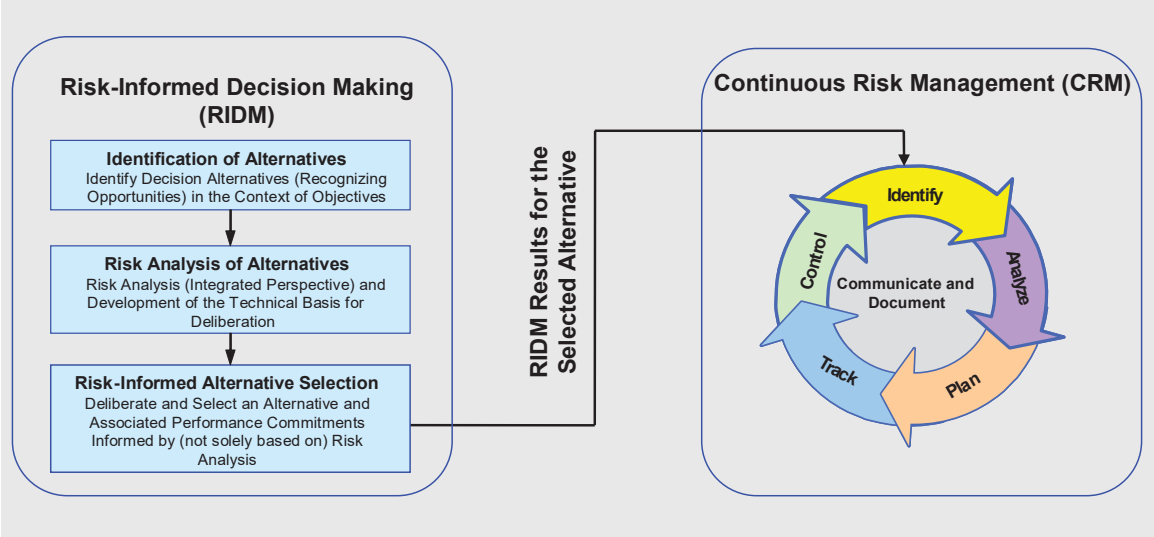

Figure 2.1: NASA's Risk Management framework, consisting of Risk-Informed Decision Making and Continuous Risk Management [59]

Uncertainty mitigation strategies which operate in the proactive regime generally act in two primary ways. First, where feasible, they seek to reduce uncertainty through rigorous analysis and quantification of responses for the system under design. This can often be a costly proposition, though, so the second approach consists of merely enveloping the impacts of uncertainty sources, enabling confidence in decision making despite their presence.

In 2010 NASA published the *Risk-Informed Decision Making Handbook*, which, together with its Continuous Risk Management process, forms a part of the overall Risk Management strategy advocated by that agency. [89] The relationship understood between Risk-Informed Decision Making (RIDM) and Continuous Risk Management (CRM) is the following: "Decisions made during the course of a program [via RIDM] ultimately 'burn in' the risk that must be managed [via CRM] during the life cycle of the program." [59] Clearly, RIDM is the process in play during architecture selection. The fact that these early decisions define the risk landscape which all subsequent development program efforts must navigate relates closely to the observations in Section 1.2.1 regarding the influence of early decisions on program cost.

If improving decision making during the architecture selection phase of LV design is the goal of this research, it is worth taking a closer look at NASA's RIDM process to understand how it might apply, and to assess if there are any gaps preventing an immediate implementation. The RIDM process is composed of six main steps, organized into the three major parts depicted in Figure 2.1.

2.1 Identification of Alternatives

According to the definition provided in Section 1.2, a decision-making process fundamentally entails the consideration and weighing of alternatives; a decision-maker seeks to discern amongst the available alternatives which ones are the most preferred in the context of the decision-maker's perspective or world view. Clearly, defining metrics to measure value and generating candidate alternatives are two important steps that must occur at the beginning of any decision-making process. These are indeed the first two steps in NASA's RIDM process.

2.1.1 Definition of Figures of Merit

In the first step to implementing an RIDM process, the top level requirements and objectives for a program are decomposed to quantifiable measures of "goodness;" that is, measures having an identifiable direction of improvement. The NASA RIDM Handbook refers to these as "Performance Measures;" however, the term "Performance" is used broadly in reference to how an alternative performs against any particular requirement or objective, and does not necessarily refer to vehicle or mission performance. In order to avoid any confusion due to terminology, Performance Measures will be referred to generically as Figures of Merit (FOMs).

The FOMs used in decision making are derived from a mix of formal requirements and less formal stakeholder preferences. Particularly in the architecting phase, there may be more preferences than fully fleshed out requirements. Most real world situations will

involve multiple FOMs, but at a minimum, there are two categories of FOMs that must be considered, described in the NASA Systems Engineering Handbook as: [24]

Cost "The cost of a system is the value of the resources needed to design, build, operate, and dispose of it."

Effectiveness "The effectiveness of a system is a quantitative measure of the degree to which the systems purpose is achieved."

FOMs should be objective (not a matter of opinion), quantitative (cardinal scales preferred over ordinal, and ordinal over nominal), and measurable (can actually be measured and known in time to support decision making). [90] So long as a decomposition of program requirements and stakeholder preferences is adequately performed, there is no "right" or "wrong" list of FOMs, and the list may vary from study to study.

2.1.2 Alternative Generation

The second step in NASA's RIDM process assembles the alternatives for consideration in the decision to be made, employing the Design Solution Definition Process described in the NASA Systems Engineering Handbook. [24] This process is described at a very high level, but within this framework there are a number of approaches to generating, or "enumerating," alternatives. These generally follow some form of system decomposition, and can be more physically or functionally focused. A common issue encountered in decomposition based alternatives enumeration is that the number of alternatives available grows very rapidly in what has been referred to as the "combinatorial explosion." [91] Techniques for addressing this challenge include compatibility/feasibility rules, subject matter expert prioritization, and set-theoretical transformations. [92, 93, 91]

Several enumeration techniques from literature are described here next.

Trade Tree

A Trade Tree as depicted in Figure 2.2 presents decisions as tree branch points, with options available for the given decision down each of the connected branches. Generation of a unique concept is complete when the full length of the tree has been traveresed, so that a complete branch, from root to leaf, has been identified. The example in Figure 2.2 shows twelve complete alternatives highlighted in green. The trade tree is the primary approach to enumerating alternatives suggested by NASA's systems engineering publications. [24, 89] The primary drawback of a trade tree is that, as a graphical technique, there is a limit on how many alternative branches can be displayed legibly. The tree in Figure 2.2 only displays 189 branches of a possible 1620 due to space constraints.

Morphological Matrix

A morphological matrix, or matrix of alternatives, captures the option space for decision making into a matrix form. Morphology is "a study of structure or form;" it is commonly used in biology in reference to physical features of plants or animals, and in linguistics in reference to word and sentence structure. [94] Zwicky is credited with expanding the application of morphological analysis, and of morphological matrices, to the broader context of concept formulation. In his 1969 book entitled *Discovery, Invention, Research - Through the Morphological Approach*, Zwicky himself made this statement: [95]

> "I have proposed to generalize and systematize the concept of morphological research and include not only the study of the shapes of geometrical, geological, biological, and generally material structures, but also to study the more abstract structural interrelations among phenomena, concepts, and ideas, whatever their character might be."

A morph matrix organizes decisions into rows that contain available options or features. In doing so, decision spaces are represented in a much more compact fashion than is possi-

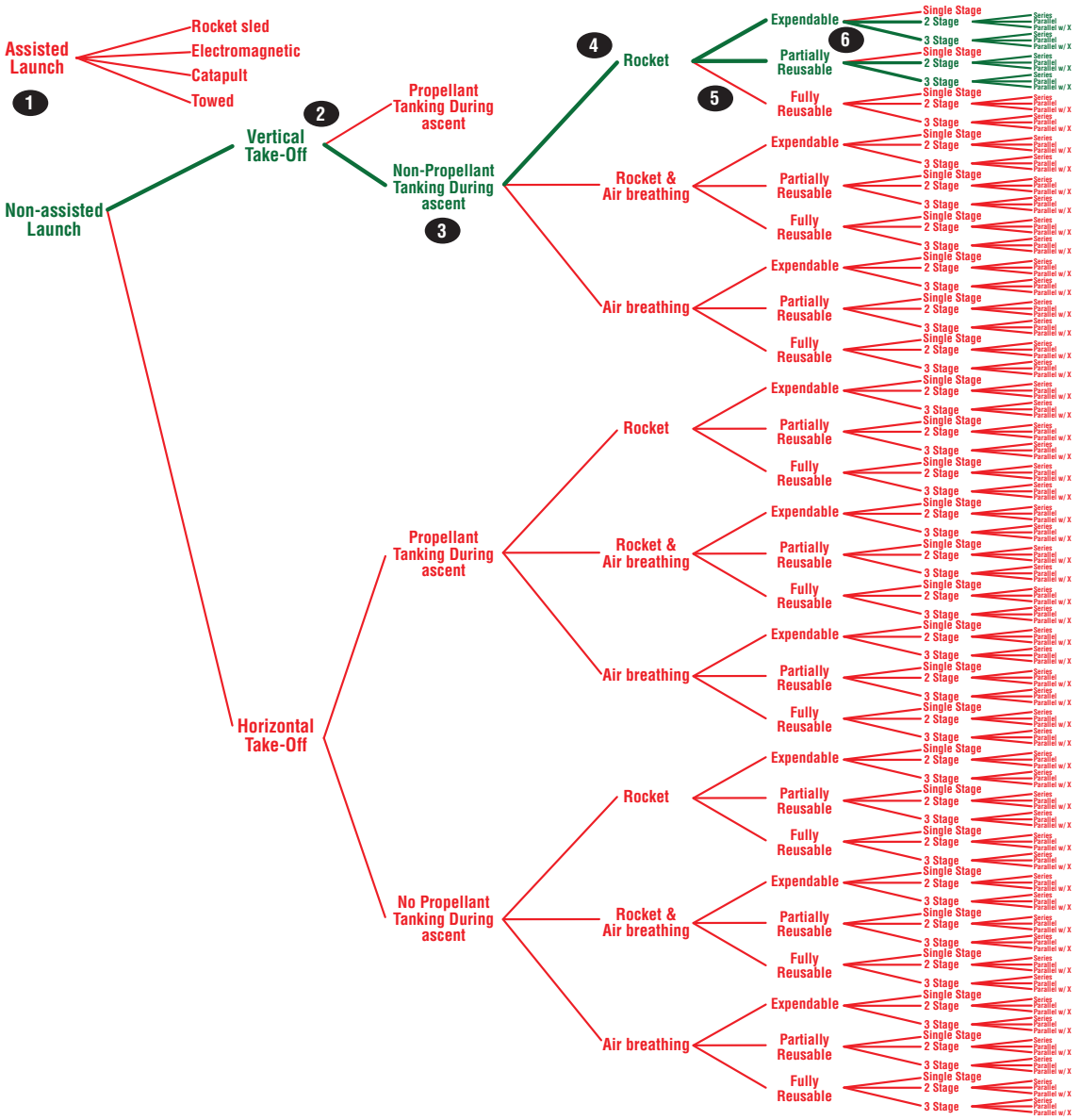

Figure 2.2: Top level trade space from NASA's ESAS Study [32] depicted as a trade tree. The green path denotes the branches selected by NASA for further study.

Table 2.1: ESAS decision space depicted in Morph Matrix form

Choice	***Option 1***	***Option 2***	***Option 3***	***Option 4***	***Option 5***
Launch Assist	None	Rocket sled	EM	Catapult	Towed
Take-off	Vertical	Horizontal			
Propellant Tanking	No	Yes			
Propulsion Type	Rocket	Air-breating	Both		
Reusability	Expendable	Partial	Reusable		
Staging	1-stage	2-stage	3-stage		
Configuration	Series	Parallel	Parallel w/ X		

ble with trees. For example, Table 2.1 presents the complete set of 1620 alternatives which could not be shown in Figure 2.2. A single unique concept is assembled by selecting one option from each row in the matrix.

Graph Methods

A variety of other methods have been formulated for the enumeration and assembly of alternatives using graph theoretic approaches. A few of these include Koo's Object-Process Networks [96], Arney's rule-based graph traversal algorithm [97], Iacobucci's Rapid Architecture Alternative Modeling (RAAM) [98], and Lafleur's application of Markov Decision Processes. [99] One of the main benefits of graph-based techniques is that they are easily interpreted and executed by computers. This allows for very large populations of alternatives to be generated and evaluated in an automated fashion. Like the trade tree, graphs can often become too large to take in quickly in a visual manner; however, they generally provide a higher degree of flexibility than either trade trees or morph matrices in terms of being able to capture variations in both systems and concepts of operations. Graphs also provide the capability to establish requirements, constraints, and other assumptions within the trade space as explicit model structural elements.

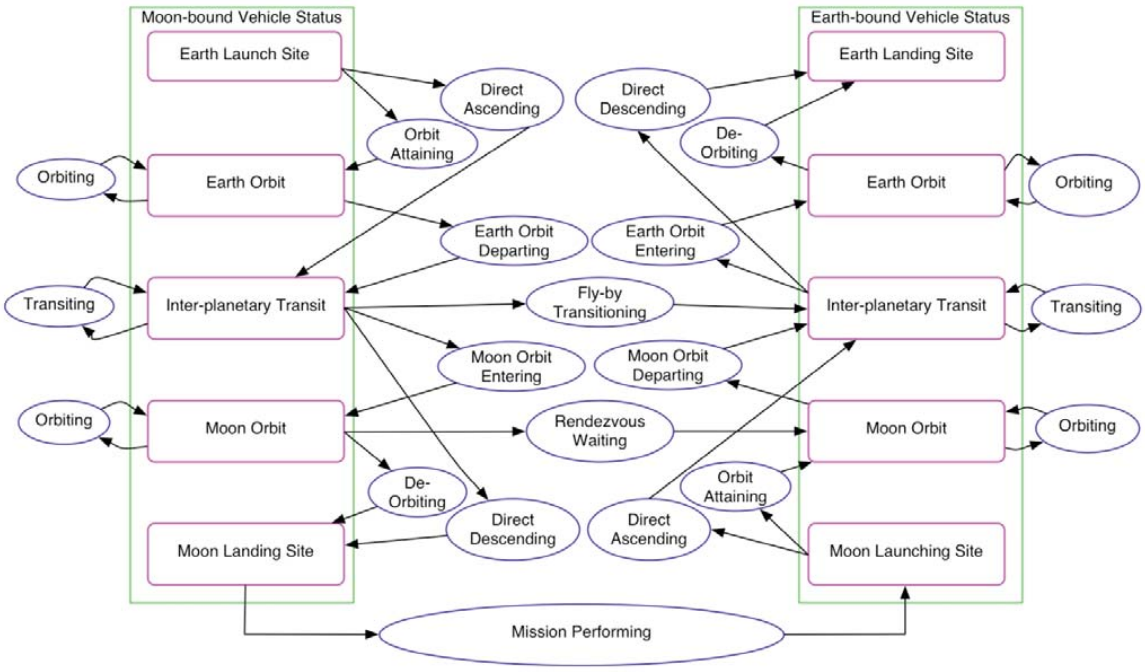

Figure 2.3: Depiction of Koo's Object-Process Networks [96]

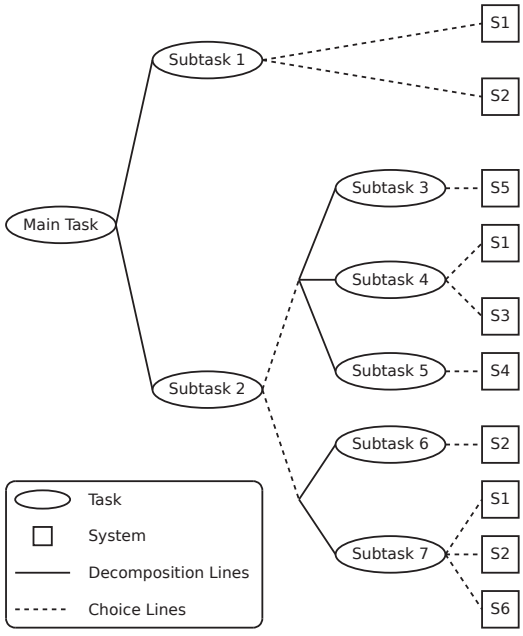

Figure 2.4: Depiction of Iacobucci's Rapid Architecture Alternative Modeling (RAAM) [98]

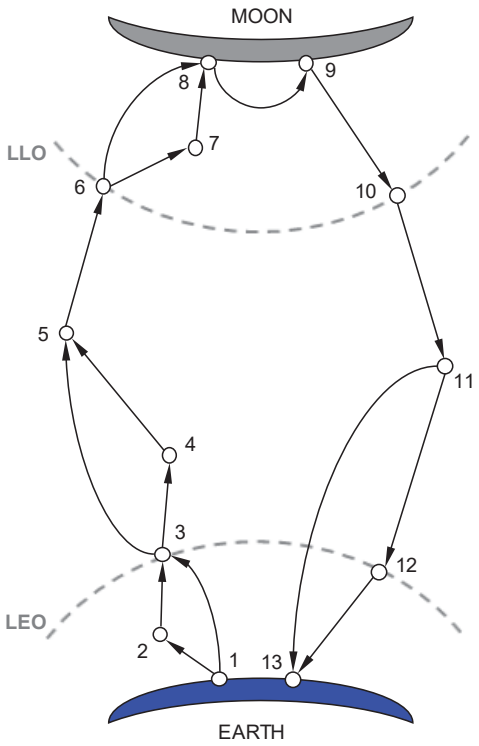

Figure 2.5: Depiction of Arney's rule-based graph traversal algorithm [97]

2.1.3 Set-Based Philosophy

The idea put forward in Section 1.3.3, that an architecture concept cannot be adequately represented by any single point, is in accord with the philosophy at work in the Set-Based Design paradigm. Set-Based Design (SBD), which first emerged in the 1990s through its practice by Toyota, generically consists of a process in which initially broad "sets" of potential solutions are whittled down over time to a final converged solution. [100] This stands in contrast to traditional design, in which an initial point design is identified early on, and then subjected to numerous refinements until it meets all requirements and constraints.

The ideas and terminology in SBD come from the field of Set Theory, and so it is helpful to establish some definitions to serve as a basis of understanding the SBD philosophy. Table 2.2 provides such a list. In SBD, a design concept is treated as the "set" of all variations that are possible within the defined properties for the concept. This formulation is useful in that it allows for the gradual refinement of the concept definition, enabling a large design

Table 2.2: Key terms and definitions from Set Theory [101]

Term	Definition
Universe	"the totality of all the things that exist pertaining to the domain of interest"
Set	"a collection of elements or members from a universe of interest"
Family of Sets	a set in which members are themselves sets
Classical Set	a set where "it is possible to determine uniquely whether any given individual is or is not a member"
Fuzzy Set	a set where individuals' memberships cannot be determined uniquely

space to be carried forward until enough knowledge is generated to support a downselection decision. [102]

Sharma developed a set-based methodology for representing architectures in his dissertation entitled *STASE: Set Theory-Influenced Architecture Space Exploration*.[91] Of greatest note here is the mapping STASE established between the Architecture, Design, and Objective spaces. The Architecture space is composed of the same alternatives that would otherwise be represented in a trade tree or matrix of alternatives; the Design space represents all of the parametric design attributes pertinent to any given concept selected from the Architecture space; and the Objective space is defined by the FOMs of interest. The Architecture space, as it is made up of a countable number of individuals, is finite. The Design and Objective spaces are both infinite, as they are both composed of continuous parameters.

In LV architecting, the universal set marked as P in Figure 2.6 is the architecture trade space from which the architecture selection will be performed. The members P_A, P_B, and P_C, which are themselves sets, represent choices that must be made in specifying a complete architecture definition. Each of their respective members are options available to be chosen. STASE posits a mapping relationship between distinct Architecture and Design spaces; an alternative but complementary interpretation from Set Thoery is that the Design

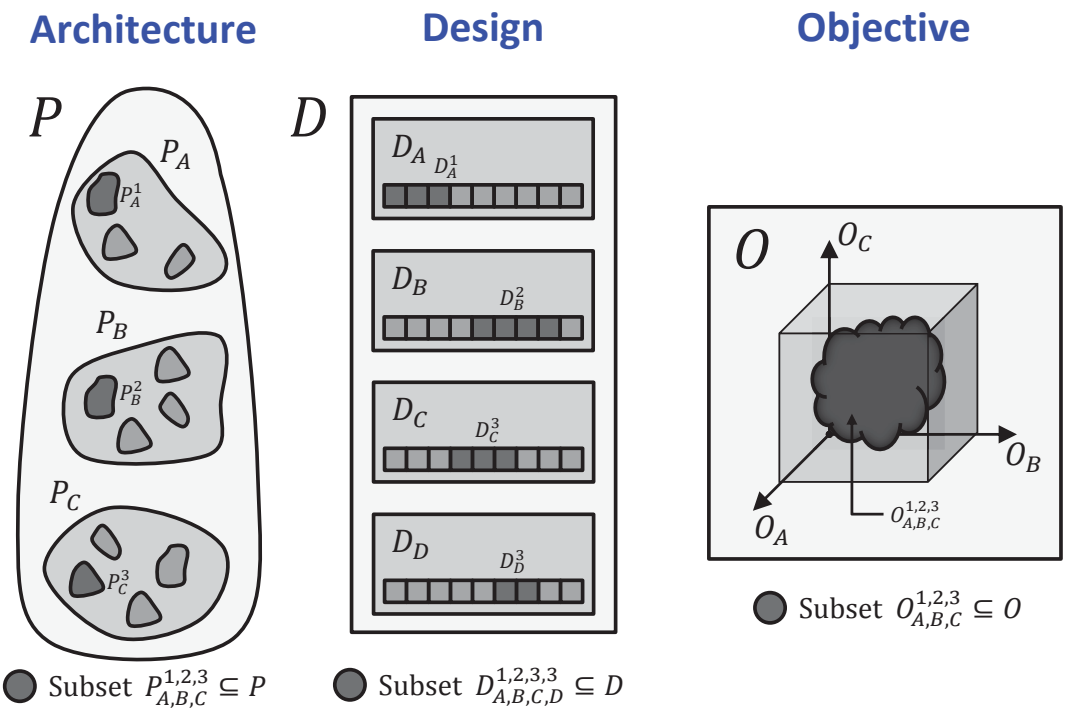

Figure 2.6: Architecture, Design, and Objective space mappings from STASE [91]. Markings in blue added

space is comprised of properties that define the Architecture space subset members via the "rule method." [101] Either way, the effect is that individuals in the Architecture space possess a set representation in the Design space which corresponds to all of the design property values that individual is allowed to take. While the Architecture family of sets, made up of individuals and their Design space property ranges, is Classical, sets in the Objective space are Fuzzy. This is because there is the potential for significant overlap between individuals within the Objective space, with a non-unique mapping back to the Architecture individuals they represent. Knowing an individual's location in the Objective space is not sufficient for identifying that individual uniquely.

Since an architecture's value to decision-makers is measured in the Objective space, characterizing a LV architecture amounts to mapping an individual defined in the Architecture space to its representative set in the Objective space. Because there is non-unique mapping from the Objective space back to the Architecture space, a single point is not sufficient representation for any LV architecture – it could just as easily stand for any number of different LV concepts. So, it is necessary to characterize and populate the full set to provide a solid basis for decision-making.

Sets are a concept already employed in the realm of uncertainty modeling and analysis. [101] Their application in the context of modeling volitional uncertainty is even more pointed, due to the stated intent in SBD of delaying design decisions for as long as possible. Since volitional uncertainty is the uncertainty due to as-of-yet unmade design decisions, it is clear that SBD in fact advocates for tolerating volitional uncertainty rather than reducing it. So, in a way, volitional uncertainty can be viewed as a risk perspective on design freedom.

2.2 Risk Analysis of Alternatives

The third step consists of selecting the appropriate analysis tools and frameworks for quantifying the performance measures selected. Care is given to ensuring the fidelity of the anal-

yses is matched appropriately to the types of metrics being quantified, and to the types of decisions being made. In the fourth step, the risk analysis is performed by evaluating each of the alternatives through the analysis framework assembled. This is necessarily a probabilistic assessment, with the variability from sources of uncertainty propagated through to the performance measures in order to quantify their potential impact.

Once alternative architectures have been identified, the next step is to evaluate their value to the decision makers, as defined by the FOMs. This evaluation equates to characterizing each architecutre's footprint in the Objective space by propagating its representation in the Design space through a "transfer" function composed of analyses, either physics-based or other, that can compute the FOMs based on design parameter values. There is no particular form imposed on this transfer function; it can be a simple analytic function of the inputs, or it can represent a large-scale M&S environment. Fundamentally, the fuction takes the form of Equation (2.1); in keeping with the notation in Figure 2.6, $\mathcal{O}$ is the realization of the concept in the Objective space and D is the description of the concept in the Design space.

$$\mathcal{O} = \mathcal{F}\big(\mathcal{D}\big) \tag{2.1}$$

It is important to note that the dimensionality of $\mathcal{D}$ may vary between different architecture concepts. For example, a 3-stage LV will possess parameters defining the design attributes of a 3^{rd} stage, while a 2-stage LV will not. This indicates that different alternatives under consideration in the same decision process may reside in distinct Design spaces $\mathcal{D}$. So long as the alternatives can be evaluated within a common Objective space, this is not a showstopper. However, it does necessitate that a specific form of $\mathcal{F}$ be developed for mapping from each of the Design spaces $\mathcal{D}$ into $\mathcal{O}$.

2.2.1 Architecture Characterization

Hull Finding

The "hull" of a set is the subset of points that form the enclosing boundary of that set, and its identification is an important part of algorithms and techniques in a variety of fields including data mining, computer vision, and machine intelligence. [103] Hulls, which can be either convex or concave, are an important attribute in the geometrical interpretation of sets. Sharma showed that the hull for an architecture's representation in the Objective space can be found by employing multi-objective optimization routines designed for finding Pareto fronts. [91]

In the context of decision making, the most interesting portion of a hull is that which forms the set's Pareto frontier. The Pareto front is composed of design points for which an improvement in any one FOM comes at the expense of another FOM.[104] Points that lie on the Pareto Front are called "dominant" or "non-dominated," while points that lie inside the Pareto front are dominated. The non-dominated points are of great interest, as they essentially define the "best" that can be achieved within a given LV concept family. Figure 2.7a shows three example Pareto fronts, with the direction of improvement towards the lower left corner (notionally minimizing both objectives). While these each depict convex fronts, it is also possible to have non-convex Pareto fronts.

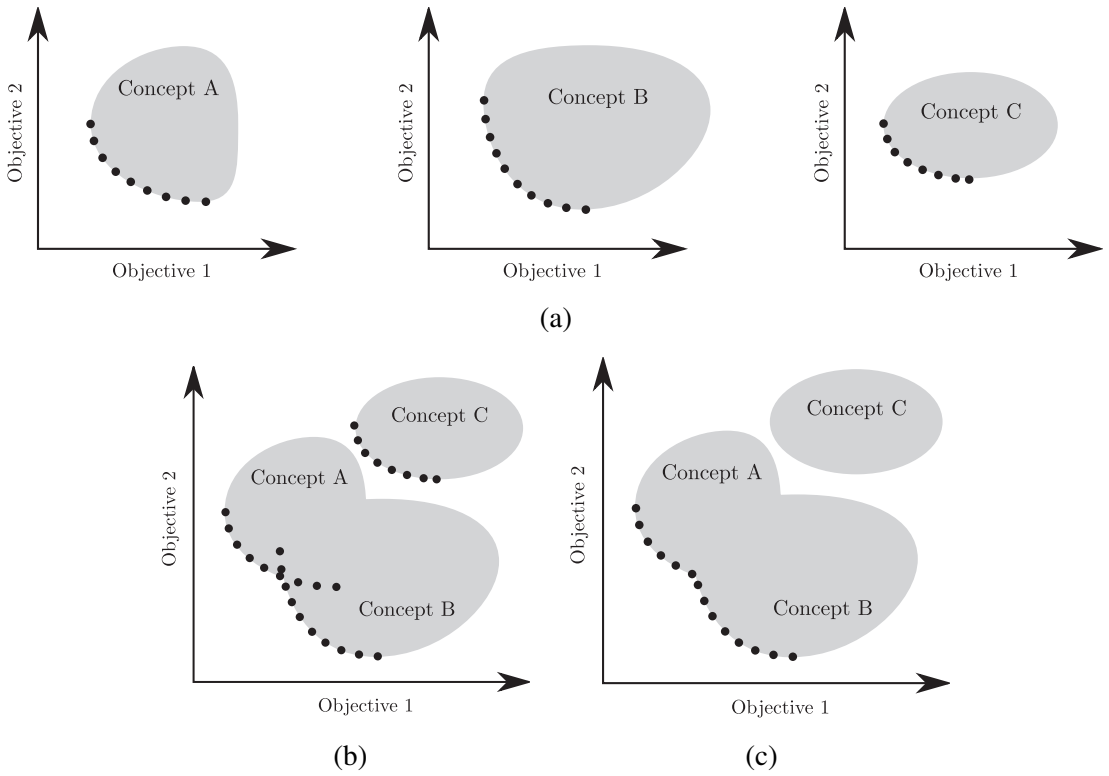

Figure 2.7: Depiction of (a) local pareto fronts (b) overlayed to form a (c) global pareto front. Images from [105]

The concept of the Pareto front also extends to the scenario where multiple architectures are considered simultaneously. In this case, the "global" Pareto front is composed of a subset of non-dominated points from the "local" architecture fronts, while some locally non-dominated points become dominated by other architectures at the global level. Some local Pareto fronts may become completely dominated in the global context, leaving their respective LV concept families with no representation on the global Pareto frontier. Both of these situations are show in Figures 2.7b and 2.7c: A portion of the Pareto fronts for both notional concepts A and B become dominated with the overlap between the two sets, while Concept C becomes completely dominated.

Though the Pareto front is an important feature to capture in characterizing the potential of any given architecture concept, neither it nor the set hull is sufficient for representing a concept family on its own. The Pareto front shows what can be achieved if all degrees

of freedom within the design space were fully leveraged to optimize some objective expressed as a function of the FOMs. Due to the nature of projecting higher dimensional data onto lower dimensions, non-dominated points do not necessarily appear in the tails of the marginal distributions; however, the reality is that non-dominated points do reside in the "tail" of multidimensional probability density functions. Reliability-based design methods emphasize accuracy in characterizing the tails of uncertainty distributions; however, architecture selection is focused on robust design, which is more interested in the denser mass of the uncertainty distribution. [88] So while the Pareto front captures the boundary of the possible, it does not provide any information about where in the objective space an architecture's design space tends to congregate.

Optimization

In characterizing an architecture concept, all of the studies reviewed in Section 1.3.4 put forward individual design points as representatives of each alternative under consideration. While it is not exactly clear how each architecture representative was selected, a very logical approach would be to perform some form of optimization routine to produce the "best" candidate from each architecture design space. This optimization might exercise gradient-based or stochastic search algorithms, and its design could be to minimize/maximize either a one-dimensional (in the form of an overall evaluation criterion) or multi-dimensional objective function. Regardless of the formulation applied, so long as the optimizer operates on the full set of FOMs defined in the Objective space, the resultant design should reside on the architecture's Pareto front. In the case of multi-objective, population-based optimizers, the final result may amount to an approximation of the full Pareto front. Either way, optimization can be viewed in this context as a more targeted and specific variation on hull finding.

Density Estimation

Density Estimation seeks to map the topology of the space enclosed by a set's hull. In probabilistic analyses, density estimation is aimed at quantifying the probability density function (PDF) or its integral, the cumulative distribution function (CDF) in the Objective space. and so in keeping with the set-based interpretation of uncertainty, quantifying the PDF is also a goal of LV architecture set characterization. In this case, the volitional uncertainty propagation can be viewed as simply another perspective on design space exploration. There are many different approaches presented in literature for propagating uncertainty to estimate the PDF; a few of the most common ones are presented here.

In practice, the aim of probabilistic assessments is to develop a cumulative distribution function (CDF), which is the cumulative integral of the PDF, and can be used to describe the likelihood that a response of interest falls within some specific range. There are a couple of ways to assemble a CDF, depending on the objectives of the probabilistic assessment and the nature of the analysis tools being exercised. Bandte describes these as: [106]

1. Fast Probability Integration on exact analysis, producing an analytical approximation of the CDF

2. Direct Monte-Carlo simulation on exact analysis, producing an empirical approximation of the CDF

3. Monte-Carlo simulation on surrogate model of the exact analysis, producing an empirical approximation of the CDF

The latter two methods mention Monte Carlo simulation specifically; however, in reality these can be viewed as sampling methods, where pure Monte Carlo is just one available strategy.

Fast Probability Integration & Expansion Methods Fast Probability Integration (FPI) is built around analyzing Most Probable Points (MPPs), and estimating their likelihood of

occurence in the Objective space. FPI performs a transformation on the input space, and then is able to infer an MPP for a specific value in the Objective space based on some Limit State Function (LSF) of interest. An Expansion technique is then exercised around the MPP to characterize the PDF and CDF values of the MPP in the Objective space.

Expansion methods, or Approximate methods as they are sometimes called, utilize a Taylor series expansion and the moments from the input variable distributions to approximate the moments of the response variable distribution. [101] An example showing the second order computation of the first and second moments of the response is presented in (2.2) and (2.3):

$$\mu_O = F(\mu_D) + \frac{1}{2}\sum_{i=1}^{n} \frac{\delta^2 F(\mu_D)}{\delta D_i^2}\sigma_{D_i}^2 \tag{2.2}$$

$$\sigma_O^2 = \sum_{i=1}^{n}\Big(\frac{\delta F(\mu_D)}{\delta D_i}\Big)^2\sigma_{D_i}^2 + \frac{1}{2}\sum_{i=1}^{n}\sum_{j=1}^{n}\Big(\frac{\delta^2 F(\mu_D)}{\delta D_i \delta D_j}\Big)\sigma_{D_i}^2\sigma_{D_j}^2 \tag{2.3}$$

The derivatives for the calculation are obtained by finite-differencing the Objective function, and so there are either $n+1$ or $2n+1$ function evaluations required, depending on the differencing scheme. It is also possible to extend the calculation to higher order moments. [107]

This approach can provide an extremely efficient estimation of a quantile of interest; however, because it is based on the Taylor series expansion about specific targeted points, its accuracy drops off in areas away from the centers of expansion. This can be problematic if the objective function is very nonlinear, multi-modal, or if a more accurate representation of the entire response probability distribution is needed. The analysis can be repeated for multiple values of the LSF, providing a sequence of points against which to regress an analytic CDF. However, the benefits of FPI begin to diminish, as larger numbers of transfer function evaluations begins to approximate a sampling method.

Sampling Methods The most frequently applied and broadly applicable approach to density estimation is sampling. In sampling, selected inputs are propagated through and their resulting outputs recorded. There are a couple of different statistical fromulations to sampling, including Monte Carlo, Quasi-Monte Carlo, and Design of Experiments.

Monte Carlo Monte Carlo is by far the most prevalent form of sampling employed today. As its casino namesake would suggest, it amounts to stochastic sampling of the input space; a random number generator draws from each of the uncertainty distributions to create a case, which is propagated to the Objective space. Given a large enough sample size, Monte Carlo can achive any degree of accuracy required. It is also extremely flexible, being able to work with almost any form of input variable or distribution, and imposing no assumptions or requirements on the nature of the transfer function $\mathcal{F}$. Also, Monte Carlo is immune to the "curse of dimensionality" in that the sample size required does not depend on the number of uncertainty sources, only on the response behavior and the resolution required. Monte Carlo's main drawback is that it exhibits very slow convergence, especially for situations where distribution extremes must be resolved finely. This can make complex or high-fidelity analyses prohibitively expensive to perform. The stochastic nature of Monte iCarlo sampling means that relatively small sample sizes run the risk of possessing some incidental statistical bias in their structure; Monte Carlo relies on the law of large numbers (through large sample sizes) to achieve unbiased samples.

Quasi-Monte Carlo Quasi-Monte Carlo methods achieve faster convergence rates by employing quasi-random number generators, which implement some form of sequence auto-correlation in order to reduce "discrepancy." Discrepancy is defined as the extent to which a sample differs from a uniform distribution. [108] Reducing discrepancy somewhat alleviates standard Monte Carlo's reliance on the law of large numbers; the auto-correlation provides assurance of low bias even for small sample sizes. However, in doing so, Quasi-Monte Carlo techniques become somewhat sensitive to the dimensionality of the input

space, losing one of the benefits of pure Monte Carlo sampling. Examples of Quasi-Monte Carlo sampling include Sobol and Hammersley sequences. [109, 110]

Design of Experiments An experiment is a "test or series of tests in which purposeful changes are made to the input variables of a process or system so that we may observe and identify the reasons for changes that may be observed in the output response." [111] Clearly, density estimation can be understood as an experiment in which "purposeful changes" in the input variables $\mathcal{D}$ are propagated through the system $\mathcal{F}$ in order to observe the resulting output response $\mathcal{O}$. Design of Experiments (DOE) is a branch of applied statistics focused on the "the process of planning, designing and analysing the experiment so that valid and objective conclusions can be drawn effectively and efficiently." [112] Many different DOE formulations have been created for different application scenarios, including process characterization, process optimization, and product design. [111] For the role of a sampling method aimed at density estimation, unbiased and uniform representation of $\mathcal{D}$'s mapping to $\mathcal{O}$ is desired, as described previously. Space-filling DOE strategies seek to provide this very thing. One drawback of space-filling DOE methods is that they generally require the a priori selection of sample size. Adding additional cases to a Latin-Hypercube DOE, for example, does not preserve the space-filling nature of the DOE. [113]

Surrogate Modeling When dealing with transfer functions that are relatively expensive to evaluate, sampling methods can overwhelm the resources available for performing probabilistic analysis. In these situations, a common approach is to perform the sampling with a "surrogate" of the expensive analysis. Surrogate modeling, which leverages reduced order modeling and advanced regression techniques (Empirical models), requires an up front investment in developing a set of data against which to "train" the model. Depending on a combination of the behavior of the response to be modeled and the goals of the assessment, this initial investment may not be deemed worthwhile. Some of the more sophisticated and effective techniques also require familiarity with their mathematical formulation, a knowl-

edge base that is far from ubiquitous.

2.2.2 Research Question 1

Since the architecture selection process has been identified as an application for robust design rather than reliability-based design, FPI can be ruled out from consideration, as it is geared primarily towards reliability-based design. The remianing methods rely on sampling techniques for performing uncertainty propagation, so based on the brief summary of available sampling strategies provided in the previous section, an important question that must be answered emerges as:

> **Research Question 1a: What is the best sampling strategy for propagating LV volitional uncertainties from the Design space to the Objective space?**

In addition, further specification between probabilistic design methods 2 and 3 from the previous section implies a decision regarding whether to use full mechanistic models or empiric ones. It is already common practice for black or gray box models to be used in LV sizing. However, as seen in Section 1.3.4, full numerical trajectory modeling is also part of the standard approach. Research Question 1b follows from this observation:

> **Research Question 1b: Is it feasible to use explicit trajectory optimization to characterize LV architectures in an RIDM process?**

2.3 Risk-Informed Alternative Selection

The fifth step seeks to summarize the probabilistic results by establishing a "performance committment" for each alternative. This committment, in the form of performance measure values at a particular confidence level, allows for a risk-normalized basis of comparison between alternatives. Finally, step six consists of the actual selection process, and includes a variety of perspectives that must be weighed by the decision makers.

2.3.1 Setting Performance Commitments

Once an architecture has been fully characterized in the Objective space, it is then ready to be evaluated against other alternatives in a decision-making process. However, due to the volitional uncertainty contained, an architecture's representation in the $\mathcal{O}$ space is a probability density function rather than a point. As such, it is necessary to identify a process by which alternative architectures can be compared. Decision making techniques generally are formulated to work on point value vector representations of alternatives, and so it is necessary to define a method for summarizing an architecture's uncertainty in such a way as to enable risk-informed decision making.

Risk-Normalized Performance

The approach recommended in NASA's RIDM process for setting performance commitments aims to establish a "risk-normalized" basis for comparing alternatives. This ensures the performance commitments selected for each alternative all possess a common risk posture with respect to each of the performance measures. The approach for doing this follows three basic steps. First, the decision makers' allowable risk must be identified for each of the performance measures, or FOMs, individually. Second, the specific order in which to apply the risk tolerances must be set, with the recommendation that order be set according to increasing risk tolerance. Finally, the performance commitments for each FOM are computed sequentially, selecting the confidence level corresponding to the risk tolerance set. This process is depicted for two performance measures in Figure 2.8

The FOM values selected are drawn from the conditional distributions rather than the marginals, in order to inoculate the process to correlations between FOMs. [89] In the end, the probability that all performance commitments will be met is computed by Equation 2.4.

$$P = \prod_{i=1}^{\#PMs} (1 - RT_{PM_i}) \tag{2.4}$$

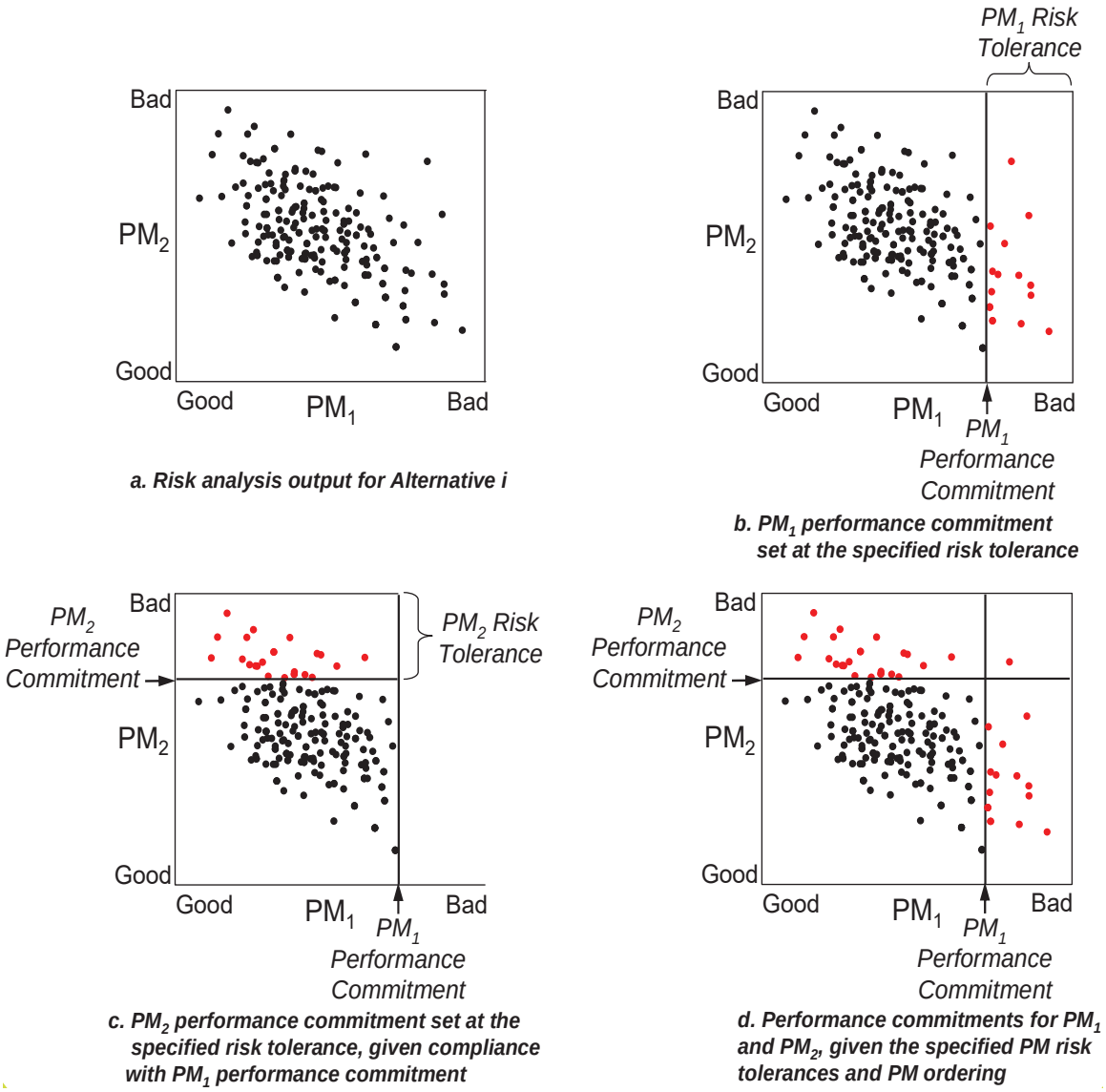

Figure 2.8: Depiction of NASA's RIDM sequential pruning the space to establish performance commitments. [89]

The result of this process is that each alternative is summarized with a vector of point values for every FOM, with a common risk posture among all alternative points.

Performance-Normalized Risk

Just as it is possible to establish a risk-normalized basis for comparison, a performance-normalized basis can also be established. In this case, the commitment made is to a particular risk level rather than a set of performance measures. This process takes place when specific target or "threshold" values for the performance measures have been set as requirements. This approach is the core of the Joint Probabilistic Decision Making (JPDM) technique formulated by Bandte. [106] The result of applying this perspective is that each alternative is summarized by a vector of risk values, where each element represents the subject alternative's risk with respect to the particular target FOM value. Figure 2.9 shows a graphical interpretation of JPDM's risk assessment; the gray region represents the portion of the distribution that meets all performance requirements, so one minus this value is the risk.

2.3.2 Alternative Selection

The culmination of a risk-informed decision making process is the point of downselection. Once performance commitments have been identified for each alternative under consideration, alternative selection can proceed as a standard Multi-Criteria Decision Analysis (MCDA) process. The field of MCDA is defined as "a collection of formal approaches which seek to take explicit account of multiple criteria in helping individuals or groups explore decisions that matter." [115] Within MCDA it is common to distinguish between Multi-Attribute Decision Making (MADM) and Multi-Objective Decision Making (MODM) techniques. Generally, MADM techniques are viewed as dealing with small sets of alternatives having large numbers of criteria; examples include Pugh Matrices, Analytical Heirarchy Process (AHP), and Quality Function Deployment (QFD). Similarly,

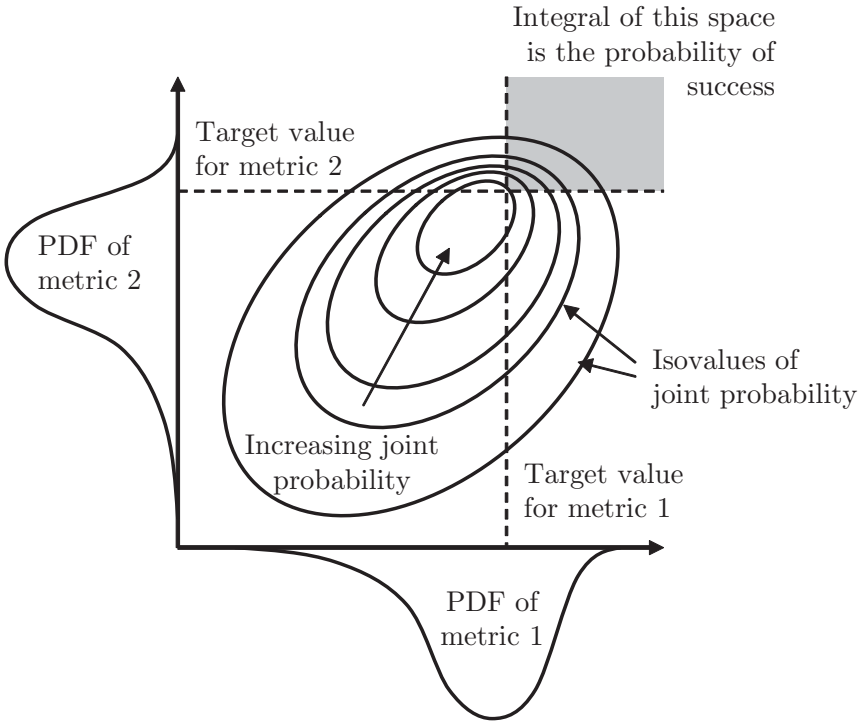

Figure 2.9: Example of JPDM approach to calculating performance-normalized risk. [114]

MODM techniques are seen to deal with large sets of alternatives and smaller numbers of criteria; Multi-Objective Optimization, which is itself a field with many methods and techniques, is a leading example of MODM. [106] These observations regarding application to various classes of decision problems may even go as far as the interpretation that MADM operates in discrete alternative spaces, while MODM operates in continuous alternative spaces. [116] However, there is clearly a continuum of decision spaces, and the suitability of various MCDA methods map to different portions of the continuum.

A very large number of MCDA algorithms have been developed, each formulated with different perspectives and assumptions on the decisions process and options space being explored. The number and diversity of techniques has led to the formulation of a meta-decision problem: Deciding on which decision making algorithm to use. [117] From qualitative to quantitative, deterministic to stochastic, MCDA provides a wealth of techniques for addressing decision making problems of various types. [118]

This is the point where the subjectiveness of a decision-maker's sense of preference must be accomodated. During this "deliberation," it may be decided that further analysis or higher fidelity analyses must be performed. This may occur when it is discovered that the difference between alternatives cannot be satisfactorily resolved. In the end, the information provided by the quantification of risk provides a solid basis for justifying decisions made. Here the concept of the Pareto front emerges again. In any group of candidate architectures, there weill be a "dominant" subset that envelopes the others with respect to either the performance commitments or the risk commitment (depending on whether risk-normalized commitments or performance-normalized risk is used). This can be interpreted as the risk-informed Pareto Front.

2.4 Launch Vehicle Performance Modeling

The overall objective for this thesis is focused on developing a methodology for risk-informed LV architecture selection. Since trajectory performance analysis was observed in Section 1.3.2 to be the most significant challenge in the execution of LV architecture studies, a closer inspection of LV performance modeling is merited. This begins first with a review of general types of models, after which a more specific review of LV performance models is performed.

2.4.1 Types of Models

In the literature, a variety of different modeling taxonomies are available to choose from. At a very high level, *Modeling and Simulation in the Systems Engineering Life Cycle* identifies four main categories of models: [119]

Iconic "physical models that 'look like' the real system"

Graphical "model the system as a network of nodes connected by edges"

Table 2.3: Models from Reddy's *Applied Data Analysis and Modeling for Energy Engineers and Scientists* [120]

Model Type	Description
Intuitive	"where the systems behavior is summarized in non-analytical forms because only general qualitative trends of the system are known"
Empirical	"where the properties of the system can be summarized in a graph, a table or a curve fit to observation points"
Mechanistic	"based on mathematical relationships used to describe physical laws such as Newtons laws, the laws of thermodynamics, etc."

Analog "use a different set of characteristics to represent the characteristics of a system of interest"

Mathematical "use mathematical language, which consists of mathematical symbols, expressions, relationships, operations, and logic, to describe a system"

Of these, it is clear that the mathematical category is the appropriate one for LV performance models. However, even within this category, there are a variety of more specific model types.

In his book on *Applied Data Analysis and Modeling for Energy Engineers and Scientists*, Reddy differentiates between three main types of models, Intuitive, Empirical, and Mechanistic. [120] These are outlined briefly in Table 2.3. Bonate, writing in the field of pharmacokinetics, only lists two primary modeling approaches, Models of Data and Models of Systems. The definitions for these, provided in Table 2.4, show close alignment with Reddy's empirical and mechanistic categories. [121] Another perspective on model categories proceeds from the field of system identification, and is based on the nature of insight and knowledge available regarding the primary system. [122] Table 2.5 provdes definitions for these, denoted as Black Box, Grey Box, and White Box models. This taxonomy has in its Grey Box category a model type that resides at the intersection of Empirical/Models

Table 2.4: Models from Bonate's *Pharmacokinetic-Pharmacodynamic Modeling and Simulation* [121]

Model Type	Description
Models of Data	"Useful when little is known about the underlying physical process from which the data are generated yet one still must make some conclusions regarding the data"
Models of Systems	"Based on physical and physiological principles and should have as many features of the system incorporated into the model as the data allow"

Table 2.5: Models from Keesman's *System Identification: An Introduction* [122]

Model Type	Description
White Box	A model based "on physical laws and additional relationships with corresponding physical parameters"
Grey Box	A model where if "some of [the physical] parameters are uncertain or not well known...the parameters [are] estimated from the data"
Black Box	Models "which do not necessarily refer to the underlying physical laws and relationships of the process"

of Data and Mechanistic/Models of Systems. Here, models are informed both by the laws of physics and the patterns of observations. Finally, Bungartz et. al. identify three modeling strategies available in general M&S applications, namely Heuristic, Analytic, and Numerical. [45] These are defined in Table 2.6.

All four of these can be synthesized into one cohesive picture with some massaging. Reddy and Bonate's ontologies are essentially the same, with Bonate leaving out Reddy's "Intuitive" model class. This is not a significant omission in the context of LV performance estimating, though, as the qualitative nature of Intuitive models would preclude them from any utility in design. Bungartz's models are simply more specific types of the other models; analytic and numerical models fall into the mechanistic class, while heuristic models fall somewhere along the boundary between Intuitive and Empirical. This relative ordering is

Table 2.6: Models from Bungartz et. al.'s *Modeling and Simulation: An Application-Oriented Introduction* [45]

Model Type	Description
Heuristic	"Strategies to get closer to the unknown solution" using "plausibility arguments"
Analytic	A "formal analytic construction of the solution," "including existence and uniqueness proofs"
Numerical	Models "A numerical algorithm provides the...solution"

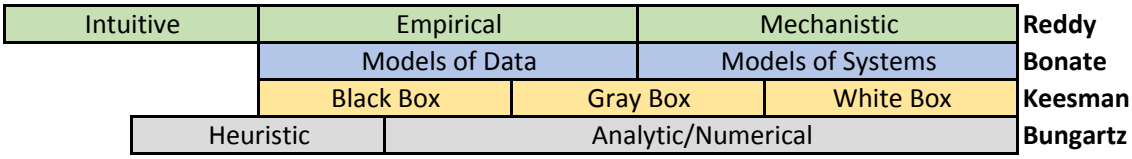

Figure 2.10: Continuum of mathematical modeling types

seen in Figure 2.10.

2.4.2 Trajectory Performance Models

As discussed previously, increased "quality" in conceptual studies results from increasing design knowledge and reducing uncertainty. Dealing with uncertainty generally requires probabilistic treatment, which places a premium on the ability to evaluate large numbers of designs. Similarly, an important part in generating increased knowledge is performing more comprehensive trade studies and analyses of alternatives. From these avenues for quality improvement it is possible to infer three desired characteristics for any model used in conceptual design:

Accurate Reflecting the outcomes of higher fidelity analyses closely enough to support architecture level decision making.

Fast Fast to implement and fast to execute, enabling significant analysis throughput.

General Able to accommodate many architectural variations, including variations in virtual staging, allowing for greater diversity in analyses of alternatives.

Based on the definitions for modeling and simulation provided in Section 1.2.2, it could be said that there is actually no such thing as a LV performance model; rather, the performance is an observed outcome derived by inserting a LV model into an environment model, and them simulating its mission. However, if a high level view is taken, with an agnostic perspective towards the internal workings of the performance estimation process, the predicted performance can be said to be a model of the real world performance. It is this form of "model," with the implicitly embedded LV model, environment model, and mission simulation, that will be reviewed here.

Numeric

Numeric models are the most flexible type of models, capable of modeling any trajectory problem that can be formulated within the software framework in which they are implemented. Fundamentally, numerically modeling LV performance entails integration of the equations of motion subject to some form of a steering program. The steering program is necessary to ensure insertion into the target orbit within specified tolerances. The presence of a steering program in turn introduces the need for optimization, as there is a non-unique set of steering programs that will satisfy the orbital insertion criteria. The real interest is in finding trajectories that not only achieve the desired orbit, but that do so in an efficient manner; typically, the desire is for the trajectory with lowest propellant consumption, though other objectives can be defined.

Several methods of addressing this problem exist, composed of combinations between two distinct implementation of the optimization problem, Indirect and Direct, with two available approaches to the numerical integration of the equations of motion, Shooting and Collocation. Each of these is described briefly in the sections that follow.

The Indirect Method The indirect method applies the Calculus of Variations to the optimal control problem to derive necessary conditions for optimality. The trajectory optimiza-

tion problem is then converted to a multi-point boundary-value problem (BVP), which is solved numerically to identify the set of trajectories which satisfy optimality conditions as extremals; the trajectory with the best objective function value is then selected as the optimal solution.[123]

Indirect methods are very powerful, and yield very accurate results. However, deriving the necessary conditions for complex systems can be very challenging. On top of this, the derived necessary conditions are unique to each problem, so there is a need to repeat this process for every new problem addressed. Constraints are brought into the optimization process as costates, resulting in an increased number of optimization variables. This complicates the solution, as with no physical meaning, good initial guesses for costates can be difficult to obtain.

Indirect methods have been studied extensively, and the general consensus on these methods is summed up in the following quote by Betts[124]:

> "The main difficulty with these methods is *getting started*; i.e., finding a first estimate of the unspecified conditions at one end that produces a solution reasonably close to the specified conditions at the other end. The reason for this peculiar difficulty is the extremal solutions are often *very sensitive* to small changes in the unspecified boundary conditions... Since the system equations and the Euler-Lagrange equations are coupled together, it is not unusual for the numerical integration, with poorly guessed initial conditions, to produce "wild" trajectories in the state space. These trajectories may be so wild that values of $x(t)$ and/or $\lambda(t)$ exceed the numerical range of the computer!" [125]

Because of this, indirect methods have not been widely implemented in many general trajectory optimization problems [124, 126].

The Direct Method The direct method transforms an optimal control problem from the infinite dimensional space, in which it naturally resides, to finite dimensions through a

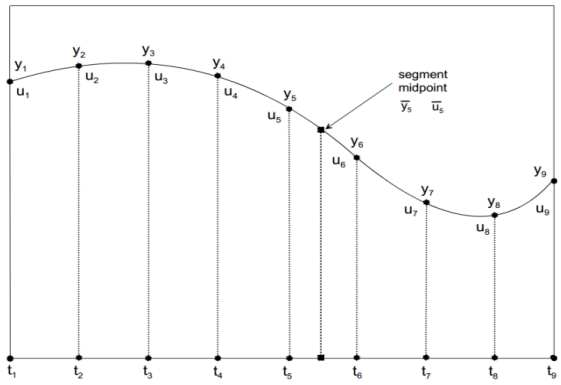

Figure 2.11: Trajectory and control discretization [127]

process called transcription. The result is a trajectory represented as a sequence of phases, as depicted in Figure 2.11. This produces an optimization problem that fits within the domain of nonlinear programming (NLP). With this, it is then possible to apply a variety of common optimization algorithms.[123]

Direct methods have the advantage of being relatively robust and simple to implement, and as such have been applied extensively in trajectory optimization codes. [124, 126]. However, they suffer from a number of drawbacks. When an optimal control problem is transcribed, the resulting NLP problem inherently has fewer degrees of freedom than the original, and as a result, solutions can become sub-optimal, even if the NLP problem solution is itself solved optimally. [128] In this the Direct method is revealed to be less accurate than Indirect method. [129] Additionally, the NLP problem posed by the Direct method has been shown to be highly multi-modal in nature. [130, 131] The optimizers traditionally used with the Direct method are gradient based, or local, and so this poses an additional problem with sub-optimal solutions. [73]

Shooting Shooting, the first of two approaches to the solution of the equations of motion, is also sometimes referred to as time stepping. It calculates the current state vector based on state information from either the current and/or the previous time steps. Essentially, at each time step the system equations are calculated, and the resulting derivatives are used to update the state to the next time step. There are several techniques on how the derivatives

are used to update the state. Euler methods are shown in Equation 2.5

$$x_{k+1} = x_k + h_k \left[\theta \mathbf{f}_k + (1-\theta)\mathbf{f}_{k+1}\right] \tag{2.5}$$

where $\mathbf{f}_k = \dot{\mathbf{x}}$ and h_k is the time step. When θ is 1, the method is called Euler forward, because the next state is dependent entirely on the information from the previous state. This type of numerical integration is called explicit integration [132]. When θ is 0, the Euler backward method is used [133]. In this case the next step is dependent on the previous state values but derivatives from the next state. These methods are called implicit integration methods because the state x_{k+1} is on both sides of the equation [132]. Because of this, the equations must be solved iteratively. In general, explicit methods are easier to implement and more computationally efficient, but not as numerically accurate as implicit methods.

Euler methods are the simplest form of shooting methods; [134] the most common numerical integration method is an explicit fourth order Runge-Kutta method. [135] Both of these are single-step methods, as only one point is used to compute the second point (even though implicit methods require the current and previous point). There are several other types of single-step methods, such as Heun and Taylor algorithms. Another class of numerical methods uses several of the previous steps (once the algorithm has been started) to compute the next step. These are known as Predictor-Corrector methods. Predictor-Corrector methods are generally more complex, but can be more accurate. One example used in spaceflight trajectory optimization is the Adams-Bashforth-Moulton method [136].

Collocation In literature, collocation is sometimes referred to as transcription. [124, 137] Note, the word transcription is used differently when speaking in the context of Direct optimization methods. To avoid confusion, transcription will be used here only in the context of Direct methods, and collocation will be used to refer to the method of numerically solving differential equations.

Collocation employs an interpolating function, usually in the form of a polynomial, to

approximate the state of the system. At collocation nodes, constraints are used to compare the derivative of the approximating function to the solution of the system of equations at that point. These constraints are called defect constraints and are shown in equation 2.6.

$$\xi = \mathbf{X}(t_j) - \mathbf{f}(\mathbf{x}(t_j), t_j) \tag{2.6}$$

Frank [138] summarizes the collocation method as construction of "a polynomial that passes through y_0 and agrees with ODE at s nodes on $[t_0, t_1]$. Then [...] let the numerical solution be the value of this polynomial t_1." Because of the way the collocation method solves differential equations, namely solving for all the variables at once, it is considered an implicit method.

The optimization method (Direct vs Indirect) and the numerical integration method (Shooting vs Collocation) can be combined in any way to form four different numerical solution approaches. Regardless of the approach selected, though, the strengths and weaknesses of this type of model are still generally the same. Numerical modeling achieves the highest fidelity possible, allowing for any trajectory problem that can be formulated within code to be modeled. However, this comes at a price, as numerical models can be extremely expensive from both computational and man-hours perspectives.[68, 71, 72]

Analytic

Generically, an analytic model is one that is "treated or treatable by or using the methods of algebra and calculus." [139] From a mathematical perspective, it is "a solution to a problem that can be written in 'closed form' in terms of known functions, constants, etc." [140] A combination of these definitions is true of analytic LV performance models, as methods of algebra and calculus are leveraged to develop either partially or fully closed form solutions for modeling LV missions of a defined scope.

The most well known closed-form analytic LV performance model is without question

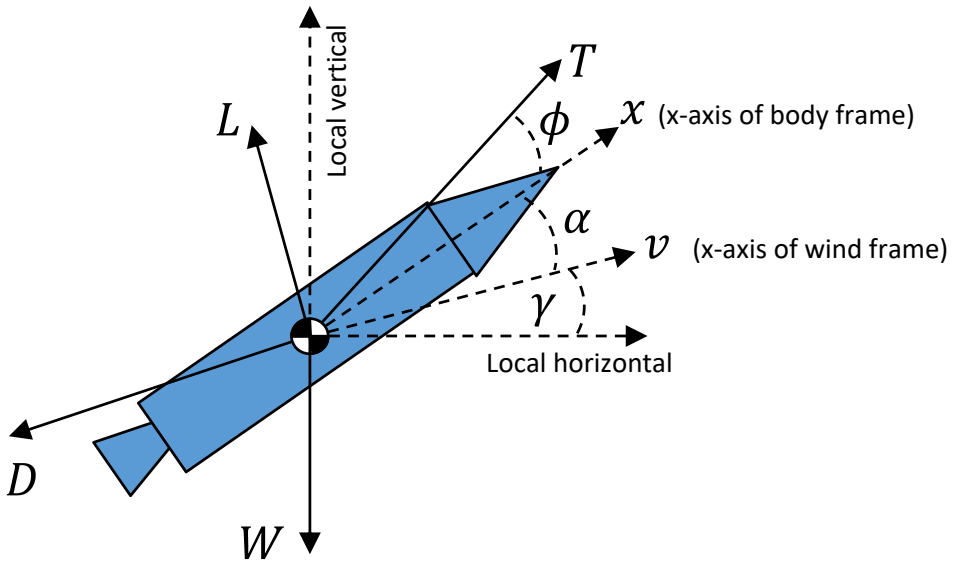

Figure 2.12: Free body diagram of forces used in Rocket Equation derivation

the Rocket Equation, and any discussion on LV performance modeling must necessarily begin with this fundamental relationship. The Rocket Equation, also commonly referred to as Tsiolkovski's Rocket Equation, describes the dynamics of a system propelled by the expulsion of mass (i.e. a rocket). The name is for Konstantin Tsiolkovsky, a Russian rocketeer often credited with first publishing the derivation. Derived from the momentum equation, the most commonly used and familiar form of the Rocket Equation was depicted in (1.2). The equation estimates a rocket's performance capability, measured as the potential for change in velocity, ΔV, as a function of the velocity of the expelled mass (or exhaust), v_e, the initial system mass, m_0, and the final system mass, m_f. The exhaust velocity is interpreted as a measure of propulsive efficiency, and the ratio m_0/m_f, also known as the Mass Ratio, MR, indicates the amount of propellant expelled relative to the overall mass of the system.

Arriving at (1.2) requires that a number of assumptions be made to simplify the Rocket Equation that emerges directly from the derivation. It is instructive to examine these assumptions closely, as they are related to some of the fundamental issues in LV performance. The raw result of the derivation, prior to application of the usual assumptions, is presented

Table 2.7: Explanation of loss terms appearing in (2.7), the Rocket Equation

Term	Description
$\left[1-\left(1-\overline{p_a}\frac{A_{exit}}{T_{vac}}\right)cos(\overline{\alpha+\phi})\right]$	This term represents two different types of thrust losses: Thrust loss due to the propulsion system fighting atmospheric pressure at the exit plane of the nozzle; and thrust loss due to the thrust vector being directed off of the velocity axis during steering.
$\frac{\overline{qC_DA}}{T_{vac}}$	This term represents the drag losses incurred during ascent to orbit. The drag is averaged across the entire flight.
$\frac{\overline{W}}{T_{vac}}sin\overline{\gamma}$	This term represents the losses incurred due to fighting gravity. Losses are greater for lower thrust-to-weight (T/W) ratios and for steeper flight path angles.

here (with accompanying free body diagram in Figure 2.12):

$$\begin{aligned}\Delta V = \Big\{1-\Big[1-\Big(1-\overline{p_a}\frac{A_{exit}}{T_{vac}}\Big)cos(\overline{\alpha+\phi})\Big] \\ -\frac{\overline{qC_D}A}{T_{vac}}-\frac{\overline{W}}{T_{vac}}sin\overline{\gamma}\Big\}v_{e_{vac}}\ln\left(\frac{m_0}{m_f}\right)\end{aligned} \tag{2.7}$$

Equation 2.7 presents the Rocket Equation in its truer form, as derived from the equations of motion. If all of the possible simplifying assumptions are applied to (2.7) – that is, if all of the terms in the bracketed expression that are being subtracted from unity are set to zero, the more commonly known form of the Rocket Equation as presented in (1.2) emerges. The additional terms in (2.7) represent real world losses, and are described in Table 2.7:

These losses are experienced by all real LVs, and so it becomes obvious that the ΔV depicted in (1.2) is really idealized for the case where there are no losses. Because of this, the quantity is known as the ideal ΔV, and the following relationship is used to describe its relation to real world quantities:

$$\Delta V_{ideal} = \Delta V_{mission} + \Delta V_{thrust\ loss} + \Delta V_{drag\ loss} + \Delta V_{gravity\ loss} \tag{2.8}$$

Assuming some of these losses to be zero is appropriate and useful in certain cases. For example, any flight that occurs in a vacuum, such as an ascent from the lunar surface, will not experience drag losses or those thrust losses attributed to atmospheric backpressure. Similarly, a vehicle that flies a trajectory primarily perpendicular to the local gravity field will experience no gravity losses. Approximately all of these conditions coincide for many in-space maneuvers (the flight path angle is not always exactly perpendicular to the gravity field, but for large enough T/W, the gravity loss is still negligibly small), and so assuming zero losses is often acceptable.

It is clear that none of these losses can be ignored for LVs ascending to orbit through a planetary atmosphere. Because of this, to design a LV capable of achieving the $\Delta V_{mission}$ set by a specified mission, it is necessary to estimate the expected losses, which are then added to the $\Delta V_{mission}$ to arrive at the ΔV_{ideal} the LV must be sized to. This estimation of ΔV_{losses} is the process that will be referred to here as LV performance modeling.

The strengths and weaknesses of the Rocket Equation epitomize the Analytic class of models. Under a specific set of assumptions, it provides an excellent estimate of performance; however, as those assumptions are violated, its accuracy quickly degenerates. Efforts to develop more sophisticated and comprehensive models have shown the true limitation of the Analytic approach. Simplifying assumptions that must be made due to the non-analytic nature of many parameters in real world problems can severely limit the scope of applicability[45]; specifically, nonlinearities due to LV aerodynamics and high accelerations have been found to be too significant for a purely analytic solution.[69]

Historically, a significant amount of research and development has been invested into the derivation of models which fall under a less stringent definition of analytic, where models are not strictly closed-form in nature. These "guidance" or "steering" laws generally leverage analytic manipulations to reduce the dimensionality of solving for optimal steering programs, and can be used to rapidly (often in real-time) compute near-optimal ascent paths. This approach has proved to be extremely fruitful, as it dramatically increases the

scope of problems that can be addressed from the limited cases available to closed-form models. [69] An example of this modeling approach is presented in a reference text compiled at the Jet Propulsion Laboratory in 1963 entitled *Flight Performance Handbook for Powered Flight Operations*.[141] In it, the authors derive an exact, closed-form solution to the exoatmospheric flight of a LV stage under the following assumptions:

1. The magnitude of the acceleration due to gravity is a constant during the burning period.

2. The variation in radial distance while burning is small compared to the initial distance from the attracting mass.

3. Thrust and propellant flow rate are constant with time.

4. Motion occurs in a plane.

5. Thrust attitude varies linearly with time.

Perhaps the most well known of these is the Linear-Tangent Steering, which provides the optimal steering program for exoatmospheric flight, regardless of thrust variation with time.[142] These "guidance," or "steering" models still require iterative numerical solution, and so they begin to merge with Numerical models.

Analytic models can be quite accurate, exact even, within the context for which they are derived. In practice, analytic models are generally applied to exoatmospheric trajectory segments, with another type of model handling endoatmospheric flight for a full LV mission simulation. They are also used effectively in conjunction with numerical models to find near-optimal solutions more efficiently.

Empiric

Webster defines empirical as "originating in or based on observation or experience."[143] Statistical regression, whether parametric or nonparametric, forms the basis for the vast

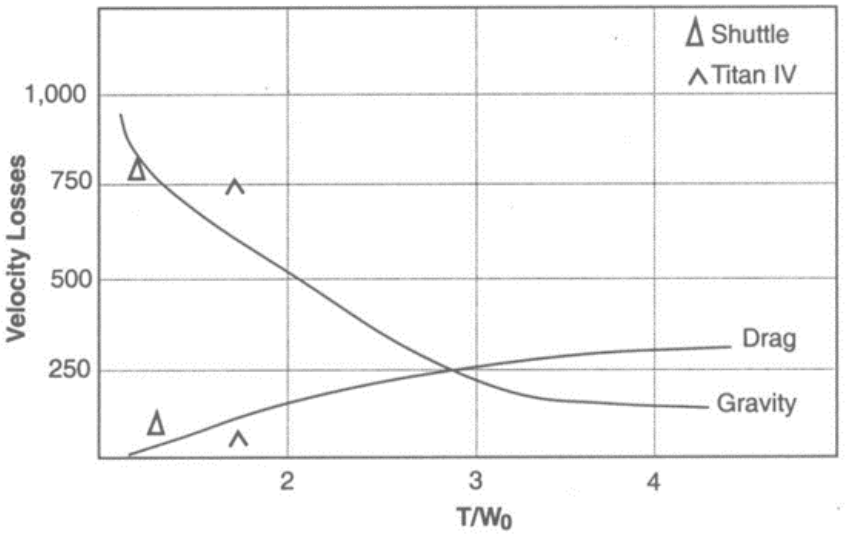

Figure 2.13: Gravity and Drag losses from Wertz and Larson [144]

majority of empirical models. The particular forms of regression employed can vary, depending on the size and nature of the data set available. This data set can proceed from a variety of different sources, including higher fidelity trajectory optimization or quoted performance of past and current operational LVs. Models that are purely empirical in nature ideally should not be used in extrapolation.[121] However, there is a class of empirical models that attempt to leverage some knowledge about the nature of the underlying physics in order to provide a structure to the regression model that could align with anticipated behaviors of the response. These begin to take on some mechanistic qualities.

The most sophisticated empirical LV performance models date back to over fifty years ago, prior to the proliferation of digital computing. [145, 146, 147, 141] In September of 1959, Dergarabedian and Ten Dyke published a technical report, entitled *Estimating Performance Capabilities of Boost Rockets*; this would prove a landmark one for conceptual LV performance modeling, as it would go on to be reprinted in various other texts [148, 149], as well as provide a starting point for more sophisticated efforts. [141] In their publication, Dergarabedian and Ten Dyke mention the following three main points as motivation for their work: [145]

1. The time required to prepare the input data and arrange for computer time can be quite long compared to the actual computation time consumed

2. The degree of accuracy required of results for preliminary design purposes is quite different from that required for detailed design

3. An analytic relationship that can be graphed may provide a better "feel" for the trades that exist for the system in question

Interestingly, these same arguments may still hold for the early stages of conceptual design, even after several decades of tremendous advances in digital computing! More recent examples on the statistical LV performance model front include the graph from Wertz and Larson's book depicted in Figure 2.13; a white paper published by John Schilling, in which he modified the model originally published by Townsend to work for more modern LVs; [150, 147] and several efforts involving surrogate modeling, in which a numerical trajectory method is used to generate a set of training data for a regression model. [151, 110, 152]

Empirical models' strengths reside in their potential for rapid evaluation and accuracy; their weakness is that they generally can only be applied within the specific context (design parameter ranges and mission profiles) from which they were regressed. They do not see widespread use in LV performance estimation today due to a combination of factors including the general availability of computing resources for numerical modeling, and a lack of empirical models that are general enough to work for a broad range LV designs and mission profiles.

Heuristic

An heuristic is "a commonsense rule (or set of rules) intended to increase the probability of solving some problem." [153] A less formal yet equally appropriate definition would be "a rule of thumb." As such, heuristics can lie on either side of the boundary between Reddy's

Intuitive and Empirical models. The difference lies in whether the heuristics are stated as qualitative or quantitative. Quantitative heuristics of LV ascent losses are found in the form of statements such as "for medium to large launch vehicles on nominal trajectories, the velocity losses due to gravity fall between 750 m/s and 1500 m/s" from Wertz and Larson's *Space Mission Analysis and Design*. [144] They are very common in the literature, and are used primarily as exemplars in reference texts [144, 154, 155], or in situations when representative values are acceptable in lieu of higher fidelity calculations [156, 157].

The strengths and weaknesses of heuristics are generally understood and accepted. While they do not provide the fidelity required to do real design trades, they are well suited to do rough order of magnitude (ROM) calculations, as they provide the fastest and ultimately most flexible of all the modeling techniques. An heuristic can be stated for any given mission or vehicle context. For example, different velocity losses are just as easily stated for launch to LEO or geosynchronous orbit (GEO) [158]; for launch from the surface of Earth, Mars, or the Moon [156]; or for different Liftoff T/W values [76].

Hybrid Models

While this section does not technically add a new model type to the list of those already reviewed, it is important to note that a common strategy in past efforts to overcome the shortcomings of the different model types has been to combine them into hybrids. The most common hybrid observed is a mixing of analytic and numeric models, where the analytic is used to provide some dimensionality reduction and guidance, while the numeric tackles the overall solution. This has proved a very successful approach for very specific applications such as for air-breathing, lifting ascent LVs [159] or strictly exoatmospheric flight. [142] Other hybrids are less common, but still occur; examples include combining empiric models of first stage flight with analytic models for subsequent stages [145], and numeric models of endoatmospheric flight with empiric models of exoatmospheric flight. [152] However, these types of hybrid models suffer from two drawbacks. First, they tend

to be somewhat limited in scope; and second, the introduction of an interface or hand-off between different models usually comes at the expense of wrapping an additional optimization loop around the models, consuming some of the gains in speed and simplicity that were the intent of the effort.

2.5 Research Objectives

Chapter 2 has sought to answer the first portion of the overarching research question posed in Chapter 1: **What are the major challenges facing LV architecture selection?** Through a review of decision making in design, uncertainty, and specific challenges related to LVs, a number of observations can be drawn. These are the following:

Observation 1: Early design decisions determine the fundamental attributes of a system, and "lock in" a large fraction of the system life-cycle cost in the process.

Observation 2: Early decisions are made in the presence of significant risk, since very little design knowledge is available for decision makers to work with.

Observation 3: Design freedom manifests itself during architecture selection as a significant source of volitional uncertainty.

Observation 4: Many methodologies have been assembled with the intent of equipping early decision makers with increased knowledge, all of which rely on some form of probabilistic techniques to account for uncertainties

Observation 5: A review of past LV architecture studies shows no evidence of these methods being employed, or of any sort of treatment for uncertainty.

Observation 6: The coupling of a Multi-Disciplinary Optimization (MDO) problem with an optimal control problem in LV sizing imposes a significant challenge to implementing techniques dealing with uncertainty in early stage decision making.

So, from these observations, the major challenges facing LV architecture selection are identified as decision making under uncertainty, and the resulting need to perform probabilistic analysis over a LV sizing process that is difficult to fully automate.

The remainder of this thesis is aimed at answering the second part of the overarching Research Objective, which is **"how can [these challenges] be addressed to enable better decision making?"** NASA's Risk-Informed Decision Making process would seem to provide an excellent starting point for incorporating uncertainty into the LV architecture selection process; however, tailoring is needed to accomodate issues specific to LVs, especially in regards to LV performance estimation. Thus, the objective for this thesis can be stated as:

> **To develop a methodology for enabling risk-informed decision making during the architecture selection phase of LV programs**

The argument put forward in Section 1.3.3 leads to the formalization of an overarching hypothesis regarding how risk-informed architecture selection might be accomplished:

> **If volitional uncertainty in the form of design freedom is quantified and propagated, decision makers will be able to perform risk-informed LV architecture selection.**

CHAPTER 3
METHODOLOGY DEVELOPMENT

In Chapter 2, NASA's Risk-Informed Decision Making (RIDM) process was identified as an ideal point of departure for tackling the objective of this thesis, **"to develop a methodology for enabling risk-informed decision making during the architecture selection phase of LV programs."** Sections 2.1 to 2.3 review the steps in RIDM, identifying applicable methods and techniques that could be leveraged in tailoring the process to LV architecture selection. Trajectory performance evaluation was observed to be the biggest challenge to implementing probabilistic analyses, so Section 3.1 discusses the approach proposed for addressing this.

3.1 Hypothesis 1: Empirical Performance Modeling for Architecture Selection

Section 2.2.2 identified sampling-based uncertainty propagation as the most appropriate approach for implementing probabilistic analyses during LV architecture studies. Research Question 1a is focused on finding the most effective sampling strategy, while Research Question 1b seeks to establsish whether full numerical trajectory optimization is feasible within the context of a sampling approach. While this question must be answered explicitly through experimentation, Section 1.3.2 provided a strong indication that explicit trajectory simulation will be too cumbersome and costly to be practical for uncertainty propagation. On the other hand, Villeneuve demonstrated the ability to analyze many thousands of LVs using an empirical regression of trajectory performance.[79] For this reason, Hypothesis 1 is proposed:

Hypothesis 1: If an empirical LV performance model is used in place of explicit trajectory optimization, then propagating volitional uncertainty

during architecture selection will become a feasible undertaking.

Section 3.2 takes a closer look at some of the more notable empirical models that have been published in the past, while Section 3.3 examines the primary elements involved in the creation of an empirical model.

3.2 Review of Empirical Performance Models

The review performed in Section 2.4.1 revealed that a number of empirical LV performance models have been developed in the past. With narrowing the focus for this methodology to empirical modeling, it is appropriate to go and examine each of these historical models more closely. Of interest would be an assessment of each model's predictive capabilities. In Section 2.4.2, the possibility that historical models have lost their utility in the face of modern LV design practices was acknowledged; therefore, benchmarking these models is desirable, if possible. While a true benchmarking in a controlled setting that ensures "apples-to-apples" comparisons would require access to the original datasets used in creating the models, an assessment of several models was performed using a set of LV data collected from literature. Altogether, 126 data points were collected for 25 LV variants. Figure 3.1 shows lineups for 20 of them. Figure 3.2 shows definitively that the rocket equation alone is not able to model the LV mission – it fails to even capture the correct trend!

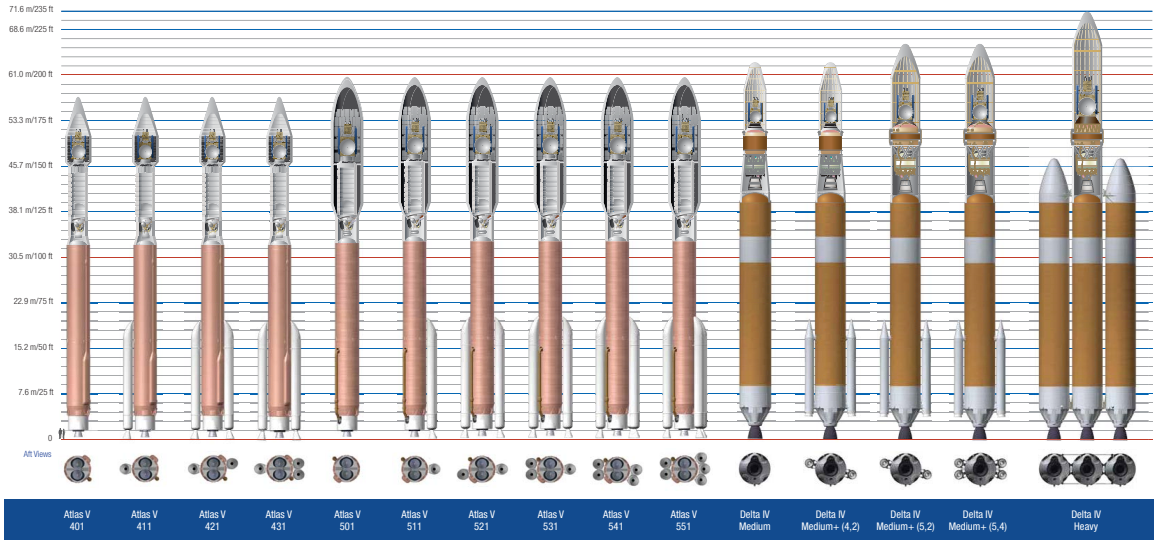

(a)

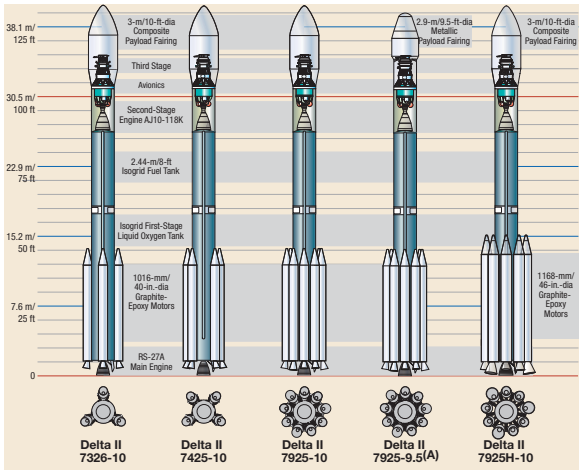

(b)

Figure 3.1: Lineup of United Launch Alliance vehicles (a) Atlas 5 and Delta 4 families, and (b) Delta 2 family [160, 64]

3.2.1 Dergarabedian & Ten Dyke, 1959

In September of 1959, Dergarabedian and Ten Dyke published a technical report entitled *Estimating Performance Capabilities of Boost Rockets*. [145] This report would prove a landmark one for conceptual LV performance modeling, as it would go on to be reprinted in various other texts [148, 149], as well as provide a starting point for more sophisticated efforts. [141] To construct their model, several hundred single-stage vehicle trajectory

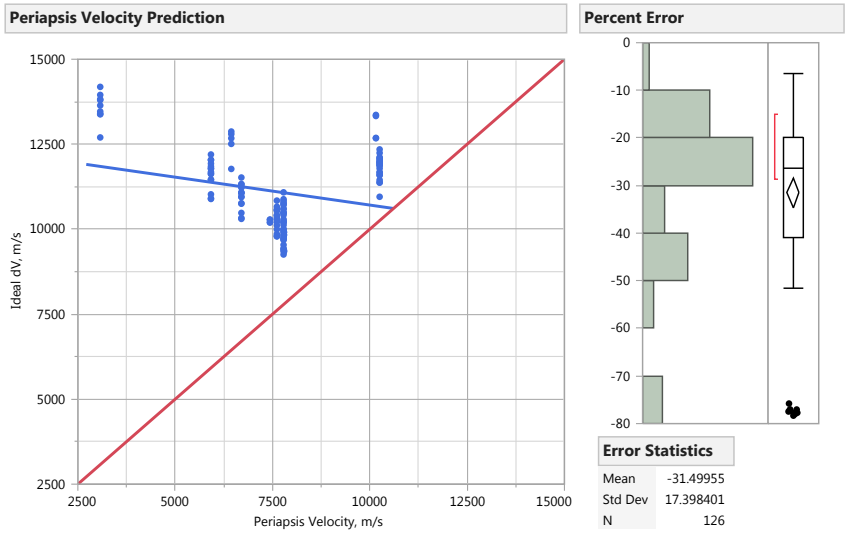

Figure 3.2: Actual ΔV_{ideal} compared to Periapsis Velocity, which is typically used as $\Delta V_{mission}$ in the literature

simulations were flown along a gravity turn to burnout, and the results were regressed using (3.1):

$$V_L = (gt_b - K_{gg})\left[1 - K_g\left(1 - \frac{1}{r}\right)\left(\frac{\beta_b}{90}\right)^2\right] + K_D\frac{C_{D_{max}}A}{W_0} + K_a \tag{3.1}$$

The regressors were selected based on an analysis of the equations of motion, and the form of the equation was custom designed based on observed and expected patterns in the data. The regression captures the values for the coefficients K_{gg}, K_g, K_D, and K_a in a sequence of four nomographs, in which they are computed based on the LV stage design parameters T/W, $I_{SP_{vac}}$, and $I_{SP_{sl}}$.

Although the detailed loss estimation regression was only performed for one-stage vehicles, the authors suggested an approach to extending the model to multi-staged vehicles. This consisted of using (3.1) to calculate velocity losses for the first stage, and then using (3.2) to calculate the losses for all subsequent stages.

$$V_L = g\left(\frac{R_e}{R_e + \bar{h}}\right)^2 t_b cos\bar{\beta} \tag{3.2}$$

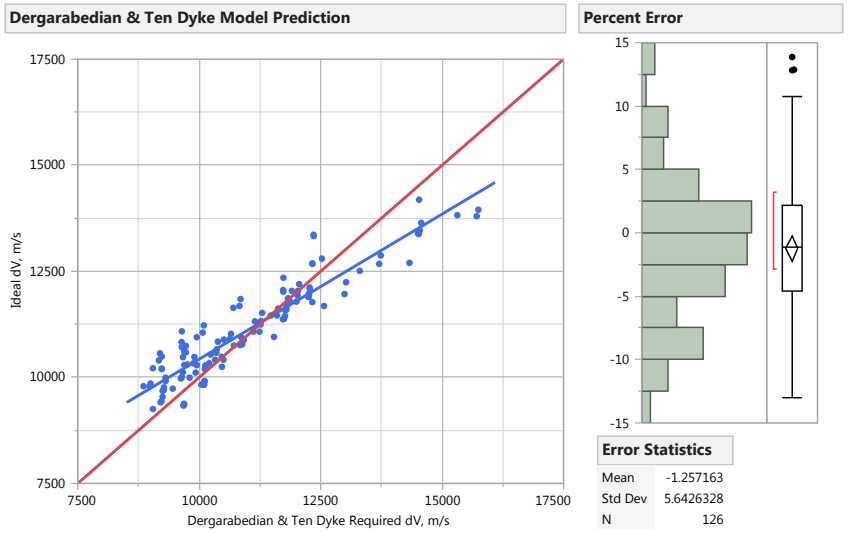

Figure 3.3: Actual ΔV_{ideal} compared to ΔV predicted by Dergarabedian and Ten Dyke's model [145]

This extension to multiple stages introduced a number of assumptions, including:

1. Propulsion system mass flow rates are all constant
2. First stages follow zero-lift trajectories (gravity turns) through the sensible atmosphere
3. All atmospheric losses (drag and nozzle backpressure) occur during flight of the first stage
4. LV drag polars all have the same shape, and are scaled in magnitude by a single parameter, $C_{D_{max}}$
5. First stages burn out at altitudes $> 200,000$ ft and flight path angles < 75 deg
6. There are no "coasting" periods between stages
7. Implicitly assumes two stage vehicles (or that all stages above the first can be analyzed as one)

3.2.2 MacKay and Weber, 1961

In 1961, researchers at NASA's Lewis Research Center published a Technical Note entitled *Performance Charts for Multistage Rocket Boosters*. [146] In it, they presented a method for conceptual LV sizing using a large set of data generated in a study characterizing the ETO performance of three stage LVs. The empirical performance model derived from the data was cataloged in a series of 61 nomographs.

The Lewis model differs from many of the other models reviewed in the predictors and responses used in its development. Unsurprisingly, the initial T/W and I_{SP} of each stage make an appearance; however, the model also used a new parameter, the propellant fraction (PF), defined in (3.3), as both a predictor and a response of the model. In modeling three stage vehicles, the PF for the first and second stages are inputs to the model, and the third stage PF required to achieve the target orbit is calculated. This sets the Lewis model apart from the other models reviewed, as the Lewis model does not directly output an estimate of the ΔV_{losses}. Instead, it implicitly captures the ΔV_{losses} by sizing the LV to provide all of the ΔV_{ideal} required, including both the $\Delta V_{mission}$ as well as the ΔV_{losses}.

$$PF_i = \left(\frac{m_{propellant}}{m_{gross}}\right)_i \tag{3.3}$$

The fundamental assumptions upon which the Lewis model is built include many of the same ones used in the two previously reviewed models. They are as follows:

1. Propulsion system mass flow rates are all constant
2. First stages follow zero-lift trajectories (gravity turns) through the sensible atmosphere; subsequent stages follow linear-tangent steering
3. All atmospheric losses (drag and nozzle backpressure) occur during flight of the first stage
4. A constant C_D of 0.4 was used for all vehicles during first stage flight

5. There are no "coasting" periods between stages

6. Explicitly assumes three stage vehicles; extendable to two stage vehicles

3.2.3 Townsend, 1962

The Martin Marietta Corporation published *Design Guide to Orbital Flight*, an expansive reference text on spacecraft flight mechanics, in 1962. [161] In this work, the "Ascent to Orbit" chapter authored by George Townsend included a method for quickly estimating LV performance losses by hand. [147] In a manner similar to Dergarabedian and Ten Dyke, Townsend developed his empirical model based on data from about one hundred distinct LVs which were analyzed on a digital computer. However, he took a much different approach to the regression modeling; rather than fitting to losses incurred by individual LV stages, Townsend opted to fit a model to the performance losses incurred across the entire ascent to a circular parking orbit.

In order to fit the LV performance regression across the entire trajectory, Townsend leveraged the simplifying assumption that the losses experienced by LVs are incurred primarily on ascent to a circular parking orbit, regardless of what final target orbit they are intended for. He justified this assumption by observing that any subsequent in-space maneuvers to achieve a specific non-circular orbit will generally occur at flight path angles very close to zero, and so gravity losses can be neglected (as can drag losses, since the maneuvers were performed in a vacuum).

The resulting regression model was published in the form of a single nomograph, providing LV ascent losses as a function of parking orbit altitude and total flight time. There were not many explicit assumptions in Townsend's approach, the biggest one regarding insertion into intermediate circular parking orbits having already been discussed. However, the extremely high level of abstraction in the model, with flight time representing the entirety of all possible LV design concepts, could be viewed as containing a host of implicit assumptions.

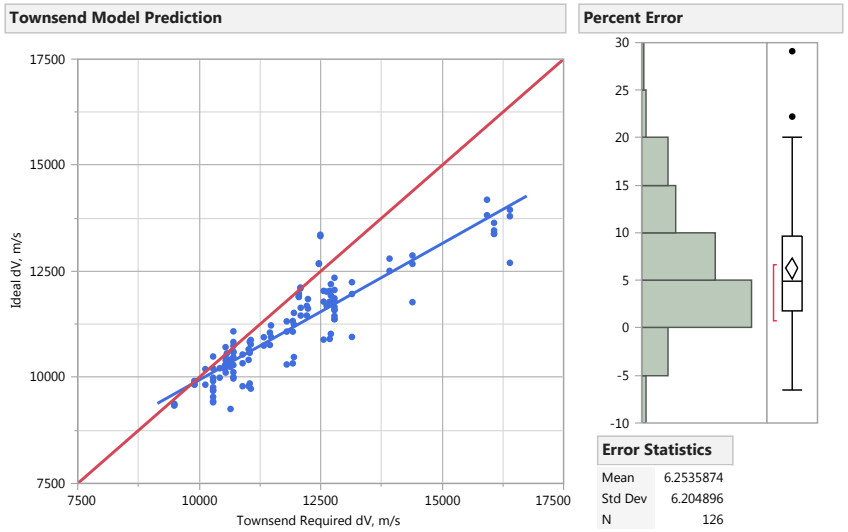

Figure 3.4: Actual ΔV_{ideal} compared to ΔV predicted by Townsend's model [147]

3.2.4 White, 1963

Rounding out the investments in empirical LV performance models of the early 1960s, Frederick White oversaw the compilation of *Flight Performance Handbook for Powered Flight Operations*, which was commissioned by the California Institute of Technology's Jet Propulsion Laboratory in 1962 to be a reference for their design engineers. [141] As stated in the preface to the book, "the backbone of the performance evaluation portion of the handbook was built around" the work published by Dergarabedian and Ten Dyke. The original model was updated and augmented, both to capture a wider range of LV design parameters and missions, as well as to provide a more accurate estimate of performance losses, especially for upper stage flight.

The resulting model was in fact a hybrid, as it leveraged the empirical approach developed by Dergarabedian and Ten Dyke, as well as an analytic model for exoatmospheric flight. Due to the complex nature of the analytic model (and because of the limited availability of computing at that time), the model was presented as a sequence of 47 nomographs! The authors acknowledge that performing this analysis by hand could take a considerable amount of time, but insist that once familiar with the approach, an engineer should

be able to complete an analysis in a couple of hours. While even this seems lengthy and tedious, it no doubt provided a unique capability at the time; in the age of modern computing, it may still fill a unique niche in LV performance analysis, assuming the information embedded in the nomographs could be codified. The assumptions used in this model are:

1. Propulsion system mass flow rates are all constant
2. Vehicles follow zero-lift trajectories (gravity turns) through the sensible atmosphere
3. All atmospheric losses (drag and nozzle backpressure) occur during flight of the first stage
4. LV drag polars all have the same shape, and are scaled in magnitude by a single parameter, $C_{D_{max}}$
5. There are no "coasting" periods between stages
6. Implicitly assumes two stage vehicles (or that all stages above the first can be analyzed as one)

3.2.5 Schilling, 2009

The latest installment in the arena of empirical LV performance models came in 2009, when John Schilling of Silverbird Astronautics published a white paper in which he presented a modification to the model developed by Townsend. [150] Schilling incorrectly states Townsend's assumptions for multistage LVs to be identical stage MR, T/W, and I_{SP}; however, in motivating the need for an update to Townsend's model, he does provide an excellent qualitative observation regarding the discrepancies between Townsend's assumptions and the behavior of modern LVs. Schilling observes that modern LVs exhibit little concern over acceleration (or T/W) for phases of flight occurring above the sensible atmosphere; he cites the Ariane 5 as an example of this.

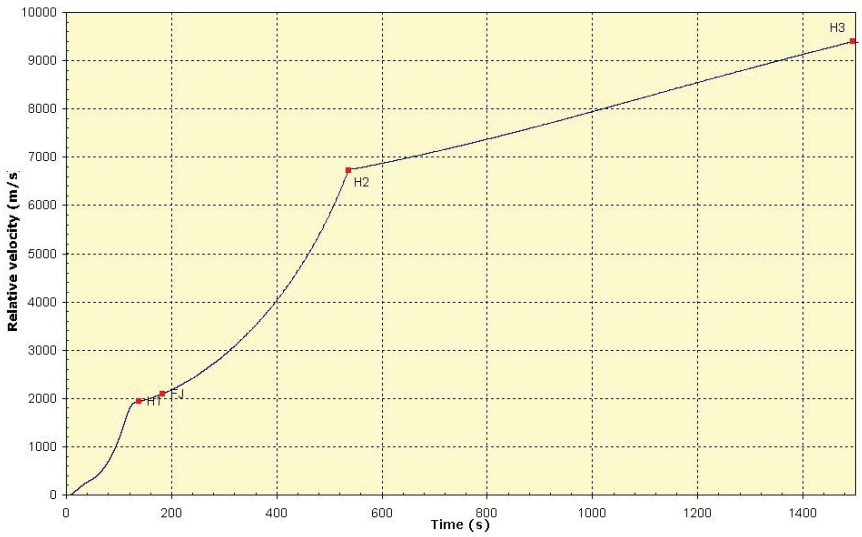

Figure 3.5: Typical acceleration profile for Ariane 5 ascent to GTO [162]

In Figure 3.5, inspection of the Ariane 5's acceleration profile for a nominal ascent to GTO reveals the vehicle averaging a brisk 1.56 g's of acceleration during the first 130 seconds of flight, then eventually settling in to a leisurely 0.28 g's of average acceleration for the last 975 seconds of burn time. [162] As observed in Section 3.2.3, Townsend varied stage T/W parametrically between 1.2 and 2.0, which clearly does not capture the behavior of the Ariane 5 upper stage. The effect is to render Townsend's model very inadequate to the task of estimating losses for the Ariane 5 and many other modern LV - hence Schilling's update of the model.

The modification Schilling made to Townsend's model consisted of replacing the original flight time regressor with a weighted average between the flight time of the actual LV under consideration, and a hypothetical three stage equivalent vehicle. With the regressor modified, Schilling then refit the model to a database of over one thousand LV performance values, consisting of known data points for seventeen modern LVs. Application of Schilling's model to the test dataset produces the results depicted in Figure 3.6.

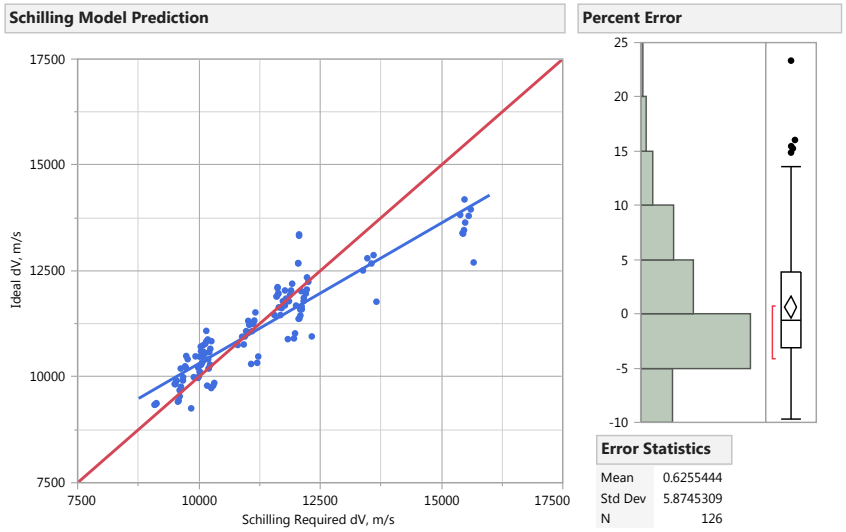

Figure 3.6: Actual ΔV_{ideal} compared to ΔV predicted by Schilling's model [150]

3.2.6 Contemporary Efforts

Several notable empirical performance modeling efforts have been published in the past decade that leverage modern LV design concepts and analyses. Qazi published an effort using stage-wise Artificial Neural Networks (neural nets for short) of $\Delta V_{required}$ in 2006; [151] one year later, he followed it with a similar study using Support-Vector Machines. [110] Steffens published a number of empirical LV performance models from 2014 to 2016. [163, 131, 130, 164, 165] Both neural nets and Response Surface Equations (RSEs) were employed. Dees [166], Walsh [152], and Zwack [167] each also published modeling efforts using RSEs. Villeneuve's models, mentioned prerviously in Section 1.3.4, also leveraged both RSEs and neural nets. [79]

While each of these has its own unique elements, they all share a number of common characteristics. All subscribe to "black box" modeling approaches, taking a purely statistical approach to model construction. Also, the intended scope for each of these models is limited to a single architecture. For example, Villeneuve's thesis studied several different LV architectures, but a separate performance model was created for each. Finally, they all utilize many more regressors than the historical models; this is made feasible by the ability

to generate large sets of training data that is afforded by modern computing and simulation technologies.

3.3 Requirements for New Model Development

Based on the discussion in Section 2.4.1, there are two primary criteria which should guide the development of a new empirical performance model: accuracy and generalization. Inexpensive evaluation is an inherent quality of empirical models once they have been trained, so the third criteria identified, speed, is implicit. In considering model accuracy, the question that must be answered is "how much is required?" Accuracy can be thought of in two separate but related ways. The first way is the standard approach in regression, where accuracy is measured as the model's error in predicting known truth values. This error is called Model Fit Error when measured against the training data, and Model Representaiton Error when measured against validation data (which was not used to train the model). [168]

Dergarabedian and Ten Dyke loosely estimated the error in their first stage loss equation to be on the order of 1.5% on the velocity achieved. They did not rigorously quantify this, and neither did they propagate this through to an estimated error for the full ascent performance. [145] MacKay and Weber explicitly state that "the accuracy of these generalized charts is adequate for preliminary design purposes," and show approximately 3% error in 3rd stage mass ratio estimation. [146] Townsend states that his results "checked generally to within 5% of the values plotted and were consistently better than 10% in error." [147] With his update to Townsend's model, Schilling claimed to achieve less than 3% error in total $\Delta V_{mission}$, and 10% in payload performance. [150] Villeneuve showed a range of empirical model errors between 1-3%; however, the simplified physics of his underlying simulation exhibited approximately 3% error when compared to higher fidelity physics, and so the empirical model error with respect to full trajectory performance was likely in the 5-6% range.

The second way accuracy can be assessed is in how decision outcomes are affected by

using the model. In the case of architecture selection, sufficient accuracy is achieved if model error does not result in the choice of different architectures than would be selected based on high-fidelity data. Specifically, only as much accuracy is needed as is required "to assess compliance with imposed constraints and support selection between alternatives." [89] This indicates that the level of acceptable accuracy is dependent on the decision being made, and may not be known a priori. For this reason, an iterative accuracy refinement process is suggested.

The second criteria that must be targeted in new model development is generalization. This is not the generalization often discussed in parametric regression modeling that deals with how overfit or underfit a regression model is. Rather, what is meant by generalization here is that the model must provide predictive capabilities spanning across multiple different architectures. Of the models reviewed in Section 3.2, all of the examples from contemporary literature were architecture specific. These models achieve a high degree of accuracy, but are only valid for evaluating concepts falling within the scope of the Design space explored (as defined by design parameter ranges) for the particular architecture modeled.

An empirical model, as defined in Section 2.4.2, consists of a statistical regression against observed data points. There are three primary elements that play into the creation of an empiric model, whether parametric or nonparametric: Responses selection, regressor selection, and model selection. These manifest themselves in the context of LV performance modeling through a sequence of three questions that must be answered: (1) How should ΔV_{losses} be defined in order to best characterize LV performance? This amounts to a question regarding what form of the response will best facilitate model creation, and is explored in Section 3.3.2; (2) What are the relevant parameters that drive LV performance, that is, which regressors should be used to develop the empirical model? This question is discussed in Section 3.3.3; and (3) How should the relevant parameters be employed to predict LV performance? This question revolves around which regression modeling approach

will be best suited to capturing the LV design space, and is addressed in Section 3.3.1.

3.3.1 Model Selection

In identifying potential regression model types for consideration, it is helpful to summarize the characteristics of the problem to be addressed as it has been described. The response of interest, as presented in Section 3.3.2, is ΔV_{losses}, which takes the form of a continuous scalar variable. Candidate regressors, discussed in Section 3.3.3, include both scalars and infinite-dimensional (functional) variables. Finally, depending on the form of regressors ultimately selected, it is possible that a large number of regressors will be necessary to describe the full spectrum of architecture variations that is targeted by the model.

Of these requirements, the need to work with functional regressors is perhaps the most specific and constraining one. In the realm of statistical regression, there are generally two main approaches to dealing with functionals. The first consists of transcribing the variables from the infinite dimensions into a lower dimensional space; the second deals directly with the functionals themselves. This latter approach is a more recent development in the field; many more candidate techniques exist that employ the first approach.

Scalar Techniques

All of the examples of empirical models from literature reviewed in Section 3.2 deal exclusively in scalar parameters. Parametric linear regression [152, 167, 166], parametric nonlinear regression [151, 164], and nonparametric regression [110] techniques are all represented in the literature reviewed. However, none of these treat the functional nature of the T/W variable; or rather, they all abstract it as a single representative scalar value.

The typical multiple regression approach for dealing with infinite-dimensional data is to discretize and/or extract summary statistics such as mean, max, or quantile values. Selection of the discretization granularity is usually ad hoc, with enough data points pulled to adequately represent the underlying behavior. However, as the number of samples in-

creases, challenges emerge: The familiar curse of dimensionality can become a factor, and collinearity due to the underlying functional destabilizes many regression techniques. [169] When such issues arise, two general approaches for dealing with them include feature selection and shrinkage methods. [170] The goal with each is to develop more parsimonious models of the given dataset.

Feature selection techniques evaluate and assemble subsets from amongst the candidate regressors. This can be done based on hypothesis testing of whether each term should be included in the model, as in Forward, Backward, and Stepwise regressions;[170] or by deriving new, uncorrelated variables from linear combinations of the original set. Deriving new variables can proceed as either an unsupervised learning, such as in Principle Component Regression (PCR), or as a supervised learning, like Partial Least Squares Regression (PLSR). [170] Feature selection techniques require that a cutoff threshold be selected for deciding when to add/drop a term from the model. As such, they behave in a discrete manner, with each term either completely "in" or completely "out" of the model.

Unlike feature selection techniques, shrinkage methods do not either retain or discard regressors in a discrete manner. Rather, they seek to constrain and "shrink" model regression coefficients by imposing penalties on their magnitudes, preventing collinearity from destabilizing the regression. Ridge and Lasso regressions are two of the most familiar shrinkage methods, with the differentiating factor between them being that the Lasso provides a means for a coefficient to become exactly zero, essentially implementing a feature selection technique. [170]

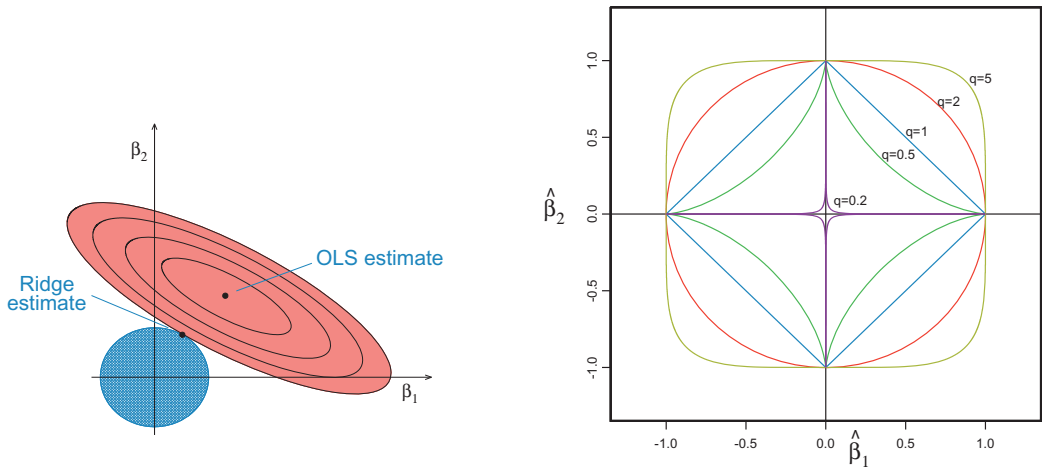

(a) (b)

Figure 3.7: (a) Graphical depiction of method for coefficient estimation in Ridge regression, and (b) generalized penalty function collapsing multiple shrinkage methods onto one continuous scale ($q = 2$ for Ridge regression depicted in (a)) [171]

The more continuous behavior of shrinkage methods tends to give them an edge over feature selection methods in regards to goodness of fit metrics. The primary argument in favor of feature selection techniques has to do with the interpretability of the resulting model; the discrete in/out nature of feature selection produces models with fewer regressor terms, allowing for some insight into the underlying structure of the response behavior to be gleaned. However, since the primary objective of this research is to develop a model with good predictive power, model interpretability is not a significant factor, and so shrinkage methods will be favored for a multiple regression approach to handling any variables pulled from the LV T/W profiles.

Functional Techniques

The term "functional" was introduced briefly in Section 3.3.3, but a more formal definition is provided here:

> "A random variable χ is called functional variable (f.v.) if it takes values in an infinite dimensional space (or functional space). An observation x of χ is called a functional data" [172]

While working with functional data sets is not a new thing, the statistical field of functional data analysis is still relatively young, having proliferated mostly in the past fifteen years. [172] What the Calculus of Variations is to Newton's Calculus is what Functional Data Analysis is (or is becoming) to the vast realm of traditional data analysis.

Regression techniques for functional data are not yet as numerous as standard regression techniques, but they are under continuous development. Already, functional linear regression, functional principal component regression, and functional partial least squares regression exist; [173, 174] nonparametric functional modeling and functional artificial neural nets have also been demonstrated. [172, 175] These developments have depended in large part on defining functional analogues to fundamental statistical parameters; an example of one such metric, the L_2 norm, is shown in (3.4).

$$\sqrt{\left(\int (\chi_i(t) - \chi_{i'}(t))^2 dt\right)} \tag{3.4}$$

Artificial Neural Networks, or neural nets as they are typically called, are a class of machine learning techniques in use across many different domains, including data mining, controls, autonomy, optimization, and artificial intelligence, among others. [176] Their formulation is inspired by and patterned after the way that neurons in the brain connect and interact. By assembling relatively simple base unit neurons, which consist of an input weighting, an activation function, and an output bias, into large networks of connected nodes and layers, highly nonlinear and complex patterns and behaviors can be discerned, learned, and leveraged.

The flexibility of neural network topologies makes them an extremely flexible family of parametric nonlinear regression. This flexibility, combined with the diversity of disciplinary fields in which they find application, means that almost any neural net graph topology that can be imagined has been applied in literature. The standard baseline neural net that serves as a starting point in many applications is the fully-connected feed forward

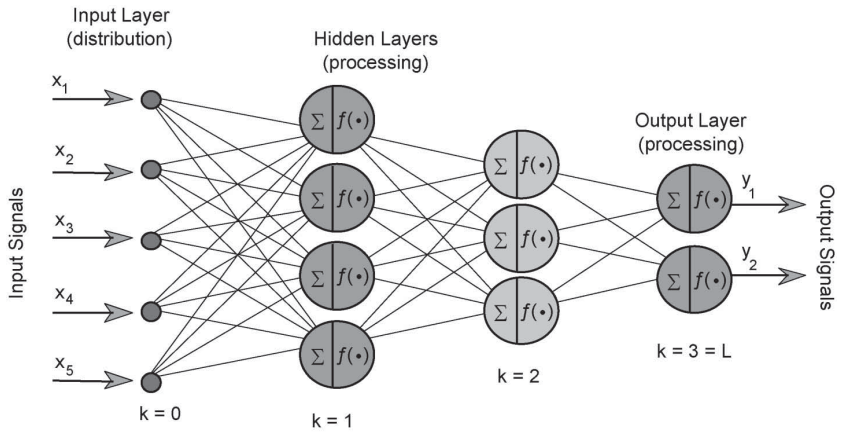

Figure 3.8: Example feed-forward neural network [177]

network, depicted in Figure 3.8. This form of neural net, when used in prediction and forecasting roles, is rightfully categorized as a nonlinear regression model for scalar responses. As such, it would fit in the previous section on Finite-Dimensional Techniques. However, there are many alternatives to the standard feed-forward network, and one family of neural nets in particular has direct application to infinite dimensional and functional problems. Recursive (or recurrent) neural networks (RNNs) are neural nets that contain cycles in their network graphs; that is, one of the paths through the network returns to the input layer rather than leading to the output layer. [176] In this way, RNNs are able to achieve "memory," as network nodes receive not only inputs pertaining to the current state, but also from the previous state. This recursion can be designed to occur in many different ways, including from output to input, output to hidden layer, hidden layer to hidden layer, or hidden layer to input. [178] This feedback loop in a network's graph allows RNNs to process of sequences of data and maintain a form of "memory" about previous steps in the sequence.

Recurrent neural nets (RNNs) specifically see use in fields from computational finance to natural language processing, among others. Most of these applications take the form of series or sequence prediction, either forecasting commodity prices or predicting the next words that will be typed in a sentence. Recurrent neural nets have also been demonstrated for time-series prediction in aerospace applications, especially in transient modeling, in-

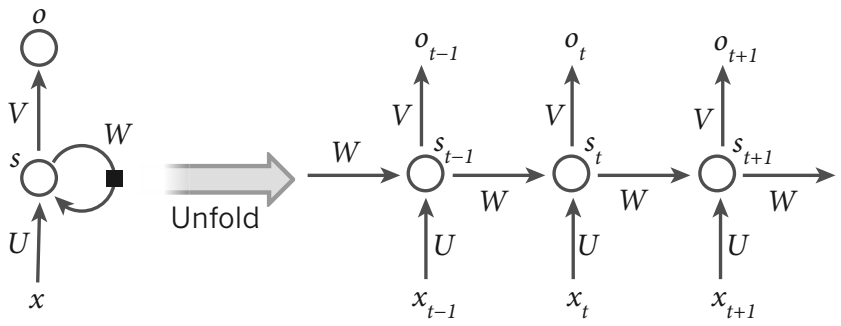

Figure 3.9: Concept of a recursive unit "unfolding" into computational recursive units [179]

cluding power systems on more electric aircraft [180], aeroelastics modeling [181], and control systems.[182] It is also possible to adapt RNNs to the task of predicting scalars from functional inputs. The only adaptation necessary is to only train and reference the value of the final output node. [183] Figure 3.9 provides a pictorial of how this recursion is handled, showing the unpacking of a recursive node into a network of nodes with a size corresponding to the length of "memory" desired in the model.

3.3.2 Response Selection

From the discussion in Section 2.4.1, it is understood that the development of a LV performance model really revolves around the estimation of the losses experienced during ascent to orbit. In this sense, (2.8) can be rewritten as

$$\Delta V_{losses} = \Delta V_{ideal} - \Delta V_{mission} \tag{3.5}$$

where all of the different losses have been rolled up into a single loss term. The traditional rocket equation as presented in (2.8) is useful for computing the ΔV_{ideal} term, and so the question that remains in identifying the proper definition of the ΔV_{losses} term is: How should $\boldsymbol{\Delta V_{mission}}$ be defined in order to best characterize LV mission requirements? To understand the possible sources from which the LV mission requirement could be derived, it is necessary to review some fundamentals of orbital mechanics.

In a two-body system, the size and shape of orbits are governed by two overarching principles: The Conservation of Energy and the Conservation of Angular Momentum. [136] Due to their constant nature, specifying both the energy, depicted in (3.6), and the angular momentum, (3.7), uniquely specifies an orbit's size and shape.

$$\epsilon = \frac{v^2}{2} - \frac{\mu}{r} \tag{3.6}$$

$$\vec{h} = \vec{r} \times \vec{v} \tag{3.7}$$

Orbits having a negative energy are "bound," being elliptical in shape; unbound trajectories, with energies greater than or equal to zero, are either parabolic or hyperbolic. The velocity, radius from the center of attraction, and flight path angle all vary continuously along an orbit, changing in such a way as to conserve energy and angular momentum. The maximum velocity is observed where the potential energy is smallest, at the orbital point where the smallest radius from the center of attraction occurs; conversely, for elliptical orbits, the minimum velocity is observed where the potential energy is largest, at the orbital point where the greatest radius from the center of attraction occurs. These points are respectively termed the periapsis and apoapsis, and are depicted in Figure 3.10.

This variation in velocity poses a problem for the would be LV designer that is seeking to quantify the $\Delta V_{mission}$ required: From which point in the specified target orbit should the required velocity be taken? If any point along the orbit is valid, the opportunistic designer would naturally select the apoapsis, as this would provide for the smallest $\Delta V_{mission}$ requirement. Of course, for circular orbits (a special case of an elliptical orbit), the choice is easy, as with a constant orbital radius the velocity is also constant, so there is only one value to choose from.

Much of the literature does not address this issue directly, quoting $\Delta V_{mission}$ values without establishing their source. [185, 186, 187, 157] Where the origin of the velocity is

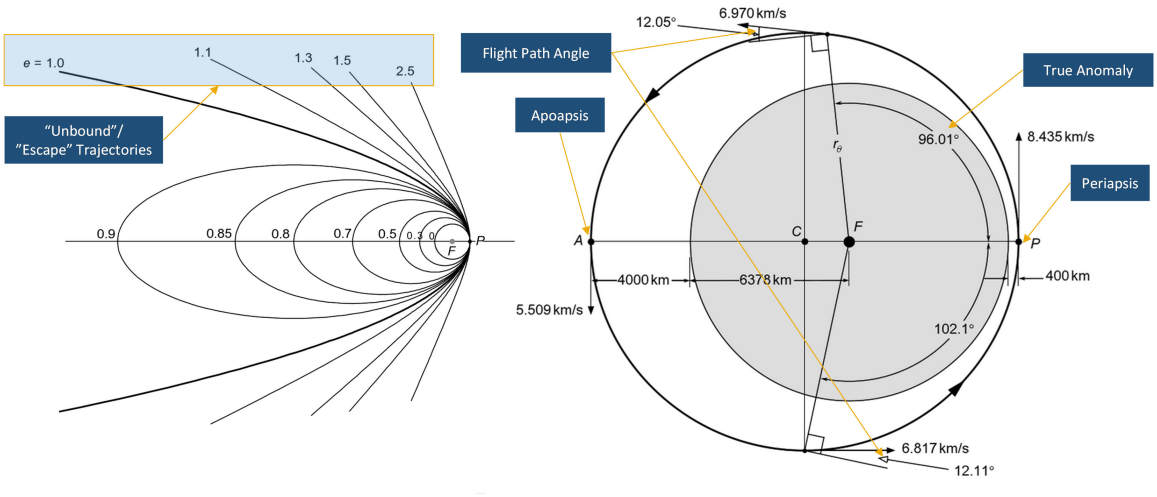

Figure 3.10: Illustration of orbital elements and concepts [184]

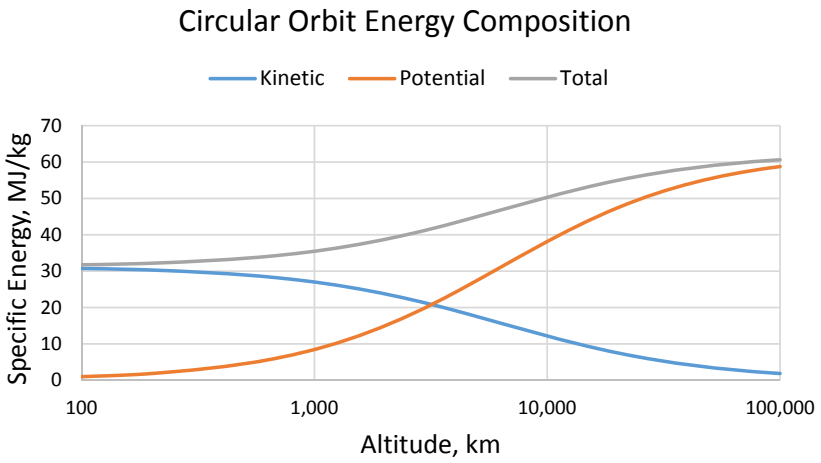

Figure 3.11: Energy composition of circular orbits

cited, however, there appears to be a consensus to using the velocity at periapsis (many use the circular velocity, which is in fact still the periapsis velocity). [188, 189, 147, 141, 150] This makes sense given that the vast majority of studies focus on ETO missions targeting LEO. Figure 3.11 shows that for circular orbits at LEO altitudes (generally 100-500km), the orbital energy is primarily kinetic in form, allowing the velocity to serve as an acceptable analogue to the energy. However, it is also clear to see that for higher orbits, including the 35,786 km altitude of GEO, the potential energy emerges as a much more significant component of the orbital energy, invalidating this approach.

It seems that the issue at the root of this question is caused by the inextricable influence the rocket equation has had on the spacecraft design community, both in its educational curriculum, as well as in its analysis practices. It is only because of the nature of the rocket equation that the mission requirements are cast in terms of velocity; otherwise, energy would seem a much more natural quantity to use in describing LV mission requirements. After all, a LV's function is primarily one of energy conversion: Chemical energy stored in the form of fuel is converted to heat, then kinetic energy of the exhaust, which then contributes to a combined increase in the LV's kinetic and potential energy states.

C_3

A form of energy is already in use for measuring LV performance to escape orbits, which are required for interplanetary missions. The term "escape" implies that the object has been imparted an energy at burnout great enough to overcome the attraction forces of the central body; this amounts to achieving a kinetic energy equal in magnitude to the potential energy, setting (3.6) to zero.

$$v_{escape} = \sqrt{\frac{2\mu}{r}} \tag{3.8}$$

If the required escape velocity, (3.8), is met exactly at burnout, the object's final velocity relative to the central body will be zero. If the escape velocity is exceeded, the object will depart with a hyperbolic excess velocity, v_∞. This is computed by equating the energies at burnout and infinity, and then substituting (3.8):

$$v_\infty^2 = v_{burnout}^2 - v_{escape}^2 \tag{3.9}$$

The resulting v_∞^2 is referred to as the characteristic energy, or C_3. It is common practice to specify interplanetary mission requirements and LV performance capabilities to escape trajectories in terms of C_3. [190, 64, 191]

Although measuring interplanetary mission requirements in terms of a required energy

is standard practice, this has not been the case for bound, elliptical orbits. The thought of extending the application of C_3 to missions targeting bound orbits degenerates under the expectation of ultimately expressing the mission requirements as $\Delta V_{mission}$, since negative C_3 values would result in imaginary velocities. However, inspiration can be drawn from this practice for use in the development of a bound orbit corollary to the characteristic energy.

Energy Velocity

The first guidance taken from the practice of measuring interplanetary mission requirements in terms of C_3 is the need to establish a reference "zero" point, or origin, from which to measure them. For interplanetary missions, it is logical to leverage the boundary between bound and escape trajectories as the origin; after all, this is in fact the point at which orbital energy transitions from negative to positive, and is exactly equal to zero. For LVs, it would seem logical to set the origin at the launch pad on the surface of the earth; however, doing so would require that mission energy requirements be measured in a relative rather than absolute fashion, as the kinematic energy state of a LV sitting on its launch pad is non-zero.

The other observation from the current practice of measuring interplanetary mission requirements as an energy is that the energy change measured from the origin can be expressed as a velocity. The hyperbolic excess velocity is essentially a measurement of energy, where all of the energy is assumed to be kinetic in form. This same practice is easily extended for the case of missions to bound orbits if mission energy deltas measured from the origin are treated as purely kinetic.

With these two ideas in mind, the last observation necessary to the development of a metric for LV mission requirements to bound orbits is found in literature relating to aircraft performance. In aeronautics, the specific energy is not defined in the same manner as astronautics. This is because for atmospheric flight, due to the comparatively small variation

in altitudes observed, it is generally acceptable to assume the gravitational acceleration to be invariant with altitude. With this assumption, the energy equation is usually written as:

$$E = \frac{mv^2}{2} + mgh \tag{3.10}$$

A rearrangement of the terms in (3.10) appears in various algebraic manipulations of the aircraft performance equations, and has come to be known as the *energy height*. This quantity, depicted in (3.11), is defined as "the altitude the aircraft would attain if its kinetic energy were completely converted into potential energy." [192]

$$z_E = h + \frac{v^2}{2g} \tag{3.11}$$

It should be reiterated that the energy height as defined in (3.11) is limited in its applicability to aircraft, due to its constant gravitational acceleration assumption.

Synthesizing all of the observations above, it is proposed that $\Delta V_{mission}$ be defined as the *energy velocity* of the target orbit, a quantity analogous to the *energy height* that is defined as "the velocity the vehicle would attain if its potential energy were completely converted into kinetic energy." This metric satisfies the need for a relative energy reference when it is defined algorithmically as

$$v_E = \sqrt{v^2 + \frac{2h\mu}{R(R+h)}} \tag{3.12}$$

where h is the altitude and R is the radius of the launch site, which implicitly includes the launch site elevation.

Figure 3.12 shows the effect of switching response parameter to the energy velocity. This figure is the equivalent of Figure 3.2, with no losses yet taken into account. It is clear to see that the energy velocity properly captures the LV orbital energy requirements, and does so in a very consistent manner across all of the data points.

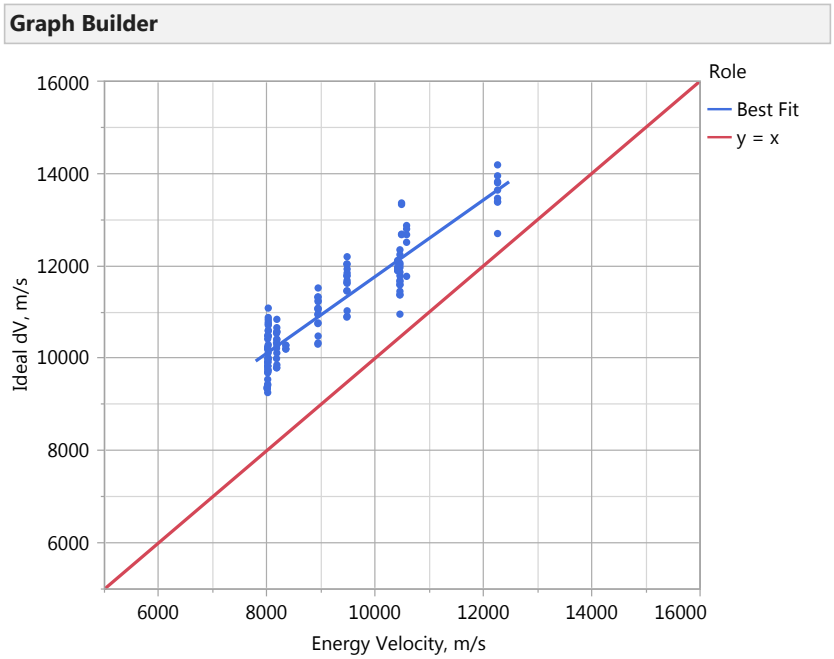

Figure 3.12: Actual ΔV_{ideal} compared to the "Energy Velocity" computed for each vehicle

3.3.3 Regressor Selection

When considering which regressors should be used to develop the empirical model, the underlying question is "what are the relevant parameters that drive LV performance?" There are three possible sources from which to draw a response to this question, and a mixture of guidance from each is expected to yield the final set of regressors. These three sources are literature, physics, and statistics.

Regressors From Literature

In developing a list of candidate regressors, it makes sense to begin by recording those which models published in the literature have used previously. It is very likely that regressors known to have predictive power in the past will prove to have predictive power once more. This expectation would be particularly strong for any regressors that make an appearance in multiple models.

Tables 3.1 to 3.5 present the regressors used in each of the respective models from liter-

Table 3.1: Regressors from Dergarabedian & Ten Dyke's model [145]

Term	Description
I	Vacuum Specific Impulse
r	Mass Ratio
N_0	Liftoff Thrust-to-Weight Ratio
$\frac{C_{DM}A}{W_0}$	Representative Ballistic Coefficient
$\frac{I_s}{I}$	Ratio of Sea-Level to Vacuum Specific Impulse
t_b	Burn Time
β_b	Velocity Angle at Burnout
h	Insertion Altitude

Table 3.2: Regressors from MacKay & Weber's model [146]

Term	Description
$\left(W_p/W_0\right)_i$	Stage propellant fraction
F/W_0	Stage initial thrust to weight
I_i	Stage specific impulse (average for $i = 1$, vacuum otherwise)
h	Insertion Altitude

ature reviewed in Section 3.2. White's model was created as an evolution of Dergarabedian and Ten Dyke's model, and so the regressors are identical except for the manner in which the Representative Ballistic Coefficient is defined. Similarly, Schilling refit Townsend's model using an updated set of LV data points, and added the acceleration at liftoff as a term to Townsend's very concise model. It is easy to observe that there are a set of common terms that appear across the majority of the models reviewed. The fact that each model may leverage these regressors differently in their algorithmic structure does not raise questions in the case for their significance, as this indicates that different approaches are displaying a

Table 3.3: Regressors from Townsend's model [147]

Term	Description
t_b	Burn Time
h	Insertion Altitude

Table 3.4: Regressors from White's model [141]

Term	Description
I	Vacuum Specific Impulse
r	Mass Ratio
N_0	Liftoff Thrust-to-Weight Ratio
$\frac{C_{D_{PD}}A}{W_0}$	Representative Ballistic Coefficient
$\frac{I_s}{I}$	Ratio of Sea-Level to Vacuum Specific Impulse
t_b	Burn Time
β_b	Velocity Angle at Burnout
h	Insertion Altitude

Table 3.5: Regressors from Schilling's model [150]

Term	Description
t_b	Burn Time
h	Insertion Altitude
A_0	Liftoff Acceleration

form of agreement. These "consensus" terms are generalized here with a brief discussion on their observed roles:

Insertion Altitude: The insertion altitude term appears in each of the models reviewed. Given the previous discussion in Section 3.3.2 regarding the inadequacy of velocity alone for describing the LV mission requirements, including altitude can be viewed as a method of capturing the additional information regarding the LV's final energy state. Because of this, the insertion altitutde is interpreted primarily as a descriptor and correction factor for $\Delta V_{mission}$ rather than a predictor of ΔV_{losses}.

Burn Time The total burn time appears explicitly in four of the five models reviewed; even in the fifth model it resides implicitly in the terms that do appear, and a simple algebraic manipulation can reveal its presence. The flight time is important due to the fact that the acceleration of gravity gets integrated over time; reducing the flight

time would thus reduce the gravity losses. However, as noted in Section 3.2.5 and depicted in Figure 3.5, modern LVs circumvent this correlation by spending a significant portion of their ascent accelerating at very low flight path angles. For this reason, total burn time may carry less predictive power for modern designs than it did for LVs of the past.

Initial Thrust-to-Weight The initial thrust-to-weight (T/W) at liftoff also appears in four of the five models reviewed. Schilling's model uses the liftoff acceleration, which simply states T/W in units of acceleration rather than g's, and subtracts out the acceleration of gravity. MacKay and Weber's model implements the initial T/W not only of the first stage, but of every stage in the LV.

Specific Impulse The specific impulse already plays a prominent role in all of the models in that it is an integral part of the ideal rocket equation. However, several of the models also use it in their calculation of the loss term that modifies the ideal rocket equation. The specific impulse in vacuum is used most frequently, and typically only for the first stage; the one exception is MacKay and Weber's model, where, like T/W, the specific impulse is specified stage-wise. In their model, they also state that the median specific impulse (midway between vacuum and sea-level values) is used for the first stage, while the vacuum value is used for all subsequent stages.

Regressors From Physics

Given that the modeling intent is to capture the behavior of a response that is subject to the laws of physics, another logical source for candidate regressors is physics itself. By inspecting the equations governing the performance and motion of LVs as they ascend to orbit, it should be possible to identify key parameters that bear influence over the trajectory. This thought process is the very one at work in the Grey Box modeling paradigm described by Keesman. [122] Dergarabedian and Ten Dyke provide an appendix to their model that

walks through this very process, showing how it not only helped identify terms for their model, but also the manner in which the terms should be applied.

$$\Delta V = (1 - K_{loss})\Delta V_{ideal} \tag{3.13}$$

The full Rocket Equation as presented in (2.7) can be rearranged so as to more clearly show the exact terms governing the various sources of loss. The result in (3.13) shows that the losses can be considered as a loss factor, K_{loss}, which will always be between 0 and 1. This loss factor is simply the sum of the three loss terms described in Table 2.7, as expected. With one algebraic manipulation, multiplying the drag term by $\overline{W}/\overline{W}$, the loss factor becomes (3.14).

$$K_{loss} = \left[1 - \left(1 - \overline{p_a}\frac{A_{exit}}{T_{vac}}\right) cos(\overline{\alpha + \phi})\right] - \frac{\overline{qC_D}A}{\overline{W}}\frac{\overline{W}}{T_{vac}} - \frac{\overline{W}}{T_{vac}} sin\bar{\gamma} \tag{3.14}$$

In this form, one new candidate regressor can be identified, as well as a couple of familiar ones. The new term is A_{exit}/T_{vac}, which directly interpreted is the inverse of the thrust per unit exit area of the engine. Further algebraic manipulations could uncover nozzle parameters such as expansion ratio, throat area, and potentially others. With the rearrangement of the drag term, the ballistic coefficient emerges, a regressor previously observed in use by two of the models from literature. Also appearing prominently, the T/W term would seem to show a strong inverse relationship with the loss factor. This is only partially true, as Figure 2.13 shows increasing T/W actually increasing the drag losses observed. Section 3.3.3 discusses this phenomenon in more detail.

Regressors From Statistics

All empirical models consist of statistical regressions of some form, whether linear or nonlinear, parametric or nonparametric. Many of the diverse techniques and approaches available involve some form of regressor selection, be it implicit or explicit. Some, such as

Stepwise regression, decide on including or excluding variables on a case by case basis, often by some form of hypothesis testing. [193] In other approaches, regressor selection is performed in a more implicit manner. For example, a particular statistical technique may end up only giving significant weighting to a subset of the candidate regressors provided, effectively pruning those with very low or even zero weightings; examples of this implicit regressor pruning include Ridge regression and Lasso regression, among others. [170]

Ultimately, the statistical methods available for regressor selection will be related to the model type and approach selected, a topic discussed in Section 3.3.2. As will be shown there, some modeling approaches have been built around various model feature selection strategies. It should be noted that all statistical approaches to choosing model terms are Black Box approaches - they do not leverage any additional knowledge that may be available concerning the underlying mechanisms of the response being modeled. As such, it is expected that applying statistical analyses will aid in the overall process, but will not be as effective as an approach that also incorporates some mechanistic knowledge.

The Importance of Thrust-to-Weight

A critical observation can be gleaned by comparing the candidate regressors identified from both literature and physics. It is evident that T/W is a critical parameter affecting LV trajectory performance, as it is the one regressor most consistently present in the sources reviewed. In fact, all but one of the literature sources reviewed identify T/W as a critical regressor. The one omission came in Townsend's model, which was the most parsimonious model reviewed, with only two regressors. However, the increased acceleration provided by higher T/W translates into shorter flight times, so its impact is accounted for implicitly even here.

The importance of T/W agress with intuition informed by physics. The higher acceleration associated with higher T/W is understood to reduce gravity losses by reducing the time a vehicle spends flying at high flight path angles; the quicker a LV can get up and out

of the dense atmosphere, the sooner it can pitch over and continue the remainder of its flight at depressed flight path angles. [144] However, higher acceleration also means the vehicle achieves a higher velocity in the lower atmosphere, producing increased drag losses, and potentially causing increased heating and structural loads for the vehicle. Thus, the T/W remains an important parameter, but its relationship with velocity losses is not simple.

A significant complication emerges on considering T/W further. While all of the models from literature used T/W as a single scalar regressor (MacKay and Weber differed only in that they used a single T/W regressor from each stage), in reality, T/W is not constant, but varies continuously throughout the trajectory; weight decreases rapidly as propellant is consumed, and thrust varies due to changing atmospheric pressure and/or throttle profiles. Figure 3.13a shows an acceleration profile for the flight of an Atlas 5 first stage.

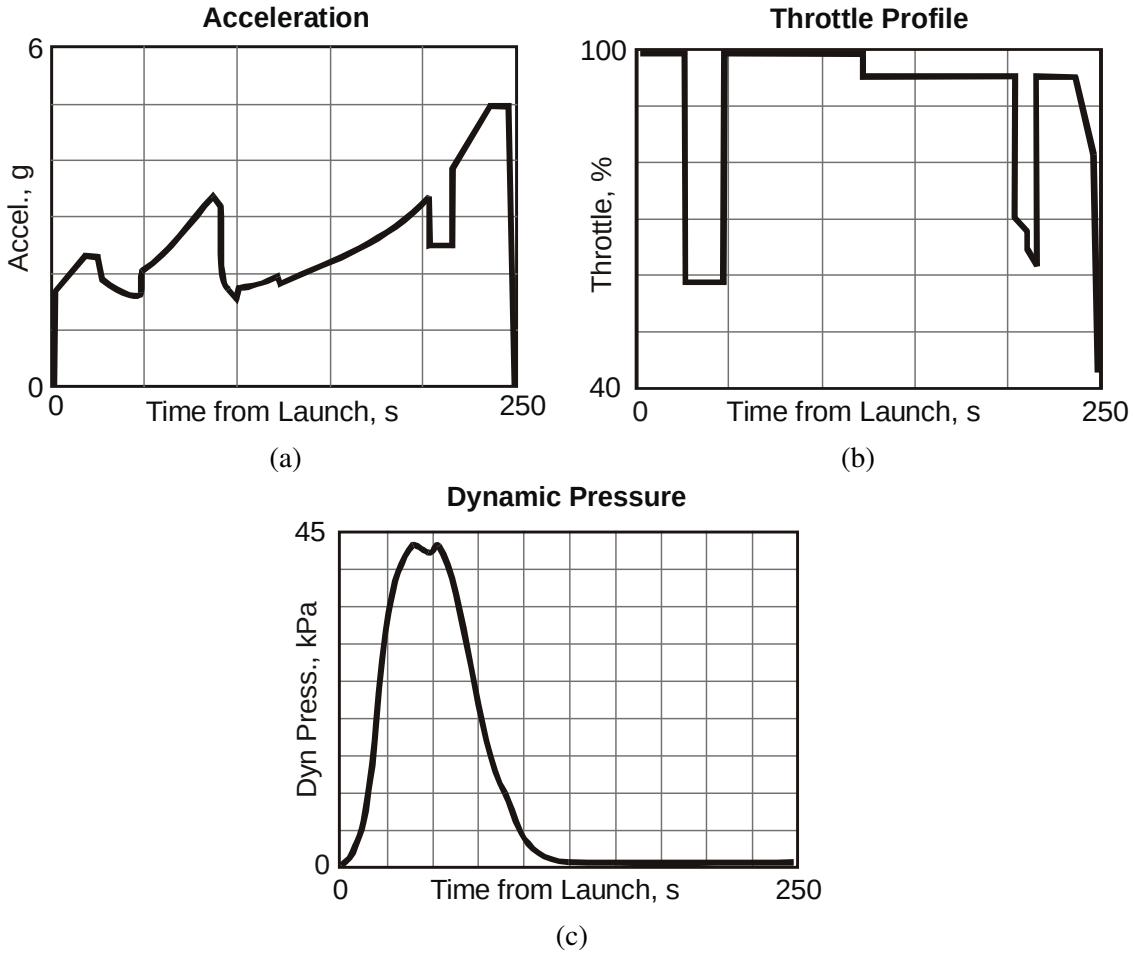

Figure 3.13: Atlas V 552 first stage ascent profile for a mission to LEO [194]

Choosing to represent all of the variation in T/W for the powered flight of a stage by a single parameter, then, is a significant abstraction of reality; choosing to represent all of the variation of T/W for an entire vehicle by a single liftoff T/W all the more so. As was observed in the velocity profile of the Ariane 5 in Figure 3.5, modern LVs often employ high T/W first stages with lower T/W upper stages to achieve overall more efficient trajectories. The simplifying assumption made in all of the models reviewed that allowed for the use of a single T/W parameter was that the mass flow rates were all assumed to be constant during the operation of each stage. However, this is not a good assumption in reality, as changing mass flow rates result from liquid rocket engine throttling and solid rocket motor grain geometries, both of which are observed in Figure 3.13.

The difficulty at hand really stems from the fact that T/W is not finite-dimensional like most other LV variables which can be fully captured in a scalar or set of scalars; it is an infinite-dimensional variable. Variables such as T/W which can be discretized as finely as desired (at least in theory) can be thought of as functions. Thus, they are referred to as functional variables. [174]

It was stated in Section 2.4.2 that transcribing optimal control problems into NLP problems incurs error and introduces a discrepancy that may cause optimal NLP solutions to be suboptimal in the functional space. In the same way, transcription of a functional variable into finite dimensional space is a potential liability to the generalization and accuracy of the intended regression. Thus, since T/W undeniably carries significant predictive power, the need to develop an approach to incorporating it into a general regression model requires careful attention. This leads to another research question: **How might T/W best be incorporated into an empirical model, given its functional nature?**

3.3.4 Hypothesis 2: Functional Regression for Launch Vehicle Performance Modeling

Figures 3.14 and 3.15 show some preliminary results obtained by a naive application of functional regression. A simplistic interpretation of the T/W profile was created for each

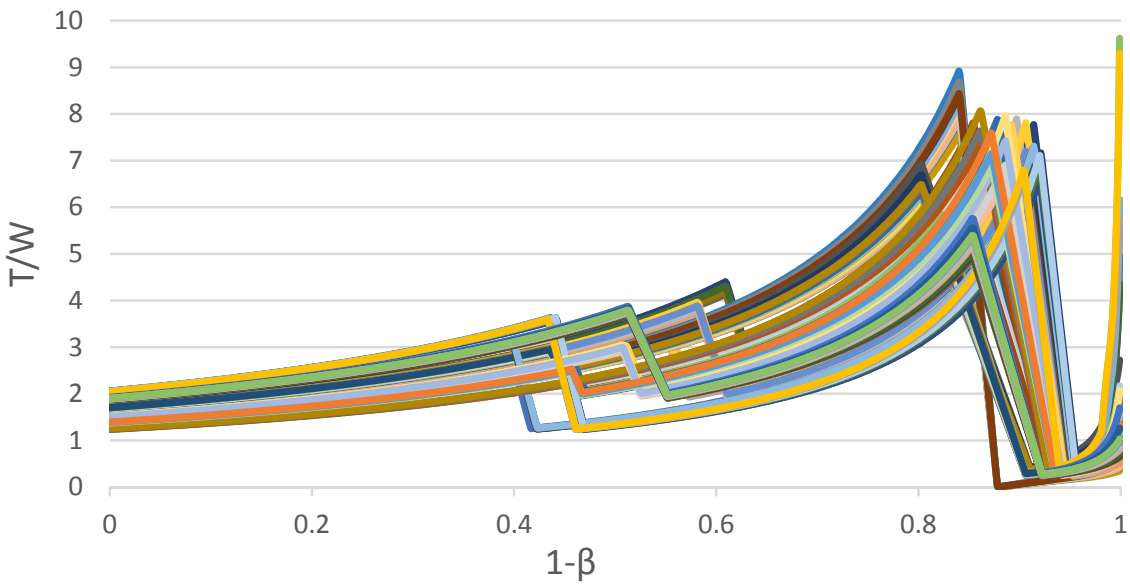

Figure 3.14: T/W profiles for the 126 LV data points collected from literature. Prepared for functional regression by non-dimensionalization of time axis

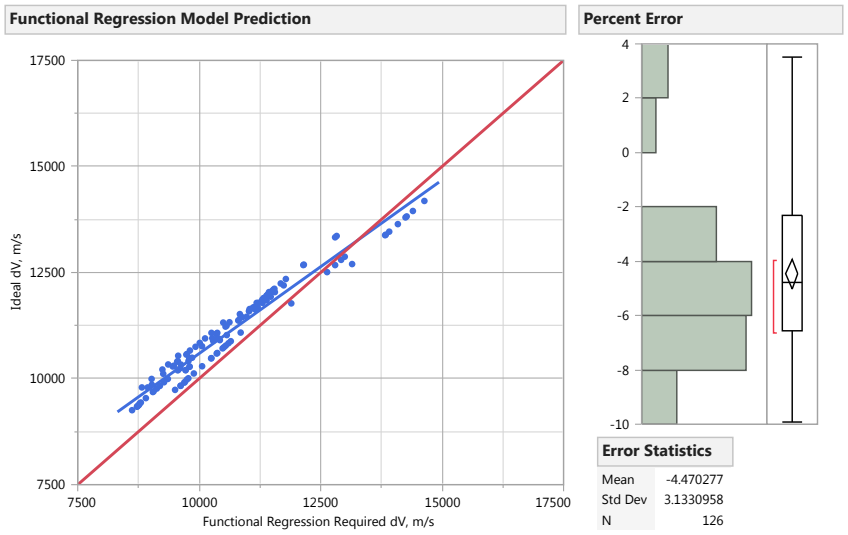

Figure 3.15: Actual ΔV_{ideal} compared to ΔV predicted by naive application of nonparametric functional regression

of the 126 LV data points collected from literature; these were then fed into a canned functional regression routine in R as a learning exercise. The regression results, depicted in Figure 3.15, show a surprisingly well behaved trend given the ad hoc nature of the implementation.

Hypothesis 2: If the functional nature of the T/W profile is leveraged directly, it will enable the building of an empirical model that is general to a broader range of LV architectures

3.4 Summary of Research Questions & Hypotheses

Chapter 2 concluded by stating the overall research objective for this thesis as: **To develop a methodology for enabling risk-informed decision making during the architecture selection phase of LV programs.** In Chapter 3, NASA's Risk-Informed Decision Making (RIDM) process was set as the baseline methodological framework within which to work towards meeting this objective. A review of the steps in RIDM identified the following observations regarding the LV architecture selection:

Observation 1 There are multiple techniques available for generating alternative architectures, any of which meet the needs of LV architecture selection

Observation 2 A LV architecture cannot be adequately represented by any single point design. The volitional uncertainty present is only properly described by a "set" in the Design space

Observation 3 In order to properly characterize an architecture for robust decision making, its representation in the Objective space must be established by propagating volitional uncertainty from the Design space to the Objective space

Observation 4 A sampling-based approach to uncertainty propagation is the most well suited to characterizing a LV architecture

Research Question 1a What is the best sampling strategy for propagating LV volitional uncertainties from the Design space to the Objective space?

Observation 4 Mission performance estimation via trajectory optimization presents the biggest challenge to performing probabilistic analysis during architecture selection

Research Question 1b Is it feasible to use explicit trajectory optimization to characterize LV architectures in an RIDM process?

Research Question 3 How might T/W best be incorporated into an empirical model, given its functional nature?

Hypothesis 2 If the functional nature of the T/W profile is leveraged directly, it will enable the building of an empirical model that is general to a broader range of LV architectures

In order to enable a risk-informed decision making process during LV architecture selection, the questions presented in this chapter must be answered, and the hypotheses tested. This will be accomplished through numerical experiments, which will be presented in the next chapter.

CHAPTER 4
EXPERIMENTS & RESULTS

This chapter seeks to provide experimental observations in support of testing the hypotheses and answering the research questions posed in this thesis. Along the way, derived research questions and hypotheses may emerge; these will be presented in the order in which they are motivated by experiment results. However, it is important to summarize here the questions and hypotheses that have been formulated thus far.

The overall research objective for this thesis was stated as **"To develop a methodology for enabling risk-informed decision making during the architecture selection phase of LV programs."** In Section 1.3.3, the broad "design freedom" that underlies each candidate LV architecture was identified as a significant source of volitional uncertainty for the decision maker. Because many other forms of uncertainty are enveloped by this volitional uncertainty, the overarching hypothesis was stated that **"If volitional uncertainty in the form of design freedom is quantified and propagated, decision makers will be able to perform risk-informed LV architecture selection."**

Chapter 3 reviewed the steps in NASA's Risk-Informed Decision Making process to identify how it might be adapted to the problem of LV architecture selection. Due to its flexibility in handling arbitrary Objective space topologies, and because of the added value of enabling predictive modeling, a sampling-based approach to volitional uncertainty propagation was identified as best meeting the needs of decision makers. From this, a couple of interrelated research questions emerged focused on developing a sampling approach for LV architecture uncertainty propagation. These questions are addressed by Experiment 1.

The rest of this chapter is organized as follows: Section 4.1 introduces the experimental apparatus employed, including LV architecture and design trade spaces selected for experimentation, as well as the design and analysis models used. Section

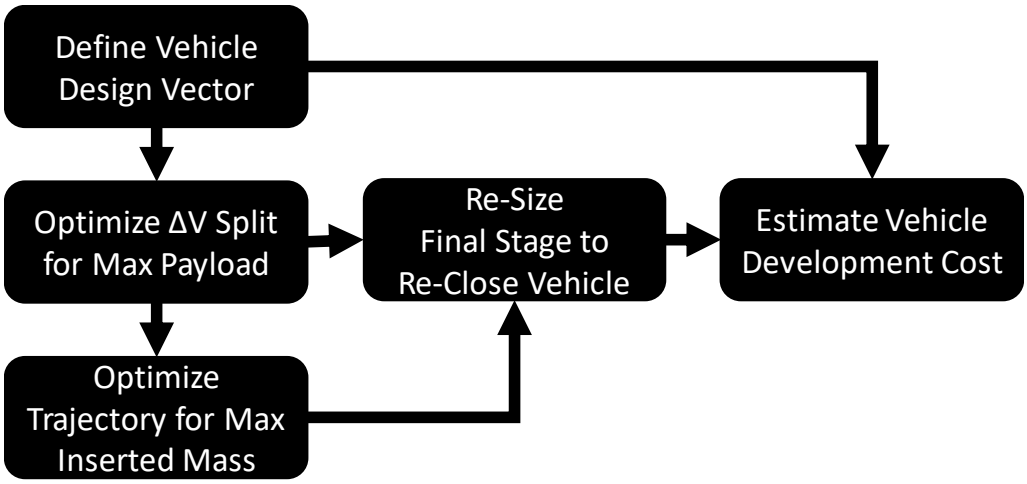

Figure 4.1: Implemented process flow for LV sizing

4.1 Experimental Apparatus

In order to carry out the experiments necessary for testing the hypotheses and answering the research questions of this thesis, a LV architecture evaluation testbed was created. Each experiment performed required the use of some part of the experimental apparatus assembled. Discussion of the details specific to each experiment is reserved for the section in which the experiment is presented; however, the LV architecture trade space and analysis models selected are common across all experiments, and so they are summarized first here.

The overall LV design process flow implemented is depicted in Figure 4.1. The sizing was performed subject to the ground rules and assumptions (GR&A) presented in Table 4.1. A more detailed walkthrough of the design process, along with some benchmarking of the LV analyses implemented, is presented in Appendix A.

4.1.1 LV Architecture Trade Space and Parameterization

Because the focus of this thesis has been directed towards addressing the role that volitional uncertainties have in architecture evaluation and selection, it is necessary to establish an experimental trade space that includes both LV architectural options and the parameters that represent the "design freedom" that resides within each architecture concept.

Table 4.1: Relevant GR&A implemented in the LV sizing analyses

Name	Description
Gross Liftoff Weight	Launch vehicle gross liftoff weight shall be equal to $5,000,000$ lbs
Target Orbit	Payload shall be delivered to a 220×220 nmi orbit
Max Burn Duration	Burn time for any single stage shall be greater than 60 seconds and less than 1200 seconds
Max Dynamic Pressure	Maximum dynamic pressure encountered shall not exceed 750 psf
Max Acceleration	Maximum sensed acceleration shall not exceed 5g

Architecture Trade Space

Since the focus of the methodology under develoment is on RIDM during architecture selection, the trade space in question is first and foremost an architecture trade space. What constitutes an architecture is somewhat a matter of perspective, but in the very earliest stages, a high level abstraction of the vehicle architecture consists of the types and arrangement of stages that comprise the vehicle. Based on the high-level decomposition performed in Section 1.3.1, and with the aim of addressing the very earliest phases of architecting, the LV architecture trade space selected for testing and demonstrating the developed methodology is presented in Table 4.2 and Figure 4.2.

Table 4.2: Table with architecture numbering used in experiments

	Boosters	**1st Stage**	**2nd Stage**	**3rd Stage**
Architecture 1	RP1	RP1	None	None
Architecture 2	RP1	LH2	None	None
Architecture 3	LH2	RP1	None	None
Architecture 4	LH2	LH2	None	None
Architecture 5	None	RP1	RP1	None
Architecture 6	None	RP1	LH2	None
Architecture 7	None	LH2	RP1	None
Architecture 8	None	LH2	LH2	None
Architecture 9	None	RP1	RP1	RP1
Architecture 10	None	RP1	RP1	LH2
Architecture 11	None	RP1	LH2	RP1
Architecture 12	None	RP1	LH2	LH2
Architecture 13	None	LH2	RP1	RP1
Architecture 14	None	LH2	RP1	LH2
Architecture 15	None	LH2	LH2	RP1
Architecture 16	None	LH2	LH2	LH2
Architecture 17	RP1	RP1	RP1	None
Architecture 18	RP1	RP1	LH2	None
Architecture 19	RP1	LH2	RP1	None
Architecture 20	RP1	LH2	LH2	None
Architecture 21	LH2	RP1	RP1	None
Architecture 22	LH2	RP1	LH2	None
Architecture 23	LH2	LH2	RP1	None
Architecture 24	LH2	LH2	LH2	None

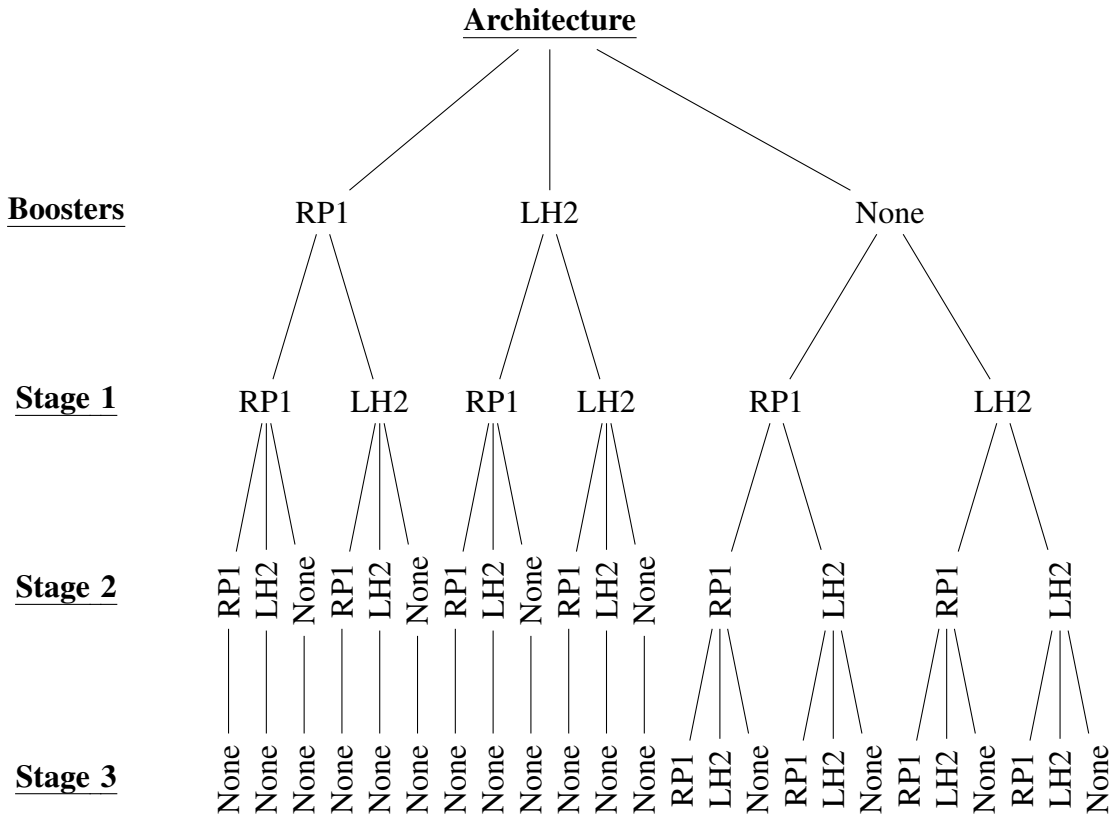

Figure 4.2: Tree depiction of LV architecture trade space examined

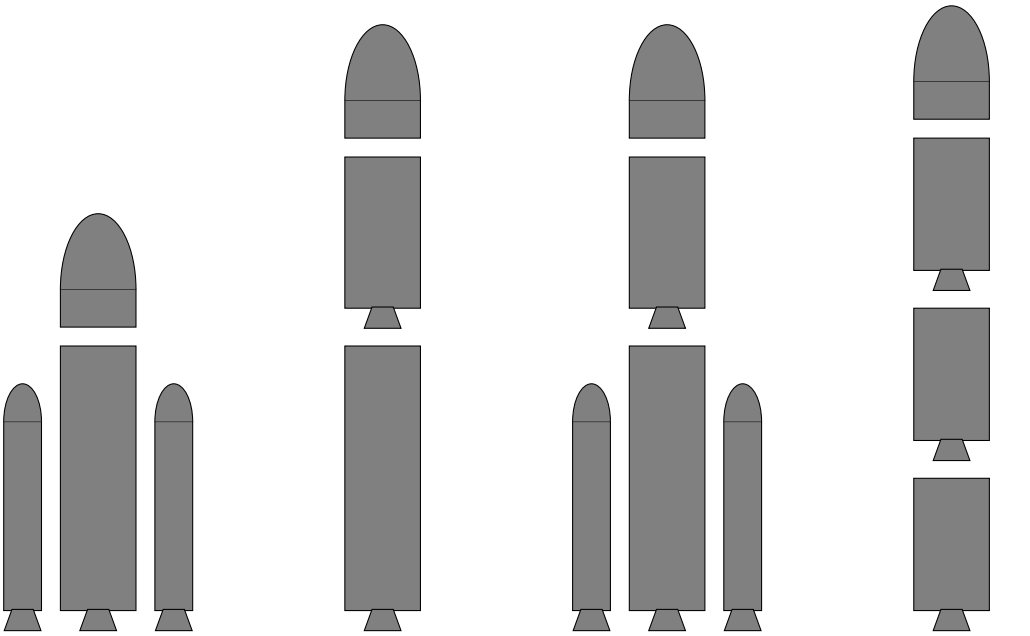

(a) 1.5 Stages (b) 2 Stages (c) 2.5 Stages (d) 3 Stages

Figure 4.3: LV architecture configurations

Design Parameterization

The parameterization selected for the vehicle level representation in these experiments was designed to capture all of the major elements at play during LV design in the real world. As discussed in Section 1.3.2, aerodynamics, propulsion, and structures/weights are all integral to any analysis of LV mission performance. Propulsion and structures also play directly into the cost of a vehicle. So, to assemble a viable proof of concept with which to test the developed methodology, it is necessary to select a minimum acceptable representation of these factors to form the experimental design space.

In Section 1.3, the propellant mass fraction (PMF) was defined mathematically with (1.1). PMF can be interpreted as a factor representing LV structrual sizing, relaying the relative amount of propellant that can be carried for a given vehicle structural weight. While this ratio is a very simple one, it displays discernable scaling trends for expendable launch vehicles, as can be seen in Figures 4.5 and 4.6. In these, the structural sizing is represented by Net Mass Fraction (NMF), a parameter equivalent to PMF. It is also convenient to assign a range of possible PMF or NMF values for a given propellant loading, allowing for its use as a measure of structural efficiency; in this way, it can also be viewed as a technology "dial." This is exemplified in Figures 4.5 and 4.6 by the blue diamonds. These data points come from LV stages that employ a common bulkhead propellant tank layout, and reveal that there is generally a significant structural efficiency advantage over conventional tank configurations (represented in red). While PMF is clearly an extremely high-level parameter, practically any effect of design features or technologies applied to a vehicle can be accounted for by an appropriate change in PMF.

The propulsion system performance for a rocket can be encapsulated at the top level by a thrust parameter and a specific impulse value. I_{SP} is a major player in the Rocket Equation; thrust is absent from the ideal Rocket Equation (2.8), but plays a major role in real trajectory performance, as evidenced by its presence in the full Rocket Equation (2.7). Since these parameters are independent, they clearly must each have a representation

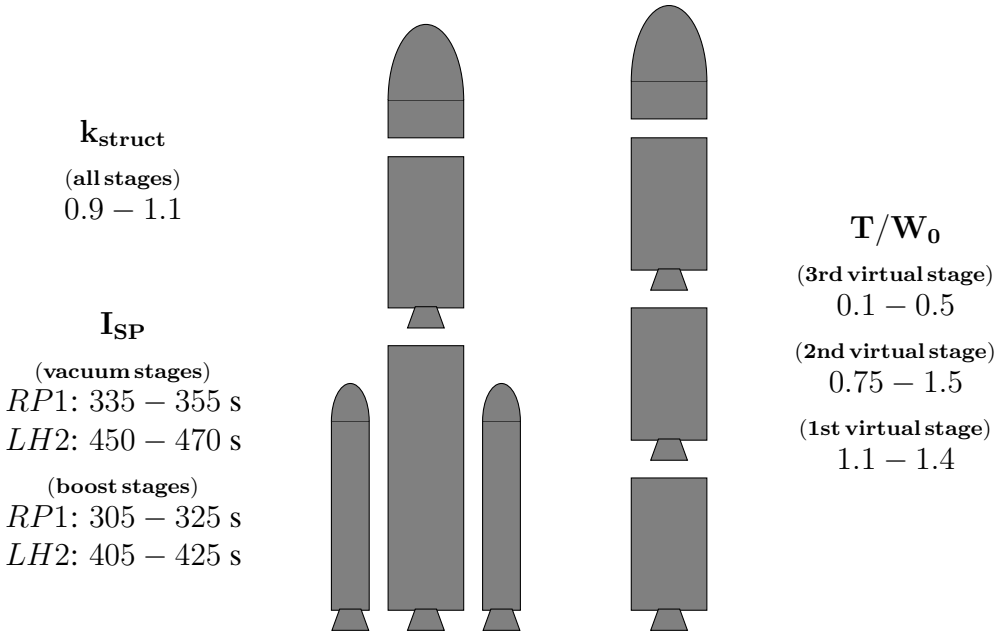

(a) 2.5 Physical Stages (b) 3 Virtual Stages

Figure 4.4: LV architecture configurations

in the parameterization to capture the variability that would exist in a real design space. Although thrust is an independent parameter, its feasible ranges are tightly linked to the weight breakdown of the vehicle; 50,000 lbs of thrust may be appropriate for an upper stage of an Atlas V class vehicle, but it would grossly underpower the full LV at liftoff. For this reason, T/W was chosen to parameterize thrust, so that the absolute thrust value would be compatible with the scaling of the stage it pertains to.

4.1.2 Vehicle Sizing

In order to perform sizing, there must be some set of requirements and/or assumptions regarding the capabilities a vehicle must have and the scenario/environment in which it must operate. The specified set of ground rules and assumptions drives the sizing and synthesis process. For LVs, there are two common perspectives from which trade studies are often performed. The first starts with a foundational requirement of delivering some defined payload to a specified orbit. The vehicle sizing proceeds from there, usually trying to achieve an optimal value of some objective function such as cost or gross liftoff weight. The second

perspective starts rather with a requirement or constraint placed on the vehicle itself, such as a gross liftoff weight; the sizing process then produces a capability assessment of how much payload the specified LV can deliver to various orbits.

For the experiments performed in this thesis, the latter approach is implemented within DYREQT, the Dynamic Rocket EQuation Tool. This choice was made for the primary reason that payload delivered to orbit is perhaps the most intuitive measure of value in any LV trade study. DYREQT, an in-house tool used within the Aerospace Systems Design Lab at Georgia Tech, is based primarily in NASA's OpenMDAO framework. [195] It implements a particular variation on the MDF algorithm that is tailored to launch vehicles and space transportation systems. [196]

Weight Estimation

While LV mass estimation is not a center piece of this dissertation, it is a necessary part in any LV sizing study. As with most disciplines, the approach typically used in calculating vehicle mass varies by design phase. Historical regressions and first principles analyses in early conceptual design give way to finite element analysis and eventually a weight rollup of actual parts as design maturity increases. The increasingly realistic treatment of physics (reducing "abstraction") is accompanied by an increase in the "resolution" of the models; designs are represented by ever more granular physical decompositions and parameterizations.

Architecture selection takes place in the very earliest stage of design, when, from a fidelity standpoint, only a relatively simple analysis model is required. A low-resolution model may actually be preferred at this stage over higher-resolution models, as design details are very sparse; requiring more detailed definitions be developed for the concepts to be evaluated would increase the level of effort involved dramatically. Ultimately, the analysis models used are dictated by the trade space under consideration. Advanced or novel concepts often do not have precedent in historical databases, necessitating the use of

more physics-based analyses. [197]

The trade space scoped out in Section 4.1.1 is a very conventional one, so it is reasonable to choose a mass estimation approach based on historical data. A review of mass estimating relationships (MERs) available in the public domain turned up several published LV MER databases; however, they all require a higher level of model resolution than this thesis intends to develop.[198, 199] For example, in the MER database developed for NASA by Brothers, a stage weight rollup is performed from MERs for tanks, intertanks, skirts, and other such structures. For each of these, parameters such as total component surface area are used as regressors, implying that a vehicle geometry must be defined. A similar model was used by Villeneuve. [79]

In order to provide a LV mass model consistent with the vehicle parameterization described in Section 4.1.1, a custom set of MERs were created based on LV data published in the *International Reference Guide to Space Launch Systems*. [200] The MERs were fit at the LV stage level, and based on anticipated scaling/sizing behaviors presented in [201], the Net Mass Fraction (NMF) was selected as the response of choice. The form of equation used in the stage MER regression is shown in (4.1):

$$NMF = k\left[a_0 + a_1\left(\frac{w_{propellant}}{d}\right)^{-\frac{2}{3}}\right] \tag{4.1}$$

where NMF is defined as $w_{dry}/w_{propellant}$, and d is the stage's propellant bulk density. The term in parentheses can be interpreted as a representative volume for the stage; stage propellant mass scales with tank volume, while stage structures tend to scale more closely with tank surface area. Thus, a rudimentary dimensional analysis points to the selection of the $2/3$ power term. Two different sets of a coefficients were computed, one for stages with storable propellants (RP-1, UDMH, Aerozine-50, etc.), and another for cryogenic stages (all LH2 in this case). Figures 4.5 and 4.6 show the resulting relationships plotted against the data points. The k coefficient in (4.1) is included as a technology factor

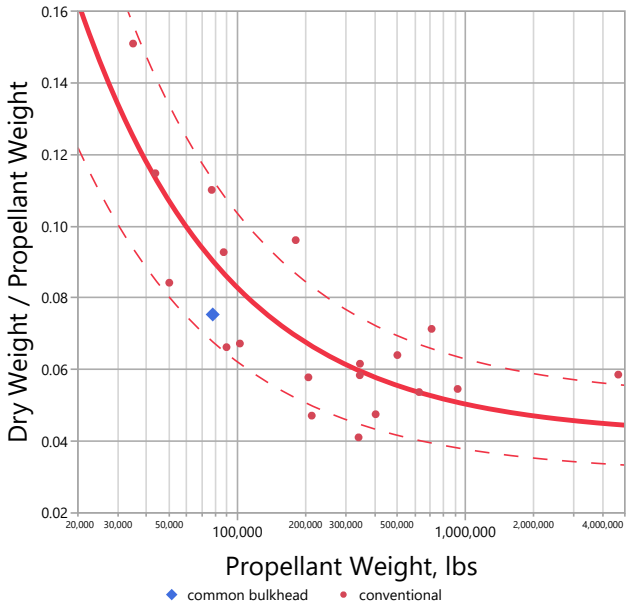

Figure 4.5: Storable propellant stage regression. Dotted lines show the range captured by a k value from 0.75 to 1.25.

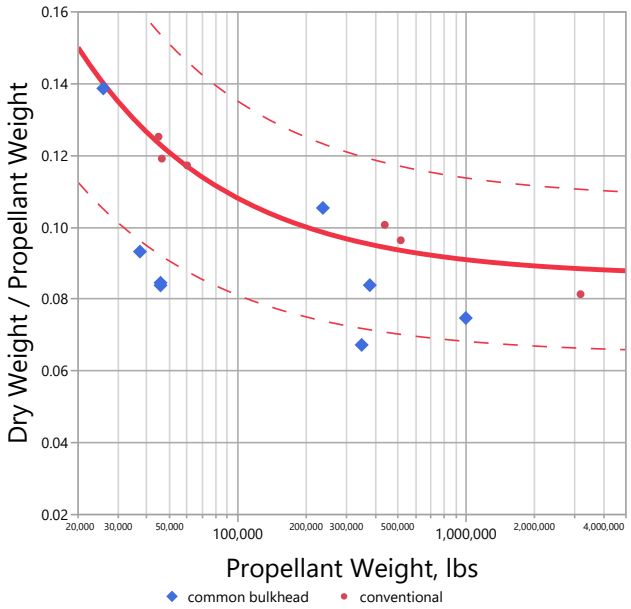

Figure 4.6: Cryogenic propellant stage regression. Dotted lines show the range captured by a k value from 0.75 to 1.25.

on structural efficiency. As shown in Figures 4.5 and 4.6, some stages were identified as employing common bulkhead tanks, an advanced structural concept in which the oxidizer and fuel tanks share a common wall between them. In most cases, common bulkhead stages achieve significantly higher structural efficiency than predicted by the MERs (which were fit only to conventional data points). There is some variance in the data around the curve fits that may be attributable to other design factors not captured by the simple structure of the MERs used; the k coefficient accounts for the effect of these factors, allowing the MERs created to span the full space of historical LV design points.

The NMF regression does not include the weight of engines in its estimation. The choice to model engine weight separately from the rest of the stage was made for two reasons. First, a statistical model of the form used in (4.1) assumes that the non-propellant stage weight is strongly correlated with, and thus can be predicted primarily from, the propellant weight. This seems like a logical starting assumption for items such as propellant tanks, skirts, and intertank structures; however, there is much less reason to expect engine weight would be explained by propellant weight. This argument is supported by a second factor, which is data from the real world: The Atlas V's payload planner's guide advertises the availability of either single- or dual-engine variants of its Centaur upper stage. The single-engine Centaur (SEC) and dual-engine Centaur (DEC) are identical in dimension and weight breakdown, except for a weight delta of 474 lbs. [190] Of this, 370 lbs is the weight of a second RL-10A-4-2 engine; the remainder can be explained as additional feed system and thrust structure weight. [202]

$$w_{engine} = a_0 + a_1 \log(T_{vac}) + a_2 \frac{\dot{m}}{d} + a_3 \log(T_{vac}) \frac{\dot{m}}{d} + a_4 \left(\frac{\dot{m}}{d}\right)^2 \tag{4.2}$$

In order to create a weight estimation model for rocket engines, publicly available data was collected on 37 existing engines. Since the engine weight estimation is only a supporting analysis intended to provide more realism to the LV sizing behavior of the experimental apparatus assembled, a high degree of accuracy is not required. Because of this, a relatively

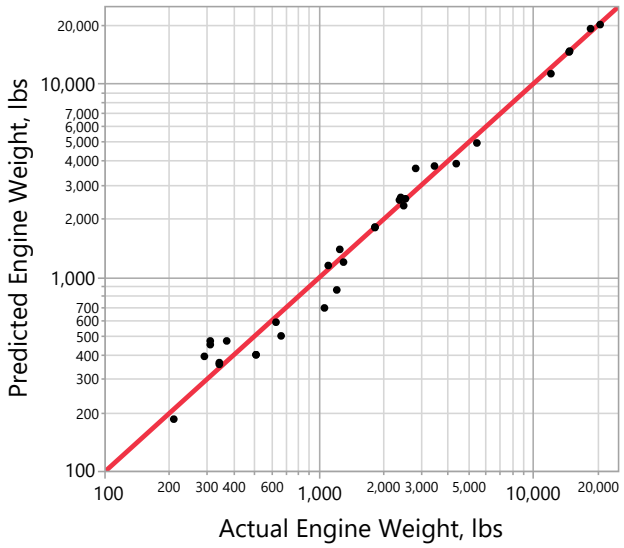

Figure 4.7: Actual by predicted plot for engine mass estimating relationship used

simple relationship structure was assumed, and the data was fit by linear regression on Equation 4.2. The result of fitting engine weight data is presented in Figure 4.7.

With stage dry weight and engine weight models comprising the LV weight modeling decomposition, the full vehicle gross liftoff weight can be calculated according to (4.3).

$$w_{gross} = w_{payload} + \sum_{i=1}^{stages} \left(w_{propellant_i} + w_{dry_i} + w_{engines_i} \right) \tag{4.3}$$

Additionally, with propulsion and weight properties defined for each of the stages in a vehicle, other overall vehicle properties can also be calculated. An important one for the experiments to be performed is the calculation of the vehicle's T/W profile. Figures 4.8 and 4.9 show some example profiles for two of the architectures in the trade space. Note that the plateau in T/W achieved by several of the profiles is due to an acceleration constraint applied as one of the requirements/assumptions on the trajectory.

Performance Analysis

As observed previously, the vast majority of LV studies employ some form of explicit trajectory simulation for calculating LV mission performance. Section 1.3.2 notes that

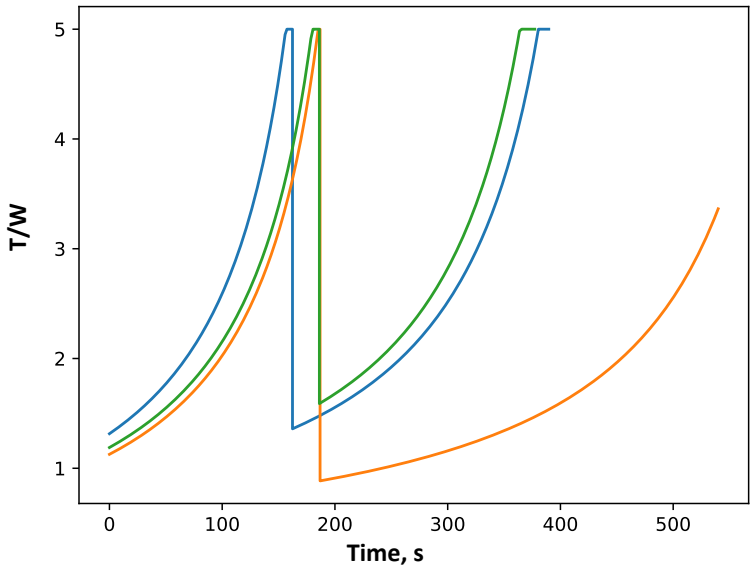

Figure 4.8: A few example T/W profiles for Architecture 1.

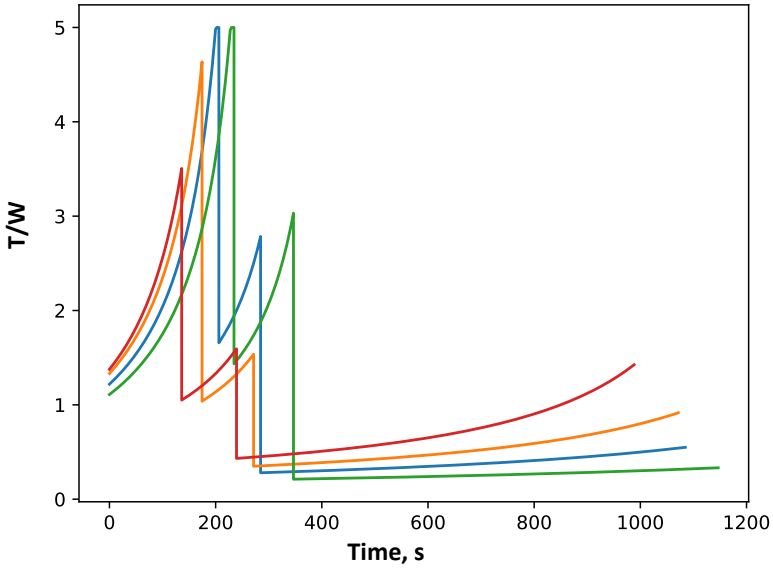

Figure 4.9: A few example T/W profiles for Architecture 21.

this analysis accounts for a significant portion of the effort expended in these studies, and because of this, one of the research questions under investigation in this thesis seeks to identify whether architecture analysis of alternatives studies might resort to using empirical models without compromising the subsequent decision-making. Therefore, two distinct performance analysis models are necessary to carry out the experiments that follow.

The first LV mission performance model selected represents the baseline approach, implementing explicit trajectory optimization via the Program to Optimize Simulated Trajectories (POST). POST is an industry-standard tool originally developed by Martin Marietta, and maintained at the NASA Langley Research Center. [124] It implements a Direct-Shooting approach, and while it exhibits all of the challenges associated with solving an NLP approximation of the optimal control problem, recent efforts by this author and his coworkers have developed a library of wrappers and subroutines that significantly improve POST's ability to execute in an automated fashion. [131, 164, 163, 166] One of the key accomodations made to the lack of robust convergence in POST is to run many repetitions of each case, each with a different initial control vector guess. While this significantly increases the execution time required for a given case, it shifts the burden from the human to the computer.

The second LV performance model is extremely simple, assuming that an empirical model of ΔV_{losses} is provided. The estimated loss term is added to the $\Delta V_{mission}$ to produce the ΔV_{ideal} according to Equation 3.5. This sets the performance requirement the vehicle design must be sized to. Outside of the model that predicts ΔV_{losses}, this approach is very simplistic; however, even the full trajectory optimization approach can be viewed as fitting into this pattern, where the losses are simply computed by numberical integration of the equations of motion rather than some empirical relationship.

4.1.3 Cost Analysis

As discussed in Section 2.1.1, decision makers typically deal with FOMs that take the form of either "cost" or "effectiveness." Often there are multiple FOMs comprising an n-dimensional Objective space. Section 2.2.1's discussion on the various aspects of set characterization accomodates this in that both of the attributes discussed, Pareto dominance and probability density, are explicitly multi-objective.

Since the "benefit" perspective in this experimental setup is provided by the payload delivered to orbit, it is necessary to introduce a "cost" metric in order to assemble a realistic testbed for LV architecture selection. There are many types of costs, including all of the various constituents of life-cycle cost, as well as non-monetary figures such as schedule. An architecture selection exercise in the real world would likely include multiple FOMs from both the cost and benefit categories; however, so long as the developed methodology provides for easy extension to problems with multiple objectives, it is only necessary here to demonstrate it with a single cost metric and a single performance metric.

The cost metric selected for incorporation into the experimental apparatus is the vehicle development cost published by Dietrich Koelle in his well known cost model TRANSCOST. [201] This model estimates the cost of an expendable LV by rolling up the separate costs of engine development and stage development, with a factor to account for integration of the separate systems. Equations 4.4-4.6 show the equations in the form in which they were used for this thesis.

$$S = \frac{98.5}{k_{pmf}} w_{inert}^{0.555} \tag{4.4}$$

$$E = 277 w_{engine}^{0.48} \tag{4.5}$$

$$V = 1.04^n \left(\sum_{i=1}^{n} \left(S_i + E_i \right) \right) \tag{4.6}$$

where S is the stage development cost, E is the engine development cost, and V is the total development cost of an n-stage vehicle. In TRANSCOST, these equations have some additional terms to account for things such as experience of the team doing the development, management style, etc. While these all have a tremendous influence on absolute costs, they were left out here for two reasons. First, the cost comparison will be done in terms of a relative normalized cost, anchored with the minimum cost vehicle design set to a cost of 1. Second, no experiments are designed to leverage or test any variations in these additional parameters, so their values are all effectively defaulted to 1.

4.2 Experiment 1: Volitional Uncertainty Propagation

4.2.1 Background

This first experiment seeks to answer the following two research questions:

> **Research Question 1a: What is the most efficient sampling strategy for propagating LV volitional uncertainties from the Design space to the Objective space?**
>
> **Research Question 1b: Is it feasible to use explicit trajectory optimization to characterize LV architectures in an RIDM process?**

These are closely related in that the sampling performance achieved by the approach selected in the first question will indicate the answer to the second question.

In order to answer Research Question 1a, it is first necessary to identify how "efficiency" should be defined. In sampling, convergence is observed when a stationary solution emerges; that is, when the change in a metric of interest with the addition of new samples becomes very small. In this context, the most efficient approach should exhibit the fastest convergence. The particular convergence desired here is in the empirical approximation of the true value of the metric or characterisitc being estimated.

The PDF was identified previously as the metric of interest in LV architecture characterization. In literature, the most common approach to calculating the error of a sample density distribution with respect to the true distribution is the mean integrated squared error (MISE): [203]

$$MISE = \mathrm{E}\Big[\int \big(\hat{f}(x) - f(x)\big)^2 dx\Big] \tag{4.7}$$

A closely related metric is the MIAE, which simply replaces the squaring of the error residual with an absolute value:

$$MIAE = \mathrm{E}\Big[\int \big|\hat{f}(x) - f(x)\big| dx\Big] \tag{4.8}$$

These both are of interest here, as they place emphasis on slightly different aspects of the PDF, and can together provide a more robust estimate of PDF representation error. [171]

With MISE and MIAE identified as the key measures of density distribution approximation accuracy, the only remaining part necessary for carrying out Experiment 1 is a set of candidate sampling strategies. All of the sampling strategies reviewed in Section 2.2.1, Monte Carlo, Quasi-Monte Carlo, and Design of Experiments meet the basic requirements for propagation of volitional uncertainty. They seek to sample the input space in an unbiased manner, distributing points according to the assumed input variable uncertainty distributions. Different formulations of each emphasize a slightly different perspectve on how this uniformity is to be achieved, and it is not clear which ones will prove most suitable. For this reason, several varieties will be tested here.

Table 4.3 presents several space-filling DOEs initially examined. In addition, the Sobol quasi-random number sequence was introduced to test the effectiveness of Quasi-Monte Carlo techniques.

The experimental testbed developed, composed, of LV sizing, performance evaluation, and cost estimation provides the "transfer" function between the Design and Objective spaces.

Table 4.3: Sampling of space-filling DOEs, with succinct descriptions from [204]

Type	Description
Sphere Packing	"maximizes the minimum distance between pairs of design points. The effect of this maximization is to spread the points out as much as possible inside the design region."
Latin Hypercube	maximizes the minimum distance between design points subject to the constraint that even spacing is maintained between factor levels
Maximum Entropy	maximizes the Shannon information of the experiment with the assumption of normally distributed data
Gaussian Process IMSE	"minimize the integrated mean squared error of the Gaussian process model over the experimental region"

4.2.2 Execution

Two initial LV architectures were selected to serve as test subjects for this first experiment. These correspond to Architectures 1 and 21 as presented in Table 4.2. An initial population of LV designs was run through the "high-fidelity" environment defined earlier in this chapter. These were sized to the ground rules and assumptions presented in Table 4.1; the sizing process followed the flow presented in Figure 4.1.

First, the LVs were sized by optimizing the ratio of propellant loadings between the stages to provide the maximum payload to orbit. The initial sizing was done for a ΔV_{ideal} of $32,500 ft/s$, after which the sized vehicles were flwon through the trajectory optimization of POST. The updated trajectory performance was then brought back to the sizing environment, where the upper stage and payload were resized in order to correct for the surplus or shortfall in propellant calculated by POST. The designs produced by this process for Architecture 1 can be seen in Figure 4.10, and for Architecture 21 in Figure 4.12.

This initial data generated was used to regress surrogate models of the payload and cost responses for both Architectures. The surrogates were fit using a feed-forward artificial

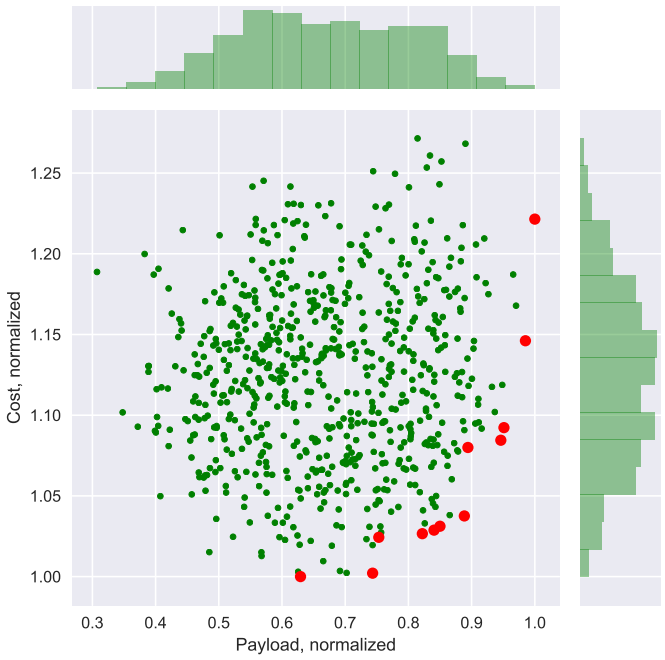

Figure 4.10: Five hundred LV designs from the Architecture 1 family. Pareto front marked in red.

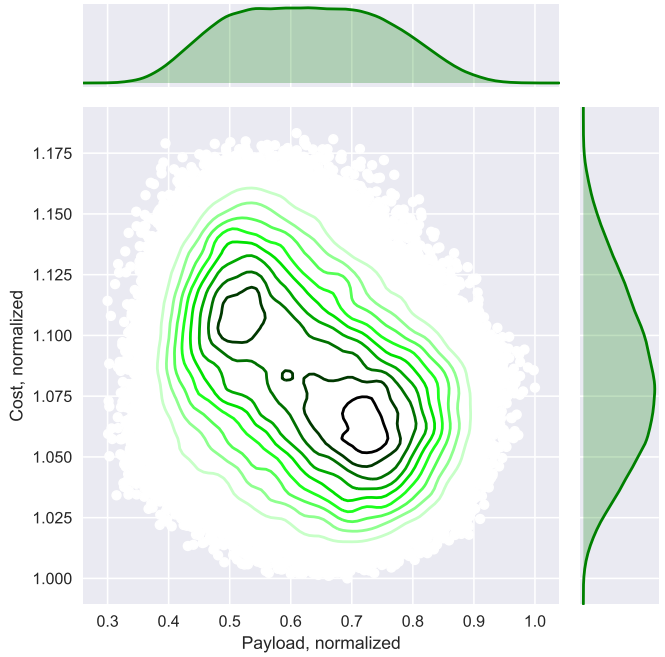

Figure 4.11: "True" density distribution for Architecture 1 in the Objective space. Data points appear as white dots in background; density contours and marginal distributions approximated by Kernel Density Estimators.

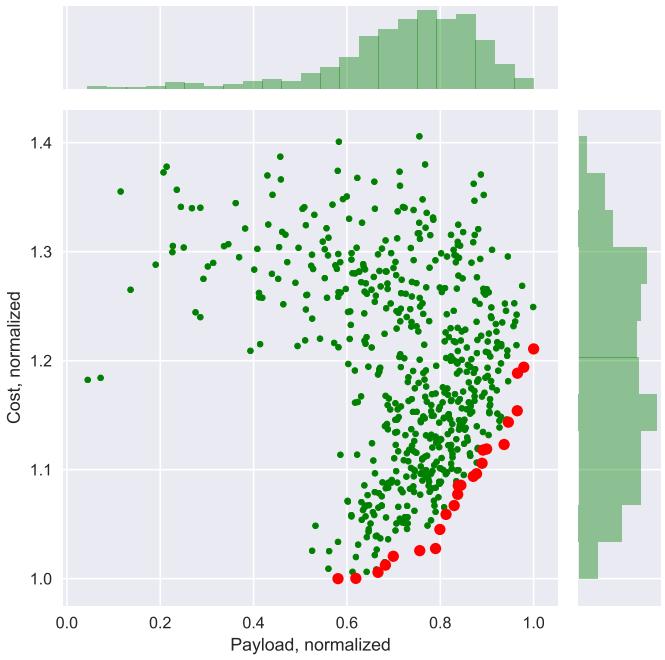

Figure 4.12: Five hundred LV designs from the Architecture 21 family. Pareto front marked in red.

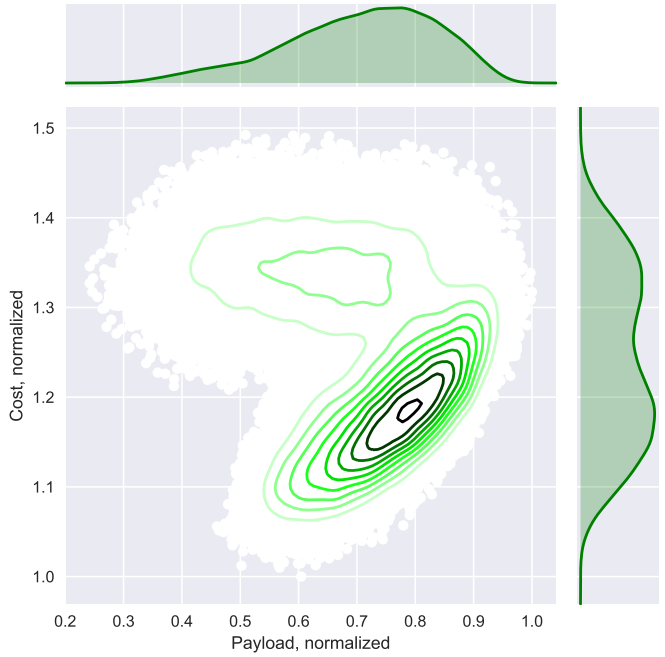

Figure 4.13: "True" density distribution for Architecture 21 in the Objective space. Data points appear as white dots in background; density contours and marginal distributions approximated by Kernel Density Estimators.

neural network using the same approach as presented in [164]. Using the payload and cost surrogates, a 100,000 point Monte Carlo simulation was run over uniform distributions of the independent parameters, creating an extremely dense representation of each architecture in the Objective space. A nonparametric model of the joint density distribution was fit using a Kernel Density Estimator routine. The resulting probability density functions were set as the "true" PDFs for Architectures 1 and 21.

To characterize the performance of Monte Carlo sampling, which is viewed as the baseline sampling approach, it was necessary to perfrom multiple simulations with different random draws. Because Monte Carlo points are selected completely at random, it is possible for there to be non-zero bias in any given sample. This is particularly true for small sample sizes, becoming less of an issue as samples become more orthogonal with greater size. To bound this randomness, the bootstrapping technique was applied 100 times for sample sizes ranging from 25 to 450. The upper and lower bounds on sample error were then identified, and are plotted as dotted lines in Figures 4.14 to 4.17.

In order to test the space-filling DOE and Sobol sequence strategies, 4 different samples having 50, 100, 200, and 300 cases were created for each type. While the DOE methods do not employ random sampling as Monte Carlo does, their creation is not necessarily deterministic – two Maximum Entropy designs of the same size may nonetheless contain different points. To overcome this issue, and to ensure a design that best achieves the underlying statistical objectives, it is common to run refinement routines on the designs, each starting with different initial seeds. This was performed using the JMP software, in which 10 random starts were used to develop the final designs. Once created, the execution of each design ws trivially easy with the surrogate model developed.

4.2.3 Observations and Discussion

The convergence behaviors for each of the different sampling routines are presented in Figures 4.14 to 4.17. The upper and lower bounds of the Monte Carlo sampling performance

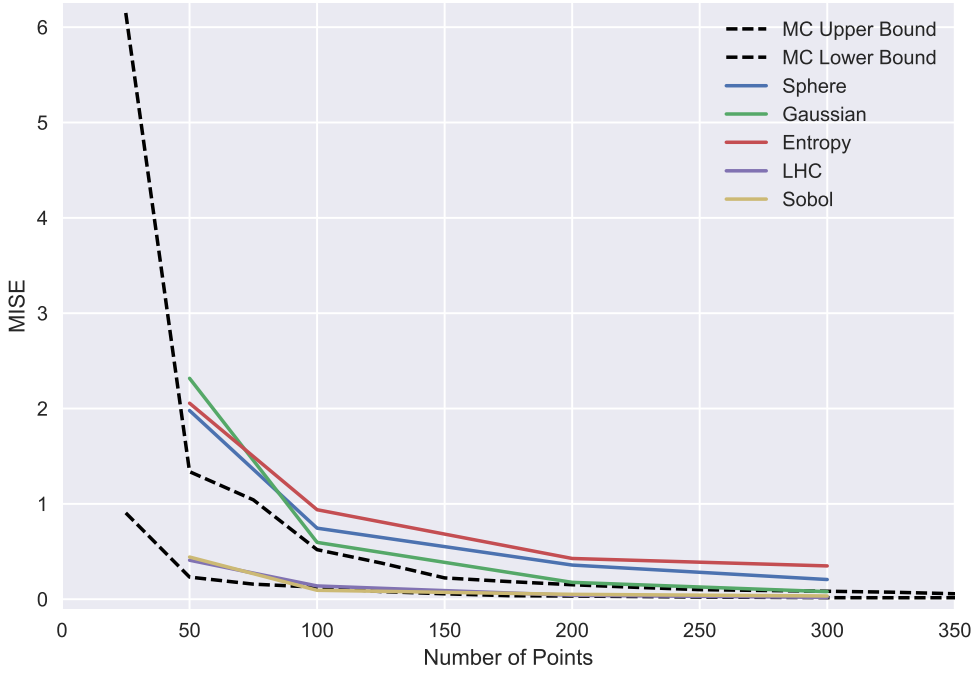

Figure 4.14: Sampling strategy convergence in MISE for Architecture 1.

are overlayed for comparison purposes. These do not represent the performance of any real Monte Carlo; instead, they bound the corridor in which Monte Carlo sampling is expected to fall.From this data, it appears that Maximum Entropy and Sphere Packing designs perform consistently worse than direct Monte Carlo sampling. The Gaussian IMSE design appears to follow the upper boundary of the Monte Carlo trend, while Latin-Hypercube and Sobol sequence sampling follow the lower bound.

From these results, it is clear that the Latin-Hypercube DOE and the Sobol sequence Quasi-Monte Carlo techniques yield the most efficient samples, performing as well as the hypothetical "best" Monte Carlo. All of the strategies begin to converge with Monte Carlo performance as the number of samples grows, an expected result as the law of large numbers comes into play.

There is one significant difference between Latin-Hypercube and Sobol strategies. As a DOE, the Latin-Hypercube requires that the sample size be selected a priori. In general,

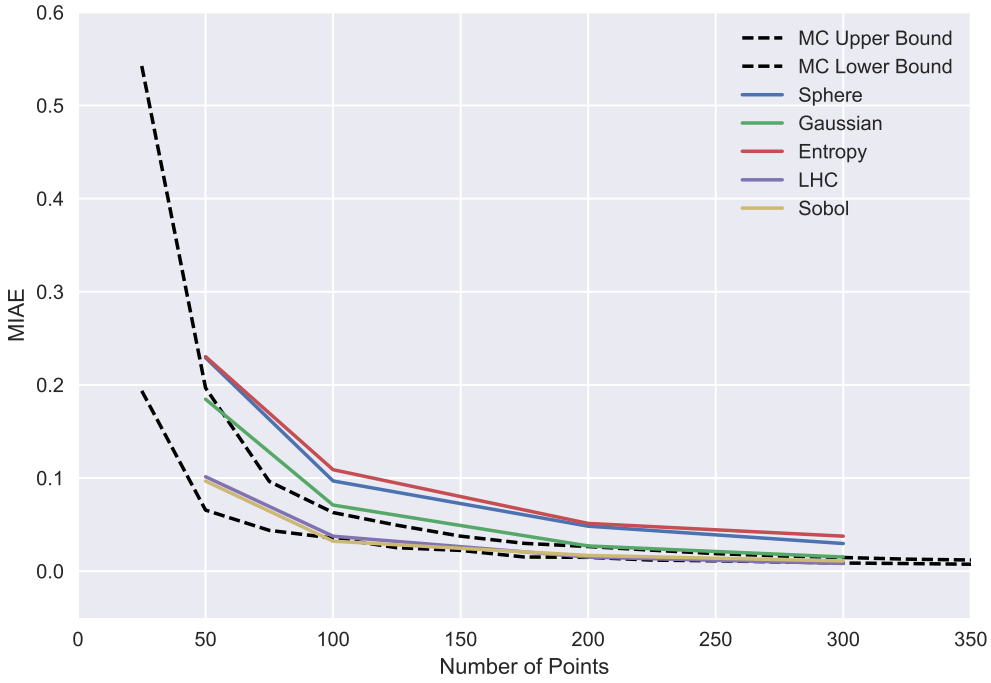

Figure 4.15: Sampling strategy convergence in MIAE for Architecture 1.

DOEs are not additive, in that combining the samples collected from two DOEs employing the same sampling strategy does not necessarily preserve the statistical characteristics of the underlying strategy. This produces a loss in efficiency, as two Latin-Hypercubes concatenated together do not have the same space-filling qualities of a single larger Latin-Hypercube. Attempts to alleviate this degradation in sequential sampling include the development of Nested- and Sliced-Latin-Hypercubes, but even these require a priori selection of nubmer of nestings/slices/samples, etc. [113]

The Sobol sequence, on the other hand, is a quasi-random number generator that is designed to be operated sequentially (as its name suggests). Description of the Sobol algorithm is very involved, and so will not be reproduced here. For reference, see [205]. This sequentail nature frees the analyst from the need for selecting sample size a priori; additional data can be collected and added to the already existing set at any time, and the space filling qualities of the aggregate sample will only be enhanced. For this reason, the

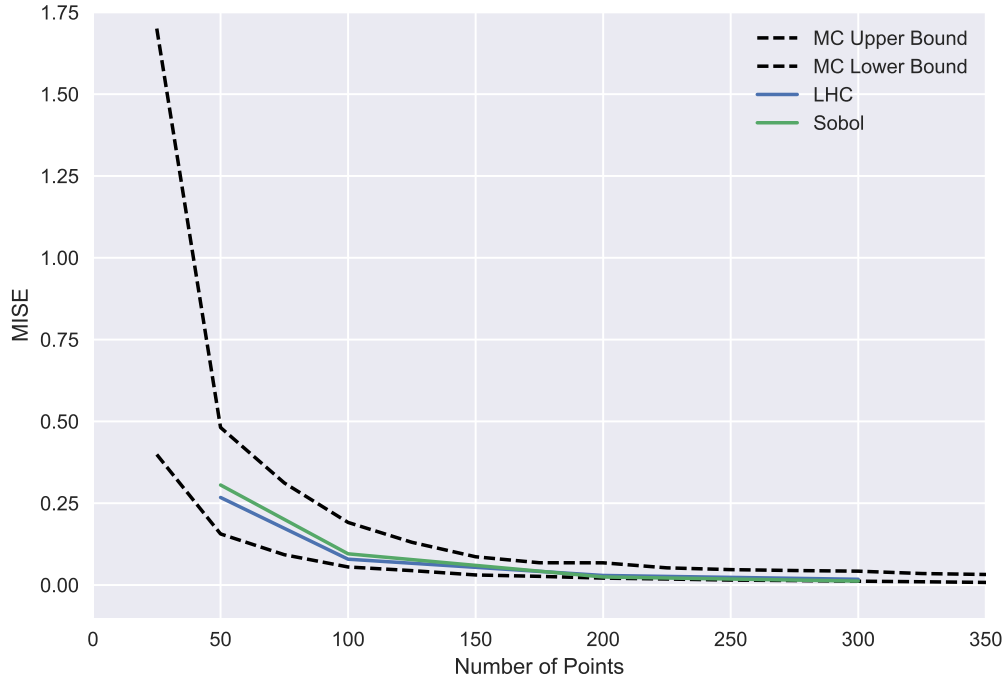

Figure 4.16: Sampling strategy convergence in MISE for Architecture 21.

Sobol sequence may be viewed as preferred over the Latin-Hypercube approach.

Having answered Research Question 1a, Research Question 1b can now be considered. By its nature, any quetion regarding feasible levels of effort will have an answer specific to the organization performing the assessment, their resources, and their objectives/requirements. However, there are a few observations that can be drawn from the experiments performed towards an answer for this question. First, it appears that architecture characterization begins to converge somewhere in the range between 200 and 300 data points analyzed. On its own, this does not immediately seem infeasible; for example, Orbital Sciences reported evaluating "several hundred" concepts in the initail phase of one of their LV assessments for NASA. [77] However, this does become a major undertaking in light of the desire to perform RIDM for architecture selection. This implies the need to evaluate 200 to 300 distinct LV designs for every architecture considered.

A trend seen in the review of LV architecture studies performed in Section 1.3.4 was

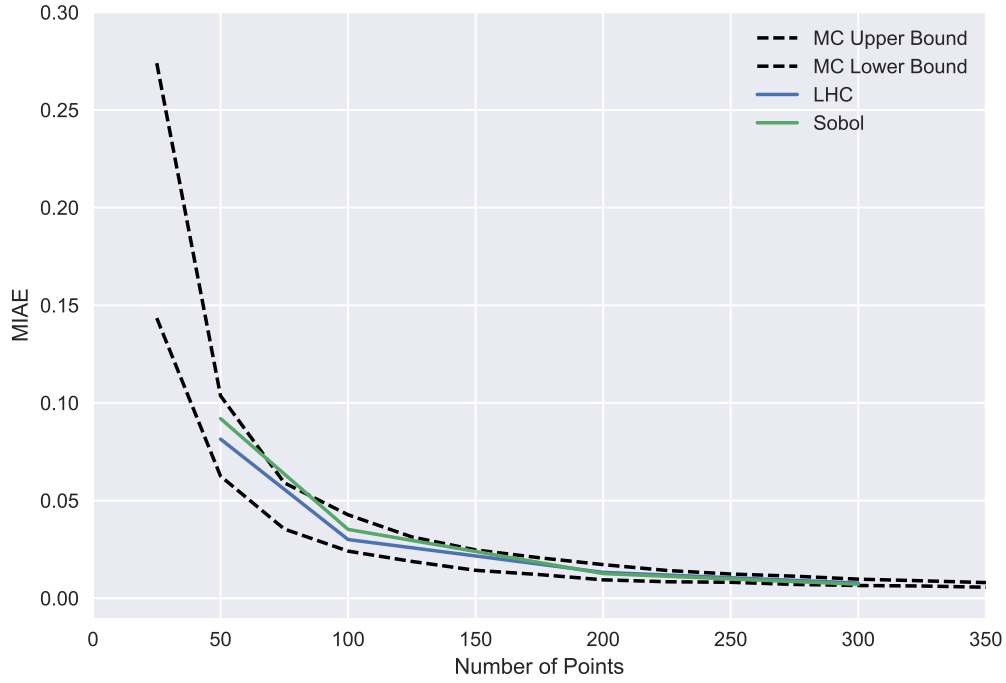

Figure 4.17: Sampling strategy convergence in MIAE for Architecture 21.

an affinity for selecting on the order of 30 concepts for deliberation. The recurrence of this number may be happenstance, but it serves as reasonable rough order of magnitude estimate of the number of architectures that would need to be analyzed. This translates to a requirement to analyze on the order of $10,000$ individual vehicle assessments, a number that is more than two orders of magnitude greater than what traditional architecture trade studies employing explicit trajectory optimization entail. Because of this, Research Question 1b is considered to be answered in the negative.

4.3 Experiment 2: Existing Empirical Model Performance

4.3.1 Background

The results of Experiment 1 showed that performing explicit trajectory simulation in the analysis of alterantive architectures is a very difficult proposition from the standpoint of

level of effort requiredo. It is desirable, therefore, to find another way to perform the assessments that is less costly. The RIDM Handbook provides encouragement in this direction, stating "modeling can commence at a low level of detail; the level of detail can be increased in an iterative fashion based on the requirement to reach a robust decision." [89] It goes on to define a couple of different levels of modeling fidelity that may be acceptable depending on the analysis required:

First-Order Estimating Methodology *"First-order estimates involve the use of closed-form or simple differential equations which can be solved given appropriate bounding conditions and/or a desired outcome without the need for control-volume based computational methods. The equations may be standard physics equations of state or empirically-derived relationships from operation of similar systems or components."*

Detailed Simulation Estimating Methodology *"Estimates using a detailed simulation require the construction of a model that represents the physical states of interest in a virtual manner using control-volume based computational methods or methods of a similar nature. These simulations typically require systems and conditions to be modeled to a high-level of fidelity and the use of meshes or network diagrams to represent the system, its environment (either internal, external, or both), and/or processes acting on the system or environment. Examples are computational fluid dynamics (CFD) and finite-element modeling."*

So, it is acceptable to consider lower-fidelity alternatives to explicit trajectory optimization whose computational expense may be significantly less. The most important thing, as explained in Section 1.3.3, is that the uncertainty in the analysis model should not prevent decision makers from distinguishing correctly between alternatives. For example, if an assessment performed using the Rocket Equation produces analysis of alternatives results which agree with the same assessment performed with trajectory optimization, the higher fidelity should not be required.

There was one work reviewed in Section 1.3.4 that performed a study in which the number of LV designs analyzed was in fact an order of magnitude greater than the $10,000$ estimated from Experiment 1. Villenueve accomplished this by using empirical trajectory models, regressed as surrogates for the actual physics-based code. [79] Combining this observation with the NASA RIDM's allowance for "First-Order Estimating" leads to the formulation of Hypothesis 1:

Hypothesis 1: If an empirical LV performance model is used in place of explicit trajectory optimization, then propagating volitional uncertainty during architecture selection will become a feasible undertaking.

The review in Section 3.2 highlighted a number of different empirical models that have been created in past research efforts. A few of these published their actual model in such a way as to enable reproduction and reuse by others; specifically, Dergarabedian [145], MacKay [146], Townsend [147], White [141], and Schilling [150] all published models in their entirety. Based on their availability, a question that bears asking is the following:

Research Question 2: Do any existing empirical LV performance models provide enough accuracy to support an RIDM process?

Experiment 2 is intended to answer this question.

The majority of these historical models estimate LV performance in terms of velocity losses, ΔV_{losses}. The $\Delta V_{mission}$, as shown in Equation 3.5, is then combined with the ΔV_{losses} predicted, providing a value with which to size the vehicle using the Ideal Rocket Equation. Because their evaluation is decoupled from the Rocket Equation, these models are very easy to swap in and out. MacKay's model is the one exception to this; in it, the required mass ratio of the final stage (assuming a 3 stage vehicle) is predicted. This mass ratio implicitly accounts for the ΔV_{losses}, as it dictates the scaling of the final stage required in order to complete the ascent to orbit.

Of the five existing empirical LV models reviewed in Section 3.2, only two were quantitatively analyzed. The models by White and by MacKay and Weber are both embedded in a very large set of nomographs, which must be approached with a ruler and a whole afternoon to evaluate! The models by Dergarabedian and Ten Dyke, Townsend, and Schilling are more approachable; however, in designing Experiment 2, it was decided to leave Townsend's model out for two reasons: (1) Schilling's model is essentially an updated and refit version of Townsend's model, and (2) Townsend's model performed the worst of the three in the initial quantitative test performed in Section 3.2.

4.3.2 Testing

Before the test could be performed, each model had to be transcribed from the equations, figures, and nomographs in which they were presented in their original source. This process required the use of graph digitization software, followed by parametric regression in order to encapsulate the models in an executable form. Once completed, carrying out the actual test for Experiment 2 was quite straight-forward. The exact same LV designs which were evaluated in Experiment 1 were resized twice, once with Dergarabedian and Ten Dykes' model replacing POST, and once with Schilling's model replacing POST. The results of these analyses are plotted in Figures 4.18 and 4.19.

It is clear by visual inspection that both models overestimate the payload capacity of both architectures, and show somewhat less variance in payload performance as well. In the case of Architecture 21, both empirical models appear to completely miss the trend dispersing and decreasing payload performance for higher cost concepts (see green POST design points in upper left quadrant of Figure 4.19). Another observation is that, while payload performance clearly show a sizeable error compared to the POST data, the two empirical models do not significantly impact the development cost estimation. There are two reasons for this: First, the cost estimation method used is primarily weight based, with some complexity factors acting to modify the baseline model for capturing the effects of

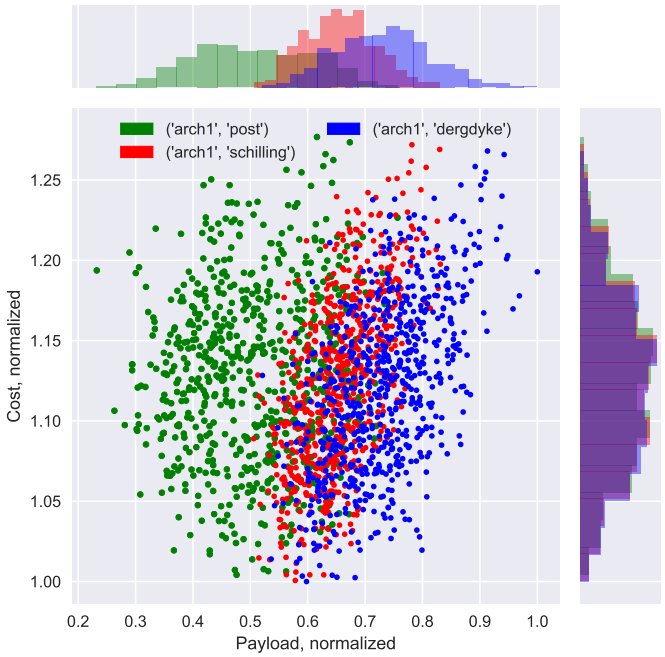

Figure 4.18: Comparison between POST (green), Schilling (red), and Dergarabedian and Ten Dyke (blue) performance models for Architecture 1.

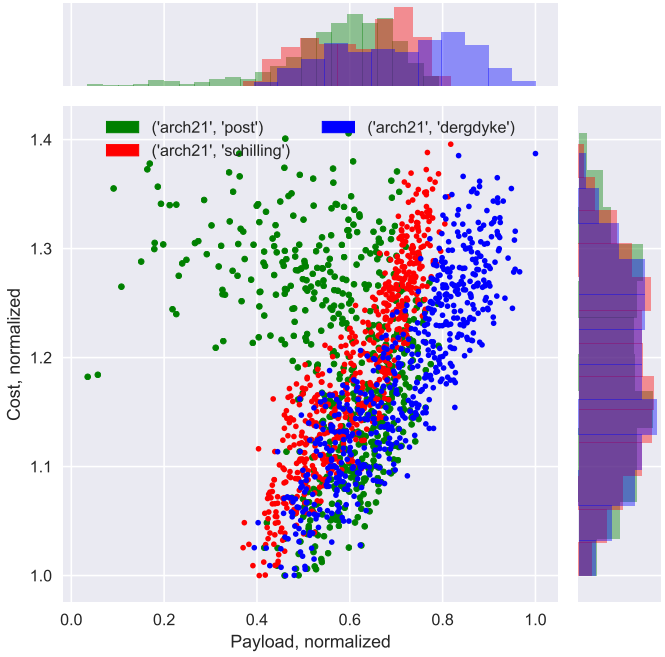

Figure 4.19: Comparison between POST (green), Schilling (red), and Dergarabedian and Ten Dyke (blue) performance models for Architecture 21.

technologies and systems integration tasks. Since the empirical models do not directly impact vehicle structural sizing, cost deltas are not a main effect of the empirical models. The second reason cost does not show a significant impact of using what appear to be somewhat inaccurate empirical performance models relates to the sizing process implemented (depicted in Figure 4.1). Because there is no iteration loop between trajectory performance and the vehicle sizing optimization, there is no opportunity for an optimizer to sieze on the change in models to dramatically shift the design point. This is neither a flaw nor a benefit of the sizing process selected, but it is important to note.

One of the primary hinge points of the RIDM process lies in the selection of a "performance commitment." As discussed in Section 2.3, this does not refer specifically to trajectory performance (as opposed to cost, or any other FOM); rather, it is more a development program performance value, with a commitment to deliver a product at least as good as the performance commitment. [89] As such, the performance commitment is a probabilistic one, usually associated with some specified confidence level.

With this in mind, the risk from using an surrogate model in an RIDM process lies in the possibility of selecting a performance commitment based on some desired level of confidence, when in reality the probability of meeting that commitment is quite different. Note that the error introduced by a model could go in either direction; that is, an 80% confidence performance commitment developed from a surrogate model could correspond to either greater or lesser confidence when measured against a high-fidelity assessment. While underpredicting confidence may be viewed as less risky than an overprediction, conservatism is not necessarily beneficial in decision making, especially when unintended. [44]

So, a measure of the risk incurred by using a surrogate could be quantified as the difference between the desired confidence and the actual confidence delivered. To give a quantitative look at this concept, points corresponding to 50% confidence (with marginal probabilities in payload and cost selected to be equal to each other) were selected for each architecture using both models. The actual confidence levels achieved are shown in Table

Table 4.4: Architecture characterization errors for existing empirical models

Model	**Schilling**	**Dergarabedian & Ten Dyke**
Architecture 1	0.147	0.044
Architecture 21	0.339	0.099

4.4. These show the extreme risk introduced by the model error.

4.3.3 Observations and Discussion

It is clear from the results of Experiment 2 that both of the already existing empirical models tested fail to capture the behavior observed in the higher-fidelity performance model. In both architecture comparisons performed, the models show evidence of overpredicting payload capabilities. In the case of the 3-stage vehicle, the error is more than a mere bias in prediction; they both fail to capture the second mode of the Architecture 21 PDF, which was depicted clearly in Figure 4.13.

Closer inspection of the data for Architecture 21 reveals the driver of this distinct density feature to be the T/W of the final stage. This is seen clearly in Figure 4.20, which shows that low T/W values place vehicle designs in the lower cost region (blue), higher T/W values place designs in the dominated high cost region (red), with middling values of T/W occuring most frequently in the elbow between (gray). This behavior makes sense in light of the sizing optimization process that produces these data points. Higher thrust implies larger engines, which will be more expensive, and while higher thrust will provide better trajectory performance, the increased weight will negatively impact stage mass ratio. This, in turn, will require a larger sized stage to carry more propellant, taking away payload given the $5,000,000$ lb GLOW constraint. So, cost will be higher, but payload performance may see relatively little change.

With these observations, the answer to Research Question 2 is considered to be answered in the negative. So, it appears that if a satisfactory empirical model is to be found,

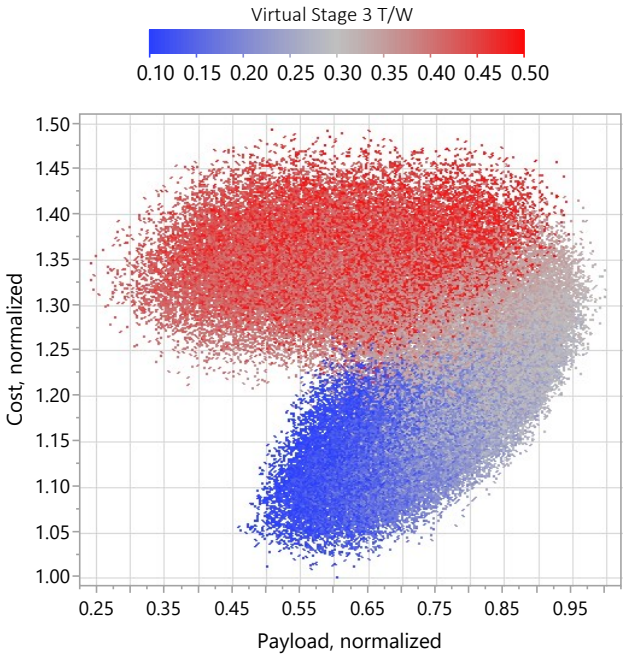

Figure 4.20: T/W of the 3^{rd} virtual stage drives the multi-modal behavior of Architecture 21's PDF.

it will have to be created.

4.4 Experiment 3: Functional Regression Performance

4.4.1 Background

Hypothesis 1 proposed the use of an empirical LV performance model for propagating volitional uncertainty during architecture analysis of alternatives. This approach is not unprecedented, as evidenced by the contemporary modeling efforts reviewed in Section 3.2. However, each of these efforts was focused on design space exploration within a fixed LV architecture. Only Villenueve's thesis used empirical models for performance estimation while varying architecture, but he did so by creating a separate surrogate model for each architecture. Because creating individual models for every architecture concept is considered to be cost prohibitive for studies evaluating large numbers of alternatives, an architecture-spanning model is sought. Experiment 2 examined if any existing empirical models might still be used, despite most of them being out of date. The results indicated that the historical models contain too much error, to the point of even failing to capture the correct trends in the data. This leads to the posing of Research Question 3, which states:

> **Research Question 3: Is it possible to develop a multi-architecture spanning surrogate of LV performance that provides enough accuracy to support risk-informed architecture selection?**

In pursuing a model that is able to predict the performance of diverse architectures, Section 3.3 pointed out the conflicting nature of model generalization and model accuracy. Out of necessity, any model meant to generalize across Design spaces of differing dimensions must operate at some level of abstraction, relying only on parameters that are common to all LVs for predictive power. Essentially, this amounts to establishing a parsimonious mathematical basis for the model to be built on in which every concept has equal representation. In Section 3.3.3, examining the potential regressors that could serve in such a model led to the observation that the T/W profile, when considered as a whole, might be considered a single variable if viewed as a functional. Because T/W exerts so much influence on LV

trajectory performance, Hypothesis 3 was proposed:

> **Hypothesis 2: If the functional nature of the T/W profile is leveraged directly, it will enable the building of an empirical model that is general to a broader range of LV architectures**

The aim of Experiment 3 is to see if leveraging functional data will enable a single surrogate model to span across multiple architectures.

4.4.2 Testing

Since the intent of Experiment 3 is to test the feasibility of regressing an empirical model of LV performance that spans a broad architecture trade space, it was necessary to expand the trade space above and beyond what was used in Experiments 1 and 2, and to provide training data for regression testing. To that end, the high-fidelity sizing environment was run for 250 LV designs from each of the 24 architectures outlined in the trade tree in Figure 4.2. To feed the functional regression testing, the T/W profiles of the LV designs analyzed had to be compiled. Usually these might be conveniently lifted from the trajectory simulation outputs; however, since the intent is to develop a model able to predict LV performance without running a trajectory optimization, a subroutine had to be created to generate predicted thrust profiles based on vehicle design characteristics.

From the literature review, two models were selected to evaluate the feasibility of performing functional regression across all 24 architectures modeled. One was recurrent neural networks (RNNs); the other was nonparametric regression techniques published by Ferraty and Vieu. [172] This experiment did not seek to apply the candidate models to the LV sizing process. Rather, the intent was to train each model to the LV data generated, and evalute the techniques based on their accuracy. Other factors to evaluate include model portability, spead of training, and speed of execution.

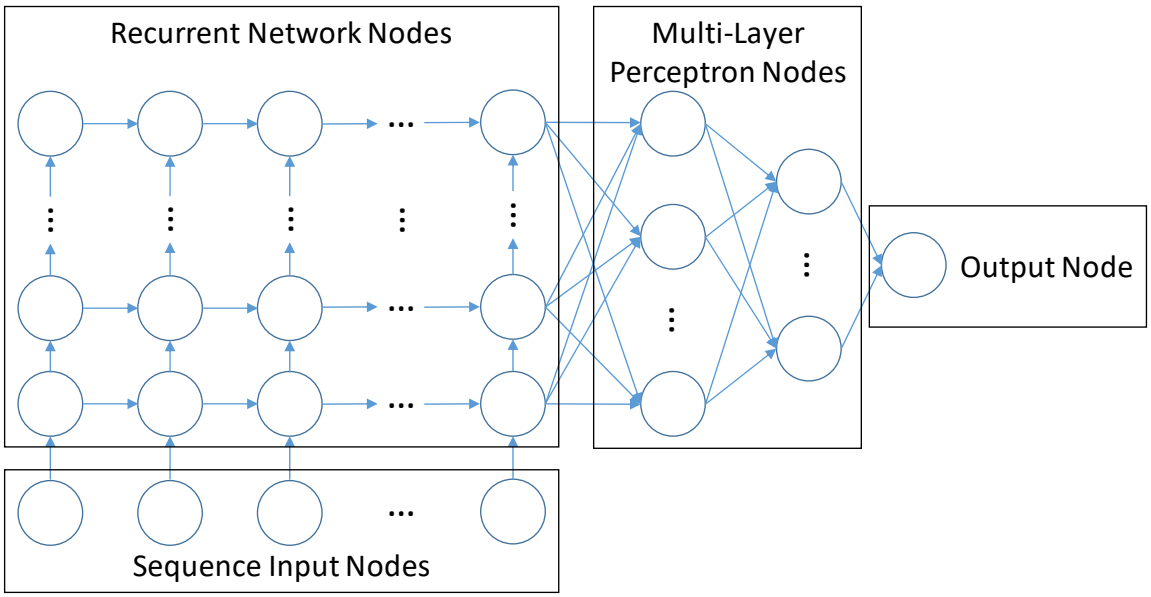

Figure 4.21: Network topology for Recursive Neural Net implemented in Experiment 3.

Recurrent Neural Networks

The RNN architecture selected for application in this experiment is based on that published in [183]. This choice was made due to the simliarity in modeling objectives and problem formulation. An image of the network topology implemented is provided in Figure 4.21. The recurrent portion of the network accepts the T/W profile as a sequence of inputs; the internal states and final output node of the recurrent network are all fed into a fully connected feed-forward network, which is then responsible for developing the final ΔV_{losses} prediction. The model was constructed in the Tensorflow framework, and a variety of network parameters were varied in order to tune the topology to the data set. Final results from model training are presented in Figure 4.22.

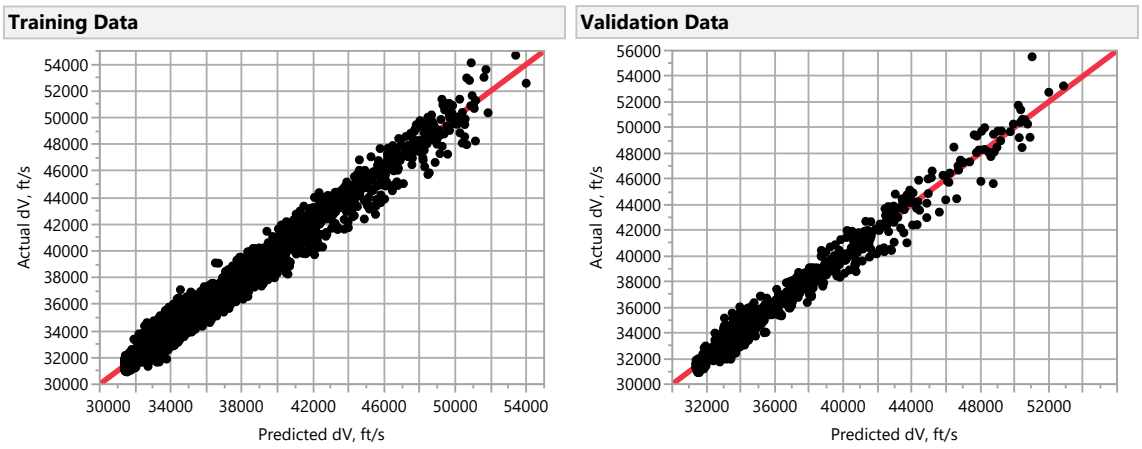

(a)

(b)

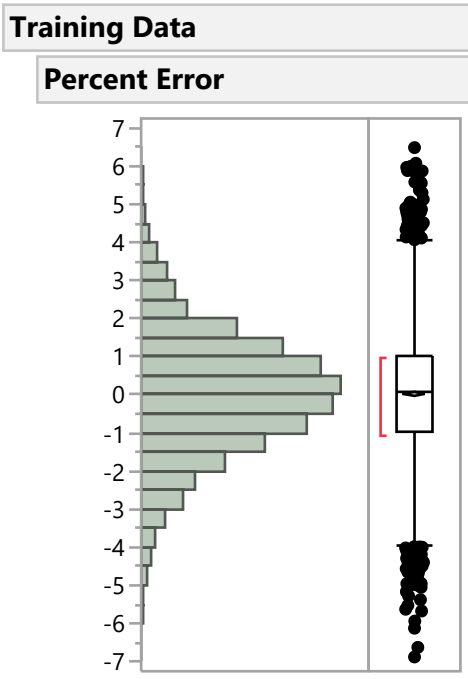

Summary Statistics	
Mean	0.0272899
Std Dev	1.651089
Std Err Mean	0.023179
Upper 95% Mean	0.0727308
Lower 95% Mean	-0.018151

(c)

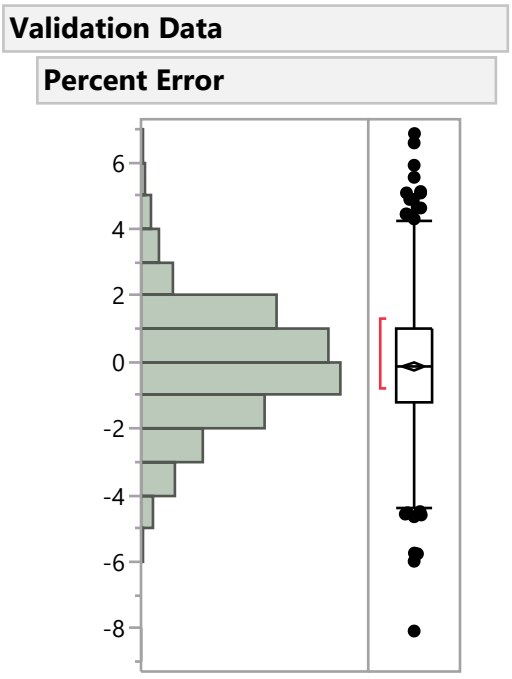

Summary Statistics	
Mean	-0.127565
Std Dev	1.7471083
Std Err Mean	0.0490637
Upper 95% Mean	-0.03131
Lower 95% Mean	-0.22382

(d)

Figure 4.22: Fitting results for best recurrent neural net model; training data in (a) and (c); validation data in (b) and (d)

Nonparametric Functional Regression

An initial application of nonparametric functional regression performed in Section 3.3.1 showed significant promise; however, of the 126 data points with which that initial test was performed, there were actually less than 20 distinct vehicle designs, and these were all variants of just three core vehicles: The Delta II, Delta IV, and Atlas V. So, the results achieved there are not a good measure of how the techniques might apply to a broader design space.

The framework for nonparametric functional data analysis (NPFDA) put forward by Ferraty and Vieu adapts a variety of kernel based techniques and algorithms for use on functional data. Within this framework, there are several different modeling types, including supervised classification, unsupervised classification, time series prediction, and scalar-on-function prediction. Of these, the last is the application of interest, where the T/W functional input is used to predict the ΔV_{loss} scalar response.

Several modeling techniques exist in the NPFDA library for scalar-on-function regression. Since the concept of functional prediction of LV performance is a completely new one, there is no evidence, and very little intuition, about which type will be best suited to the problem. For this reason, the first step taken was to do a broad sweep of model types, varying some of the key tuning parameters along the way. The results from this sweep are presented in Table 4.6, with descriptions of the model attributes in Table 4.5. From these results it is clear that the Nearest-Neighbor techniques, denoted by a leading "knn," seem to perform the best in general. Another overarching trend observed is that six principal components in the distance semimetric provides for lower error. The best fit was selected from this set, and analyzed further in Figure 4.23.

Table 4.5: Nonparametric functional model key

Model Key	Description
kernel_cv	Kernel estimator with bandwidth selected by cross-validation
knn_lcv	Nearest-neighbors kernels estimator, local number of neighbors selected by cross-validation
knn_gcv	Nearest-neighbors kernels estimator, global number of neighbors selected by cross-validation
quadratic	Quadratic kernel shape
triangle	Triangular kernel shape
pca(n)	n-number of functional principal components to use in distance calculations

Table 4.6: Functional kernel regression results

Model Specification	RMSE
kernel_cv_quadratic_pca(3)	1667.46726
kernel_cv_quadratic_pca(6)	1434.785907
kernel_cv_quadratic_pca(9)	1528.598865
kernel_cv_triangle_pca(3)	1622.301844
kernel_cv_triangle_pca(6)	1377.674715
kernel_cv_triangle_pca(9)	1481.835457
knn_lcv_quadratic_pca(3)	1217.164962
knn_lcv_quadratic_pca(6)	712.507135
knn_lcv_quadratic_pca(9)	767.4183793
knn_lcv_triangle_pca(3)	1209.283218
knn_lcv_triangle_pca(6)	704.0450135
knn_lcv_triangle_pca(9)	758.7156721
knn_gcv_quadratic_pca(3)	1147.165683
knn_gcv_quadratic_pca(6)	668.9859682
knn_gcv_quadratic_pca(9)	741.1395204
knn_gcv_triangle_pca(3)	1145.333333
knn_gcv_triangle_pca(6)	662.0195153
knn_gcv_triangle_pca(9)	730.7184805

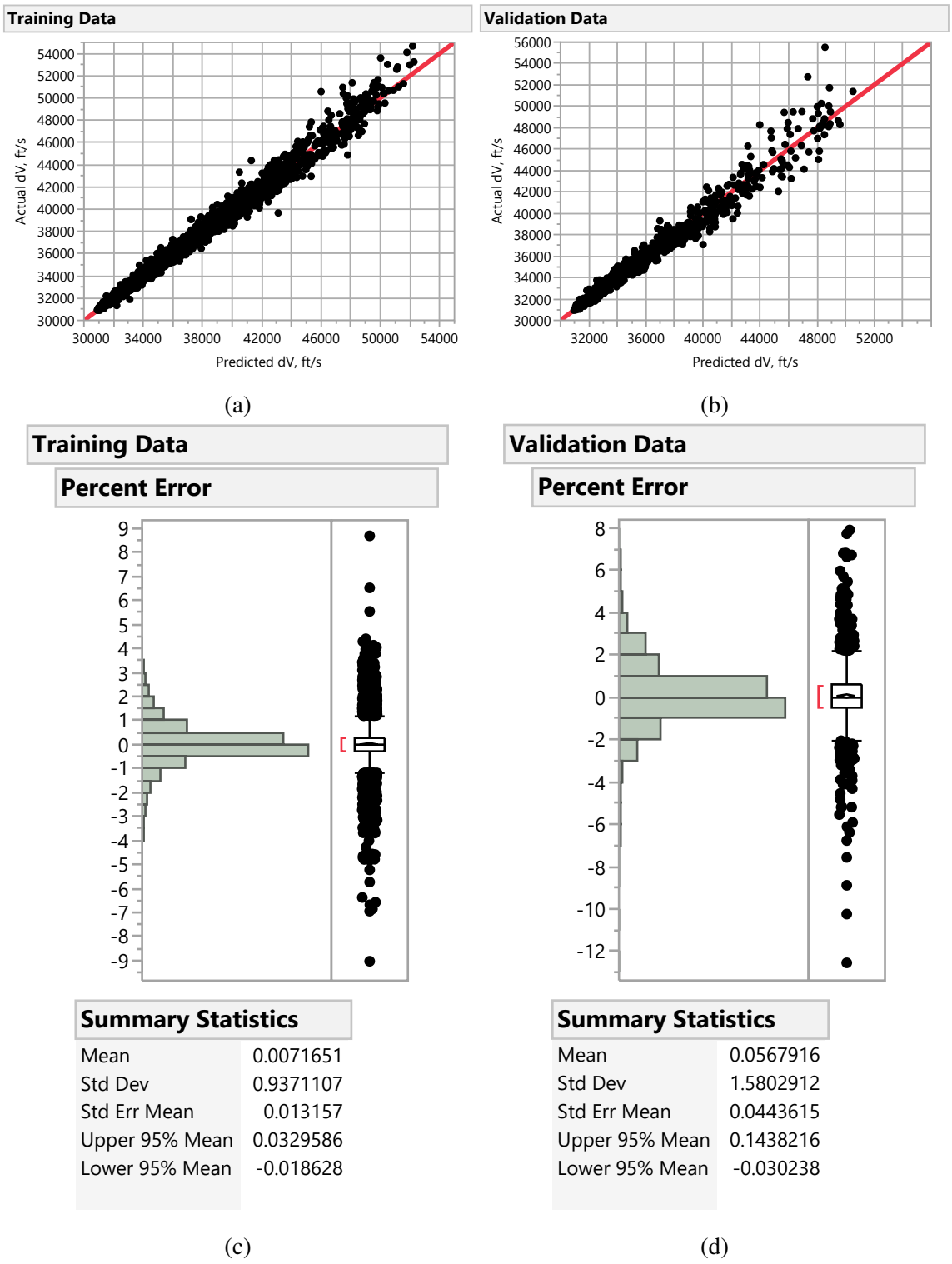

Figure 4.23: Fitting results for best nonparametric regression model; training data in (a) and (c); validation data in (b) and (d)

4.4.3 Observations and Discussion

Both RNN and NPFDA approaches show very strong predictive power with the T/W profile functional as the lone regressor. This confirms the argument in favor of a functional treatment of T/W. In addition, the fact that the data used in the training and validation comes from a diverse set of LV architectures which could not be expressed in a common finite-dimensional basis proves that the functional treatment provides a means of creating architecture-spanning models. Non-functional approaches to empirical modeling of the trajectory such as those demonstrated in [79, 152, 164] would require at least four different models to be fit across the subject architecture trade space. With these results, Hypothesis 3 is considered confirmed.

With regards to accuracy, both functional modeling approaches can predict velocity losses with an accuracy of $+/-$ 4% error. This is comparable to the best historical models based on the accuracies they claimed at the time of their creation. The most significant differentiating factor between the two approaches tested lies in the effort required, both manual and computational, to build and train the model. The RNN required more effort to design and setup the appropriate network topology, and took significantly longer to train on the data provided. The NPFDA model, on the other hand, provided nearly "out-of-the-box" capability. Given its nonparametric approach to modeling, the NPFDA approach could potentially become prohibitively expensive for extremely large data sets; however, the data set used in this experiment is considered to be a fair representation of what might be encountered for LV architecting problems. Because of these observations, the NPFDA model was selected as the preferred approach for implementing a functional regression of LV trajectory performance.

4.5 Proof of Concept

The three preceding experiments developed and demonstrated the elements necessary for implementing sampling-based uncertainty propagation in the earliest phase of LV design. These set the stage for a demonstration proving the overarching hypothesis that ”if volitional uncertainty in the form of Design Freedom is quantified and propagated, decision makers will be able to perform risk-informed LV architecture selection.”

With the empirical model developed, the volitional uncertainty resident in the architecture trade space can be propagated to the Objective space. Figure 4.24 shows the results. In it, density contour plots for each architecture alternative have been plotted, along with their corresponding marginal plots for both Cost and Payload. A number of high-level observations can be made immediately by visual inspection. First of all, the variability of the responses present in the architecture trade space selected is significant; there is a nearly 90% increase in cost from the lowest cost to the most expensive LV concept, and a variability of nearly 500% from the lowest to the highest payload performance. Secondly, a distinct Pareto Front can be discerned, and multiple different LV architectures are seen to reside on the Front.

Additional observations can be drawn by parsing through the individual architecture contour plots, which are presented in Appendix B due to their number. It is clear to see that some architectures exhibit far more variability than others, with some even displaying multi-modal behaviors in their densities. Vehicles with more stages, whether core stages or boosters, contain the greatest variability, an expected outcome given their greater number of uncertainty sources.

The overarching hypothesis in this dissertation posits that **”if volitional uncertainty in the form of Design Freedom is quantified and propagated, decision makers will be able to perform risk-informed LV architecture selection.”** With this new dataset available, it should now be possible to assess the value provided by the inclusion of uncertainty into

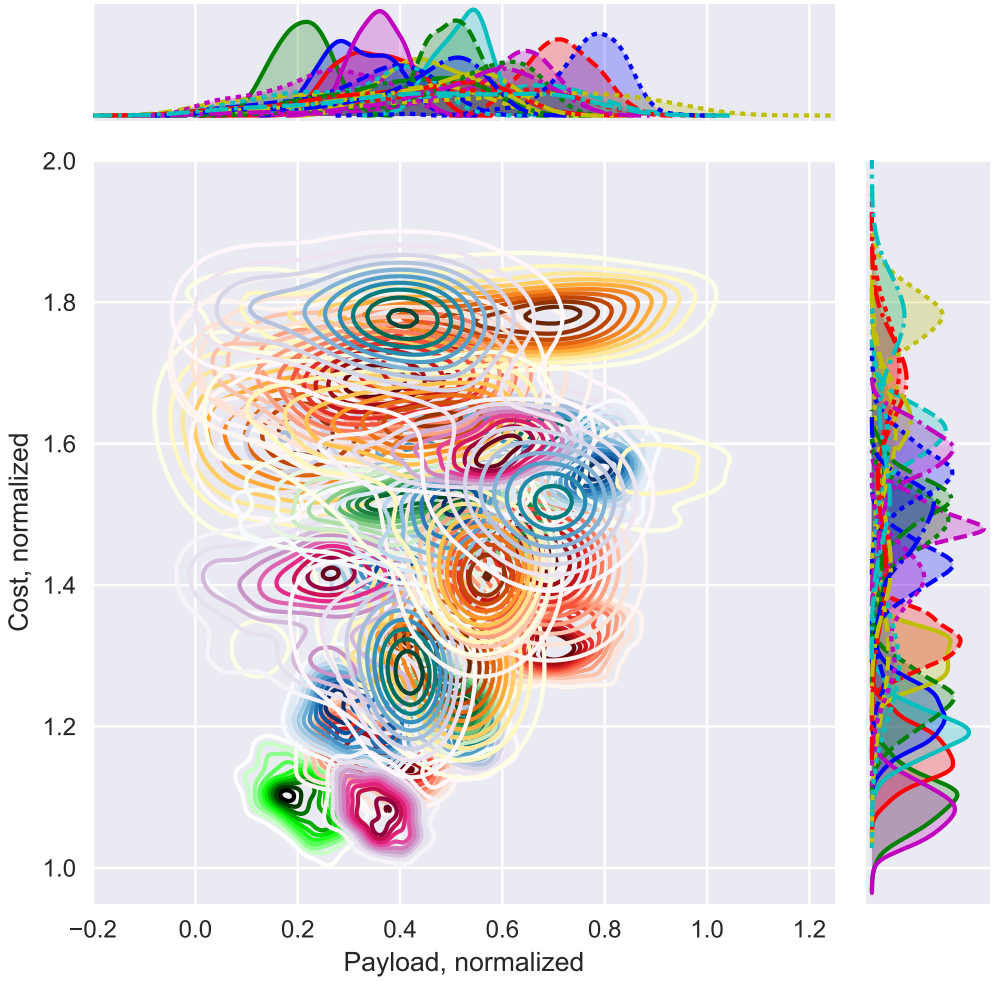

Figure 4.24: Plot of probability density distributions for all 24 architectures considered.

the architecture evaluation. While Figure 4.24 is too messy to do any probabilistic analysis by visual inspection, the data plotted contains all of the information necessary to establish probabilistic performance commitments for each architecture.

A key question to consider in evaluating the merit of the overarching hypothesis is whether the explicit treatment of uncertainty leads to any substantially different decision options or outcomes. In order to explore this, several distinct scenarios are explored with the data presented in Figure 4.24. These are presented in the sections that follow.

4.5.1 Dominant Architecture Identification

In any LV architecture analysis of alternatives, each architecture under consideration is characterized by a representative design point. These design points are typically used as the basis of comparison between alternatives, and provide a tangible concept for decision makers to weigh and deliberate over. While many studies do not reveal exactly how each architecture representative was selected, a very logical approach would be to perform some form of optimization routine to produce the "best" candidate from each architecture design space. In Section 1.3.4, it was observed that LV architecture studies rely almost exclusively on deterministic analyses to identify representative design points. The only exception is the reliability analysis performed by the ESAS study; however, even this analysis was based on a deterministically-sized vehicle. For this reason, deterministic optimization is taken here as the baseline approach for LV architecture characterization.

Figure 4.25 presents a scatterplot of the 24 architectures defined in Section 4.1.1, as reprsented by design points selected by an optimizer. The particular optimization scheme employed was a very basic approach to stochastic optimization: A Monte Carlo random search was executed over the nonparametric functional regression created in Experiment 3 to densely populate the design space, and the optimal design points were selected from the Pareto Front for each architecture using a uniformly weighted Technique for Ordered Preference by Similarity to Ideal Solution (TOPSIS) algorithm. In this case, the performance

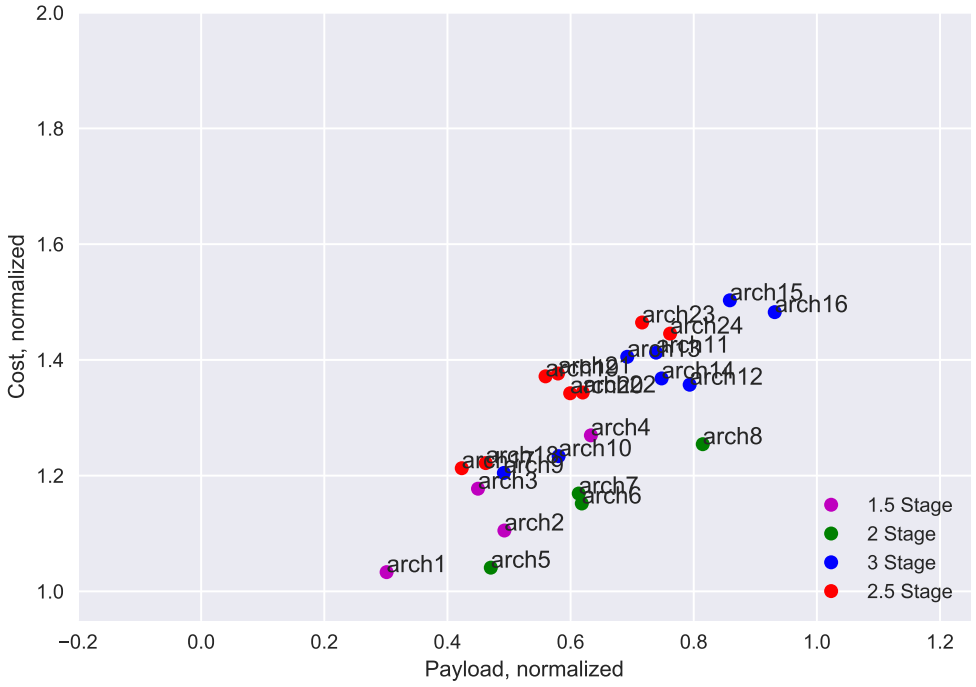

Figure 4.25: Architecture performance commitments based on an optimizer-selected LV design point

commitment (as used in the RIDM process) corresponds to the actual cost and payload capabilities of a specific vehicle.

From the results obtained, a clear Pareto front of architectures can be observed. Architectures 2, 5, 6, 8, and 16 comprise the dominant set, and 1.5, 2, and 3-stage vehicles all exist within this set. To view how a risk-informed perspective might alter this decision space, a set of probabilistic architecture representatives was created, initially selected according to an aggressive risk tolerance (which was defined as 20% confidence for the commitments in both cost and payload). The performance commitments were not derived from specific individuals within the Monte Carlo set of designs; rather, univariate Kernel Density Estimator (KDE) functions were fit to the Monte Carlo data for both cost and payload (as depicted by the side plots on Figure 4.24), and these were querried for the 20% confidence intervals on both FOMs. Figure 4.26 presents these results.

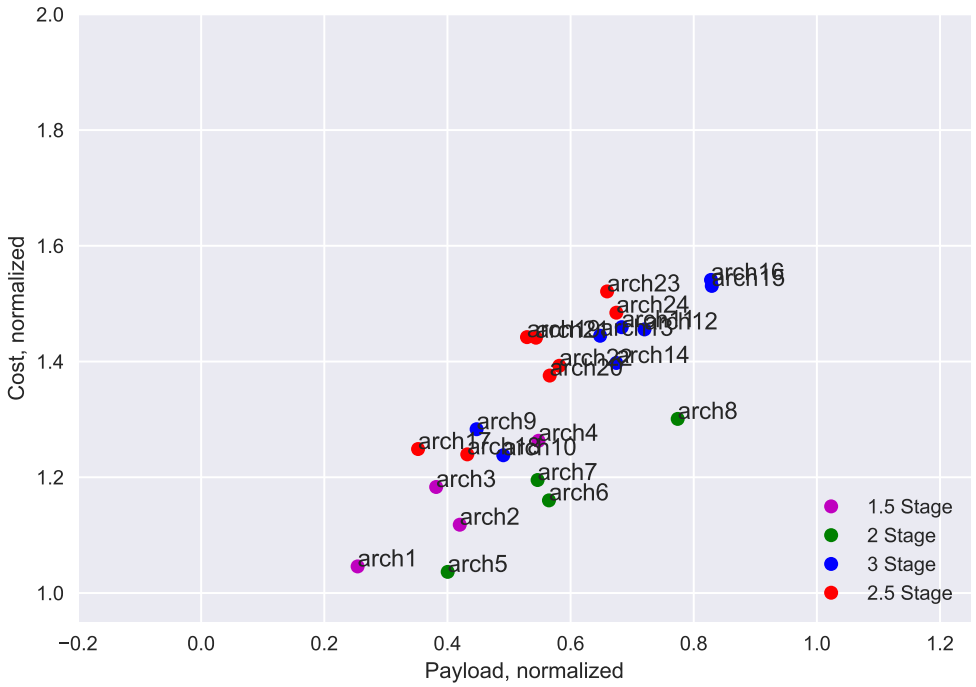

Figure 4.26: Architecture performance commitments for an aggressive decision-making risk posture

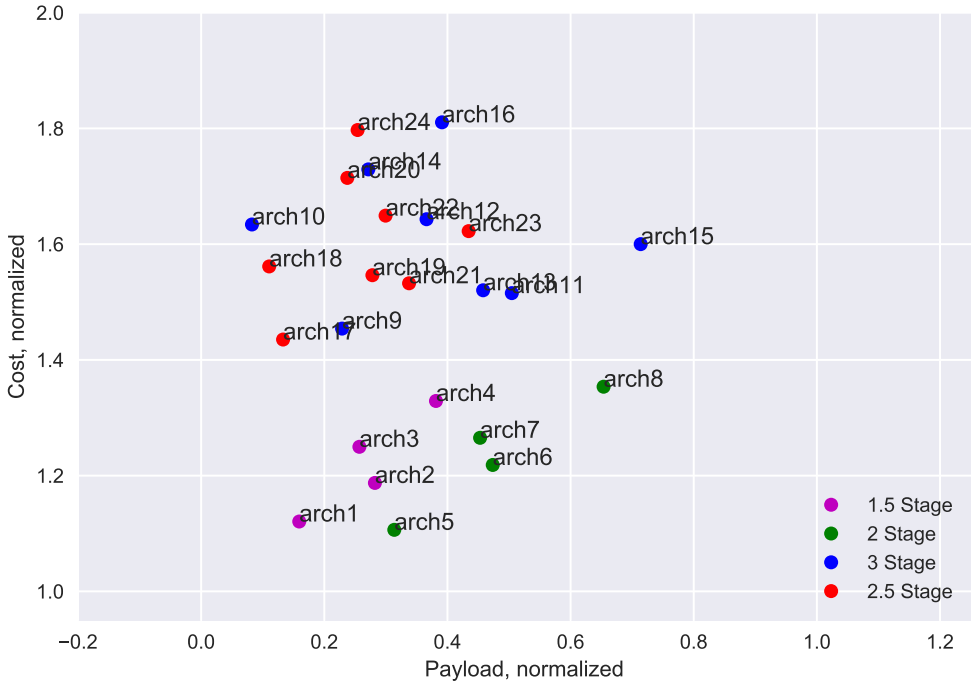

Figure 4.27: Architecture performance commitments for a conservative decision-making risk posture

The results obtained from the probabilistic analysis with the aggressive risk stance do not differ significantly from those arrived at by the deterministic optimization. There is an overall shift of the points towards lower payload and higher cost, which may influence decision makers towards a different portion of the Pareto frontier as they search for preferred solutions. This may be particularly true in the case where specific cost or payload requirements have been identified, which would lead to decision making with a "performance-normalized risk" rather than "risk-normalized performance" perspective (as discussed in Section 2.3.1). However, the dominant set of architectures shows only a minimal delta from the deterministic case: Architecture 16 has been supplanted by Architecture 15, but only by a marginal amount. The two alternatives are so close as to be considered as equivalent options for this decision making risk posture.

One more probabilistic case was evaluated, identified as a conservative risk posture,

with 80% confidence required for both cost and payload commitments. Using the same KDEs developed for populating the aggressive risk-informed decision space, the performance commitments were reevaluated for each of the architectures. As can be seen if Figure 4.27, some significnat shifts have occurred in the data, revealing a distinct clustering of the results by architecture type. Architectures with 3 virtual stages (either 2.5 or 3-stage vehicles) exhibit the most significant shifts, with average decreases of 20% and 40% for cost and payload commitments, respectively. The increased sensitivity of these architectures over that of 2 virtual stage architectures is not altogether unexpected, as increasing the number of sources of uncertainty should increase the variance in architecture performance. Nonetheless the significance of the shift is striking.

Also of note is the change in the Pareto front. Architectures 5, 6, and 8, all 2-stage vehicles, have become the most clearly dominant options. Architecture 15, still technically non-dominated, only provides five percentage points more payload performance than Architecture 8, at the cost of 20 percentage points increase in cost. Architecture 2, the only 1.5-stage option on the deterministic Pareto fron, is now fully dominated; also, Architecture 16, originally dominant over Architecture 15, is now revealed to be very poor performing within the conservative risk posture perspective. The dramatic shift of this architecture as risk tolerance is dialed back reveals the peril of performing architecture selection with a deterministic analysis: There is no accomodation for architecture sensitivity, and so there is very little understanding generated on how a particular baseline concept may behave as the design space matures through subsequent phases of design.

CHAPTER 5
CONCLUSION

5.1 Recapitulation

In Chapter 1, affordability was observed to be the single biggest objective in all the LV programs of today. Governments seek assured access to space that can be realized within constrained budgets, and commercial entities vie for survival, profitability, and market-share. From literature, it is clear that the biggest opportunity for affecting cost savings resides in improving decision-making early on in the design process. However, a review of historical and recent studies revealed very little progress in improving the quality of knowledge provided to decision-makers tasked with performing LV architecture selection. Specifically, no significant improvements in the quantification or reduction of uncertainty appears to have been achieved, as all the analyses employed in architecture analysis of alternatives are executed in a deterministic fashion. Because of this, the main objective for this thesis was stated as: **"To develop a methodology for enabling risk-informed decision making during the architecture selection phase of LV programs."**

An analysis of the key issues at play in this earliest phase of design leads to the identification of Design Freedom as the most significant source of uncertainty, and so the overall hypothesis formulated posits that **"if volitional uncertainty in the form of Design Freedom is quantified and propagated, decision makers will be able to perform risk-informed LV architecture selection."** Taking NASA's Risk-Informed Decision Making (RIDM) process as a point of departure, a number of research questions emerged relating to its implementation in LV design. The first two research questions arose upon concluding from a review of probabilistic analysis techniques that a sampling-based approach would best meet the need to accurately construct the probability density function (PDF):

Research Question 1a What is the most efficient sampling strategy for propagating LV volitional uncertainties from the Design space to the Objective space?

Research Question 1b Is it feasible to use explicit trajectory optimization to characterize LV architectures in an RIDM process?

The results from Experiment 1 indicate that Sobol Sequence sampling, a Quasi-Monte Carlo technique, provides the most efficient and flexible strategy for propagating LV volitional uncertainties. Even with this approach, though, experiment results show that somewhere between $200-300$ samples are needed to resolve an architecture's probability density in the Objective space. Because of this, the volume of analyses that would be required to perform a full architecture analysis of alternatives would be at least two orders of magnitude greater than traditional LV architecture trade studies, leading to the answering of the second research question in the negative.

The same review of probabilistic analysis techniques indicated that sampling with an approximating "surrogate" of computationally expensive processes might provide a feasible approach instead. A number of examples from literature support this, leading to the formulation of Hypothesis 1:

Hypothesis 1 If an empirical LV performance model is used in place of explicit trajectory optimization, then propagating volitional uncertainty during architecture selection will become a feasible undertaking.

A literature survey uncovered a variety of empirical models constructed in the past, with the most comprehensive ones dating back to the late 1950s and early 1960s. This finding makes sense given the need at that time to perform preliminary analyses by hand prior to seeking refined numerical integration solutions on mainframe computers. Several of these models were published in their entirety, and so it is of interest to answer the naturally arising question:

Research Question 2 Do any existing empirical LV performance models provide enough accuracy to support an RIDM process?

Experiment 2 tested two of the historical models against the sizing data set that was generated in Experiment 1. Initial results raised significant doubts regarding their suitability for reuse. The performance of the two models was inconsistent between the two different architectures tested, but with significant error in both cases. For the first LV architecture, a 1.5 stage concept, both empirical models appear to agree with the higher-fidelity data, though with significantly overpredicted payload performance; in the other, a 2.5 stage configuration, they altogether failed to capture a distinct feature of the PDF constructed from higher-fidelity analyses. Based on these inital results, there is very little confidence in either historical model's ability to support future LV studies. Since it has been stated that "uncertainty in the analysis model should not prevent decision makers from distinguishing correctly between alternatives," a final conclusion on the historical models' potential for reuse would more conclusively be decided in the context of comparing decision-making outcomes. This analysis will follow, but it appears that a new empirical modeling approach is needed.

When considering the development of a new empirical LV performance model, a common observation among the majority of models in literature is that they are constructed for one architecture at a time. If a study is to evaluate multiple architectures, it uses a different model for each one. This is seen as a significant impediment, as it has the potential to require more analysis effort than a direct Monte Carlo. In short, it might be cheaper to characterize an architecture's PDF by Monte Carlo sampling than to generate the data required to regress the surrogate model intended for use in carrying out the Monte Carlo! Because of this potential showstopper, the only feasible option would be if a single model were able to span across multiple architecture concepts. The research question regarding this issue is:

Research Question 3 Is it possible to develop a multi-architecture spanning surrogate of

LV performance that provides enough accuracy to support risk-informed architecture selection?

In examining the potential regressors that could serve in such a model, the T/W parameter was identified as being a key driver of LV performance. This finding was supported by both a review of regressors in literature, as well as an examination of the physics governing trajectory performance. Further examination revealed that the T/W profile, when taken as a whole, might be considered a single variable if interpreted as a functional. Taking this perspective would allow for all architectures to be described in the same infinite-dimensional basis, making available a variety of functional regression techniques that might be able to provide an architecture-spanning predictive capability. Because T/W exerts so much influence on LV trajectory performance, Hypothesis 2 was proposed:

Hypothesis 2 If the functional nature of the T/W profile is leveraged directly, it will enable the building of an empirical model that is general to a broader range of LV architectures

Experiment 3 carried out a test of this hypothesis by regressing two distinct models using the T/W functional alone as a regressor. Results showed significant success in producing empirical models with good predictive power and gaussian error distributions. The accuracy achieved by these models is in line with the accuracies quoted for the best of the historical models in the era in which they were constructed. For this reason, Hypothesis 2 was accepted.

A final implementation of the risk-informed methodology for LV architecture selection was performed over the trade space of 24 architecture concepts, and the ability to establish a risk-informed Pareto Front based on a decision maker's desired risk posture was demonstrated.

5.2 Final Methodology

The objective of this research was stated as the development of a methodology for risk-informed LV architecture selection. Through a literature review, NASA's Risk-Informed Decision Making (RIDM) process was identified as a good baseline approach. A further decomposition of the problem and accompanying review of literature revealed the "Risk Analysis of Alternatives" to be the only step where a significant gap existed for LV analysis. Specifically, the difficult, often manual process of trajectory optimization, generally known within the community as necessary for quantifying LV performance and performing sizing, was identified as an impediment to performing uncertainty propagation. The methodology proposed in response to these challenges consisted of the adaptation of RIDM to accomodate sampling-based uncertainty propagation using surrogate models of the trajectory performance. The specific surrogate modeling implementation selected consists of a functional regression of performance as a function of the T/W profile, a single, infinite-dimensional predictor variable. The final methodology as exercised in the Proof of Concept in Section 4.5 is depicted in Figure 5.1.

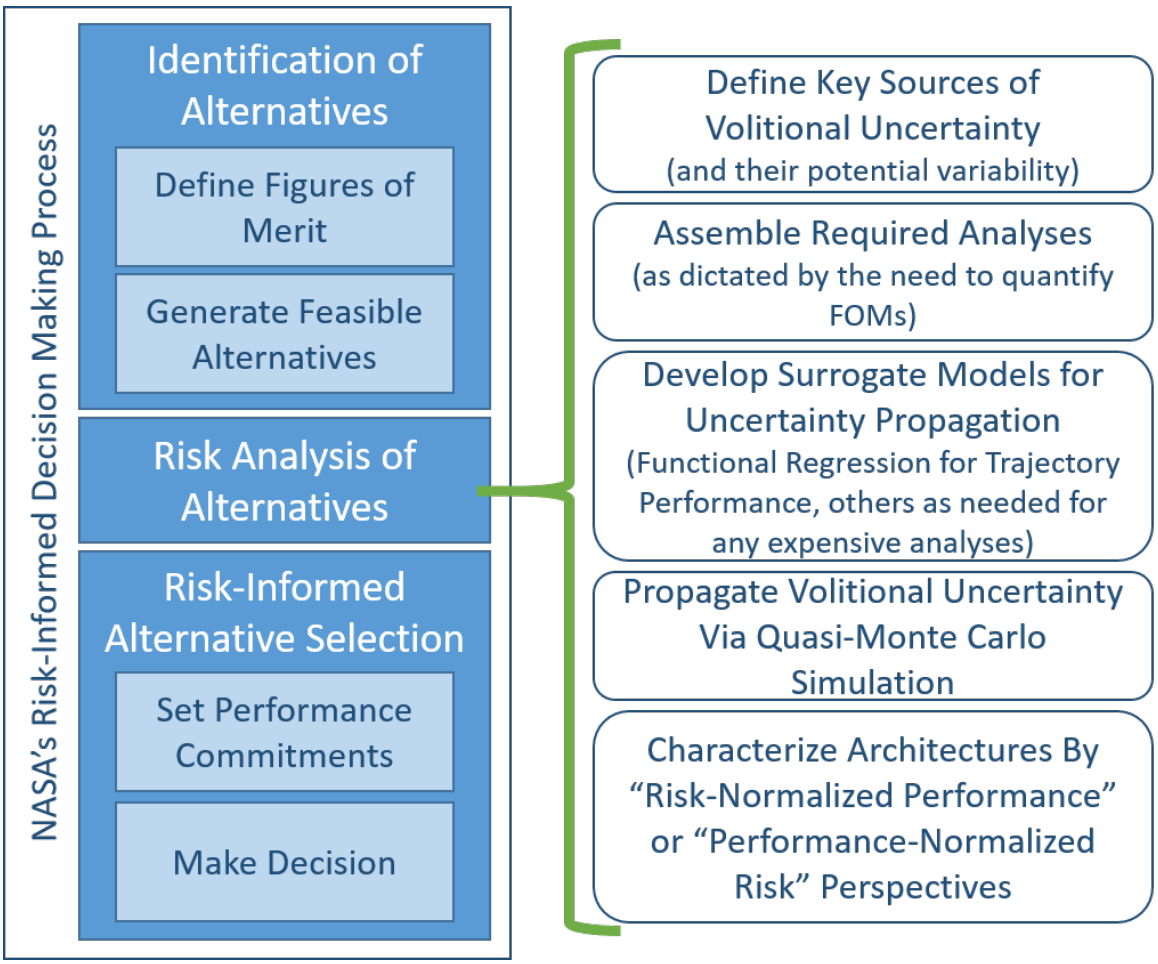

Figure 5.1: Mapping of methodology developed as an enhancement to NASA's RIDM process.

5.3 Final Thoughts

This thesis set out to identify the major challenges facing LV architecture selection, and to find a way of addressing them such that better, more informed decision making would result. The absence of any treatment for uncertainty in this earliest stage of design was identified as a significant problem. The large amount of design freedom that exists early on manifests itself in the form of volitional uncertainty, and so this was selected to be the targeted uncertainty in developing a risk-informed LV architecture selection methodology. The biggest challenge to performing probabilistic analysis in early LV design was identified as LV mission performance estimation via trajectory optimization, but the introduction of architecture-spanning empirical performance models provided a means of overcoming this. All of the identified methods and techniques fit into the overall risk-informed decision making methodology, which has now been demonstrated as a feasible approach to performing LV architecting studies.

5.3.1 Future Work

Many other enhancements and research tracks branch off from the work performed here, so many as to make this thesis seem very small in comparison. A few of the unexplored avenues of research include:

- How do other types of analysis relating to aspects such as manufacturing, operations, and the supply chain fit into this type of risk-informed decision making framework? These are responsible for the remainder of the life-cycle cost, and all the recurring costs, so selecting affordable alternatives will require their consideration at some level.

- How should other types of uncertainty be handled? The case was made briefly that volitional uncertainty during architecture selection is large enough to envelope many other types of uncertainty; however, this was not tested explicitly, and may not be

true as more detailed design attributes or assumptions come into play.

- This thesis focused on implementing the first instance of functional regression and proving that the T/W profile carries signiciant predictive power. It did not test the functional treatment of the complex T/W profiles developed by solid rocket motors, but this would be a natural extension that would be very valuable.

- Implementation of a fully-fledged multidisciplinary optimization routine may uncover some additional challenges for integration. The use of empirical models in iterative solution schemes may place tighter requirements on their acceptable error

These, among others, all seem to be potentially fruitful avenues of research to pursue. The work done in this thesis serves as a foundation for any of these, as performing probabilistic LV mission performance and sizing analysis is a critical capability in many other studies.

Appendices

APPENDIX A

LAUNCH VEHICLE DESIGN PROCESS & BENCHMARKING

The design process implemented in the experimental apparatus presented in Section 4.1 is intended to provide data with sensitivities and correlations realistic to what would be observed in real world LV design studies. The design process was not, however, assembled to produce globally optimal LV concepts; instead, the analysis flow is laid out to achieve fully closed LV designs in a robust, rapid, and repeatable way. The specific workflow implemented is presented in Figure A.1; the sections that follow in this appendix describe all of the major steps taken, except for one. The Vehicle Development Cost estimation is a very simple step in which the final closed design is evaluated through the cost estimating relationships as presented in Section 4.1.3.

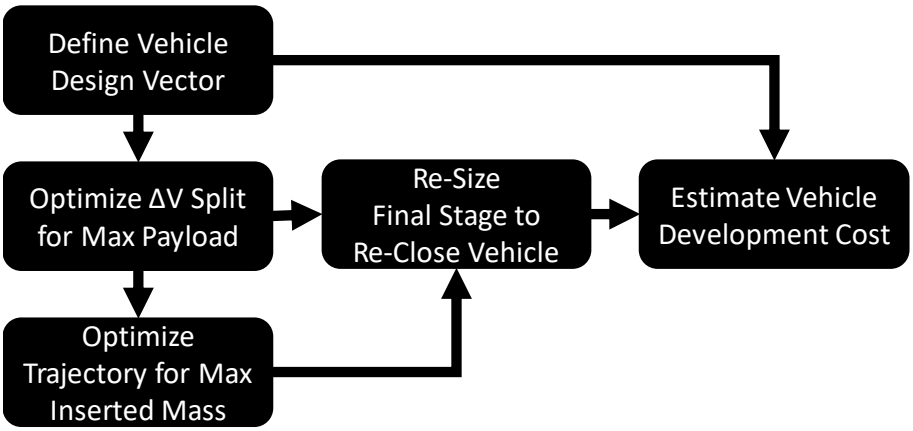

Figure A.1: Implemented process flow for LV sizing

A.1 Define Vehicle Design Vector

The design process kicks off with the definition of a high-level set of vehicle design parameters that uniquely identify a LV architecture concept. These parameters include architecture descriptions of the number and types of stages, plus the relevant ranges for key stage design parameters. Figure 4.2, reproduced for convenience here in Figure A.2, presents the discrete architectural tradespace considered by the experiments in this thesis. Figure A.3 conveys the key parameter ranges selected as representative of the design spaces available for each of the different architecture elements.

In order to proceed with a single vehicle design, a specific vector of parameter values is selected from within the ranges of the assembled vehicle parameterization. In the experiments performed, these selections were made by use of a sampling technique such as Latin Hypercube Design of Experiments, Monte Carlo, or Sobol Sequence Sampling. Once fully populated, the vehicle architecture and high-level design vector are then ready to be fed into the vehicle sizing process described in the next section.

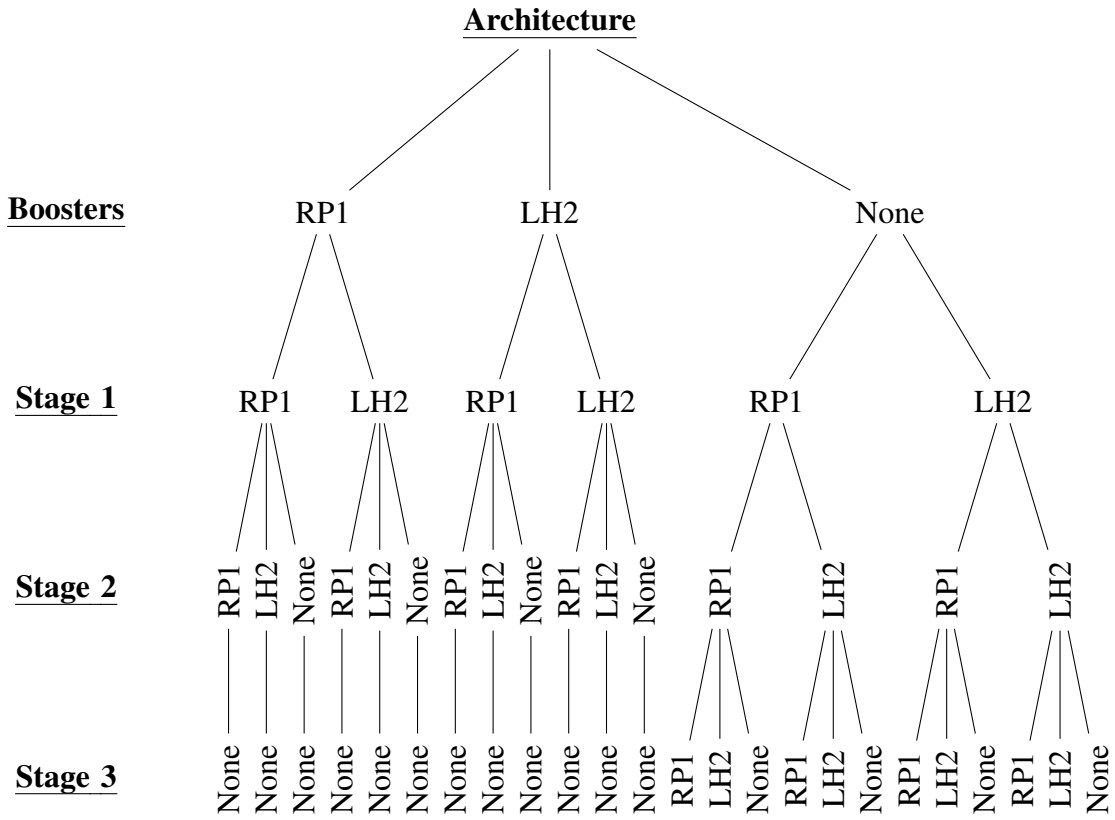

Figure A.2: Tree depiction of LV architecture trade space examined

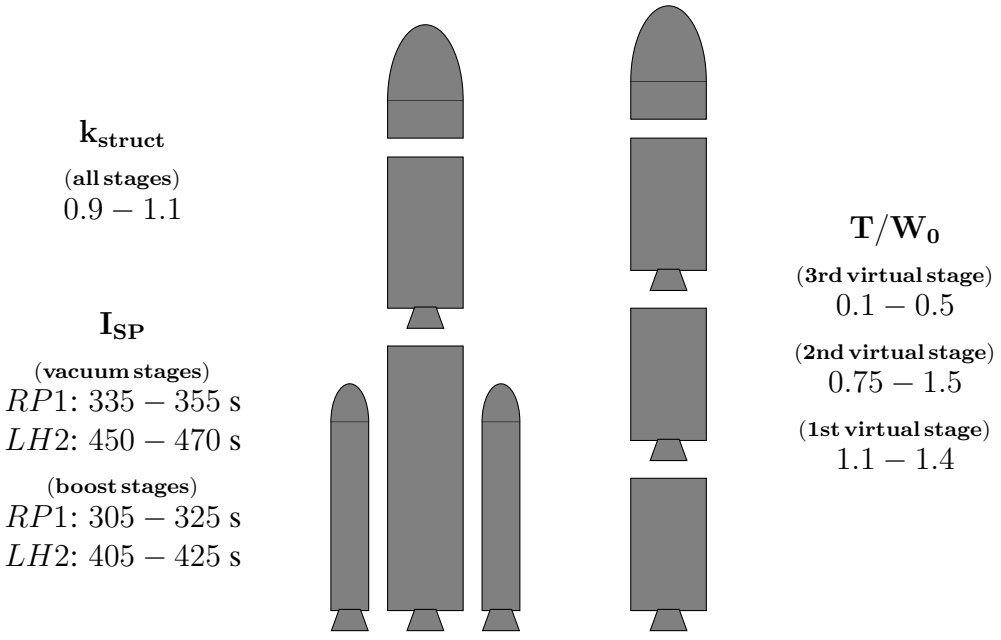

(a) 2.5 Physical Stages (b) 3 Virtual Stages

Figure A.3: LV architecture configurations

A.2 Optimize ΔV Split for Max Payload

The specific vehicle description assembled in the previous step is fed into the LV sizing environment instantiated in the DYnamic Rocket EQuation Tool (DYREQT), which implements a multidisciplinary optimization process to size the vehicle for a mission to Low Earth Orbit (LEO). This mission is represented very simply in DYREQT as a $\Delta V_{required}$, which is assumed to encompass both the energy required to achieve orbit, as well as the losses that would be encountered during ascent. The optimization procedure in DYREQT proceeds with the following formulation:

$$
\begin{aligned}
\text{maximize} \quad & f(\vec{x}, \vec{y}) \\
\text{subject to} \quad & GLOW = 5,000,000.0 \quad lbm \\
& \Delta V_{required} = 32500.0 \quad fps \\
& 0.2 \leq y_i \leq 0.8, \; i = 1, \ldots, m-1 \\
& 60 \quad s \leq burntime_i \leq 800 \quad s, \; i = 1, \ldots, m \\
& a_{max} \leq 5g
\end{aligned}
$$

Here, the objective function, f, is quantified by the total payload capability of the LV, and is computed as a function of the high level vehicle description, $\vec{x}$, and a vector of ΔV fractions, $\vec{y}$. The $\vec{y}$ is of length $m-1$, where m is the total number of virtual stages (defined in Section 1.3.1). Sizing is also constrained by reasonable burn times for each virtual stage, as well as a maximum axial acceleration of the vehicle, a_{max}. To compute the axial acceleration constraint, all core LV stages are assumed to have a depth of throttle down to 0 (a liberal assumption, to be sure).

A.3 Optimize Trajectory for Max Inserted Mass

Once a vehicle design emerges from the ΔV split optimization routine, it is then flown through the physics of an ascent to orbit trajectory. This trajectory is modeled and optimized in NASA's Program to Optimize Simulated Trajectories (POST), which performs an optimization of the following form:

$$
\begin{aligned}
\text{maximize} \quad & f(\vec{z}, \vec{u}) \\
\text{subject to} \quad & R_{final} = 22,262,391.73 \quad ft \\
& \epsilon_{final} = -316,148,110.33 \quad ft^2/s^2 \\
& \gamma_{final} = 0.0 \quad deg \\
& \phi_{final} = 28.7 \quad deg \\
& q_{max} \leq 750 \quad psf \\
& a_{max} \leq 5 \quad g
\end{aligned}
$$

In this case, the four equality constraints represent the targeting conditions for the insertion orbit specified; the remaining two inequality constraints limit the maximum dynamic pressure (q_{max}) and axial acceleration (a_{max}) that the vehicle is allowed to encounter in its trajectory. The objective function for this optimization, $f(\vec{z}, \vec{u})$, returns the final mass inserted into the desired orbit. It is a function of the complete vehicle design vector, $\vec{z}$, and the trajectory control history vector, $\vec{u}$, which the optimizer operates on.

A.4 Re-size Final Stage to Re-Close Vehicle

Once an optimal trajectory solution is found, the actual ΔV losses can be calculated. This quantity invariably differs from the losses assumed in the initial vehicle sizing, and so the design immediately enters into a non-converged state. An obvious next step would be to trigger an iteration loop in which the updated ΔV losses are fed back into the ΔV split

optimization performed in Section A.2. This iteration loop would then continue until some convergence criteria on the ΔV losses were met. However, a second option is also available which prevents the triggering of this iteration loop at the expense of producing a slightly sub-optimal design.

The alternate approach implemented for achieving convergence with the LV designs produced by this experimental apparatus consists of a single pass resizing of the LV's uppermost stage. Whatever residual ΔV results between the initial vehicle sizing and the final optimized trajectory is absorbed into the upper stage, which is then resized to reestablish consistency. In resizing, any additional propellant required is taken directly out of the payload delivered to orbit; similarly, excess propellant is added back into the payload. The final step is to re-calculate structural size based on the updated propellant loading, with the structural weight delta adjusting the payload delivered one final time.

APPENDIX B

INDIVIDUAL ARCHITECTURE RESULTS

The LV architecture trade space defined for the experiments in this dissertation consisted of 1.5, 2,2.5, and 3 stage vehicles. The $x.5$ designation indicates a vehicle with x core stages and two strap-on liquid boosters. Besides the vehicle staging, the one additional "architecture" level variable used was the fuel-type designation for each stage. The two options used for this variable were "RP1" (Rocket Propellant 1, a refined kerosene fuel) and "LH2" (liquid hydrogen). The oxidizer for both fuels was assumed to be liquid oxygen. These two variables exercised together in a full-factorial combinatorial manner produce 24 distinct vehicle architectures, as depicted in Figure 4.2.

Conventional wisdom among the LV architect community is that architectures which place higher propulsive efficiency stages (as measured by I_{SP}) on top of lower propulsive efficiency stages provide more optimal sizing behavior. As such, it would be expected that this trend would be observable in the results obtained in that architectures with LH2 upper stages and RP1 lower stages should deliver more payload to orbit than their RP1 upper/LH2 lower counterparts.

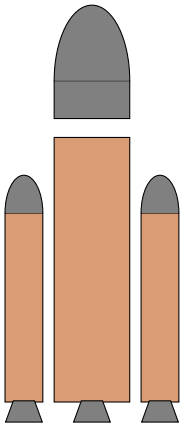

Figure B.1: “Cartoon” depiction of Architecture 1, which consists of a single RP1-fueled core stage with two RP1-fueled boosters.

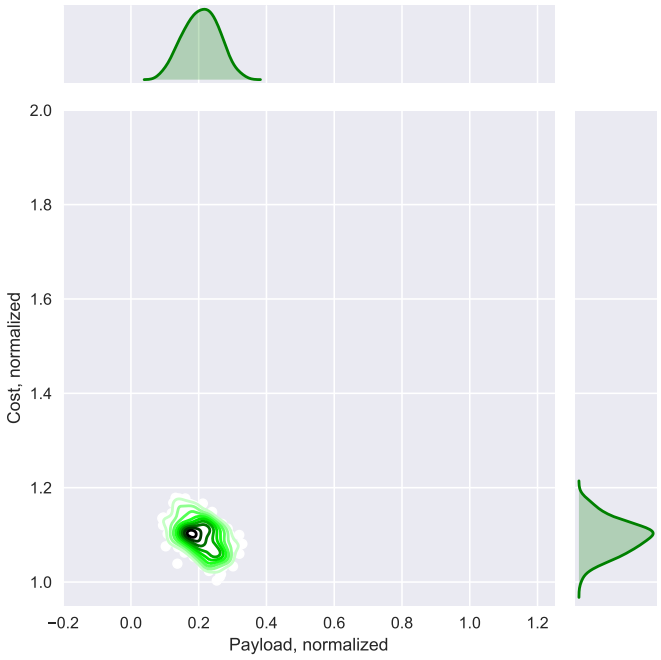

Figure B.2: Probabilistic results of Architecture 1 against Cost and Payload Performance FOMs. Axes scaled by best cost and payload observed in the overarching architecture trade space.

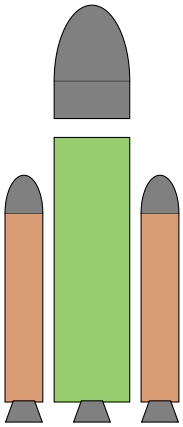

Figure B.3: “Cartoon” depiction of Architecture 2, which consists of a single LH2-fueled core stage with two RP1-fueled boosters.

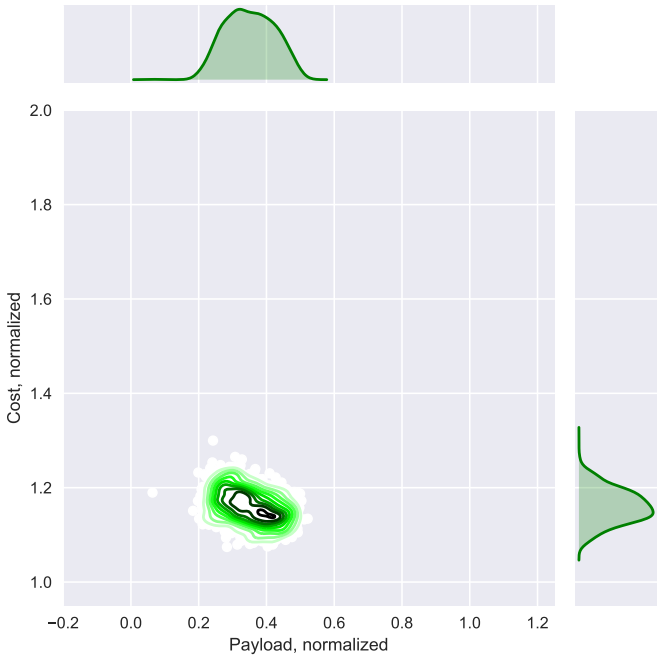

Figure B.4: Probabilistic results of Architecture 2 against Cost and Payload Performance FOMs. Axes scaled by best cost and payload observed in the overarching architecture trade space.

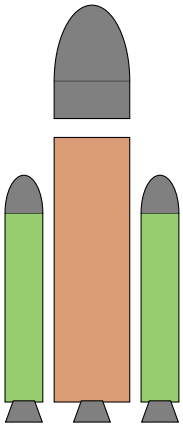

Figure B.5: “Cartoon” depiction of Architecture 3, which consists of a single RP1-fueled core stage with two LH2-fueled boosters.

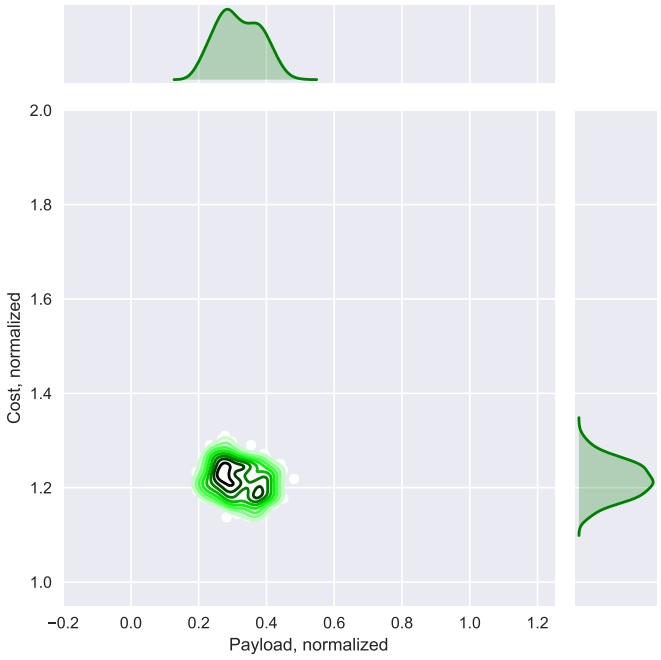

Figure B.6: Probabilistic results of Architecture 3 against Cost and Payload Performance FOMs. Axes scaled by best cost and payload observed in the overarching architecture trade space.

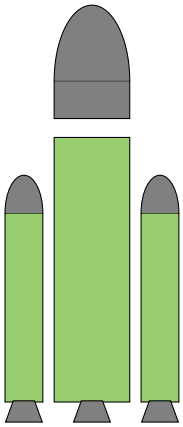

Figure B.7: “Cartoon” depiction of Architecture 4, which consists of a single LH2-fueled core stage with two LH2-fueled boosters.

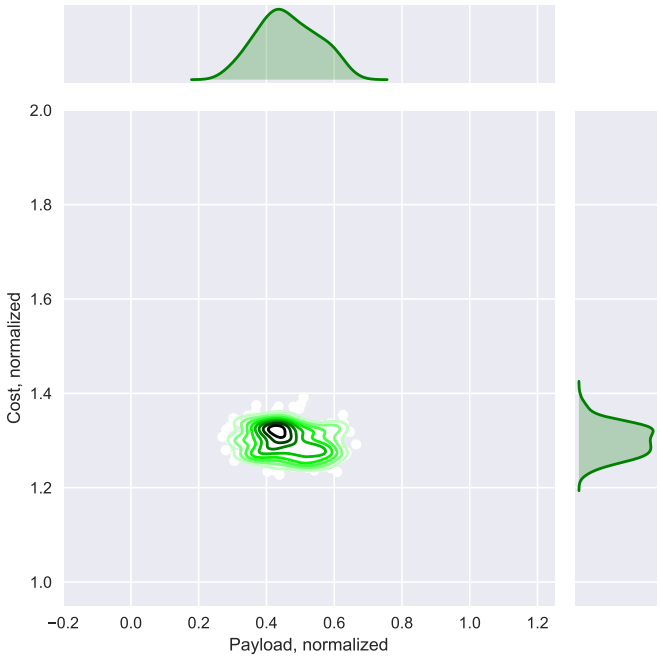

Figure B.8: Probabilistic results of Architecture 4 against Cost and Payload Performance FOMs. Axes scaled by best cost and payload observed in the overarching architecture trade space.

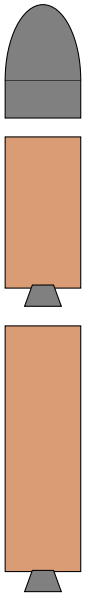

Figure B.9: “Cartoon” depiction of Architecture 5, which consists of two RP1-fueled core stages.

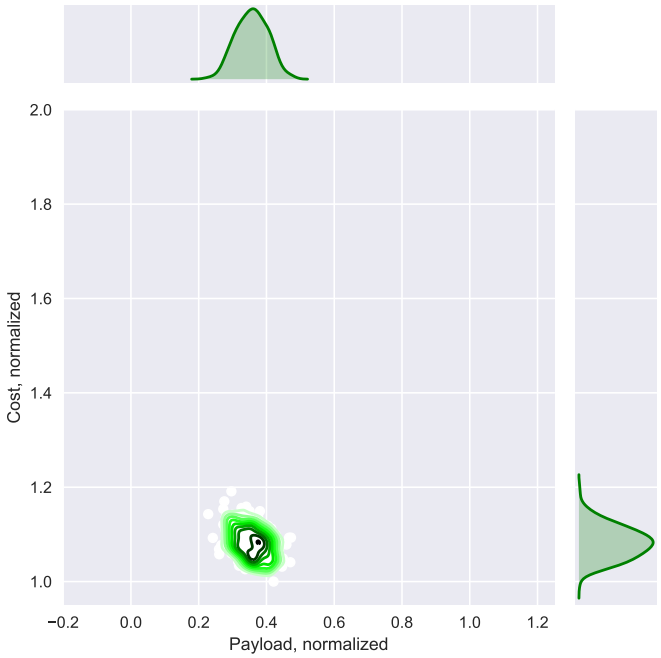

Figure B.10: Probabilistic results of Architecture 5 against Cost and Payload Performance FOMs. Axes scaled by best cost and payload observed in the overarching architecture trade space.

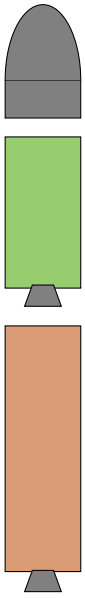

Figure B.11: “Cartoon” depiction of Architecture 6, which consists of an RP1-fueled first stage and an LH2-fueled second stage.

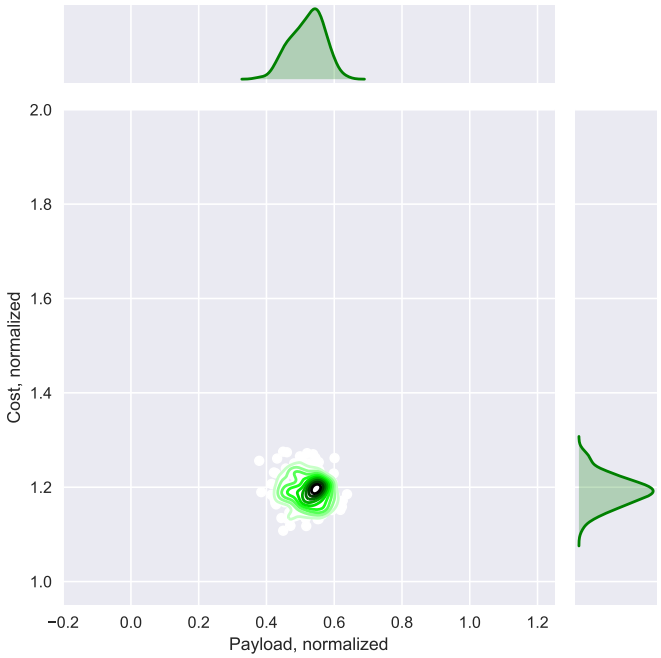

Figure B.12: Probabilistic results of Architecture 6 against Cost and Payload Performance FOMs. Axes scaled by best cost and payload observed in the overarching architecture trade space.

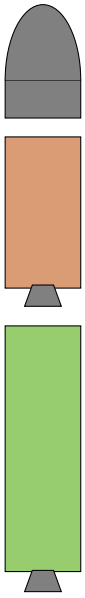

Figure B.13: “Cartoon” depiction of Architecture 7, which consists of an LH2-fueled first stage and an RP1-fueled second stage.

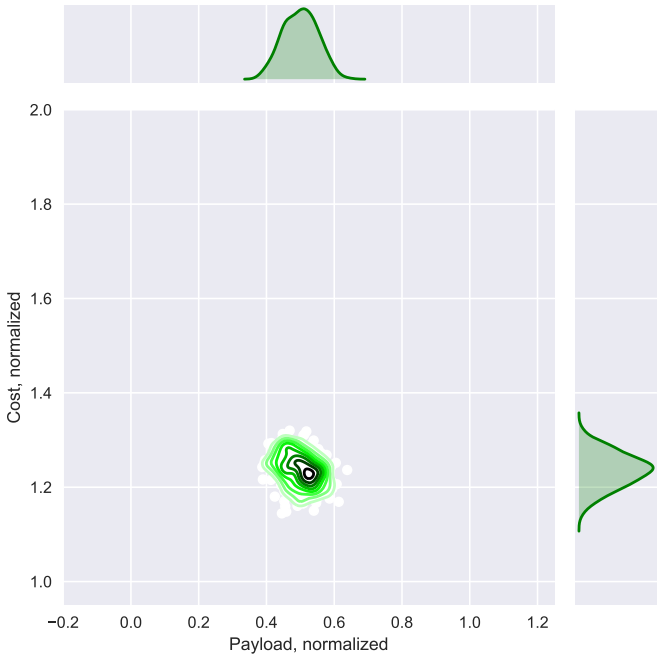

Figure B.14: Probabilistic results of Architecture 7 against Cost and Payload Performance FOMs. Axes scaled by best cost and payload observed in the overarching architecture trade space.

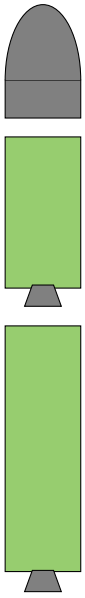

Figure B.15: “Cartoon” depiction of Architecture 8, which consists of two LH2-fueled core stages.

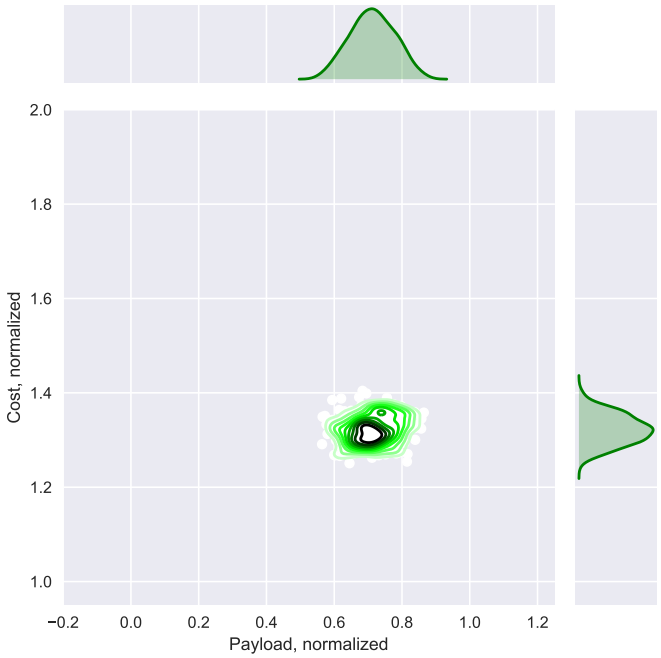

Figure B.16: Probabilistic results of Architecture 8 against Cost and Payload Performance FOMs. Axes scaled by best cost and payload observed in the overarching architecture trade space.

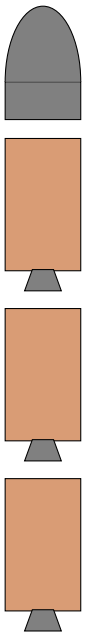

Figure B.17: “Cartoon” depiction of Architecture 9, which consists of three RP1-fueled core stages.

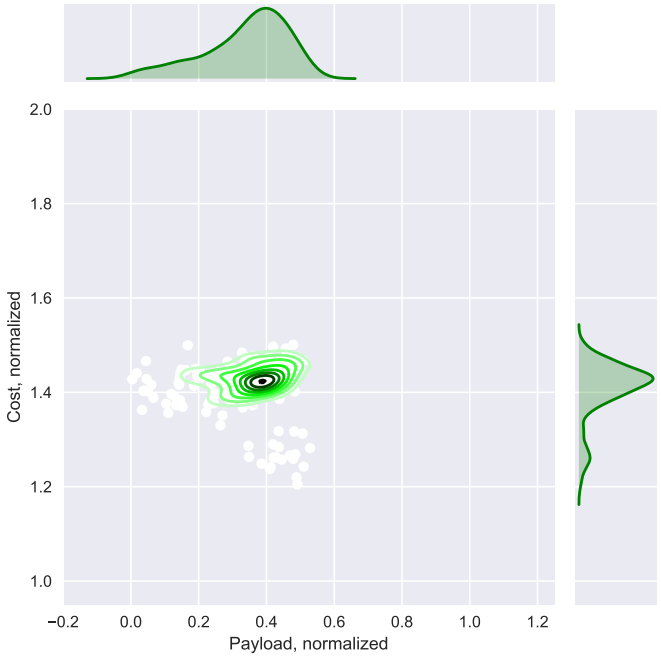

Figure B.18: Probabilistic results of Architecture 9 against Cost and Payload Performance FOMs. Axes scaled by best cost and payload observed in the overarching architecture trade space.

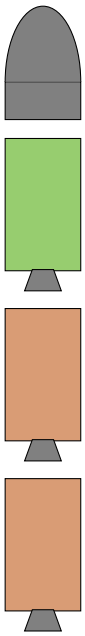

Figure B.19: “Cartoon” depiction of Architecture 10, which consists of RP1-fueled first and second stages, and an LH2-fueled third stage.

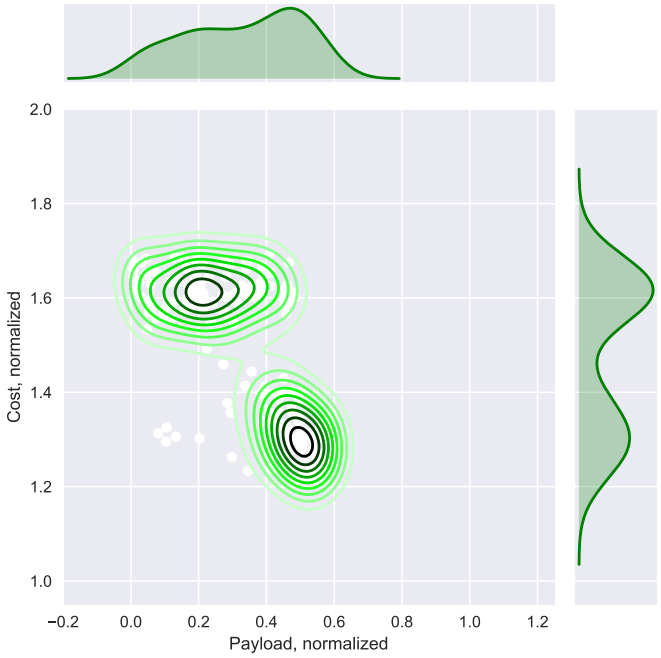

Figure B.20: Probabilistic results of Architecture 10 against Cost and Payload Performance FOMs. Axes scaled by best cost and payload observed in the overarching architecture trade space.

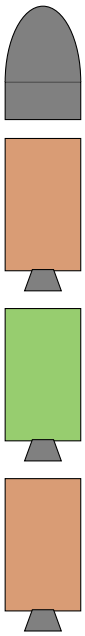

Figure B.21: “Cartoon” depiction of Architecture 11, which consists of an RP1-fueled first, an LH2-fueled second stage, and an RP1-fueled third stage.

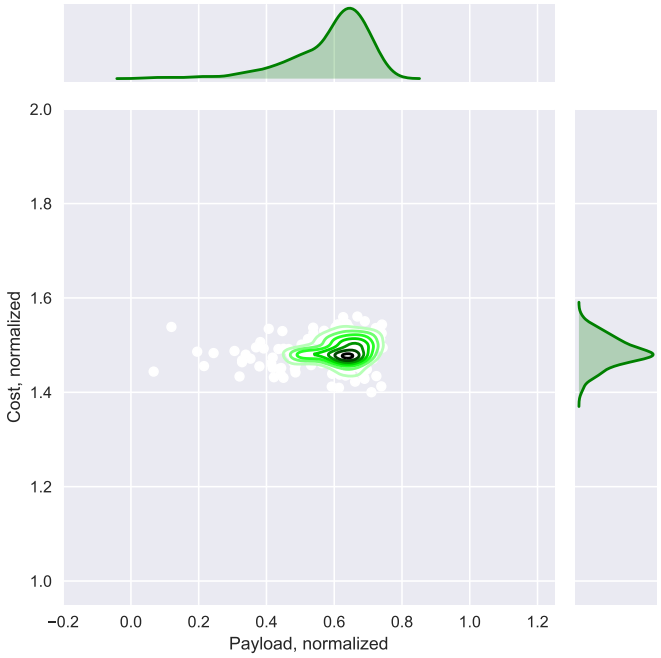

Figure B.22: Probabilistic results of Architecture 11 against Cost and Payload Performance FOMs. Axes scaled by best cost and payload observed in the overarching architecture trade space.

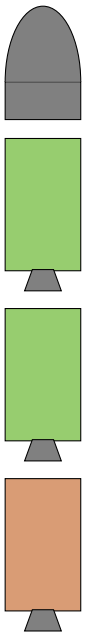

Figure B.23: “Cartoon” depiction of Architecture 12, which consists of an RP1-fueled first stage, and LH2-fueled second and third stages.

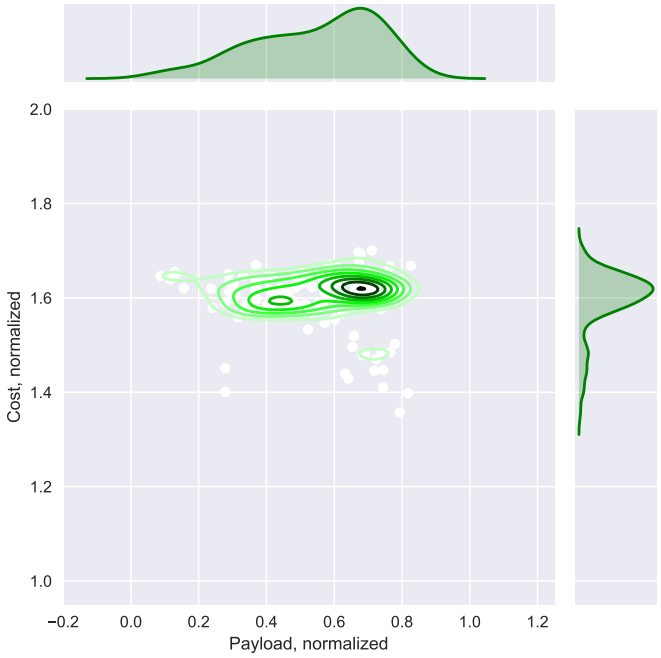

Figure B.24: Probabilistic results of Architecture 12 against Cost and Payload Performance FOMs. Axes scaled by best cost and payload observed in the overarching architecture trade space.

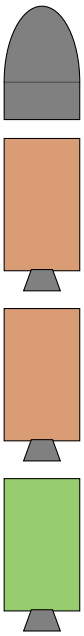

Figure B.25: “Cartoon” depiction of Architecture 13, which consists of an LH2-fueled first stage, and RP1-fueled second and third stages.

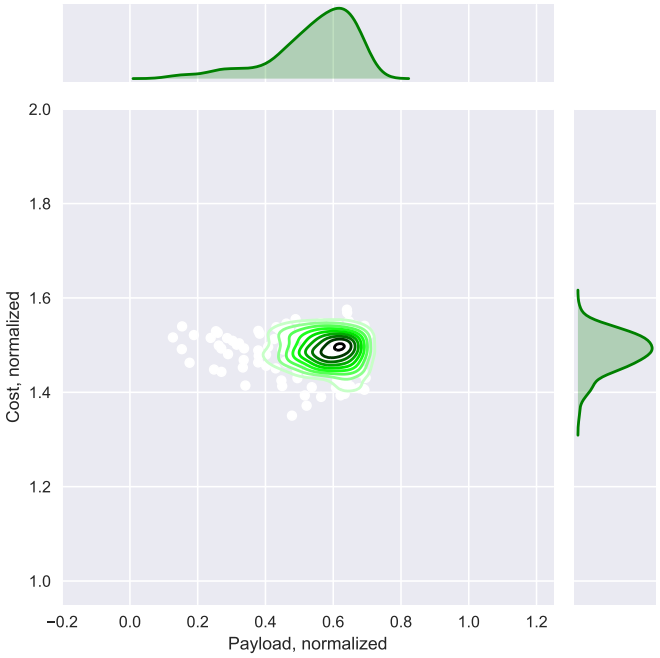

Figure B.26: Probabilistic results of Architecture 13 against Cost and Payload Performance FOMs. Axes scaled by best cost and payload observed in the overarching architecture trade space.

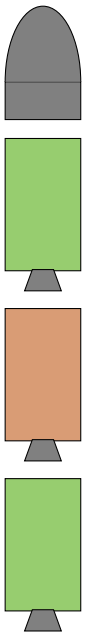

Figure B.27: “Cartoon” depiction of Architecture 14, which consists of an LH2-fueled first, an RP1-fueled second stage, and an LH2-fueled third stage.

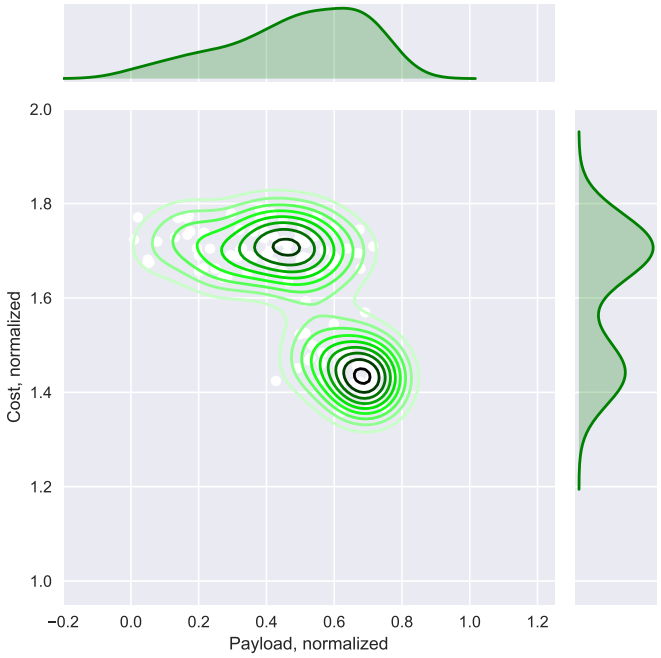

Figure B.28: Probabilistic results of Architecture 14 against Cost and Payload Performance FOMs. Axes scaled by best cost and payload observed in the overarching architecture trade space.

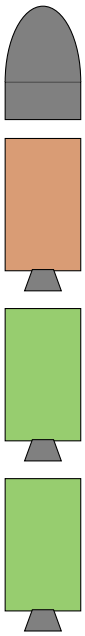

Figure B.29: “Cartoon” depiction of Architecture 15, which consists of LH2-fueled first and second stages, and an RP1-fueled third stage.

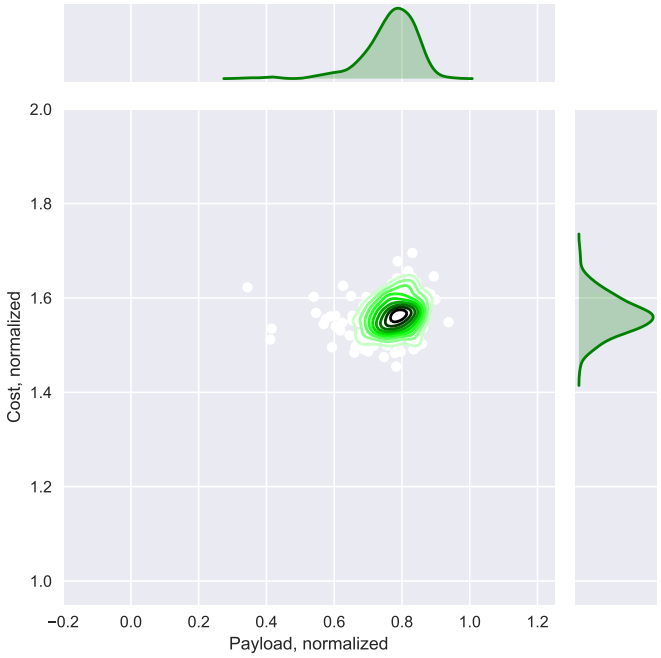

Figure B.30: Probabilistic results of Architecture 15 against Cost and Payload Performance FOMs. Axes scaled by best cost and payload observed in the overarching architecture trade space.

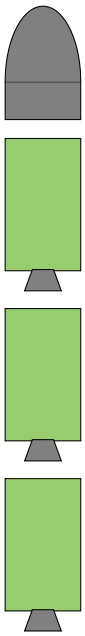

Figure B.31: “Cartoon” depiction of Architecture 16, which consists of three LH2-fueled core stages.

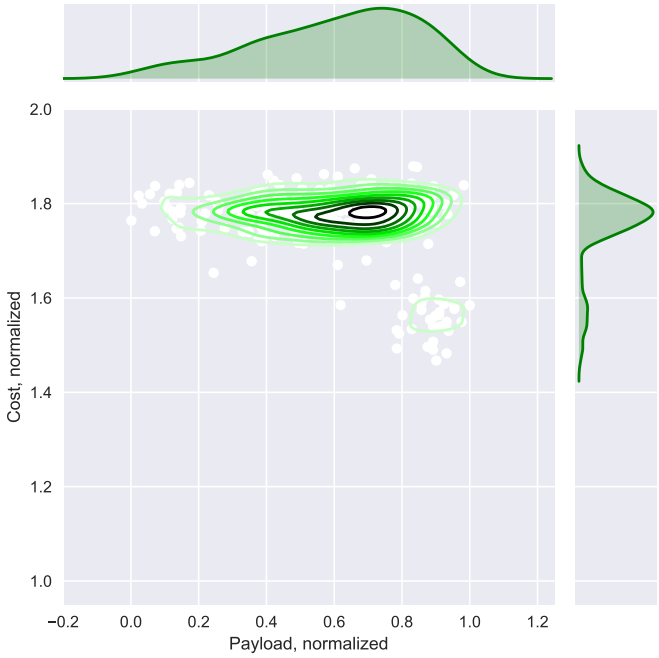

Figure B.32: Probabilistic results of Architecture 16 against Cost and Payload Performance FOMs. Axes scaled by best cost and payload observed in the overarching architecture trade space.

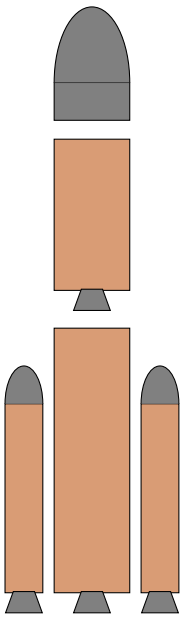

Figure B.33: “Cartoon” depiction of Architecture 17, which consists of two RP1-fueled core stages and two RP1-fueled boosters.

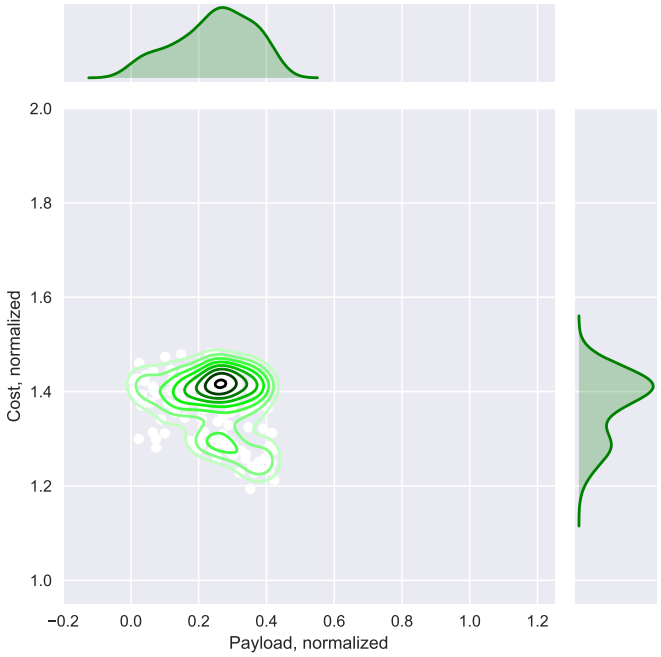

Figure B.34: Probabilistic results of Architecture 17 against Cost and Payload Performance FOMs. Axes scaled by best cost and payload observed in the overarching architecture trade space.

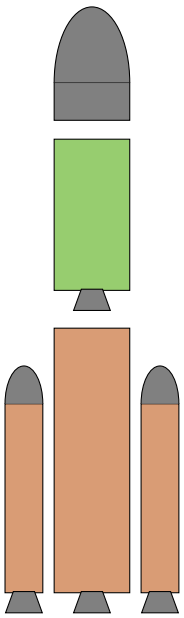

Figure B.35: “Cartoon” depiction of Architecture 18, which consists of an RP1-fueled first stage, LH2-fueled second stage, and two RP1-fueled boosters.

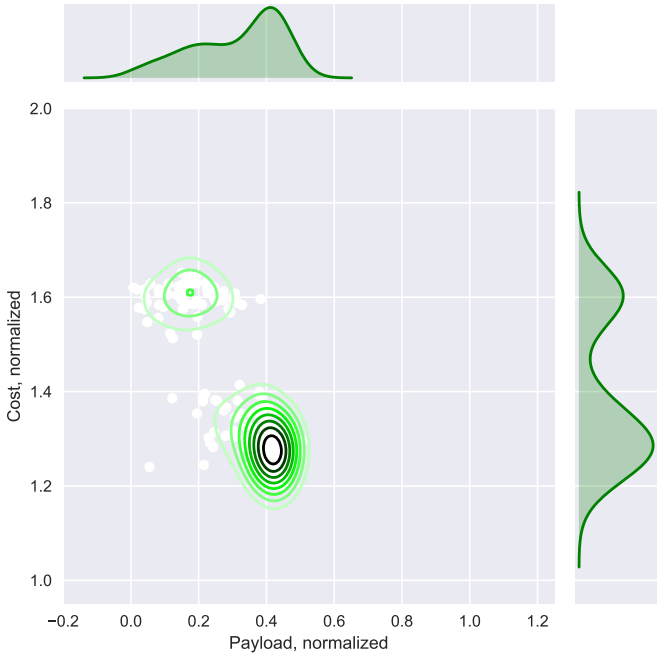

Figure B.36: Probabilistic results of Architecture 18 against Cost and Payload Performance FOMs. Axes scaled by best cost and payload observed in the overarching architecture trade space.

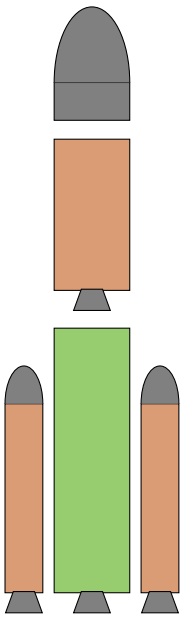

Figure B.37: “Cartoon” depiction of Architecture 19, which consists of an LH2-fueled first stage, RP1-fueled second stage, and two RP1-fueled boosters.

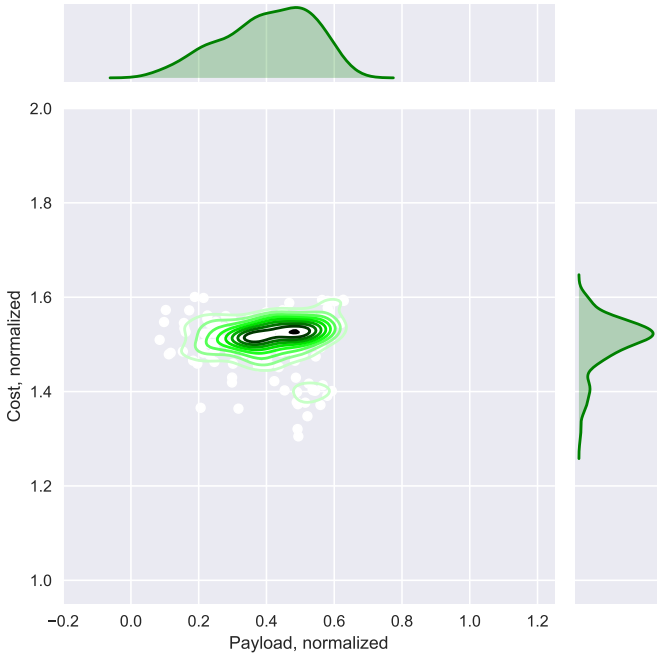

Figure B.38: Probabilistic results of Architecture 19 against Cost and Payload Performance FOMs. Axes scaled by best cost and payload observed in the overarching architecture trade space.

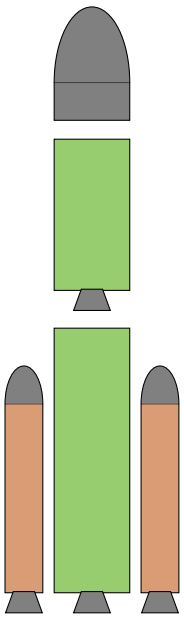

Figure B.39: “Cartoon” depiction of Architecture 20, which consists of two LH2-fueled core stages, and two RP1-fueled boosters.

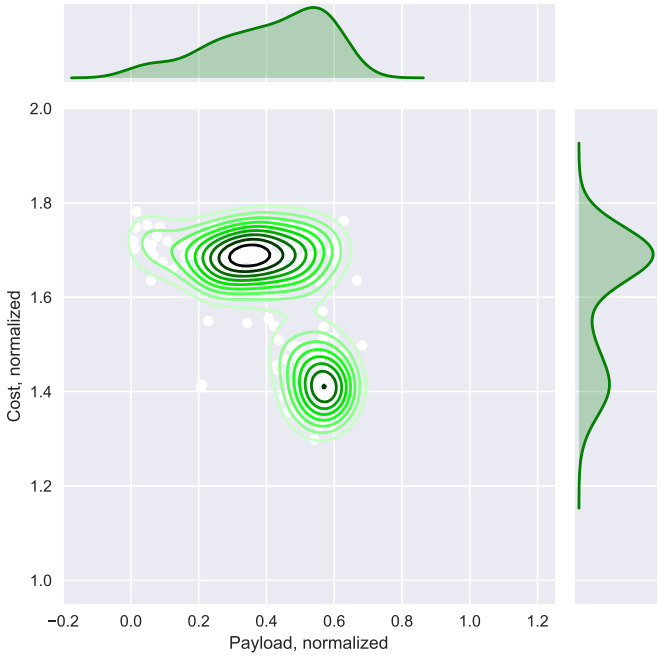

Figure B.40: Probabilistic results of Architecture 20 against Cost and Payload Performance FOMs. Axes scaled by best cost and payload observed in the overarching architecture trade space.

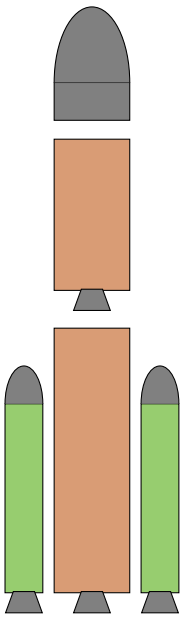

Figure B.41: “Cartoon” depiction of Architecture 21, which consists of two RP1-fueled core stages, and two LH2-fueled boosters.

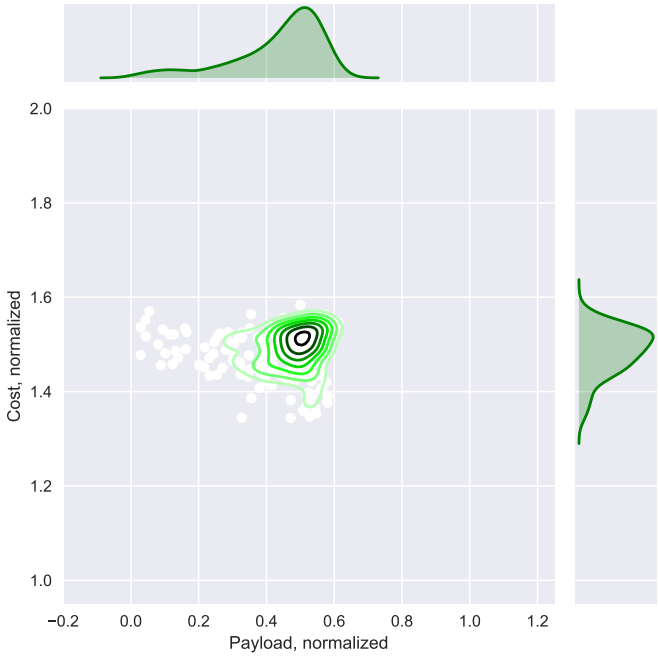

Figure B.42: Probabilistic results of Architecture 21 against Cost and Payload Performance FOMs. Axes scaled by best cost and payload observed in the overarching architecture trade space.

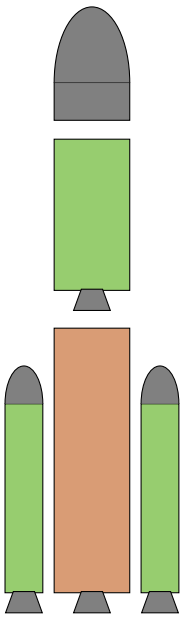

Figure B.43: “Cartoon” depiction of Architecture 22, which consists of an RP1-fueled first stage, an LH2-fueled second stage, and two LH2-fueled boosters.

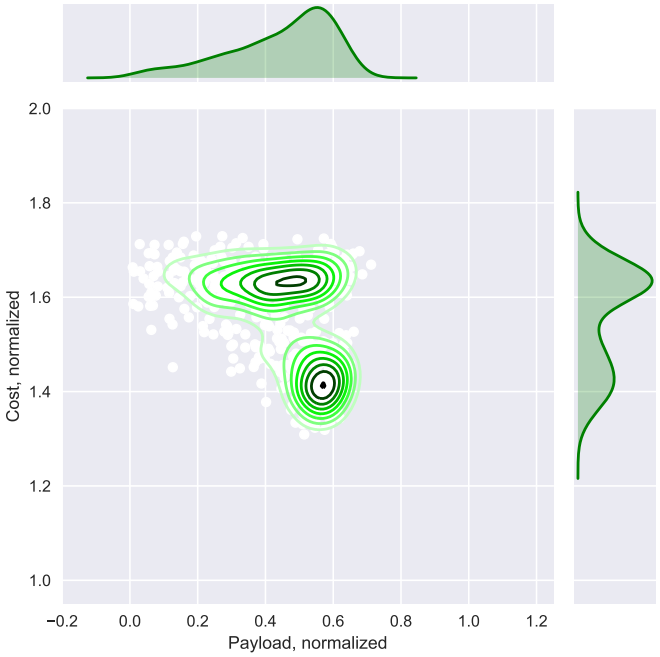

Figure B.44: Probabilistic results of Architecture 22 against Cost and Payload Performance FOMs. Axes scaled by best cost and payload observed in the overarching architecture trade space.

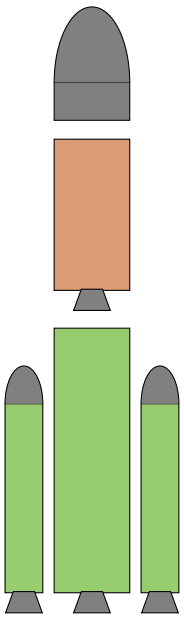

Figure B.45: “Cartoon” depiction of Architecture 23, which consists of an LH2-fueled first stage, an RP1-fueled second stage, and two LH2-fueled boosters.

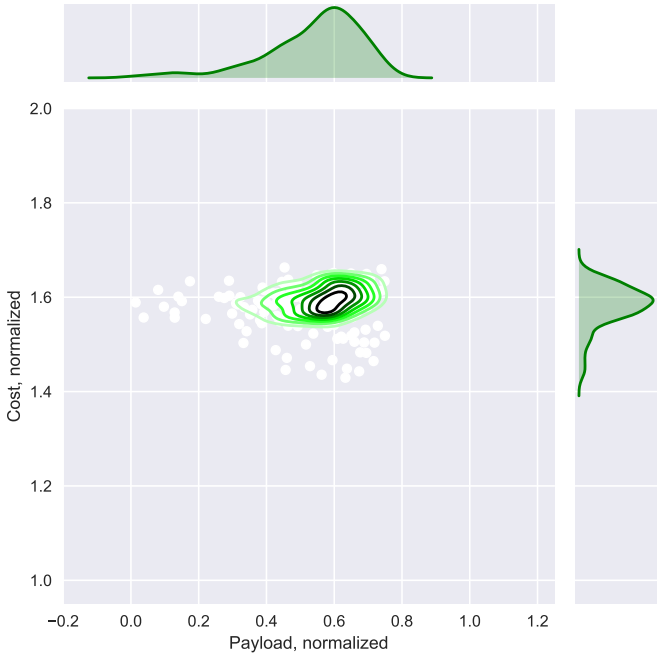

Figure B.46: Probabilistic results of Architecture 23 against Cost and Payload Performance FOMs. Axes scaled by best cost and payload observed in the overarching architecture trade space.

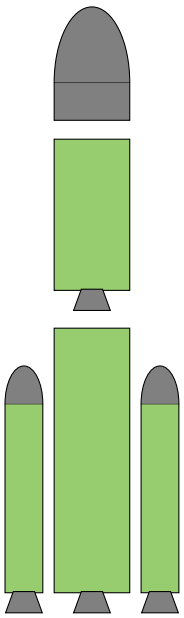

Figure B.47: “Cartoon” depiction of Architecture 24, which consists of two LH2-fueled core stages and two LH2-fueled boosters.

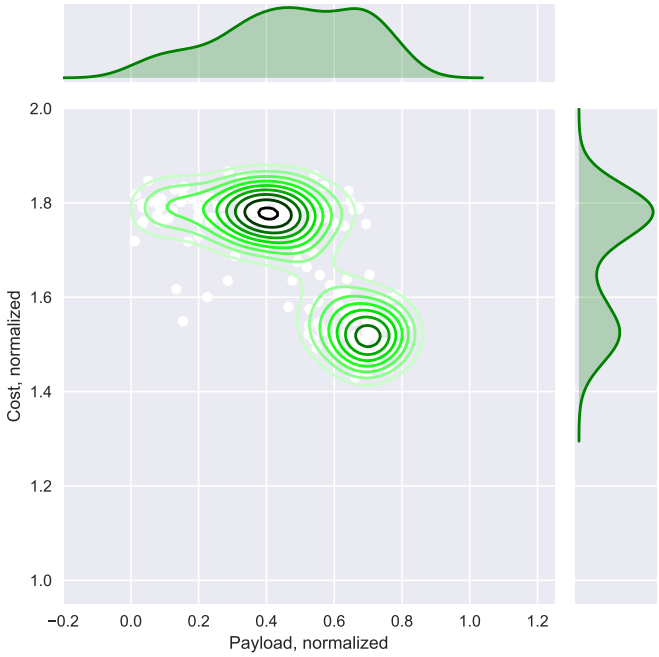

Figure B.48: Probabilistic results of Architecture 24 against Cost and Payload Performance FOMs. Axes scaled by best cost and payload observed in the overarching architecture trade space.

REFERENCES

[1] O. Acker, F. Ptscher, and T. Lefort, "Why satellites matter: The relevance of commercial satellites in the 21st century a perspective 2012-2020," Booz & Company, Tech. Rep., 2011.

[2] C. Kunstadter, "Market update," in *2014 World Space Risk Forum*, 2014.

[3] J. Brathwaite and J. H. Saleh, "Value-centric framework and pareto optimality for design and acquisition of communication satellites," *International Journal of Satellite Communications*, vol. 27, pp. 330–348, 2009.

[4] L. Kelly, *Russia to launch new heavy-lift space rocket on december 25: Interfax*, Reuters, 2014. [Online]. Available: http://www.reuters.com/article/2014/10/03/us-russia-space-angara-idUSKCN0HS0D120141003.

[5] J. Lin and P. Singer, *China is building one of the world's largest space launch vehicles*, Popular Science, http://www.popsci.com/long-march-goes. [Online]. Available: http://www.popsci.com/long-march-goes.

[6] A. Kalra, *India tests its heaviest space launch vehicle, eyes global market*, Reuters, 2014. [Online]. Available: http://www.reuters.com/article/2014/12/18/us-india-space-launch-idUSKBN0JW0HF20141218.

[7] *Interview with yasuhiro morita, epsilon launch vehicle project manager*, Japanese Aerospace Exploration Agency (JAXA), 2015. [Online]. Available: http://global.jaxa.jp/article/interview/vol58/index_e.html.

[8] (Jan. 23, 2017). Ariane 6, [Online]. Available: http://www.esa.int/Our_Activities/Launchers/Launch_vehicles/Ariane_6.

[9] J. Singer, J. R. Cook, and C. Singer, "Nasa space launch system operations strategy," in *SpaceOps 2012 Conference*, 2012.

[10] *Commercial orbital transportation services: A new era in spaceflight*, National Aeronautics and Space Administration, 2014.

[11] W. E. Hammond, *Space transportation: A systems approach to analysis and design*. American Institute of Aeronautics and Astronautics, 1999.

[12] I. Bekey, "Exploring future space transportation possibilities," in *Exploring the Unknown: Selected Documents in the History of the U.S. Civil Space Program*, J. M.

Logsdon, R. A. Williamson, R. D. Launius, R. J. Acker, S. J. Garber, and J. L. Friedman, Eds. National Aeronautics and Space Administration, 1999, vol. Volume IV: Accessing Space, ch. Exploring Future Space Transportation Possibilities, pp. 503–634.

[13] (2012). Reps. posey, culberson, wolf and olson introduce the space leadership act, US Congressman Bill Posey's website, [Online]. Available: http://posey.house.gov/news/documentsingle.aspx?DocumentID=309399.

[14] R. Pielke Jr and R. Byerly, "Shuttle programme lifetime cost," *Nature*, vol. 472, p. 38, 2011.

[15] *Access to space: Issues associated with dods evolved expendable launch vehicle program*, 1997.

[16] *Missile procurement, air force*, 2009.

[17] *Missile procurement, air force*, 2010.

[18] *Missile procurement, air force*, 2014.

[19] C. Haskins, K. Forsberg, M. Krueger, D. Walden, and R. D. Hamelin, Eds., *Systems engineering handbook: A guide for system life cycle processes and activities*. International Council on Systems Engineering, 2011.

[20] J. Singer, *Status of nasas space launch system*, Apr. 25, 2012.

[21] C. Haskins, Ed., *Systems engineering handbook: A guide for system life cycle processes and activities*, 2006.

[22] Z. C. Krevor, "A methodology to link cost and reliability for launch vehicle design," PhD thesis, Georgia Institute of Technology, 2007.

[23] K. Forsberg, H. Mooz, and H. Cotterman, *Visualizing project management: Models and frameworks for mastering complex systems*. John Wiley & Sons, Inc., 2005.

[24] *Nasa systems engineering handbook*. National Aeronautics and Space Administration, 2007.

[25] *Space project management - project planning and implementation*, ECSS-M-ST-10C Rev. 1, European Space Agency Requirments and Standards Division, 2009.

[26] M. J. Scott and E. K. Antonsson, "Arrows theorem and engineering design decision making," *Research in Engineering Design*, vol. 11, pp. 218–228, 1999.

[27] I. Kaliszewski, *Soft computing for complex multiple criteria decision making*. 2006.

[28] G. E. Deiter, *Engineering design*. McGraw-Hill, 2000.

[29] M. Zeleny, *Multiple criteria decision making*. 1982.

[30] J. Blair, R. Ryan, L. Schutzenhofer, and W. Humphries, "Launch vehicle design process: Characterization, technical integration, and lessons learned," NASA / TP–2001-210992, Tech. Rep., 2001.

[31] G. Havskjold, "Developing innovative products on budget and on schedule – part 1: Identifying and measuring cost drivers correlates technical uncertainty with rework cycles," in *45th AIAA/ASME/SAE/ASEE Joint Propulsion Conference & Exhibit*, 2009.

[32] *Nasa's exploration systems architecture study*, National Aeronautics and Space Administration, 2005.

[33] M. A. Aguirre, *Introduction to space systems: Design and synthesis*. Springer, 2012, vol. 27.

[34] F. T. Hoban, W. M. Lawbaugh, and E. J. Hoffman, Eds., *Readings in program control*. National Aeronautics and Space Administration, 1994.

[35] W. E. Hammond, *Design methodologies for space transportation systems*. AIAA, 2001.

[36] D. Schrage, T. Beltracchi, L. Berke, A. Dodd, L. Niedling, and J. Sobieski, *White paper on current state of the art*, AIAA Technical Committee on Multidisciplinary Design Optimization, 1991.

[37] D. N. Mavris, D. A. DeLaurentis, O. Bandte, and M. A. Hale, "A stochastic approach to multi-disciplinary aircraft analysis and design," in *36th Aerospace Sciences Meeting & Exhibit*, American Institute of Aeronautics and Astronautics, 1998.

[38] *Epistemology: What we can know*. Films Media Group, 2004. [Online]. Available: http://digital.films.com/PortalPlaylists.aspx?aid=8826&xtid=32715.

[39] R. Audi, *Epistemology a contemporary introduction to the theory of knowledge*. Taylor and Francis Group, 2011.

[40] Merriam-Webster, *Truth*, 2015. [Online]. Available: http://www.merriam-webster.com/dictionary/truth.

[41] ——, *Belief*, 2015. [Online]. Available: http://www.merriam-webster.com/dictionary/belief.

[42] ——, *Justified*, 2015. [Online]. Available: http://www.merriam-webster.com/dictionary/justified.

[43] R. Beheshti, "Design decisions and uncertainty," *Design Studies*, vol. 14, no. 1, pp. 85 –95, 1993. [Online]. Available: http://www.sciencedirect.com/science/article/pii/S0142694X05800079.

[44] B. E. Robertson, "A hybrid probabilistic method to estimate design margin," PhD thesis, Georgia Institute of Technology, 2013.

[45] H.-J. Bungartz, S. Zimmer, M. Buchholz, and D. Pflger, *Modeling and simulation: An application-oriented introduction*. Springer, 2014.

[46] L. G. Birta and G. Arbez, *Modelling and simulation: Exploring dynamic system behaviour*. Springer, 2007.

[47] M. L. Loper and A. Register, "Modeling and simulation in the systems engineering life cycle," in, M. L. Loper, Ed. Springer, 2015, ch. Ch. 1 - Introduction to Modeling and Simulation, pp. 3–16.

[48] D. K. Pace, "Modeling and simulation in the systems engineering life cycle," in, M. L. Loper, Ed. Springer, 2015, ch. Ch. 3 - Fidelity, Resolution, Accuracy, and Uncertainty, pp. 3–16.

[49] M. R. Zwack, "Contrast: A conceptual reliability growth approach for comparison of launch vehicle architectures," PhD thesis, Georgia Institute of Technology, 2014.

[50] J. Ceisel, P. Witte, T. Carr, S. Pogaru, and D. N. Mavris, "A non-weight based, manufacturing influenced design (mind) methodology for preliminary design," in *28TH INTERNATIONAL CONGRESS OF THE AERONAUTICAL SCIENCES*, 2012.

[51] T. R. Milner, "A risk-informed manufacturing influenced design framework for affordable launch vehicles," PhD thesis, Georgia Institute of Technology, 2016.

[52] A. Sudol, "A methodology for modeling the verification, validation, and testing process for launch vehicles," PhD thesis, Georgia Institute of Technology, 2015.

[53] Merriam-Webster, *Uncertain*, 2015. [Online]. Available: http://www.merriam-webster.com/dictionary/uncertain.

[54] J. D. Steinbruner, *The cybernetic theory of decision: New dimensions of political analysis*. Princeton University Press, 1974.

[55] M. Phillips, J. Hanson, T. Schmitt, G. Dukeman, J. Hays, A. Hill, and J. Garcia, "Preliminary performance analyses of the constellation program ares i crew launch vehicle," *Advances in the Astronautical Sciences*, vol. 128, pp. 437–462, 2007.

[56] N. Munier, *Risk management for engineering projects*. Springer, 2014.

[57] R. W. Thompson, A. W. Wilhite, D. Reeves, D. O. Stanley, and J. Wagner, "Mass growth in space vehicle and exploration architecture development," *Acta Astronautica*, vol. 66, pp. 1220–1236, 2010.

[58] J. M. Hanson and R. M. Pinson, "Calculating launch-vehicle flight performance reserve," *Journal of Spacecraft and Rockets*, vol. 49, pp. 353–363, 2012.

[59] H. Dezfuli, A. Benjamin, C. Everett, G. Maggio, M. Stamatelatos, and R. Youngblood, *Nasa risk management handbook*. National Aeronautics and Space Administration, 2011.

[60] I. Rychlik and J. Rydn, *Probability and risk analysis: An introduction for engineers*. 2006.

[61] P. R. Taylor, "The mismeasure of risk," in *Handbook of Risk Theory*. 2012.

[62] M. W. Maier and E. Rechtin, *The art of systems architecting*. CRC Press, 2000.

[63] K. A. Griendling, "Architect: The architecture-based technology evaluation and capability tradeoff method," PhD thesis, Georgia Institute of Technology, 2011.

[64] *Delta ii payload planner's guide*, United Launch Alliance, 2006.

[65] Merriam-Webster, *Jetsam*, 2014. [Online]. Available: http://www.merriam-webster.com/dictionary/jetsam.

[66] *Delta iv eft-1 mission overview*, United Launch Alliance, United Launch Alliance, 2014.

[67] F. Castellini, M. R. Lavagna, A. Riccardi, and C. Bskens, "Quantitative assessment of multidisciplinary design models for expendable launch vehicles," *Journal of Spacecraft and Rockets*, 2014.

[68] M. Balesdent, N. Bérend, P. Dépincé, and A. Chriette, "A survey of multidisciplinary design optimization methods in launch vehicle design," *Structural and Multidisciplinary optimization*, vol. 45, no. 5, pp. 619–642, 2012.

[69] A. J. Calise and M. S. K. Leung, "Optimal guidance law development for an advanced launch system," NASA, Tech. Rep. CR-4667, 1995.

[70] W. Humphries Sr., W. Holland, and R. Bishop, "Information flow in the launch vehicle design/analysis process," NASA TM-1999-209877, Tech. Rep., 1999.

[71] M. Pontani and P. Teofilatto, "Simple method for performance evaluation of multi-stage rockets," *Acta Astronautica*, vol. Vol. 94, pp. 434–445, 2014.

[72] O. von Stryk and R. Bulirsch, "Direct and indirect methods for trajectory optimization," *Annals of Operations Research*, vol. 37, pp. 357–373, 1992.

[73] D. Nelson, "Qualitative and quantitative assessment of optimal trajectories by implicit simulation (otis) and program to optimize simulated trajectories (post)," Master's thesis, Georgia Institute of Technology, 2001.

[74] L. F. Rowell and J. J. Korte, "Launch vehicle design and optimization methods and priority for the advanced engineering environment," NASA TM-2003-212654, Tech. Rep., 2003.

[75] M. B. Adams, M Beach, C. W. Cox, D. L. Crosby, R. Dobson, A. J. Goodwin, L. J. Pritchett, J. R. Quartucy, P Rosati, R. A. Sturdevant, and J. H. Young, "Nasa integral launch and reentry vehicle final report," McDonnell Douglas Astronautics Company, Tech. Rep., 1969.

[76] *Advanced transportation system studies technical area 2 (ta-2) heavy lift launch vehicle development contract final report*, Lockheed Martin Missiles & Space, 1995.

[77] M. A. Foster, "Developing a heavy lift launch vehicle systems architecture using a model based systems engineering approach," in *AIAA SPACE 2011 Conference & Exposition*, 2011.

[78] A. Aliakbargolkar, E. F. Crawley, A. C. Wicht, J. A. Battat, and E. D. Calandrelli, "Systems architecting methodology for space transportation infrastructure," *Journal of Spacecraft and Rockets*, vol. 50, pp. 579–590, 2013.

[79] F. Villeneuve, "A method for concept and technology exploration of aerospace architectures," PhD thesis, Georgia Institute of Technology, 2007.

[80] S. I. Briceo, "A game-based decision support methodology for competitive systems design," PhD thesis, Georgia Institute of Technology, 2008. [Online]. Available: http://hdl.handle.net/1853/26671.

[81] B. H. Poole, "A methodology for the robustness-based evaluation of systems-of-systems alternatives using regret analysis," PhD thesis, Georgia Institute of Technology, 2008. [Online]. Available: http://hdl.handle.net/1853/24648.

[82] I. Ordaz, "A probabilistic and multi-objective conceptual design methodology for the evaluation of thermal management systems on air-breathing hypersonic vehicles," PhD thesis, Georgia Institute of Technology, 2008. [Online]. Available: http://hdl.handle.net/1853/26478.

[83] A. P. Frits, "Formulation of an integrated robust design and tactics optimization process for undersea weapon systems," PhD thesis, Georgia Institute of Technology, 2005. [Online]. Available: http://hdl.handle.net/1853/6827.

[84] D. P. Thunnissen, "Propagating and mitigating uncertainty in the design of complex multidisciplinary systems," PhD thesis, California Institute of Technology, 2005.

[85] J. C. Domercant, "Arc-vm: An architecture real options complexity-based valuation methodology for military systems-of-systems acquisitions," PhD thesis, Georgia Institute of Technology, 2011. [Online]. Available: http://hdl.handle.net/1853/42928.

[86] F. Caron, *Managing the continuum: Certainty, uncertainty, unpredictability in large engineering projects*. 2013.

[87] G. Grote, *Management of uncertainty: Theory and application in the design of systems and organizations*. 2009.

[88] T. A. Zang, M. J. Hemsch, M. W. Hilburger, S. P. Kenny, J. M. Luckring, P. Maghami, S. L. Padula, and W. J. Stroud, "Needs and opportunities for uncertainty-based multidisciplinary design methods for aerospace vehicles," NASA Langley Research Center, Tech. Rep., 2002.

[89] *Nasa risk informed decision making handbook*. National Aeronautics and Space Administration, 2010.

[90] *Nasa space flight program and project management handbook*. 2014.

[91] J. L. Sharma, "Stase: Set theory-influenced architecture space exploration," PhD thesis, Georgia Institute of Technology, 2014.

[92] F. Zwicky, "Morphological astronomy," *The Observatory*, 1948.

[93] W. Engler, P. Biltgen, and D. Mavris, "Concept selection using an interactive reconfigurable matrix of alternatives (irma)," in, ser. Aerospace Sciences Meetings, American Institute of Aeronautics and Astronautics, Jan. 2007. [Online]. Available: http://dx.doi.org/10.2514/6.2007-1194.

[94] "Morphology," in *Merriam-Webster Dictionary*. 2016.

[95] F. Zwicky, *Discovery, invention, research - through the morphological approach*. 1969.

[96] H.-Y. B. Koo, "A meta-language for systems architecting," PhD thesis, Massachusetts Institute of Technology, 2005.

[97] D. C. Arney, "Rule-based graph theory to enable exploration of the space system architecture design space," PhD thesis, Georgia Institute of Technology, 2012.

[98] J. V. Iacobucci, "Rapid architecture alternative modeling (raam): A framework for capability-based analysis of system of systems architectures," PhD thesis, Georgia Institute of Technology, 2012.

[99] J. M. Lafleur, "A markovian state-space framework for integrating flexibility into space system design decisions," PhD thesis, Georgia Institute of Technology, 2012.

[100] D. K. S. II, A. C. Ward, and J. K. Liker, "Toyota's principles of set-based concurrent engineering," *MIT Sloan Management Review*, 1999.

[101] B. M. Ayyub and G. J. Klir, *Uncertainty modeling and analysis in engineering and the sciences*. 2006.

[102] J. I. Bernstein, "Design methods in the aerospace industry: Looking for evidence of set-based practices," Master's thesis, Massachusetts Institute of Technology, 1998.

[103] A. López Chau, X. Li, W. Yu, J. Cervantes, and P. Mejía-Álvarez, "Border samples detection for data mining applications using non convex hulls," in *Advances in Soft Computing: 10th Mexican International Conference on Artificial Intelligence, MICAI 2011, Puebla, Mexico, November 26 - December 4, 2011, Proceedings, Part II*, I. Batyrshin and G. Sidorov, Eds. Berlin, Heidelberg: Springer Berlin Heidelberg, 2011, pp. 261–272, ISBN: 978-3-642-25330-0. [Online]. Available: http://dx.doi.org/10.1007/978-3-642-25330-0_23.

[104] H. Ran, "A framework for the determination of weak pareto frontier solutions under probabilistic constraints," PhD thesis, Georgia Institute of Technology, 2007.

[105] D. A. Rousis, "A pareto frontier intersection-based approach for efficient multiobjective optimization of competing concept alternatives," PhD thesis, Georgia Institute of Technology, 2011.

[106] O. Bandte, "A probabilistic multi-criteria decision making technique for conceptual and preliminary aerospace systems design," PhD thesis, Georgia Institute of Technology, 2000.

[107] T. Aven, P. Baraldi, R. Flage, and E. Zio, *Uncertainty in risk assessment the representation and treatment of uncertainties by probabilistic and non-probabilistic methods*. 2014.

[108] K. Wu, X. Wang, L. Gu, and X.-T. Yan, "A new system design method for space launch vehicles," *Journal of Systems and Control Engineering*, vol. 227, pp. 62–69, 2013.

[109] D. R. Crowley, "An efficient approach for high-fidelity modeling incorporating contour-based sampling and uncertainty," PhD thesis, Georgia Institute of Technology, 2013.

[110] M. Qazi and H. Linshu, "Hammersley sampling and support-vector-regression-driven launch vehicle design," *Journal of Spacecraft and Rockets*, 2007.

[111] D. C. Montgomery, *Design and analysis of experiments*. 2001.

[112] J. Antony, *Design of experiments for engineers and scientists*. 2003.

[113] Z. Qian, "Computer experiments: Design, modeling and integration," PhD thesis, Georgia Institute of Technology, 2006.

[114] N. K. Borer, "Decision making strategies for probabilistic aerospace systems design," PhD thesis, Georgia Institute of Technology, 2006. [Online]. Available: http://hdl.handle.net/1853/10469.

[115] V. Belton and T. Stewart, *Multiple criteria decision analysis: An integrated approach*. 2002.

[116] M. J. Daskilewicz, "Methods for parameterizing and exploring pareto frontiers using barycentric coordinates," PhD thesis, Georgia Institute of Technology, 2013.

[117] Y. Li, "An intelligent, knowledge-based multiple criteria decision making advisor for systems design," PhD thesis, Georgia Institute of Technology, 2007.

[118] F. Roman, N. Rolander, M. G. Fernndez, B. Bras, J. Allen, F. Mistree, P. Chastang, P. Dpinc, and F. Bennis, "Selection without reflection is a risky business," in *10th AIAA/ISSMO Multidisciplinary Analysis and Optimization Conference*, 2004.

[119] R. G. Sargent, "Modeling and simulation in the systems engineering life cycle," in, M. L. Loper, Ed. Springer, 2015, ch. Ch. 5 - Types of Models, pp. 51–57.

[120] T. A. Reddy, *Applied data analysis and modeling for energy engineers and scientists*. Springer, 2011.

[121] P. L. Bonate, *Pharmacokinetic-pharmacodynamic modeling and simulation*. Springer, 2006.

[122] K. J. Keesman, *System identification: An introduction*. Springer, 2011.

[123] A. V. Rao, "Optimization and optimal control in automotive systems," in, H. Waschl, I. Kolmanovsky, M. Steinbuch, and L. del Re, Eds. Springer International Publishing, 2014, ch. Chapter 1 - Trajectory Optimization: A Survey, pp. 3–21.

[124] J. T. Betts, "Survey of numerical methods for trajectory optimization," *Journal of Guidance, Control, and Dynamics*, vol. 21, pp. 193–207, 1998.

[125] A. E. J. Bryson and Y. C. Ho, *Applied optimal control*. Wiley, 1975.

[126] B. A. Conway, "A survey of methods available for the numerical optimization of continuous dynamic systems," *Journal of Optimization Theory and Applications*, vol. 152, pp. 271–306, 2012.

[127] C. D. Eagle, *A MATLAB Script that Demostrates Aerospace Trajectory Optimization Using Direct Transcription and Collocation*. [Online]. Available: http://www.cdeagle.com/ommatlab/dto_matlab.pdf.

[128] R. Kamada, "Trajectory Optimization Strategies for Supercavitating Vehicles," PhD thesis, Georgia Institute of Technology, 2005.

[129] B. M. Shippey, "Trajectory Optimization using Collocation and Evolutionary Programming for Constrainted Nonlinear Dynamical Systems," PhD thesis, University of Texas at Arlington, 2008.

[130] M. Steffens and D. N. Mavris, "Launch vehicle performance analysis using extreme value theory," in *AIAA Space 2015 Conference and Exposition*, American Institute of Aeronautics and Astronautics, 2015.

[131] M. J. Steffens, S. J. Edwards, and D. N. Mavris, "Capturing the global feasible design space for launch vehicle ascent trajectories," in *AIAA SciTech*, American Institute of Aeronautics and Astronautics, Jan. 2015, pp. –. [Online]. Available: http://dx.doi.org/10.2514/6.2015-1910.

[132] K. E. Atkinson, *An introduction to numerical analysis*, 2nd. John Wiley & Sons, Inc., 1989.

[133] U. M. Ascher and L. R. Petzold, *Computer methods for ordinary differential equations and differential-algebraic equations*. Society for Industrial and Applied Mathematics, 1998.

[134] E. Suli. (2013). Numerical solution of ordinary differential equations. Lecture Notes at University of Oxford, University of Oxford, [Online]. Available: http://people.maths.ox.ac.uk/suli/nsodes.pdf.

[135] A. V. Rao, "A survey of numerical methods for trajectory optmization," in *AAS/AIAA Astrodynamics Specialist Conference*, 2009.

[136] R. R. Bate, D. D. Mueller, and J. E. White, *Fundamentals of astrodynamics*. Dover Publications, Inc., 1971.

[137] D. G. Hull, "Conversion of Optimal Control Problems into Parameter Optimization Problems," *Journal of Guidance, Control, and Dynamics*, vol. 20, no. 1, pp. 57–60, 1997.

[138] J. Frank, *Collocation Methods*, 2008. [Online]. Available: http://homepages.cwi.nl/~jason/Classes/numwisk/ch7.pdf.

[139] Merriam-Webster, *Analytic*, 2014. [Online]. Available: http://www.merriam-webster.com/dictionary/analytic.

[140] WolframMathWorld, *Analytic*, 2014. [Online]. Available: http://mathworld.wolfram.com/Analytic.html.

[141] J. F. White, Ed., *Flight performance handbook for powered flight operations*. John Wiley & Sons, Inc., 1963.

[142] F. M. Perkins, "Derivation of linear-tangent steering laws," Aerospace Corporation, Tech. Rep. TR- 1001(9990)-i, 1966.

[143] Merriam-Webster, *Empirical*, 2014. [Online]. Available: http://www.merriam-webster.com/dictionary/empirical.

[144] J. R. Wertz and W. J. Larson, *Space mission analysis and design*. Microcosm, 2003.

[145] P. Dergarabedian and R. TenDyke, "Estimating performance capabilities of boost rockets," Space Technology Laboratories, Inc., Tech. Rep. TR- 59-0000-00792, 1959.

[146] J. S. MacKay and R. J. Weber, "Performance charts for multistage rocket boosters," NASA Lewis Research Center, Tech. Rep. NASA TN D-582, 1961.

[147] G. E. Townsend, "Ascent to orbit," in *Design Guide to Orbital Flight*, J. Jensen, G. Townsend, J. Kork, and D. Kraft, Eds. McGraw-Hill Book Company, Inc., 1962, ch. 6, pp. 265–312.

[148] R. Bellman, Ed., *Mathematical optimization methods*. University of California Press, 1963, ch. Ch. 2: Estimating Performance Capabilities of Boost Rockets.

[149] H. S. Seifert and K. Brown, *Ballistic missile and space vehicle systems*. John Wiley & Sons, 1961.

[150] J. Schilling, "Launch vehicle performance estimation," White Paper, 2009, [Online]. Available: http://www.silverbirdastronautics.com/LaunchMethodology.pdf.

[151] M. Qazi and H. Linshu, "Nearly-orthogonal sampling and neural network metamodel driven conceptual design of multistage space launch vehicle," *Computer-Aided Design*, vol. 38, pp. 595–607, 2006.

[152] P. Walsh, A. Coulon, S. Edwards, and D. Mavris, "Creation of an upper stage trajectory capability boundary to enable booster system trade space exploration," in *AIAA Space Conference and Exposition*, American Institute of Aeronautics and Astronautics, Sep. 2012, pp. –. [Online]. Available: http://dx.doi.org/10.2514/6.2012-5129.

[153] WolfromAlpha, *Heuristic*, 2014. [Online]. Available: http://www.wolframalpha.com/input/?i=heuristic.

[154] W. Ley, K. Wittmann, and W. Hallmann, *Handbook of space technology*. John Wiley & Sons, 2009, vol. 22.

[155] M. Macdonald and V. Badescu, *The international handbook of space technology*. Springer, 2014.

[156] F. Castellini and M. Lavagna, "Comparative analysis of global techniques for performance and design optimization of launchers," *Journal of Spacecraft and Rockets*, vol. 49, no. 2, pp. 274–285, 2012.

[157] A. D. Ketsdever, M. P. Young, J. B. Mossman, and A. P. Pancotti, "Overview of advanced concepts for space access," *Journal of Spacecraft and Rockets*, vol. 47, no. 2, pp. 238–250, 2010.

[158] A. Tewari, *Atmospheric and space flight dynamics: Modeling and simulation with matlab® and simulink®*. Springer, 2007.

[159] M. J. Bayer, "Analytic performance considerations for lifting ascent trajectories of winged launch vehicles," *Acta Astronautica*, vol. 54, pp. 713–721, 2004.

[160] *Atlas v and delta iv technical summary*, United Launch Alliance, 2013.

[161] J. Jensen, G. Townsend, J. Kraft, and J. Kork, *Design guide to orbital flight*. McGraw-Hill, 1962.

[162] *Ariane 5 user's manual*, Arianespace, 2011.

[163] M. J. Steffens, "A combined global and local methodology for launch vehicle trajectory design-space exploration and optimization," Master's thesis, Georgia Institute of Technology, 2014.

[164] M. Steffens, S. Edwards, M. Diaz, D. N. Mavris, and P. Dees, "A method for launch vehicle performance analysis via surrogate modeling," in *AIAA SciTech*, 2016.

[165] M. J. Steffens, "Trajectory-based launch vehicle performance analysis for design-space exploration in conceptual design," PhD thesis, Georgia Institute of Technology, 2016.

[166] P. D. Dees, M. R. Zwack, S. Edwards, and M. J. Steffens, "Augmenting conceptual design trajectory tradespace exporation with graph theory," in, ser. AIAA SPACE Forum, American Institute of Aeronautics and Astronautics, Sep. 2016. [Online]. Available: http://dx.doi.org/10.2514/6.2016-5650.

[167] M. R. Zwack and P. D. Dees, "Application of design of experiments and surrogate modeling within the nasa advanced concepts office, earth-to-orbit design process," in *AIAA SPACE Forum*, 2016.

[168] P. A. Barros Jr., M. R. Kirby, and D. N. Mavris, "Impact of sampling technique selection on the creation of response surface models," *2004 World Aviation Congress*, 2004.

[169] M. Kuhn and K. Johnson, *Applied predictive modeling*. Springer, 2013.

[170] T. Hastie, R. Tibshirani, and J. Friedman, *The elements of statistical learning*. Springer, 2009.

[171] A. J. Izenman, *Modern multivariate statistical techniques: Regression, classification, and manifold learning*. Springer, 2013.

[172] F. Ferraty and P. Vieu, *Nonparametric functional data analysis*. Springer, 2006.

[173] P. T. Reiss and R. T. Ogden, "Functional principal component regression and functional partial least squares," *Journal of the American Statistical Association*, vol. 102, pp. 984–996, 2007.

[174] J. Ramsay and B. Silverman, *Functional data analysis*. Springer, 2005.

[175] F. Rossia, N. Delannay, B. Conan-Gueza, and M. Verleysen, "Representation of functional data in neural networks," *Neurocomputing*, vol. 64, pp. 183–210, 2005.

[176] G. Dreyfus, *Neural networks: Methodology and applications*. Springer, 2004.

[177] K. L. Priddy and P. E. Keller, *Artificial neural networks: An introduction*. 2005.

[178] J. E. Kolen and S. C. Kremer, *A field guide to dynamical recurrent networks*. 2001.

[179] Y. LeCun, Y. Bengio, and G. Hinton, "Deep learning," *Nature*, vol. 521, no. 7553, pp. 436–444, May 2015. [Online]. Available: http://dx.doi.org/10.1038/nature14539.

[180] L. L. Phan, "A methodology for the efficient integration of transient constraints in the design of aircraft dynamic systems," PhD thesis, Georgia Institute of Technology, 2010.

[181] O. Voitcu and Y.-S. Wong, "A neural network approach for nonlinear aeroelastic analysis," in, ser. Structures, Structural Dynamics, and Materials and Co-located Conferences, American Institute of Aeronautics and Astronautics, Apr. 2002. [Online]. Available: http://dx.doi.org/10.2514/6.2002-1286.

[182] R. Sclafani and P. Shankar, "Variable memory recurrent neural networks for launch vehicle attitude control," in, ser. AIAA SciTech Forum, American Institute of Aeronautics and Astronautics, Jan. 2015. [Online]. Available: http://dx.doi.org/10.2514/6.2015-1774.

[183] A. De Brébisson, E. Simon, A. Auvolat, P. Vincent, and Y. Bengio, "Artificial neural networks applied to taxi destination prediction," in *Proceedings of the 2015th International Conference on ECML PKDD Discovery Challenge - Volume 1526*, ser. ECMLPKDDDC'15, Porto, Portugal: CEUR-WS.org, 2015, pp. 40–51. [Online]. Available: http://dl.acm.org/citation.cfm?id=3056172.3056178.

[184] H. Curtis, *Orbital mechanics for engineering students*. Elsevier Science & Technology, 2009.

[185] E. Civek-Coskun and K. Ozgoren, "A generalized staging optimization program for space launch vehicles," in *Proceedings of the 6th International Conference on Recent Advances in Space Technologies (RAST)*, 2013, pp. 857–862. [Online]. Available: http://ieeexplore.ieee.org/stamp/stamp.jsp?arnumber=6581333.

[186] R. Ullah, D.-Q. Zhou, P. Zhou, M. Hussain, and M. A. Sohail, "An approach for space launch vehicle conceptual design and multi-attribute evaluation," *Aerospace Science and Technology*, vol. 25, pp. 65–74, 2013.

[187] B. Palaszewski and R. Powell, "Launch vehicle performance using metallized propellants," in *AIAA/SAE/ASME/ASEE 27th Joint Propulsion Conference*, 1991.

[188] J. Cole and I. Silvera, "Future propellants for launch vehiclesmetallic hydrogen with water and hydrocarbon diluents," in *SPACE, PROPULSION & ENERGY SCIENCES INTERNATIONAL FORMUM SPESIF-2010: 14th Conference on Thermophysics Applications in Microgravity 7th Symposium on New Frontiers in Space Propulsion Sciences 2nd Symposium on Astrosociology 1st Symposium on High Frequency Gravitational Waves*, AIP Publishing, vol. 1208, 2010, pp. 107–120.

[189] R. Jamilnia and A. Naghash, "Simultaneous optimization of staging and trajectory of launch vehicles using two different approaches," *Aerospace Science and Technology*, vol. 23, no. 1, pp. 85–92, 2012.

[190] *Atlas v launch services users guide*, United Launch Alliance, 2010.

[191] *Delta iv launch services user's guide*, United Launch Alliance, 2013.

[192] J. D. Mattingly, W. H. Heiser, and D. T. Pratt, *Aircraft engine design*. American Institute of Aeronautics and Astronautics, 2002.

[193] L. Fahrmeir, T. Kneib, S. Lang, and B. Marx, *Regression - models, mmethod, and applications*. Springer, 2013.

[194] *Atlas launch system mission planner's guide, atlas v addendum*, International Launch Services, 1999.

[195] J. Gray, K. T. Moore, T. A. Hearn, and B. A. Naylor, "Standard platform for benchmarking multidisciplinary design analysis and optimization architectures," *AIAA Journal*, vol. 51, no. 10, 2013.

[196] M. Balesdent, N. Brend, and P. Dpinc, "Stagewise multidisciplinary design optimization formulation for optimal design of expendable launch vehicles," *Journal of Spacecraft and Rockets*, 2012.

[197] D. Mavris, D. DeLaurentis, O. Bandte, and M. Hale, "A stochastic approach to multi-disciplinary aircraft analysis and design," in *Aerospace Sciences Meetings*, American Institute of Aeronautics and Astronautics, Jan. 1998, pp. –. [Online]. Available: http://dx.doi.org/10.2514/6.1998-912.

[198] R. R. Rohrschneider, "Development of a mass estimating relationship database for launch vehicle conceptual design," Master's thesis, Georgia Institute of Technology, Apr. 26, 2002.

[199] B. Brothers, "Launch vehicle mass estimating relationship database," ALPHA TECHNOLOGY, INC., Tech. Rep., Dec. 1, 1999.

[200] S. Isakowitz, J. Hopkins, and J. H. Jr., *International reference guide to space launch systems*. 2004.

[201] D. E. Koelle, *Handbook of cost engineering for space transportation systems with transcost 8.2 : Statistical-analytical model for cost estimation and economical optimization of launch vehicles*. 2013.

[202] P. W. Rocketdyne, *Rl10 propulsion system product card*, 2011.

[203] D. W. Scott, *Multivariate density estimation*. 2015.

[204] S. I. Inc., "Design of experiments guide," in *JMP 13 Documentation Library*, 2016.

[205] P. BRATLEY and B. L. FOX, "Algorithm 659: Implementing sobols quasirandom sequence generator," Universite de Montreal, Tech. Rep., 1988.